

ALMA MATER STUDIORUM A.D. 1088
UNIVERSITÀ DI BOLOGNA

SCUOLA DI SCIENZE

Corso di Laurea Magistrale in Geologia e Territorio

Dipartimento di Scienze Biologiche, Geologiche ed Ambientali

Tesi di Laurea Magistrale

A new specimen of shark from the Monte Postale
locality (Eocene, Bolca) and the rise of triakids in
ancient ecosystems

Candidato:
Gabriele Larocca Conte

Relatore:
Prof. Federico Fanti

Correlatore:
Enrico Trevisani
Paolo Guaschi

Sessione Marzo 2018
Anno Accademico 2016 - 2017

Index

| | |
|---|-----------|
| Abstract | 1 |
| Chapter 1: Introduction | 2 |
| Chapter 2: Geological setting, stratigraphic and Paleoenvironmental settings | 3 |
| 2.1 Geological setting | 3 |
| 2.2 Stratigraphic Setting of Pesciara and Monte Postale successions | 5 |
| 2.3 Age of the Pesciara – Monte.Postale fossil – fish <i>Lagerstätte</i> | 11 |
| 2.4 Paleoenvironmental setting | 13 |
| Chapter 3: Materials and methods | 18 |
| Chapter 4: Results – Overall description of MSNPV 17716 – 17717 | 25 |
| Chapter 5: Historical outline of Bolca’s shark specimens | 35 |
| Chapter 6: Discussion | 38 |
| 6.1: <i>Galeorhinus Vs Eogaleus</i> and size estimates of MSNPV 17716 – 17717 ... | 38 |
| 6.2: Comparison of body ratios between extant and living specimens | 50 |
| 6.3: Comparison of scale morphotypes between extant and living specimens ... | 55 |
| 6.4: Comparison of tooth morphotypes between extant and living specimens ... | 59 |
| 6.5: Age and size estimates | 68 |
| 6.6: Paleoecologically and Paleogeographic significances | 75 |

| | |
|--------------------------------------|-----------|
| Chapter 7: Conclusions | 79 |
| References | 80 |
| Supplementary materials | 92 |

Abstract

This thesis focused on the description of a fossil shark found in the Museo di Storia Naturale di Pavia during a complex restoration project started in 1989. The specimen consists in slab and counter – slab, and recently was assigned the inventory ID MSNPV 17716 and 17717. The specimen represents one of the rarest shark taxa from the world – renowned Eocene Bolca locality. Unlike *Galeorhinus cuvieri* and *Eogaleus bolcensis* individuals housed in the collections of Bologna, Padova, Paris and Verona, the specimen is disarticulated and lies in a massive limestone matrix, suggesting its provenience from the Monte Postale site rather than the Pesciara quarry. This study focuses primarily on qualitative and morphometrical measurements of body, vertebral centra, teeth and placoid scales. The dataset was compared to both fossil and extant taxa, in order to document divergences within fossil assemblage and to review the overall systematic assessments of the Bolca sharks at higher taxonomic levels. Overall body measurements collected from triakids and carcharhinids taxa from Bolca show several affinities, therefore the ratios dataset for each specimen was performed to estimate the size of 17716 – 17717. The total length of the individual is estimated in 175 cm. The statistical approach performed on body measurements and number of vertebrae supported that these anatomical characters are largely shared among the extant families Carcharhinidae, Hemigaleidae, Triakidae and Sphyrnidae. SEM analysis on dermal denticle collected from different segments of the body support the interpretation that the Pavia specimen is an individual of *Eogaleus bolcensis*. As teeth represent a standard and pivotal tool for taxonomic interpretation, a comprehensive dataset was used to compare dental morphologies of the living species *Galeorhinus galeus* and *Galeocerdo cuvier*, considered as standards for the families Triakidae and Carcharhinidae. A statistical approach reveals no significant results and, therefore, the general categorization is mainly based on qualitative characters and ratios between selected measurements. The comparison between fossil and extant taxa based on tooth types suggest that: 1) *G. cuvieri* is related to the genus *Galeorhinus* and differs from the extinct carcharhinid genus *Physogaleus*; 2) *Eogaleus bolcensis* significantly differs from *G. galeus*. Interestingly, the genus *Eogaleus* and *Galeocerdo* show several affinities to the triakid fossil genus *Pachygaleus*.

The correlation between averages of centra length and external regions for each fossil specimen indicates three distinct ontogenetic classes among examined individuals. To support this hypothesis, the age of the specimens was estimated following the standard Von Bertalanffy growth curves commonly applied to modern chondrichthyans. Results suggest that all specimens assigned to *G. cuvieri* are somatically and sexually immature, whereas the specimens classified as *E. bolcensis* are young – adult individuals. As the present – day *Galeocerdo*, *Eogaleus* was most likely a mesopelagic, top predator of the Ypresian lagoonal ecosystems. Stomach content of several species of *G. cuvieri* provides a deep conservation of a complex trophic network among primary consumers, which has its counterpart into the modern coral reef systems. The combination of biological and abiotic proxies suggests the Bolca setting as a possible nursery area for the juvenile – schooling individuals of *G. cuvieri*.

Chapter 1: Introduction

In 1989, the Museo di Storia Naturale of the Università di Pavia started a complex project in order to restore and catalogue all specimens housed in the main building, including the rich paleontological collections. During this process, two slabs from the Bolca locality were found uncatalogued in the collection: a first examination revealed that slabs (slab and counter – slab) host a nicely preserved chondrichthyan, one of the rarest fossils from Bolca. Luckily, the paper archive of the Museum provided pivotal information on the history of this unique specimen. Both slabs were purchased in 1825 by the Museum Director Gian Maria Zandrini together with other eight specimens from the Bolca quarry (Galeotti et al., 1831; Jucci, 1939; Rovati, 1999). Zandrini himself provided a taxonomic identification for the specimens most likely based on the early description of the Bolca vertebrates by Volta (1796 – 1808). He therefore assigned the specimen to the swamp eel *Synbranchus immaculatus?*. Lacking any illustration or photographic material dated to the acquisition of the slabs, the description provided by Zandrini was essential in identifying the shark material among the vast acquisition of the Museo in Pavia. In particular, Zandrini mentions:

- 1) *Anatomical features*. The specimens consist of an individual 43”1/2 long (measure expressed in French Inches, corresponding about 120 cm), with a bent vertebral column and smoothed head.
- 2) *Workmanship of the slabs*. The assembled blocks of both slabs lie on a basal and compact layer of nodular calcareous limestones (i.e. “Formazione Rosso Ammonitico”). Indeed, each slab is covered with black woody frame. The specimens of the Bolca batch purchased by Zandrini are designed with the same elements.

Among the wide literature of the fossiliferous area, the shark specimens have been received little attention. The evolutionary history of Paleocene Chondrichthyes is usually problematic due to the lack of non – dental characters (Cappetta, 2012). A remarkable exception to this general taphonomic setting is represented by the articulated shark specimens of the Ypresian Bolca deposits. Nevertheless, the systematic of the fossil carcharhinids assemblage is still unclear (Fanti et al., 2016; Marammà et al., 2017). The analysis of the individual allows to review the overall biodiversity of Bolca carcharhinids assemblage at higher taxonomic levels and provides additional insights on the complex coral reefs – trophic network among primary consumers at the exit of the Early Eocene Climate Optimum.

Chapter 2: Geological setting, stratigraphic and Paleoenvironmental settings

2.1: Geological Setting

Bolca is a world – renowned *Fossil – Lagerstätte* located in Alpone River Valley, about 25 km to the North – Est of Verona. Throughout the Jurassic, the area was characterized by the carbonate sediments of the Trento Platform. The latter was limited by deeper marine basins: the “Lombardo Basin” to west and “Belluno Trough” to east, (Bosellini et al., 1981; Winterer & Bosellini, 1981; Bosellini & Papazzoni., 2003; Papazzoni et al., 2014; **Fig. 1A**). According to Barbieri et al. (1982, 1991), during the Late Paleocene – Oligocene basaltic rocks were erupted at irregular intervals, due to Alpine collision. This combination resulted in gradual uplift of the area. The stasis of basaltic products contributed to the growth of carbonate platform called “Lessini Shelf” (Bosellini, 1989).

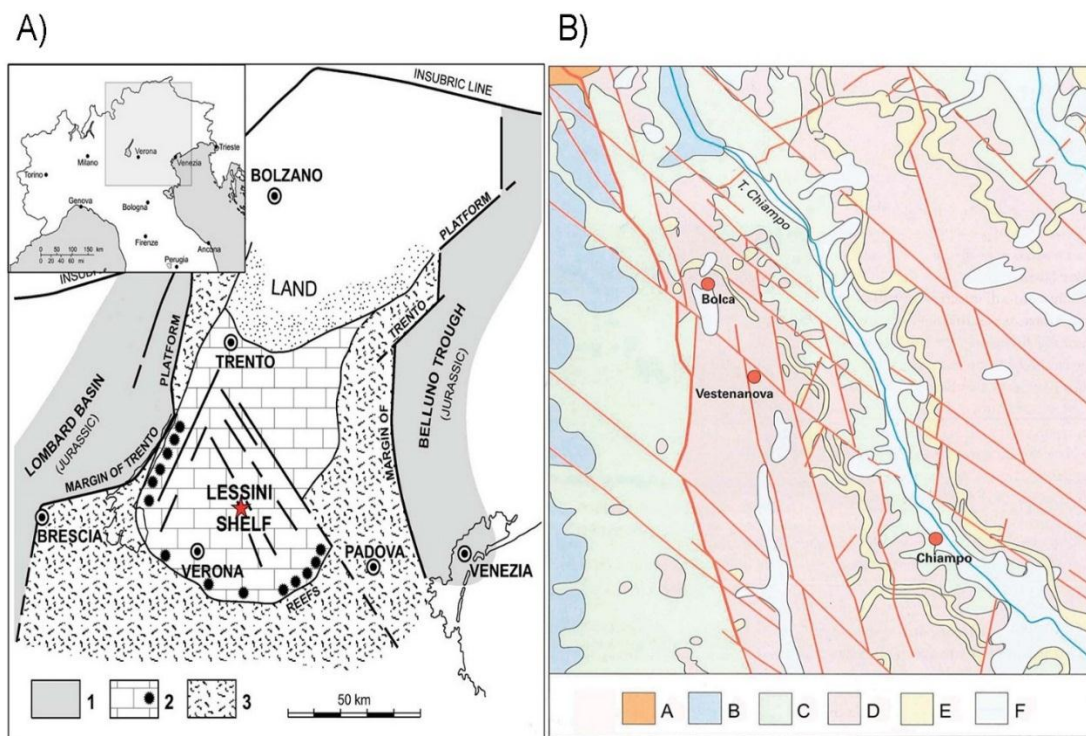


Figure 1: A) Paleogeographic reconstruction of the Lessini Shelf during Paleogene (after Papazzoni et al., 2014). The locality of Bolca is indicated by the red star. Legend: 1) deep - water sediments of Jurassic - Paleogene basins; 2) Paleogene shallow water limestones and reefs (asterisks); 3) Paleogene deep – water sediments of Jurassic Trento Platform. B) Simplified geological map of Bolca area (after Papazzoni et al., 2014). Legend: A, Triassic dolostones; B, Jurassic limestones; C, Cretaceous limestones; D, Paleocene - Eocene volcanic rocks; E, Eocene limestones; F) Quaternary deposits.

Limestones and bioclastic beds dated to lower – middle Eocene are improperly included in the “Calcarei Nummulitici” unit (Bosellini et al., 1967). The Castelvevo Fault runs NNW – SSE on

the right side of Alpone River Valley (**Fig. 1B**). The activity of this fault during the Paleocene – Middle Eocene was crucial for the developing of carbonates platforms. The fault interrupted the geographic distribution of basalts by separating a western area, with thin and widespread volcanic deposits, from an eastern one, dominated by volcanic rocks prevail. The increase of subsidence of the eastern area, created by the fault activity, promoted the formation of carbonate platforms intercalated between volcanic. This tectonic system is called “Alpone – Agno half – graben” (Barbieri et al., 1982, 1991). The tectonic stresses both generated a brittle response and tilted the volcanic and sedimentary blocks in a domino – style deformation (Barbieri & Zampieri, 1992; Zampieri, 1992, 1995), or made them collapse as olistoliths (i.e. Pesciara outcrop; Trevisani, 2015). Six volcanic stages, separated by carbonate deposits, have been recognized after a long period of open water – sedimentation, belonging to Scaglia Rossa Formation (Barbieri, 1972; Barbieri et al., 1982, 1991).

Historically, five distinct, fossiliferous sites are identified in Bolca area: Spilecco Hill, Pesciara; Monte Postale; Monte Purga e Vegroni (**Fig. 2**). Specimens discussed in this thesis were collected from Pesciara and Monte Postale sites. Therefore, the stratigraphic, environmental and paleoecologic analysis are focused on Pesciara – Monte Postale settings: The Pesciara outcrop and the top of Monte Postale succession represent the Lower Cuisian carbonate platform, established between the third and the fourth volcanic phase (Barbieri et al., 1991; Trevisani, 2015).

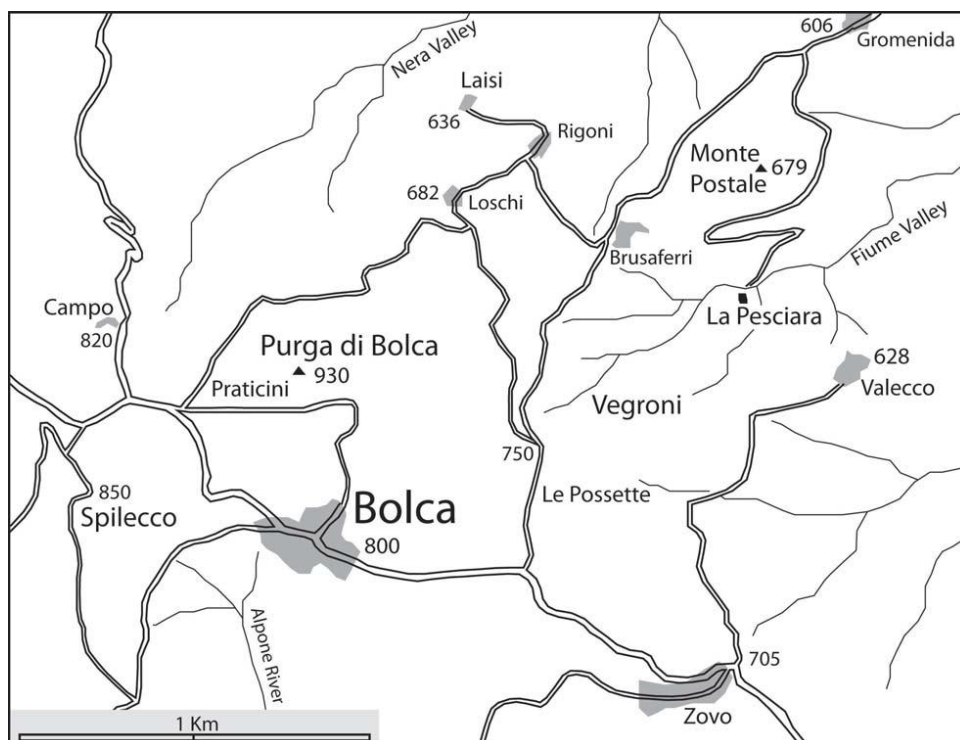


Figure 2: Location map of Bolca area (after Papazzoni et al., 2014).

2.2: Stratigraphic Setting of Pesciara and Monte Postale successions

Pesciara: This fossiliferous site is represented by a single exposure of calcareous beds about 20 m thick (**Fig. 3**), plunged to the South – East with a highly inclination range (30 – 70°), surrounded by volcanic rocks. The site is located on the right side of Val del Fiume, about 2 km to the North – East of Bolca. After early studies by Massari and Sorbini (1975), recent papers significantly increased our knowledge on the stratigraphy of the site (Trevisani et al., 2005; Papazzoni & Trevisani, 2006, Schwark et al., 2009). The main succession consists in:

- a) Metric units of grey fine – grained limestones, organized in decimeter – thick beds. The beds are laminated and separated by thin clayey levels. These levels are commonly known as “*Strati a Pesci e Piante*” (fishes and plants – bearing beds);
- b) coarse – grained biocalcarenite – biocalcirudite with molluscs and foraminifera, common known as “*Strati Sterili*” (barren beds) in regard of fishes and plants.

The vast majority of vertebrates and plants remains have been collected from five discrete limestone layers each measuring approximately 1m in thickness; in ascending order, such beds have been referred to as L1, L2, L3, L4 and L5 (**Fig. 4A**; Papazzoni & Trevisani, 2006). The L5 level is no longer exposed as it was entirely caved during the last several decades, therefore its thickness has been inferred based on stratigraphic reconstructions. Fossil remains have been quarried primarily from L1, L2 and L5 (Papazzoni & Trevisani, 2006). The L1 level is 1,6 m thick, made up by decimetric – laminated micritic layers intercalated with centimetric silty clays. This level is better known as “*Cava Bassa*” (lower quarry; Sorbini, 1967). This layer also produces yellow – green amber with maximum size of few centimeters. (Trevisani et al., 2005). Between L1 and L2 levels, there are ~3,5 m thick of ruditic biocalcarenites with nodular texture and rounded clasts. The base of this layer is erosional with an irregular conglomerate bed (maximum thickness 30 cm) and brecciated lithoclasts, often silicified. This level includes reworked foraminifera belonging to SBZ 10 biozone (“Shallow Benthic Zone”, biostratigraphic unit based on *Alveolina oblonga* foraminifer assemblages, Lower Cuisian; Serra – Kiel et al., 1998; Papazzoni & Trevisani, 2006). The biocalcarenites are formed by full – rich of miliolids peloidal grainstone and wackestone – packstone with alveolinids, corals, plant fragments, algae and bryozoans (Papazzoni & Trevisani, 2006). The level L2 consists in decimetric beds of laminated micrite with interbedded millimetric or centimetric silty clay levels. It is commonly known as “*Cava Alta*” (higher quarry; Sorbini, 1967). The top of L2 has been eroded by two horizons of molluscs – rich coarse biocalcarenites, variable in thickness (“lumachelle layers” according to Papazzoni & Trevisani, 2006; **Fig. 4A**). These strata include miliolids, corals, alveolinids (sometimes oxidized), green algae, echinoids. On top of these layers, there are laminated limestones with a thickness up to 25 cm; the top of this interval is characterized by an erosional contact. A wackestones of 60 cm – thick with peloids, miliolids and alveolinids.

The L3 level is 1 m thick and includes nine laminated micritic beds interbedded with coarser layers less than 1 cm thick (mudstone – wackestone). The reduction of laminae, compared with L1 and L2 laminated layers, is due to a slightly abundance of fine – grained bioclasts, rich of miliolids and other small benthic foraminifers, that interrupt the surfaces of laminae. In addition, the laminae are colored and undulated. Near the tunnel entrance, 0,5 m of the section is covered and follow 2,35 m of non – laminated limestones – wackestones beds with ostracods, intercalated by centimetric bioclast layers. The latter turn into thicker and more frequent upwards. The L4 level is affected by a 3 m – thick slump, interpreted as a syndepositional folding. On the top, the slump is cut by a massive 1,8 m – thick biocalcarenitic

level and its base is rich in molluscs, peloids, intraclasts and alveolinids. The biocalcarene is gradated (packstone to wackestone according to Papazzoni & Trevisani, 2006). The section ends with a packstone – wackestone of 1 m thick with peloids, miliolids and plant fragments. The top of the outcrop is made up by non – laminated mudstones with plant remains and rare foraminifers. This level is referred to L5. A collapsed boulder in the lowermost part of the Pesciara outcrop probably represents the cap of the L5. Lithological analysis of collected samples by this olistolith are interpreted as packstones with abundant nummulites, red algae and both benthic and pelagic foraminifera. Inside the section, four distinct microfacies are recognized based on lithology, fossil content, geometry of sedimentary structures and silicification of clasts (**Fig. 4B**). Roghi et al. (2015) surveyed with geoelectric methods the Pesciara site around the touristic tunnel to implement the stratigraphic knowledge of the site and establish the best area to core. The core is 40 meters length and reveal stratigraphic continuity from basaltic rocks (-40 - -35 m) to the known recent levels, suggesting high potential of exploitation of the added calcareous lithologies discovered.



Figure 3: Panoramic view of the Pesciara site (after Papazzoni et al., 2014)

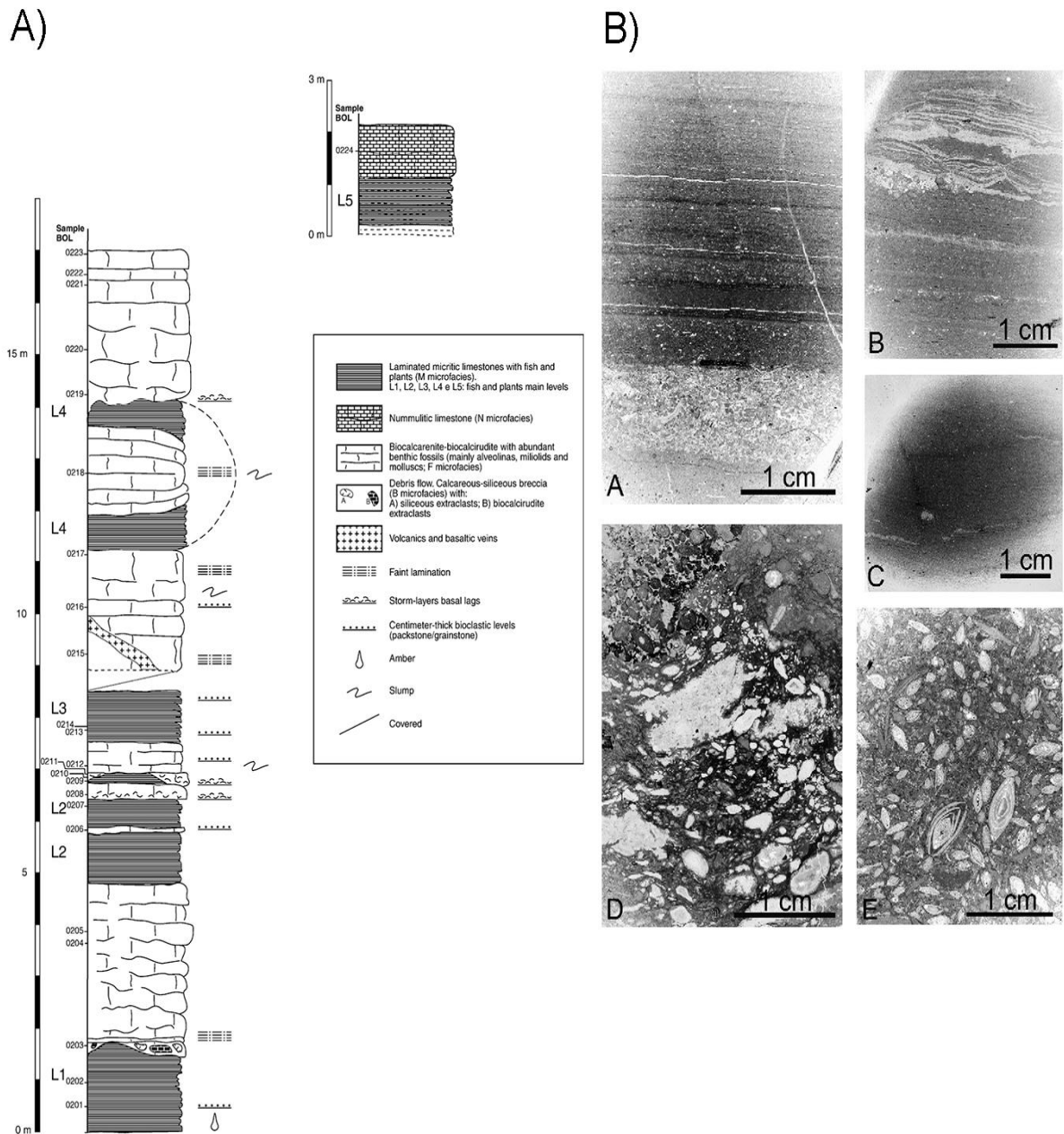


Figure 4: A) Stratigraphic section of the Pesciara succession. L5 has been inferred (after Papazzoni & Trevisani, 2006). B) Thin section of rock samples from Pesciara succession (after Papazzoni & Trevisani, 2006); A: F microfacies in the lower part and M1 microfacies in the upper part. The F microfacies consists in biocalcarenite – biocalcirudite stones with abundant benthic fossils. The M1 is characterized by weakly laminated mudstones with black laminae; B: M2 microfacies. Micritic, laminated mudstones whit white laminae; C: M3 microfacies. Micritic and massive limestones; D: B microfacies. Calcareous – siliceous breccia with extraclasts; it is found only in the lower part of the section and the foraminifera assemblage suggests an older biozone (SBZ 10); E: N microfacies. Biocalcarenite – biocalcirudite with abundant nummulites and assilinas. It is found only on the top of the section.

Monte Postale: It is located few meters north to Pesciara quarry. The mountain is cut by the Monte Postale Fault (Munier – Chalmas, 1891; Barbieri & Medizza, 1969; Trevisani, 2015) that is sub – parallel to Castelvero Fault, but locally is affected by a change of direction. Trevisani (2015) proposed a stratigraphic section divided in two sections by the fault (**Fig. 5**):

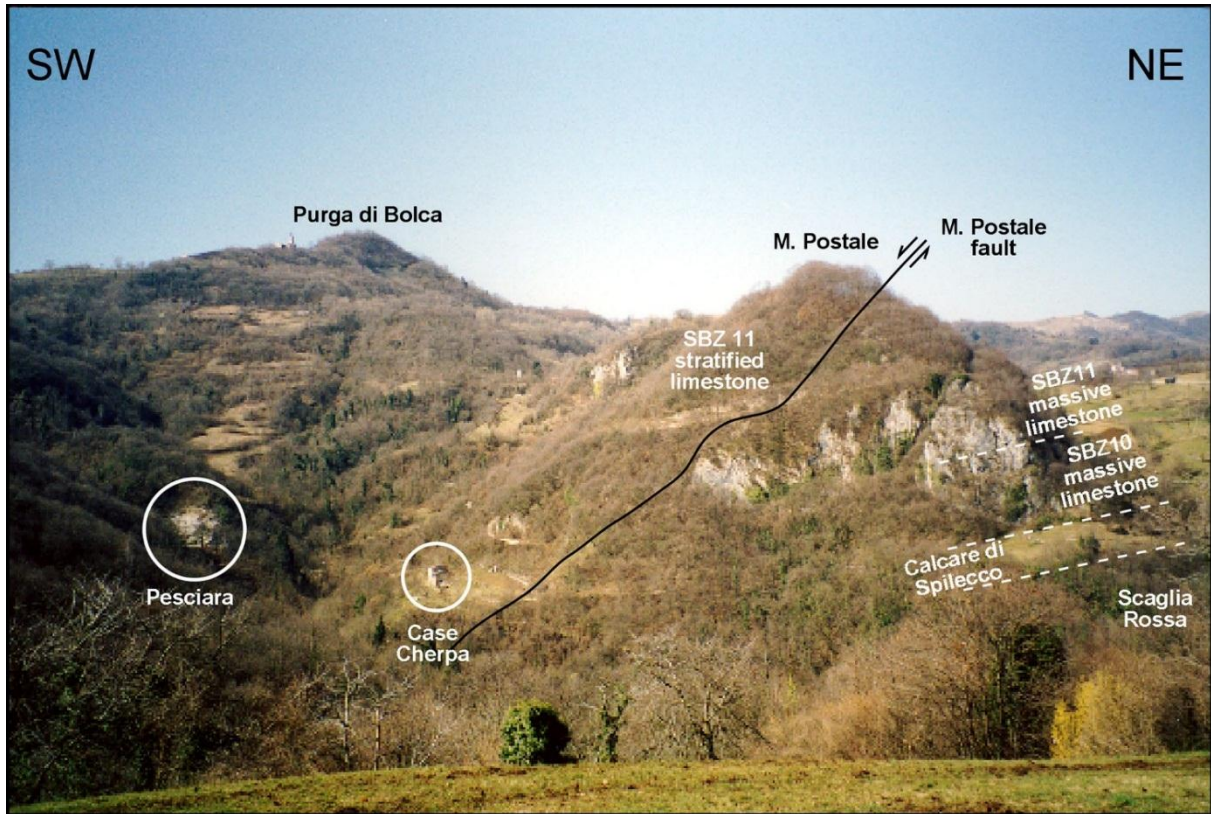


Figure 5: Panoramic view of Monte Postale from south - east slope (after Trevisani, 2015)

- a) *Monte Postale 1 section* (**Fig. 6A**). This section is ~70 m thick and includes, from bottom to top, the “Scaglia Rossa Formation” and Ilerdian limestones referred to the informal “Spilecciano” unit (covered by vegetation). In this section the Cuisian platform of Lower Eocene is established. On Ilerdian covered limestones, emerges a 4 m – thick level of massive Cuisian limestones. These are referred as packstones rich in nummulitids, discocyclinids, red algae, miliolids, peloids, and echinoderms. The occurrence of *Nummulites partichi* suggests chronostratigraphic correlations to the SBZ 10 biozone (Lower Cuisian; Serra – Kiel et al., 1998; Trevisani, 2015). There are 52 m thick of massive to weakly bedded limestones. These levels consist in wackestone – packstones including ortofragminids, nummulitids, miliolids, encrusting foraminifera, bryozoans and red algae, together with corals and molluscs. On the top, the assemblages of *Alveolina cremae*, *A. aff. croatica*, *A. decastroi*, *A. distefanoi*, *A. levantina*, *A. rugosa* are referable as the SBZ 11 (Middle/Late Cuisian; Trevisani, 2015).
- b) *Monte Postale 2 section* (**Fig. 6B**). Above the Monte Postale Fault, the section herein is ~90 m – thick and represents the Cuisian platform. It starts from Case Cherpa on the south slope of the mountain. The alveolinids assemblages are related to Monte Postale 1 and show evidences of transportation and size sorting. The succession is characterized by three different lithofacies:

- *Lithofacies 1: massive bioclastic packstone.* It is made up by massive limestones in which occur nodular structures (“mammellonar” according to Trevisani, 1994) and volcanoclastics debris clasts with a diameter up to 10 cm on the bottom of the section.
- *Lithofacies 2: stratified bioclastic packstone.* This facies is well – bedded bioclastic packstone in that occur cross lamination separated by marl layers. The thickness has a range between 10 to 50 cm.
- *Lithofacies 3: laminated lime mudstone.* It corresponds to dark lime mudstones of 10 – 20 m – thick, regularly alternated by millimetric pale and dark laminae and non – laminated paler mudstones. According to geochemical analysis leaded by Schwark et al. (2009), the darker texture of laminae is probably due to microbial mats of diatoms and cyanobacteria. This feature is also reliable to darker laminae of Pesciara limestones.

The controlled excavation between 1999 and 2004 in the upper part of Monte Postale 2 section (*Lithofacies 3*) reveals stratigraphic continuity and correlations whit L1 laminated limestone levels of Pesciara section, based on lithological, chronological, fossil and organic contents affinities. Therefore, the two fossiliferous sites are considered as part of a unique and complex system (Papazzoni & Trevisani, 2006; Trevisani, 2015; Vescogni et al., 2016; Papazzoni et al., 2017). In the next sections are described the paleo – biostratigraphic correlations and how the environmental setting promoted the optimal conditions for high degree of preservation.

2.3: Age of the fossil – fish *Lagerstätte*

Hottinger (1960) put the age of Pesciara site to Early Eocene based of foraminifera assemblage. Medizza (1975) estimated the age of the fossiliferous site to the early – middle Eocene transition according the analysis of a single sample of calcareous nannoplankton collected by himself. This sample was assigned to *Discoaster sublodoensis* Zone (NP 14; NP stands for “Calcareous nannoplankton” zones according to Martini, 1971) and the interpretation strongly disagreed with Hottinger’s proposal. He solved these conflicting results suggesting that alveolinids assemblages are clearly reworked. Massari & Sorbini (1975) remarked the non – reliability of alveolinids data. According to Papazzoni & Trevisani (2002, 2006; Trevisani et al., 2005), the alveolinids occurred only in bioclastic layers, are quite well preserved and present a low degree of abrasion, suggesting a nearly – contemporaneous transport from a related slightly shallower area. Moreover, the taxa suggest a time – consistent assemblage referred to a single biozone. Therefore, the assemblage analyzed by Hottinger (1960) and inspected by Papazzoni & Trevisani (2002, 2006; *Alveolina cremae*, *Alveolina rugosa*, *Alveolina distefanoi*, and *Alveolina rutimeyeri*, *Alveolina ex gr. canavarii*, *A. cremae*, *A. aff. croatica*, *A. decastroi*, *A. distefanoi*, *A. levantina*, *A. cf. minuta*, *A. rugosa*, *Assilina spp.*, *Asterocyclina spp.*, *Discocyclina spp.*, *Idalina sp.*, *Nummulites pratti*, *N. prelucasi*, *N. cf. rotularius*, *Orbitoclypeus sp.*, and *Orbitolites spp.*) indicates the *A. dainellii* Zone, or SBZ 11 biozone (Middle Cuisian; Serra-Kiel et al., 1998; Trevisani et al., 2005). A unique single sample collected on the top of L1 (*B microfacies*) includes reworked alveolinids referred to the *Alveolina oblonga* Zone (SBZ 10, Early Cuisian). According to Kapellos & Schaub (1973), Schaub (1981), and Serra-Kiel et al. (1998), the SBZ11 biozone is correlated to the whole of NP13 (“NP” stands for nannoplankton biozone) and the lowest part of NP14 (Beccaro et al. 2001; Papazzoni & Trevisani, 2006; Trevisani et al., 2005) and the planktonic foraminifera assemblage belong to *Morozovella aragonensis* biozone (P8; “P” stands for planktonic biozone), dated to Middle Cuisian. Finally, the correlation according to foraminifers (both planktonic and benthic specimens) and calcareous nannoplankton found suggest that the age of Pesciara is restricted to a narrow interval between the top of SBZ11, the base of NP14 and P9 zone that correspond to 49 – 50 Ma (**Fig. 7A**).

The age of Monte Postale is slightly discussed. However, it is easy reliable to the Pesciara biostratigraphic setting. Scheibner & Speijer (2008) and Höntzsch et al. (2013) elaborated a divisional scheme of the main climate events for the Late Paleocene – Lower Eocene Tethyan carbonate platforms. According to this interpretation, the Monte Postale – Pesciara system is well integrated in Stage III, more exactly after the Early Eocene climatum optimum (EECO, the fourth hyperthermal event at Paleocene – Eocene boundary, PETM; Scheibner & Speijer, 2008; Höntzsch et al., 2013; Whidden & Jones, 2012; Trevisani, 2015) that is the stage when larger benthic foraminifers (LBT), to the detriment of the relative abundance of corals in the deposits, became the predominant biota in Tethyan carbonate platforms during the Lower Eocene. According to the correlation between the climate events, benthic and planktic foraminifera and calcareous nannoplankton, the age of the Monte Postale – Pesciara system is about 49 Ma (Trevisani, 2015; **Fig. 7B**). Vescogni et al. (2016) and Papazzoni et al. (2017) attributed the age of Monte Postale depositional system in a restricted range between 50,5 – 48,96 Ma (**Fig. 7C**) The latter authors improved the biostratigraphy correlation with the description of the first assemblage of calcareous nannoplankton collected on the Monte Postale succession. The correlation is based on: the abundance of *Alveolina cremae* and *A. decastroi* (SBZ 11 according to Serra – Kiel et al., 1998); calcareous nannoplankton found that marked the CNE 5 biozone of Agnini et al. (2014; it corresponds to NP13 according to Martini, 1971; “CNE” stands for Eocene calcareous nannofossil according to Agnini et al., 2014). The assemblage could be extended until the bottom of CNE 6 (or NP14 according to Martini, 1971).

The Monte Postale succession, according to the assemblages, is associated within the end of Early Eocene Climatic Optimum event (EECO, ~49 – 53 Ma according to Luciani et al., 2016), not over as proposed by Trevisani (2015). However, all the authors agreed that the Pesciara – Monte Postale system is aged to Middle Cuisian (around 50 – 49 Ma). Sediments from Pesciara succession are coeval/sub – sequent to those of Monte Postale. The Middle Cuisian carbonate platform of Bolca area build up during the late phase or nearby the end of the Early Eocene Climatic Optimum.

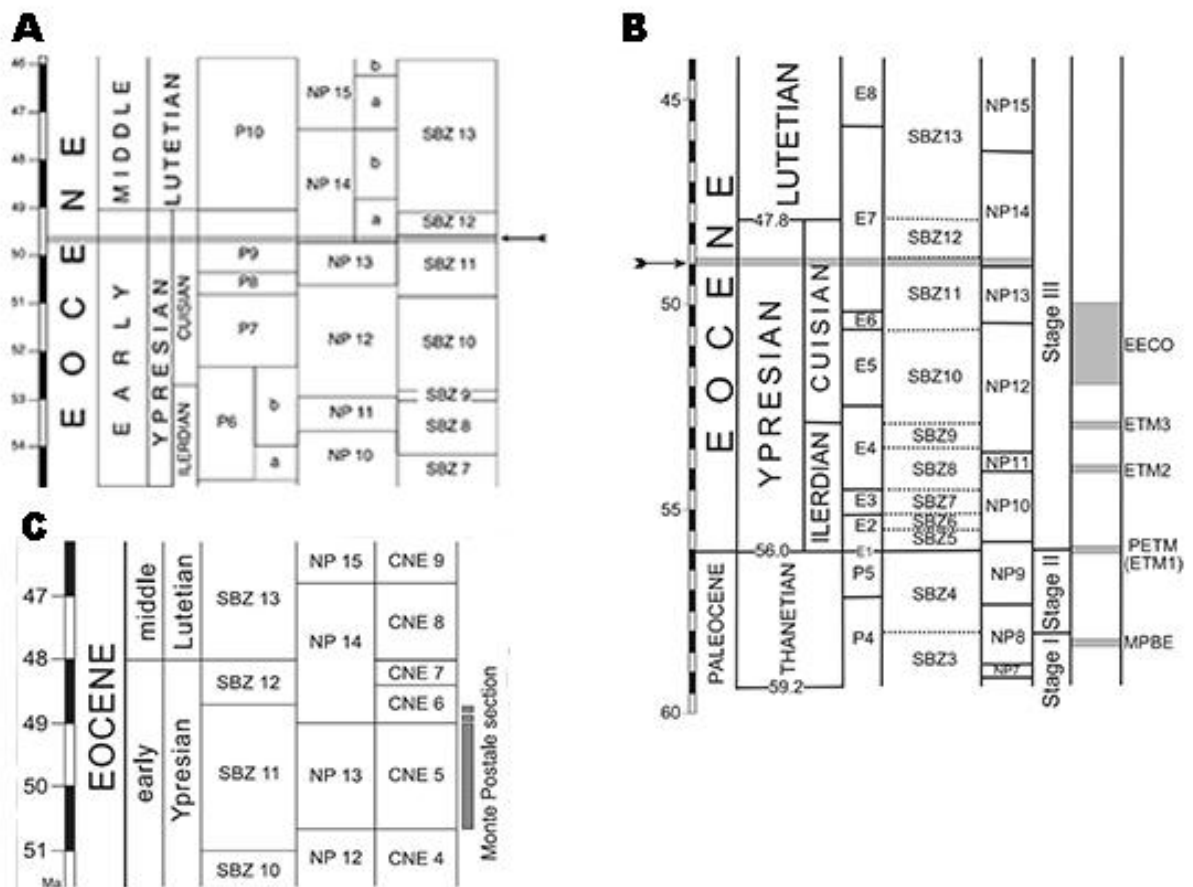


Figure 7: Correlations between benthic foraminifera and calcareous nannoplankton fauna assemblages. A) Age range of Pesciara (after Papazzoni & Trevisani, 2006); B) Age range of Monte Postale proposed by Trevisani, 2015; C) Age range proposed by Papazzoni et al., 2017

2.4: Paleoenvironmental setting

The Pesciara limestones are interpreted as sediments deposited in anoxic or poor oxygenated conditions and absence of bioturbator organisms (Schwark et al., 2009). These features are even marked by the presence of pyrite and bituminous material (Trevisani et al., 2005; Schwark et al., 2009), despite the overall light color seems inconsistent for an organic matter accumulation. The lithological and paleoecological analysis conducted on Pesciara site during the last decades give a hint on lagoonal depositional model. These evidences are confirmed by the interpretation of Papazzoni & Trevisani (2006), including relative sea – level changes and oxygen – salinity seasonal variabilities (**Fig. 8**). In principle, during a relative lowstand the buildup had protected the lagoon with more efficiency despite relative sea – level highstand periods; a relative higher water column decreased the sheltered skill of the rim, frequently exhibited by dismantlement. Therefore, the clasts and extraclasts dismembered were transported inside the lagoon and resedimented within limestones. The hypothetical seasonal conditions, combined with relative eustatic changes, implement the setting. During wet conditions occurred in relative highstand phases, the estuarine circulation prevailed, characterized by low – salinity, superficial and seaward currents rich in nutrients. The latter increased primary productivity and supported the accumulation of organic matter on the bottom. The decay of organic matter consumed the oxygen, increasing the redox boundary and anoxic condition on the bottom. On the contrary, an anti – estuarine circulation imposed during highstand with dry conditions. The high evaporation and the poor river influxes increased the salinity of water mass that sinking seaward. Therefore, the organic matter had no possibility to accumulate abundantly on the bottom, but rather than that had to be transported seaward. Moreover, the oxygen contents increased, and the salinity was almost homogeneous along the water column caused by occurring water mixing. The seasonal changes during relative lowstand periods were like to relative highstand phases, but the lagoon was better separated by open sea and prevailed permanent stagnated conditions; the oxygenating episodes were very short and limited to strong storms. These features increased the potential of preservation.

Palynologic analysis (Trevisani et al., 2005) documented the occurrence of both terrestrial (several Angiosperms, Gymnosperms, Briophyte, Pteridophyte) and shallow marine palynomorphs (mainly dinoflagellates). The abundance of continental plants and the presence of several amber and freshwater insects (dragonflies) in limestones are referred to a fluvial system close to lagoon – buildup setting. Schwark et al. (2009) conducted geochemical analysis on Pesciara limestone (L1, L2 and L3) and coarse – grained biocalcarenite – biocalcirudite samples. The organic carbon contents (TOC) of limestones is low (range between 0.16 and 0.55%), excepted for one sample collected in L1 (M1 microfacies) the value exceeds 8%TOC. According to TOC and Rock Eval data, bitumen contents indicated low mature kerogen belonging to type II, attributed to marine origin and a mix of terrigenous material. The latter is mainly given by plants fragments entrapped in limestones, probably transported by aeolian processes into the basin. The molecular biomarkers indicated that the most marine organic production is attributed to diatoms, despite their relative abundance is low. The data, together to presence of amber and palynology analysis, confirmed the paleoenvironmental interpretation.

According to Trevisani (2015) interpretation of Monte Postale 2 section, the bioclasts of *lithofacies 1* are absent in Pesciara section, representing probably the organic protection (bioclastic buildup) that allowed the development of the Pesciara lagoon (laminated limestones). The nodular structures and volcanic clasts found on lower part suggest a back –

reef position (i.e. washover fans). The *lithofacies 3* is represented by an area closer to the organic buildup than the equivalent facies of Pesciara outcrop, suggested by more fragmented clasts reduced in thickness due to a more intensive storm reworking. The occurrence of rare centimetric amber nodules and the abundance of plant remains (TOC 1,5 %) confirms the correlation. Even preliminary geochemical analysis of the kerogen content supports the interpretations of the entire setting (Trevisani et al., 2005), confirming that the carbonate buildup was the main protection of the Pesciara lagoon (**Fig. 9**). The abundance of several pelagic fish families (e.g. Scombridae, Paleorhynchidae, Euzaphlegidae) suggests that the boundary of the deep – water basin was close to the buildup system. Nevertheless, no lithological data confirm lateral stratigraphic continuity (Trevisani, 2015).

Vescogni et al. (2016) proposed an additional interpretation of Monte Postale based on fossil content. According to the relative abundance of coralgal – alveolinids – nummulites assemblages and the lateral continuity of the outcrops studied, the authors defined a detailed paleoenvironmental reconstruction of the Monte Postale – Pesciara system, based on eight distinct facies, that support the setting proposed by Trevisani (2015). They recognized:

1) *The coralgal rim*. The associated facies includes the massive – weakly stratified wackestones (coralgal boundstones, polygenic bindstone, *Alveolina* grainstone and coralgal rudestone). It is characterized by the presence of scleractian corals (66% of the overall lithology), coralline red algae, encrusting foraminifera, alveolinids, miliolids, peyssonelliacean algae, solenoporacean algae, dasycladacean algae. According to the ecological features of the assemblages, the coralgal buildup developed within the euphotic zone. The growth of the coral rim was affected by different hydrodynamic conditions; several intervals of encrusting coralgal biota rim have been found in the extremely compacted – polygenic bindstones (bioclasts <10% of the overall lithology), suggesting the growth of coral rim during high hydrodynamic processes inferred by waves and tides. The branched corals, dasycladacean algae and mud – supported bioclasts accumulation indicate the development of the coral reef during low energy conditions.

2) *Fore reef*. It includes weakly stratified limestone (coralgal rudestone, *Alveolina* – *Nummulites* limestones). The weakly stratification of beds, the abundance reduced of bio – builder specimens and the presence of *Nummulites* marks a deeper, open – marine depositional setting.

3) *Lagoon deposits*. It includes massive to bedded facies (laminated wackestone, non – laminated wackestone and graded *Alveolina* grainstone). The laminated wackestone correspond to the fishes – plants bearing beds. The non – laminated wackestone is composed by only micrite, despite the graded *Alveolina* grainstone includes alveolinids, miliolids and fragments and scleractinian corals.

To complete the setting, they added relative - rapid transgressive periods between the relative lowstand – highstand phases. This is marked by the presence of non – laminated wackestone facies because the massive texture was given probably by an increase of sea – water energy during a relative sea level rise.

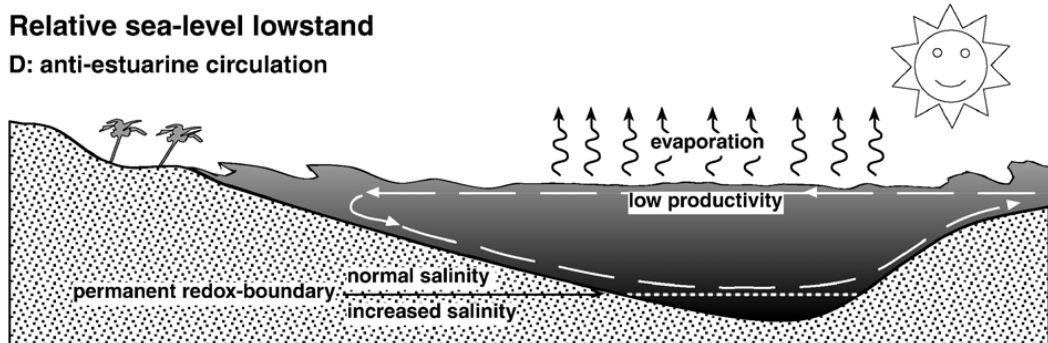
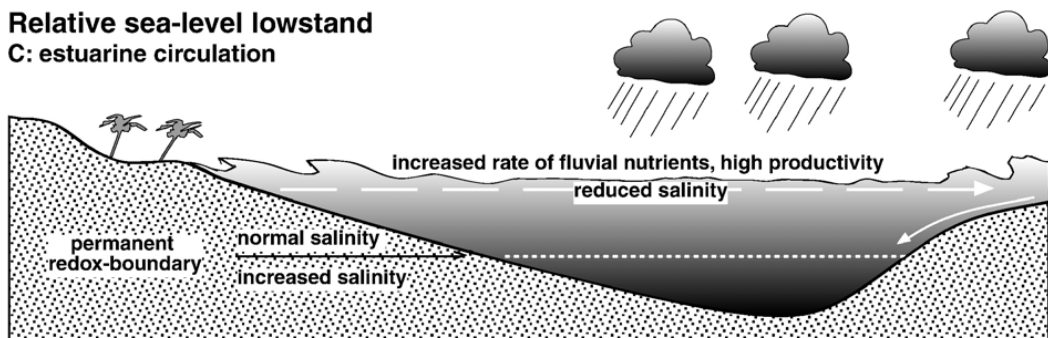
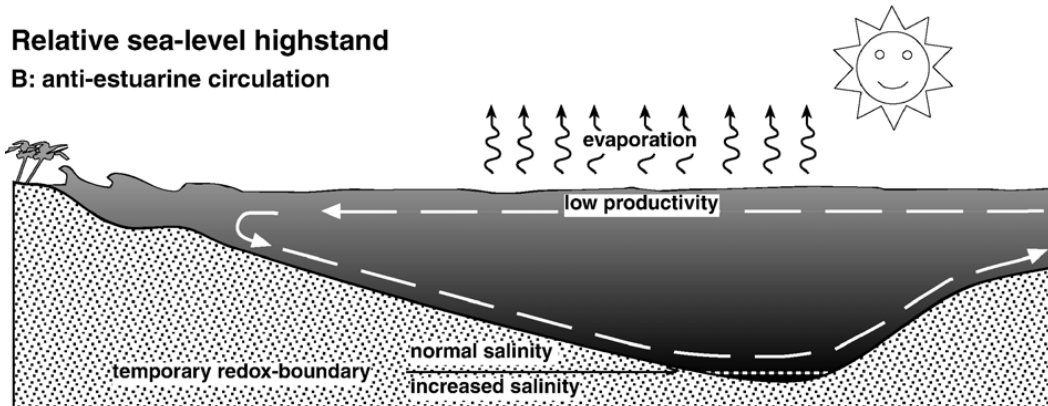
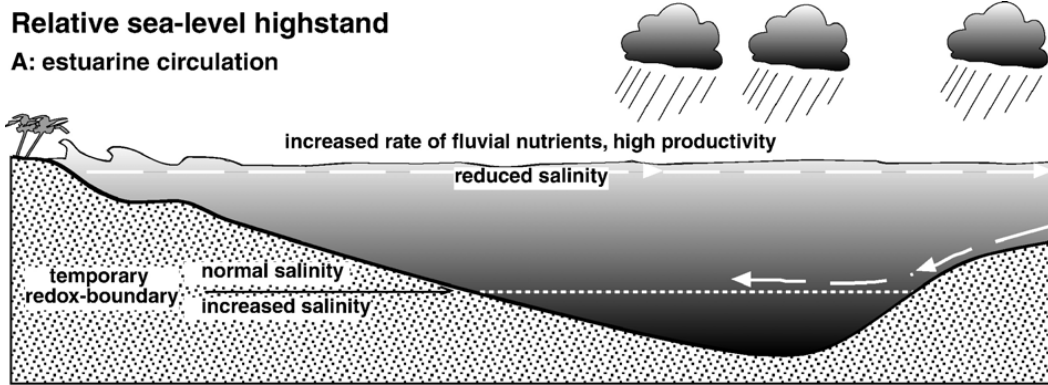


Figure 8: Scheme of depositional model of the Pesciara site (after Papazzoni & Trevisani, 2006). During relative highstand phases, water mixing occurred. The best conditions for high potential of preservation corresponds to relative sea – level lowstand. The grey tone of the water indicates, from dark to light, decreasing salinity.

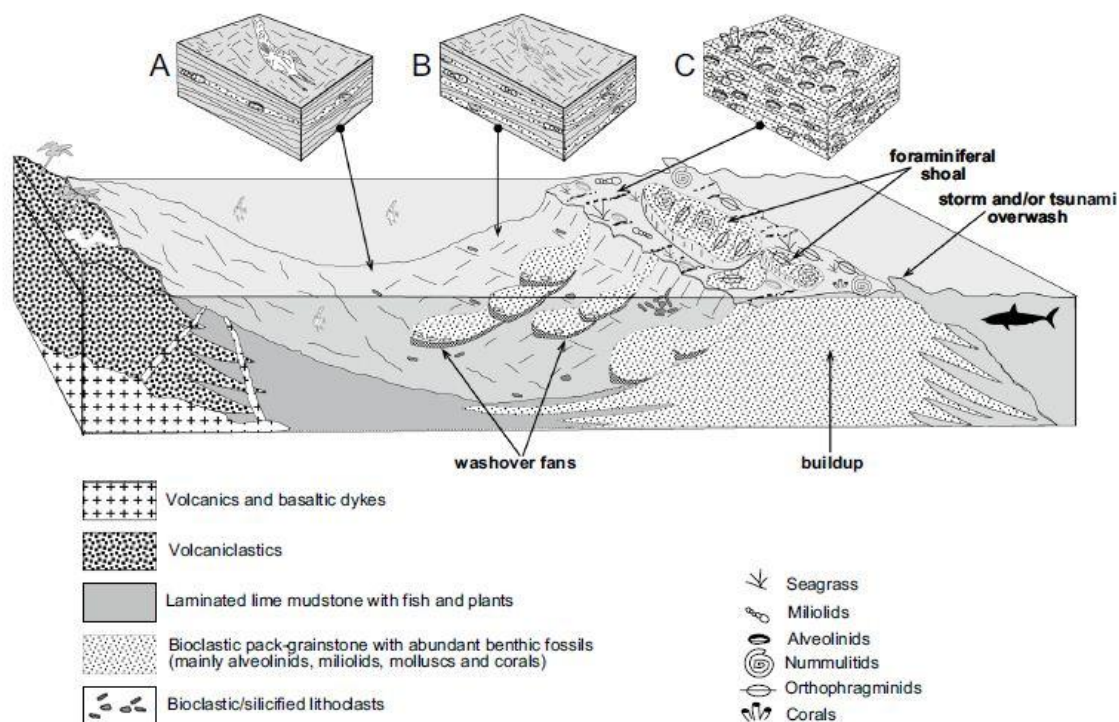


Figure 9: Depositional model of Pesciara - Monte Postale system (after Trevisani, 2015): A) ideal cross section of the Pesciara type-succession, with prevalent laminated mudstone, well-preserved fossils and rare bioclastic intervals; B) Ideal cross section of Monte Postale type-succession, with common bioclastic levels and thinner, laminated, and discontinuous mudstone intervals, with fossils commonly poorly preserved; C) Ideal cross section of the buildup type-succession, with poorly stratified bioclastic pack-grain-rudstone, rich in macro-foraminifera and miliolid.

Although the large descriptions occurred by different authors in the past, nobody has yet defined the proper fossiliferous locality of fossil specimens (i.e. Pesciara or Monte Postale). Despite these important shortages, a list of several taphonomic and lithological features can correctly define the provenience of samples according to stratigraphic and paleoenvironmental settings:

- 1) *Organic content.* Usually, Pesciara limestones include organic residuals marked by darker spots. The Monte Postale limestones show a lower content of organic residuals.
- 2) *Occurrence of benthic molluscs and bioturbations.* Benthic organisms and bioturbations are rare in Pesciara limestones, whereas occur frequently in Monte Postale laminated mudstones (Cerato, 2011; Trevisani, 2015; Marammà et al., 2016).
- 3) *Taphonomic features.* Several taphonomic features mark the differences between the two sites. The *Completeness* of Pesciara is higher than the Monte Postale succession. Around the 80% of fishes are moderately high to excellently preserved, being characterized by low degree of disarticulation of bony components (or cartilaginous

component), fins and vertebral column; in Monte Postale succession, the degree of preservation is lower. Fishes from both sites show different degree of *tetany* (i.e. postmortem muscular contraction). The samples collected from Monte Postale are usually recognizable by concave distortions of vertebral column and higher degree of disarticulation of skeletal components/fin elements (Cerato, 2011; Trevisani, 2015; Marammà et al., 2016).

Chapter 3: Materials and methods

Institutional abbreviations:

BMNH, Natural History Museum, London, United Kingdom; **BPBM**, Bernice P. Bishop Museum, Honolulu, Hawaii; **CAS**, California Academy of Science, United States; **CSIRO**, Commonwealth Scientific and Industrial Research Organization, Hobart, Tasmania; **EGV/GUR**, Eocene Gujarat Vertebrates/Garhwal University/Rana. Department of Geology, HNB Garhwal University, Uttaranchal, Srinagal (Garhwal), India; **FEV/ R**, Fuller's Heart Vertebrate/Rana. Laboratory of Vertebrate Paleontology, Department of Geology, HNB Garhwal University, Uttaranchal, Srinagal (Garhwal), India; **LACM**, Los Angeles County Museum of Natural History, USA; **KNUM**, Department of Marine Living Resource, Kunsan National University, Korea; **MCSNV**, Museo Civico di Storia Naturale di Verona, Italy; **MGGC**, Museo Geologico Giovanni Capellini, Bologna, Italy; **MGP – PD**, Museo Geologico – Paleontologico dell'Università di Padova, Italy; **MNHN** Muséum national d'Histoire naturelle of Paris, France; **MSNPV** Museo di Storia Naturale dell'Università di Pavia, Italy; **MSR**, Yano et al., (2005) catalog number; **MYB**, Méra-el-Arech, Bassin des Ouled, Abdoun, Morocco; **MZB**, Museum Zoologicum Bogoriense, Indonesia; **NCIP**, Research Centre for Oceanography, Indonesian Institute of Sciences, Jakarta, Indonesia; **NMMB**, National Museum of Marine Biology, Pingtung, Taiwan; **NMNZ**, Museum of New Zealand Te Papa Tongarewa, Wellington, New Zealand; **S**, Geological – Paleontological collection of Universität Leipzig, Germany; **SU**, Stanford University (now housed in CAS); **UM – PRE**, vertebrate paleontology collections of the Paleontology Department, University of Montpellier, France; **USNM**, Smithsonian Institution National Museum of Natural History NMNH, Washington DC, United States; **WAM**, Western Australian Museum; **ZMB**, Zoologisches Museum, Humboldt Universität, Berlin, Germany; **ZHM**, Zoological Museum Hamburg, Germany.

Anatomical abbreviations:

External terminology: 1) Total length (TL); 2) Head length; 3) Trunk length; 4) Caudal Fin length; 5) Head – First Dorsal Fin length; 6) Head – Second Dorsal Fin length; 7) Head – Pelvic Fin length; 8) Head – Anal Fin length; 9) Head Caudal Fin length; 10) Basal Lobe length; 11) Apical Lobe length; 12a) First Dorsal base length; 12b) First Dorsal anterior edge; 12c) First Dorsal height length; 13a) Second Dorsal base length; 13b) Second Dorsal anterior edge; 13c) Second Dorsal height length; 14a) Pectoral Fin base length; 14b) Pectoral Fin anterior edge; 14c) Pectoral Fin height length; 15a) Pelvic Fin base length; 15b) Pelvic Fin anterior edge; 15c) Pelvic Fin height length; 16a) Anal Fin base length; 16b) Anal Fin anterior edge; 16c) Anal Fin height length; 17) First – Second Dorsal Fins length; 18) Second Dorsal – Caudal Fin length; 19) Pectoral – Pelvic Fins length; 20) Pelvic – Anal Fins length; 21) Anal – Caudal Fins length; 22) Apical Lobe – Caudal Tip length; 23) Basal – Apical Lobes length; 24) Total Vertebra; 25) Precaudal Vertebra; 26) Caudal Vertebra.

Tooth measurements: a) root height; b) crown height; c) root length; d) total height; e) mesial edge + main cusp length; f) mesial edge; g) main cusp length; h) distal edge length; i) main cusp width.

Scale terminology: CL = crown length; CT = crown thickness; CW = crown width; ms) micro – structures; p) peak; r) ridge; ri) ridge interspace; s) spine

This study introduces an historic and undescribed shark from Bolca housed at the Museo di Storia Naturale dell'Università di Pavia. The specimen, which include slab and counterslab, has been assigned the following inventory ID: MSNPV 17716 and 17717.

Both slabs have been restored using soft brushes and malleable silicone (CTS[®] silica 110) in order to remove dust accumulated over centuries on top of the specimens. As several patches of dermal denticles, centra, and teeth were covered by mortars, selected areas of both slabs were prepared in order to remove mortar and expose preserved tissues.

Both slabs have been observed and documented photographically under natural and black light.

Samples of dermal denticles were collected from the head region of MSNPV 17716 and from the distal – dorsal part of the trunk of 17717. Placoid scales were examined with an SEM (Tescan Mira3; Voltage = 20.0 kV) at the University of Pavia. Following methodologies discussed in Fanti et al. (2016), UV light allowed to accurately discriminate preserved tissues as well as to identify areas affected by different typologies of pigmented mortar glues and sustaining blocks, assembled for the preservation of specimen. Teeth (**Fig. 10**) are described using combined terminologies of Ebert & Stehmann (2013) and Adnet & Cappetta (2008), whereas root vascularization morphology follows Hermann et al. descriptions (1989, 1991). The dermal denticles terminology follows Dillon et al. (2017).

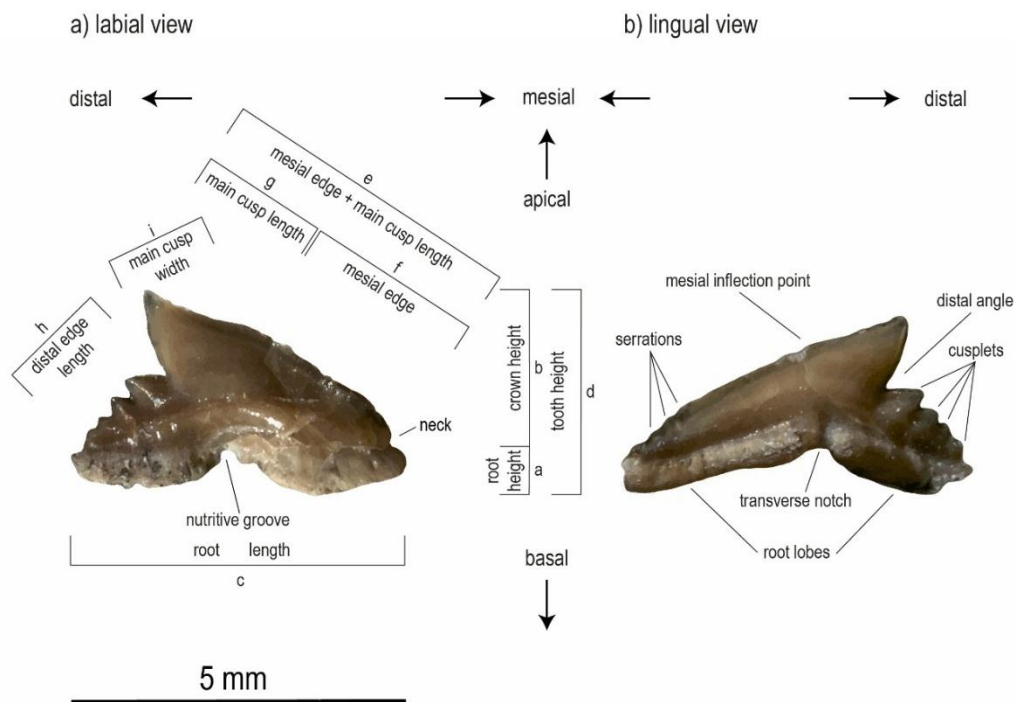


Figure 10: Terminology adopted of dental characters according to Adnet & Cappetta (2008) and Ebert & Stehmann (2013). The well – preserved teeth shown in the picture belong to MGGC 1976. The rectangles (a, b, c, d, e, f, g, h, I,) represents the measurements taken to each tooth.

The vertebral centra were counted and measured using a caliper, focusing on length variability along their axial arrangement. In this study, all measures will be expressed as percentage of total length (TL). Measurements of teeth and centra length were taken with a digital caliper to the nearest 0,5 mm for teeth and 1 mm for vertebra centra length. The measures of the single considered elements of the body were taken to the nearest 1 mm.

Bolca shark specimens (MGP – PD 8869 – 8870, 8871 – 8872, 26878; MGGC 1976; MCSNV VII.B.96 – 96, T.1124, T.311; **Fig. 11 - 12**) were analyzed with the same adopted criteria. The degree of preservation of the samples varies from medium to excellent and the outline of body is well preserved. Therefore, the exquisitely taphonomic conditions of the latter allowed to take longitudinal measurements of the body and their relative components (**Fig. 13**). The terminology is according to Cappetta (1975). Measurements from 17 to 23 were added to the morphometrical scheme of Cappetta (1975).

This approach was consistently applied also to embalmed specimen MSNPV PP119, referred to the IUCN – Red List vulnerable species *Galeorhinus galeus* (Walker et al., 2006; **Fig. 14**). In order to increase the morphometric dataset, several taxa has been included (*Apristuris exsanguis*, *A. nakayai*, *Atelomycterus erdmanni*, *Bythaelurus giddingsi*, *Carcharhinus coatesi*, *C. dussumeri*, *C. humani*, *C. sealei*, *C. sorrah*, *C. tjtjtjot*, *Cephaloscyllium fasciatum*, *C. hiscosellum*, *C. maculatum*, *C. pardelotum*, *C. sarawakensis*, *C. umbratile*, *Glyphis garricki*, *G. glyphis*, *Hemigaleus microstoma*, *Hemitriakis abdita*, *H. falcata*, *H. japonica*, *Mustelus ravidus*, *M. widodoi*, *Nasolamna velox*, *Paragaleus randalli*, *P. tengi*, *Parmaturus albimarginatus*, *P. albipenis*, *P. bigus*, *P. lanatus*, *P. profundicolus*, *Sphyrna lewini*; Compagno & Garrick, 1983; Compagno & Stevens, 1993; Compagno et al., 1996; Compagno, et al., 2008; Choy et al., 1998; Sato et al., 1999; Nakaya & Séret, 2000; White & Last, 2006; Séret & Last, 2007; Schaaf – Da Silva & Ebert, 2008; White & Ebert, 2008; Iglésias et al., 2012; McCosker et al., 2012; Weigmann, 2012; White & Harris, 2013; White & Weigmann, 2014; Famhi & White, 2015). The body sizes and ratios of the specimens reported in literature has reported with different methods and terminology. Therefore, the **Appendix A** depicts the conversions between the terminology adopted in this thesis and those reported in bibliography.

Similarly, teeth of both fossil and extant taxa have been included in the dataset (*Chaenogaleus macrostoma*, *Galeorhinus duchaussoisi*, *G. lousi*, *G. minor*, *Galeorhinus sp.*, *G. ypresiensis*, *Hemigaleus microstoma*, *Hemitriakis falcata*, *Pachygaleus lefevrei*, *Paragaleus pectoralis*, *Physogaleus latecuspidatus*, *P. secundus*, *Physogaleus sp.*, *P. tertius*; Cappetta, 1980; Compagno & Stevens, 1993; Hermann et al., 1991; Muller, 1999; Rana et al., 2004, 2006; Adnet & Cappetta, 2008). The dataset of body ratios, vertebral centra counts and measurements of Bolca well – preserved fossil individuals were performed to estimate size and body proportions of MSNPV 17716 – 17716.

The complete dataset for morphometric measurements and qualitative features of both teeth and external components were elaborated with the software Past 3.17. (Hammer et al., 2001), performing several Principal Components Analysis (PCA).

All images are edited with Adobe® Photoshop and Illustrator.

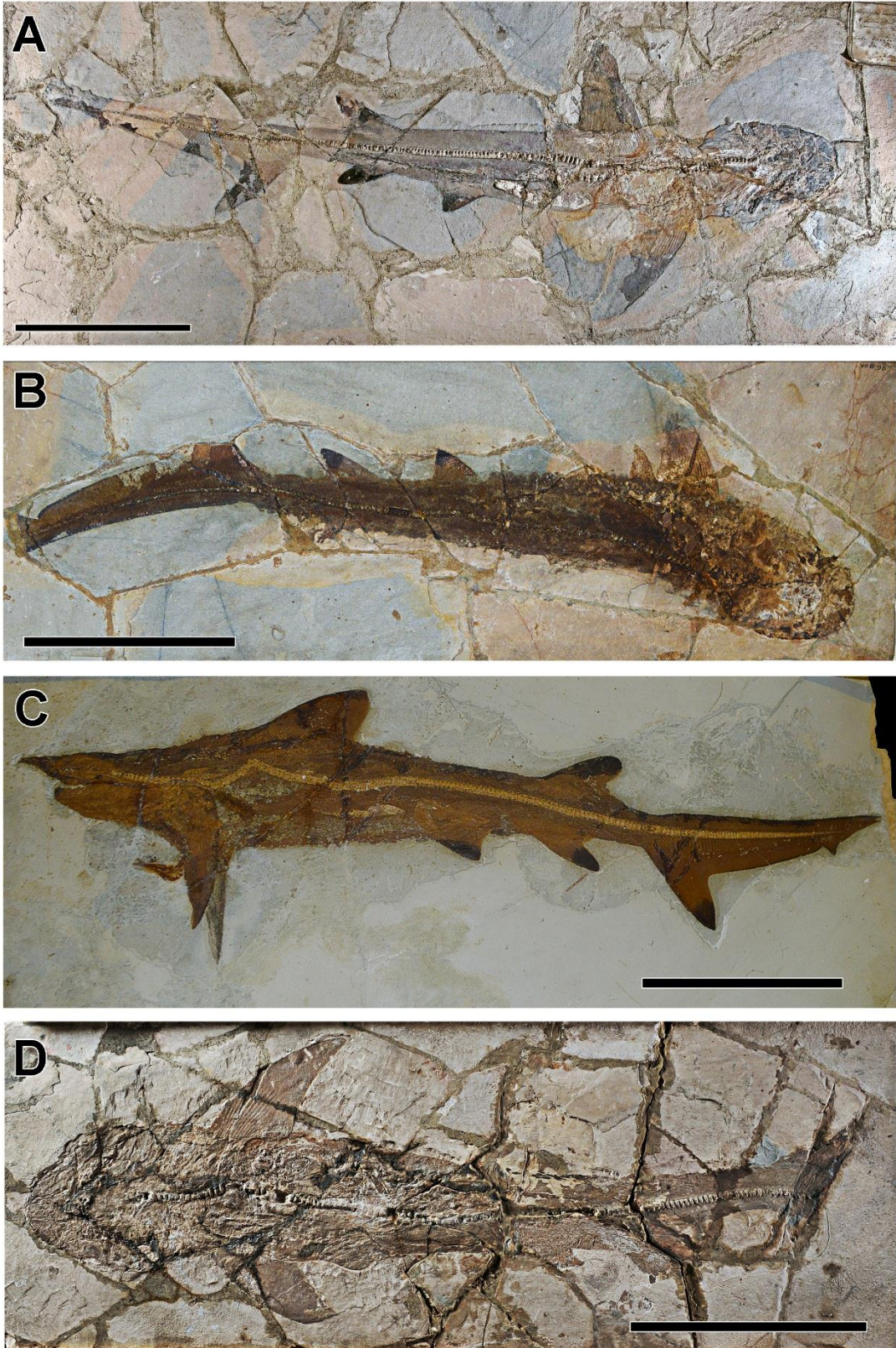


Figure 11: Bolca shark specimens: *Galeorhinus cuvieri*: A) MGGC 1976; B) MCSNV VII.B.96; C) MCSNV T.1124; D) MNHN.F.Bol.516 (holotype). Scale bar 20 cm

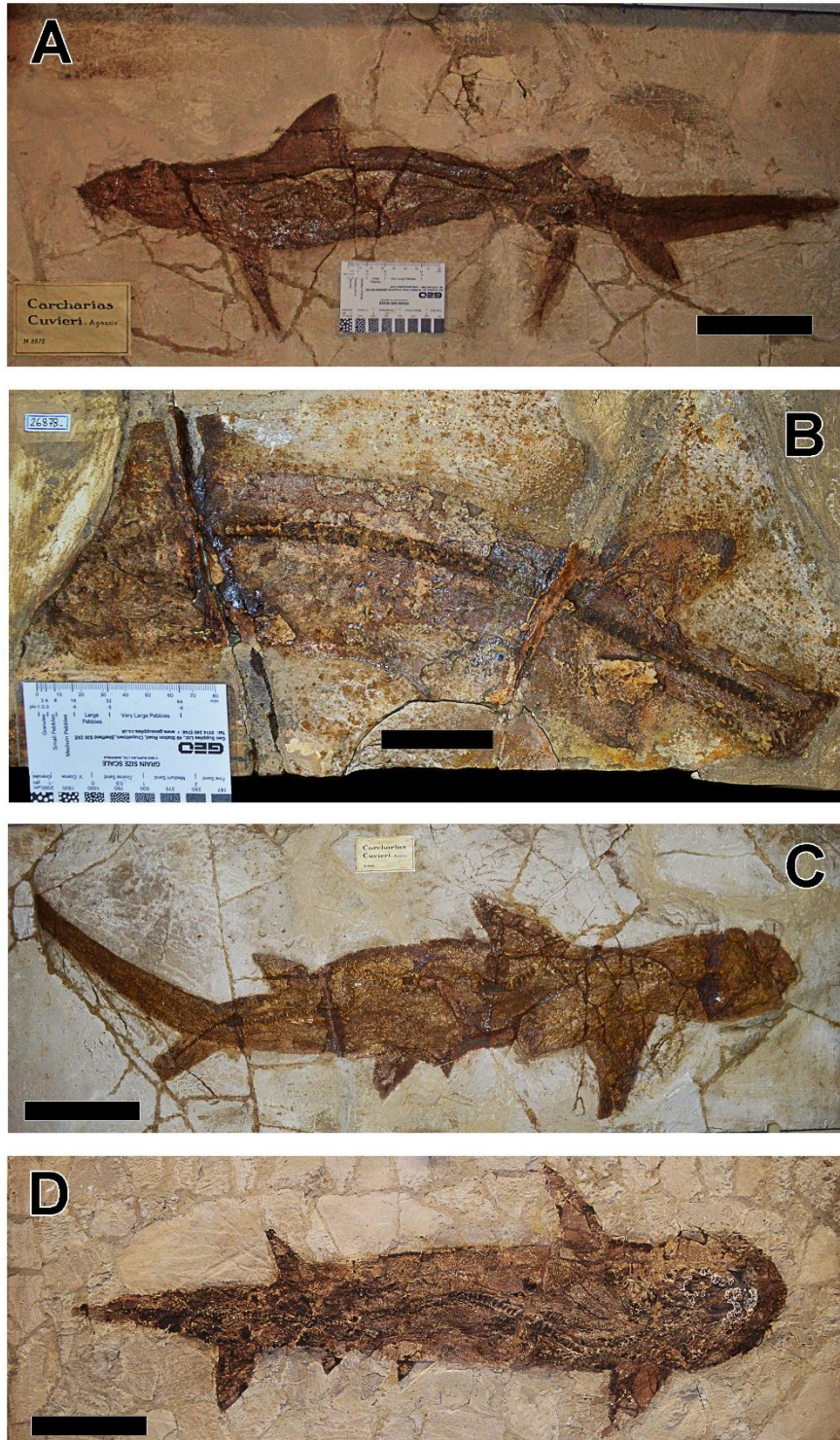


Figure 12: Bolca shark specimens: *Galeorhinus cuvieri*: A) MGP – PD 8872. Scale bar 10 cm; Unclassified specimen: B) MGP – PD 26878. Scale bar 5 cm; *Eogaleus bolcensis*: C) MGP – PD 8869; D) MCSNV T.311 (holotype). Scale bar 20 cm

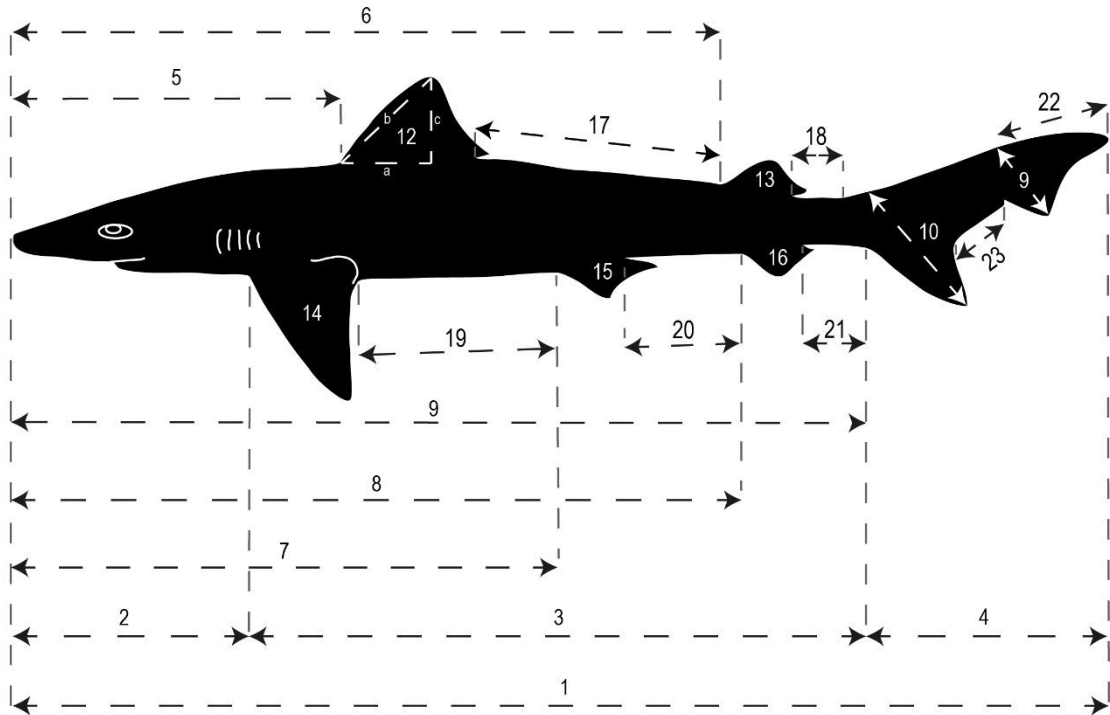


Figure 13: Terminology of longitudinal measurements following Cappetta (1975). In this thesis has been added measurements from No.17 to 23, expanding the original model. Measures list: 1) *Total length (TL)*; 2) *Head length*; 3) *Trunk length*; 4) *Caudal Fin length*; 5) *Head – First Dorsal Fin length*; 6) *Head – Second Dorsal Fin length*; 7) *Head – Pelvic Fin length*; 8) *Head – Anal Fin length*; 9) *Head Caudal Fin length*; 10) *Basal Lobe length*; 11) *Apical Lobe length*; 12a) *First Dorsal base length*; 12b) *First Dorsal anterior edge*; 12c) *First Dorsal height*; 13a) *Second Dorsal base length*; 13b) *Second Dorsal anterior edge*; 13c) *Second Dorsal height*; 14a) *Pectoral Fin base length*; 14b) *Pectoral Fin anterior edge*; 14c) *Pectoral Fin height*; 15a) *Pelvic Fin base length*; 15b) *Pelvic Fin anterior edge*; 15c) *Pelvic Fin height*; 16a) *Anal Fin base length*; 16b) *Anal Fin anterior edge*; 16c) *Anal Fin height*; 17) *First – Second Dorsal Fins length*; 18) *Second Dorsal – Caudal Fin length*; 19) *Pectoral – Pelvic Fins length*; 20) *Pelvic – Anal Fins length*; 21) *Anal – Caudal Fins length*; 22) *Apical Lobe – Caudal Tip length*; 23) *Basal – Apical Lobes length*; 24) *Total Vertebra*; 25) *Precaudal Vertebra*; 26) *Caudal Vertebra*

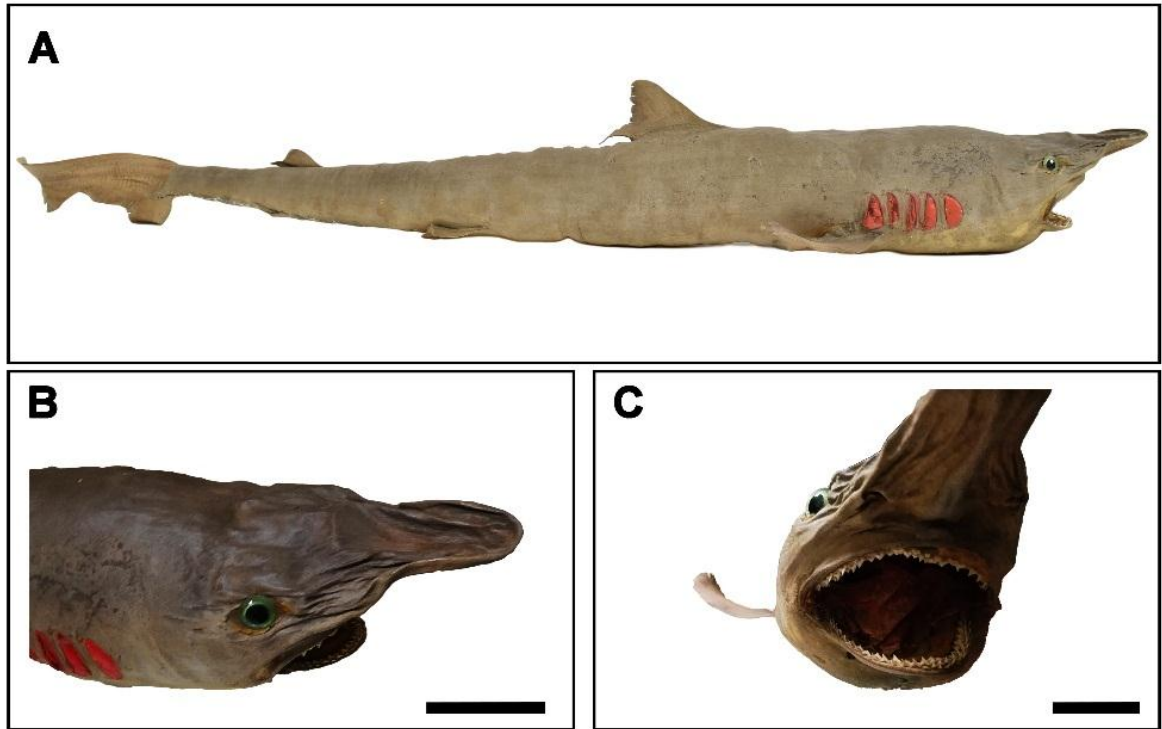


Figure 14: MSNPV PP 119, embalmed specimen of an adult female individual of *Galeorhinus galeus* (TL = 130 cm). All photographs are under natural colors: A) lateral view of the specimen; B) detail of the head region in lateral view; C) detail of the head region in frontal view. Scale bar = 5 cm

Chapter 4: Results – Overall description of MSNPV 17716 – 17717

The individual measures 120 cm (stretched body length) and lies in lateral view (**Fig. 15**). The head region and the apical area of the trunk are turned clockwise. The matrix of both slab and counter – slab is composed by massive limestones. No residuals of plants, ambers, bioturbations, and kerogens are shown on the surfaces of slabs. The preserved head measures approximately the 15% of the stretched body length. The skeletal components are fragmented and usually associated with patches of dermal denticles (**Fig. 16 – 17**). The hemimandibles are dislocated along the symphysis. The left hemimandible join distally to the palatoquadrate through the commissure. The palatoquadrate extend apically with several patched interruptions that overall mark an arched trend. The right nasal capsule extends from the middle point of palatoquadrate to apical. Ventrally to the 7th and 8th centra, a branchial arch develops laterally on 17716, covered by dermal denticles patches (**Fig. 17B**).

The teeth are few and strongly damaged on 17717. Twentyfive teeth are preserved on 17716 and are arranged laterally to longitudinal axis of head (**Fig. 18**; measurements and ratios in **Appendix B**). The roots vary from poorly to totally damaged, never higher than 1 mm, and the morphology might belong to holaulacorhizid type (i.e. deep transverse notch on the lingual face of the root and several foramina running on both labial and lingual faces of the root); observing the lingual face of tooth No. 19, the root is divided in two lobes by a transverse notch that cover a central foramen. The most teeth are in labial view, which obscure a clear understanding of the vascularization root – type assessment. Four morphotypes are recognized:

- 1) *Morphotype A*. The most representative tooth is the No.1 which is preserved in its labial view. It is sub – triangular and asymmetrical. The total height is 44% of the root length. The crown is smooth, lacking basal ornamentation. The mesial edge is straight and bears 8 serrations. In proportion, the f/e ratio is 67%. The mesial inflection point is sharp. The main cusp is approximately 20% of the root length and it is inclined distally. The distal angle is acute, approximately 45°, with a deep notch. The distal margin bears 3 secondary cusps that decrease in size distally. The distal edge is about the half of the mesial one. The root is wider than high and flat. The distal part is absent. Several foramina run along the root surface. Teeth No. 3, 11, 13,16,18 and 21 show the same characters. The total height of tooth No. 11 is 75% of the root length. The main cusp is slightly turned distally and on mesial edge it counts 3 serrations. The distal edge of No. 17 and 18 bears one small and rounded cusplet.
- 2) *Morphotype B*. Tooth No. 12 is a sub – triangular, symmetrical tooth as high as wide (d/c ratio = 100%). Mesial and distal edges are about the 25% of total height. The main cusp is erected, approximately 3/4 of the total height, and lack serrations. Crown is smooth and convex, lacking transverse ridges. The distal angle is obtuse with a wide notch. Distal edge bears 1 small secondary cusp. Medially, the root is incomplete and preserves the cast of a wide and circular central foramen.
- 3) *Morphotype C*. No. 19 is a triangular, asymmetrical tooth, higher than wide and blade – like. It is preserved in lingual view. The main cusp is slender, about three times higher than the distal edge. The distal angle is obtuse. The d/c ratio is 1,5. The distal edge is

smooth, joining to the main cusp through an obtuse distal angle apically. The mesial edge is straight (f/e ratio = 0,54) and bears 2 distally secondary cusps.

- 4) *Morphotype D*. No. 17 is a subtriangular and asymmetric tooth, preserved in labial view. The crown is smooth, lacking basal ornamentation. The mesial edge is straight and bears 2 distal serrations (f/e ratio = 0,5). The main cusp is slightly inclined distally; its width is the half of root length. The distal angle is obtuse. The distal edge bears 1 cusplet. The root is poorly preserved, and it is mainly represented by its cast.

A)



B)

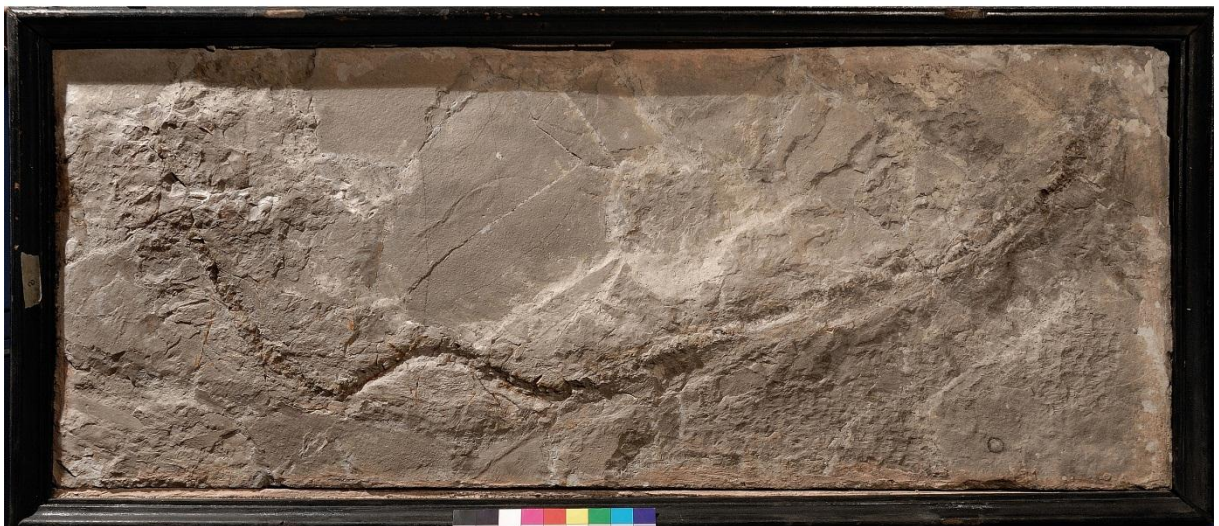


Figure 15: MSNPV 17716 (A) and 17717 (B). Images under natural colors

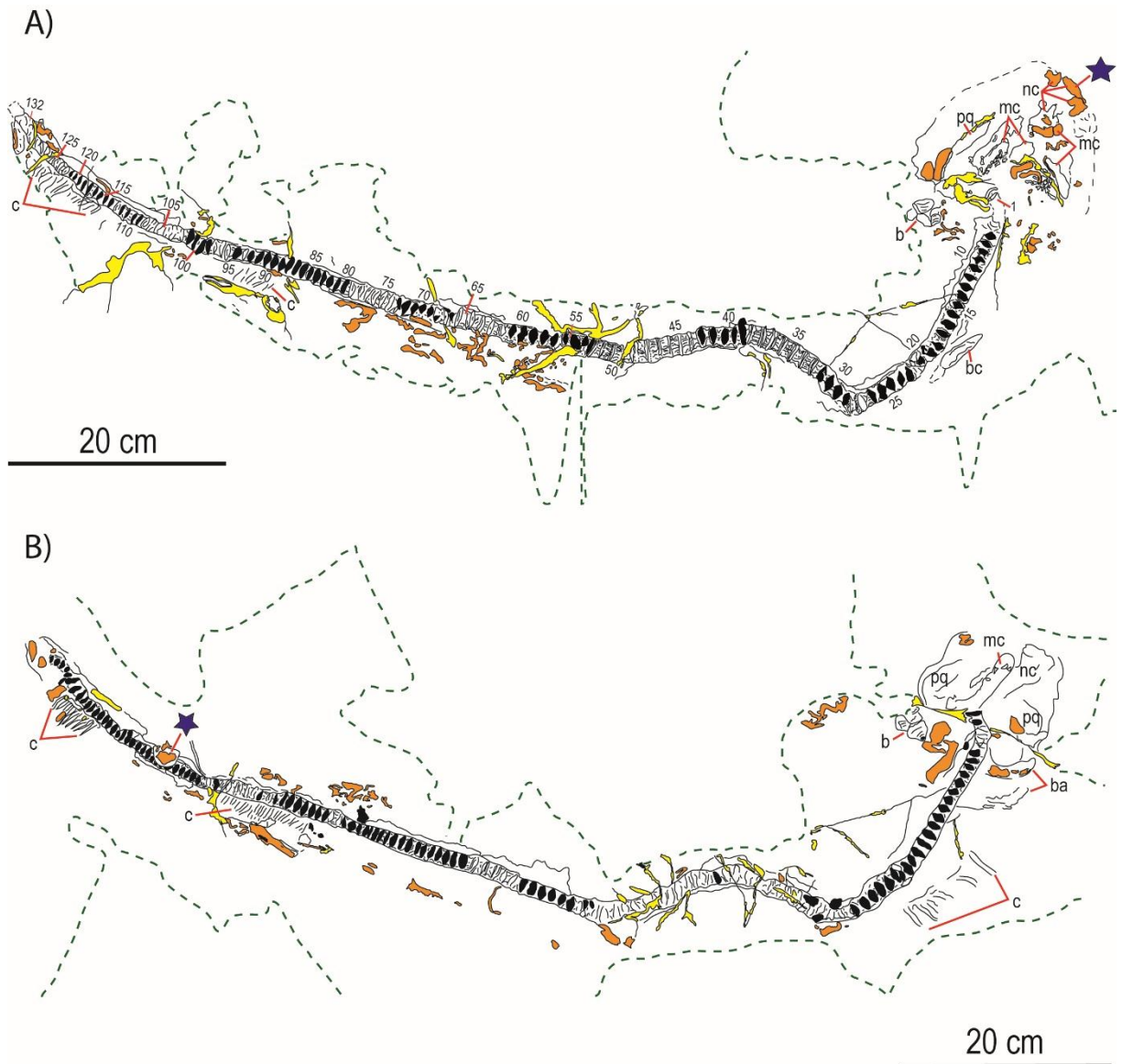


Figure 16: Anatomy of MSNPV 17716 (A) and 17717 (B). The interpretative drawing of 17717 (B) is reflected through the vertical axis of the image. Dermal denticles are widespread arranged in patches along the body (orange). The yellow patches mark the different typologies of mortar glues employed for the assemblage of the slabs. The green contour lines separate the matrix of the specimens from sustain blocks. The blue stars indicate the anatomical area where dermal denticle samples were collected. *Abbreviations:* b) benthic organisms; ba) branchial arch; c) ceratotrichia; mc) Meckel's cartilage; nc) nasal caps; pq) palatoquadrate.

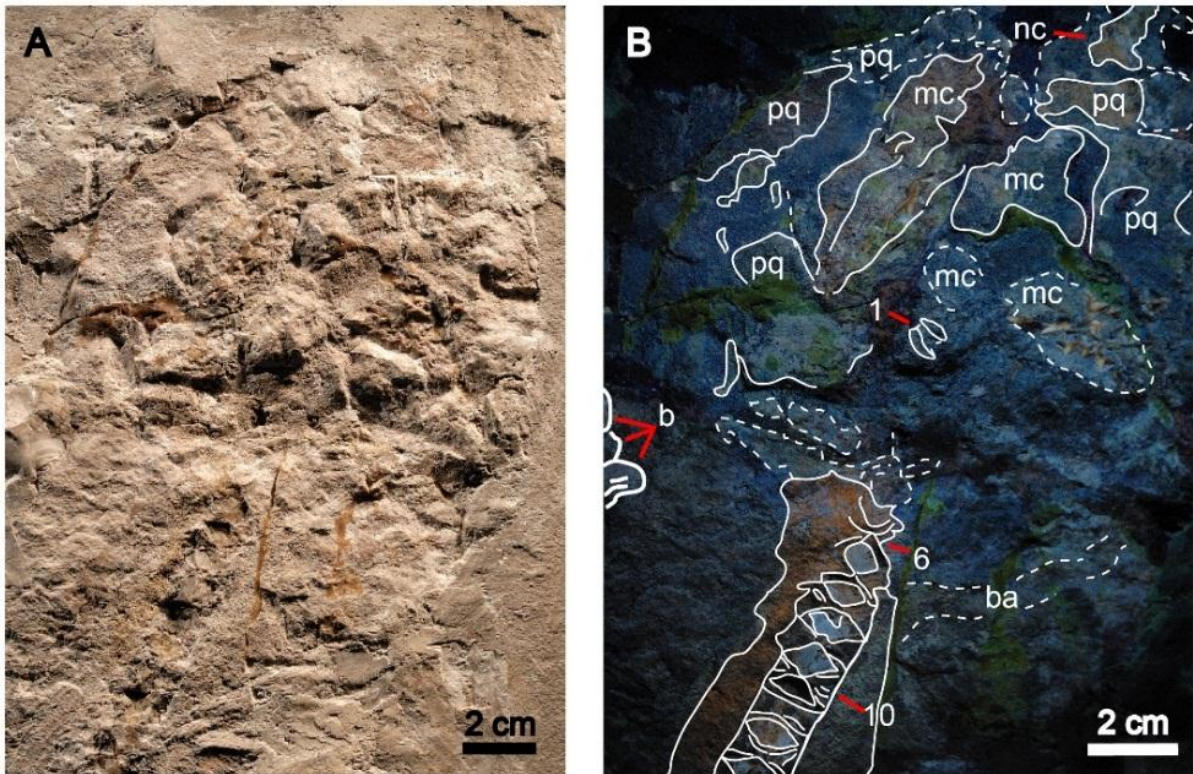


Figure 17: Dorsal view of the head region (MSNPV 17716) under natural color (A) and UV light (B). The skeletal components react under UV – light and they well differentiate from other components of the slab. *Abbreviation:* b) benthic organisms; ba) branchial arch; mc) Meckel’s cartilage; nc) nasal caps; pq) palatoquadrate

The vertebral column displays a strongly “S” – shaped bent. A total of 132 centra are preserved. Centra are wider than high with a strong, wedge – shaped intermedial calcifications. From the 2nd to the 5th, vertebral centra are estimated. The length of centra varies from millimetric to centimetric size posteriorly (**Fig. 19**), showing an inverted trend around the 40th. The 39th centrum is the widest of the series (centrum length = 16 mm). Observing the trend, the length of centra strongly oscillate distally without significant peaks until the 39th. Following, the longitudinal size decreases in several steps distally. Another peak of rapid increasing is shown by the 49th centrum.

A basal cartilage develops between 16th and 22th vertebral centra, (**Fig. 20**). The length of the basal cartilage is about the half head region preserved. Dorsal fins lack and no evidences of visceral tissues are shown. Ischiopubic and basal cartilages outlines of pelvic girdle are not preserved. Distally, two clusters of ceratotrichia are preserved in ventral position: between 88th and 98th vertebra and among the 115th and the 125th vertebral centra, 15 ceratotrichia counted (**Fig. 21**).

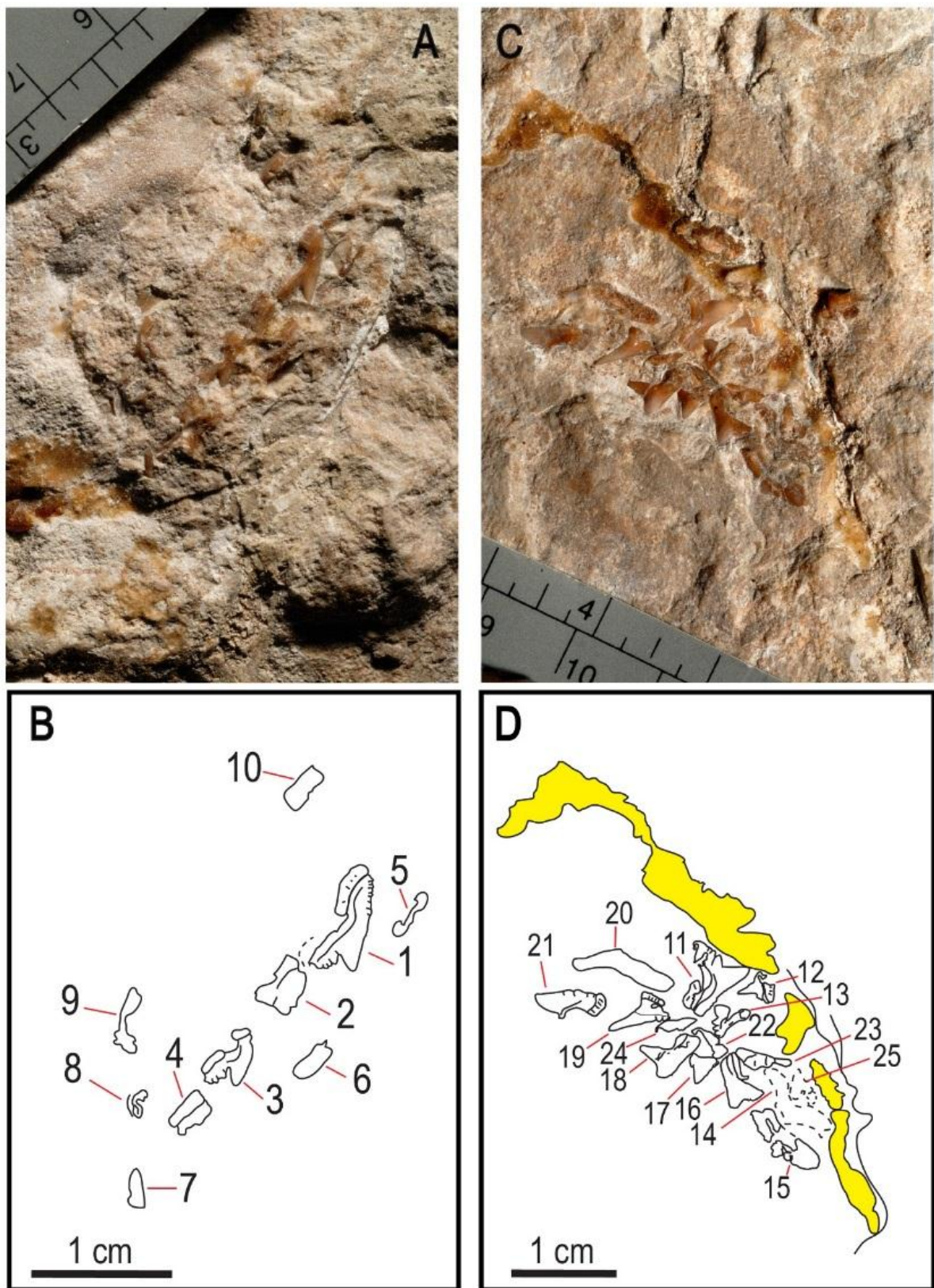


Figure 18: Preserved teeth of MSNPV 17716. Sections A and B show teeth from No. 1 to 10. No. 1 - 4 are aligned according life position. Teeth illustrated in sections C and D show scattered arrangement. The degree of preservation varies from partially to totally damaged. The yellow patches represent pigmented mortar glue.

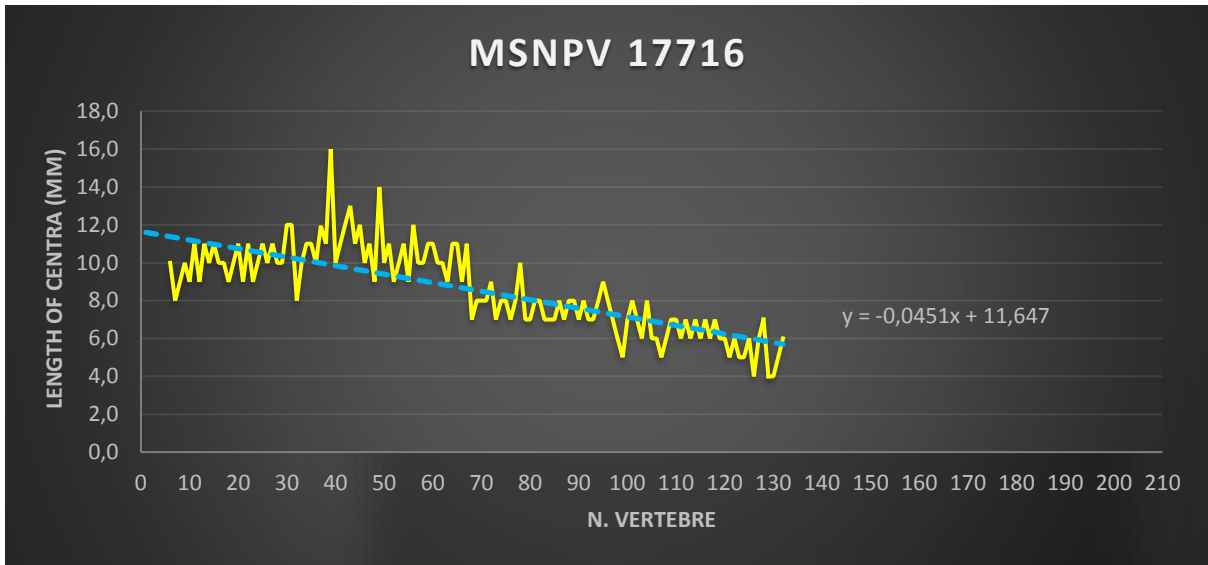


Figure 19: Length trend of vertebral centra. The size increases rapidly from 33th to the 39th (16 mm). Following, the dimension decreases slowly into 3 steps: 1) from 40th to 67th (average: 10,6 mm); 2) from 68th to 98th (average: 7,6 mm); 3) from 99th to 132th (average: 6,0 mm). X axis is vertebra count, whereas in Y axis is plotted the length of centra expressed in mm. Vertebrae are numbered from anterior (0) to posterior (132).

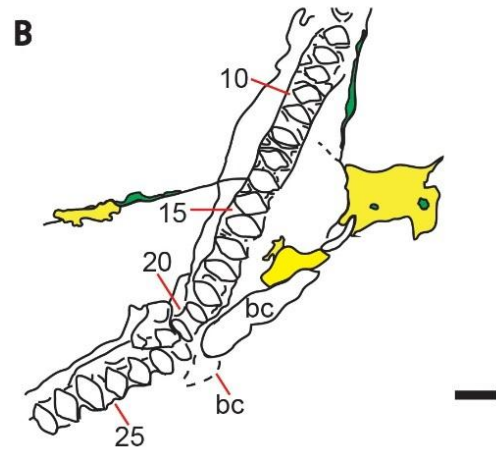


Figure 20: photograph under UV light (A) and interpretative drawing (B) of the apical area of the trunk (MSNPV 17716). The basal cartilage ventrally extends among the 16th and 22th centra. Yellow and green patches represent different typologies of mortar glue. Scale bar = 2 cm. Abbreviation: bc) basal cartilage.

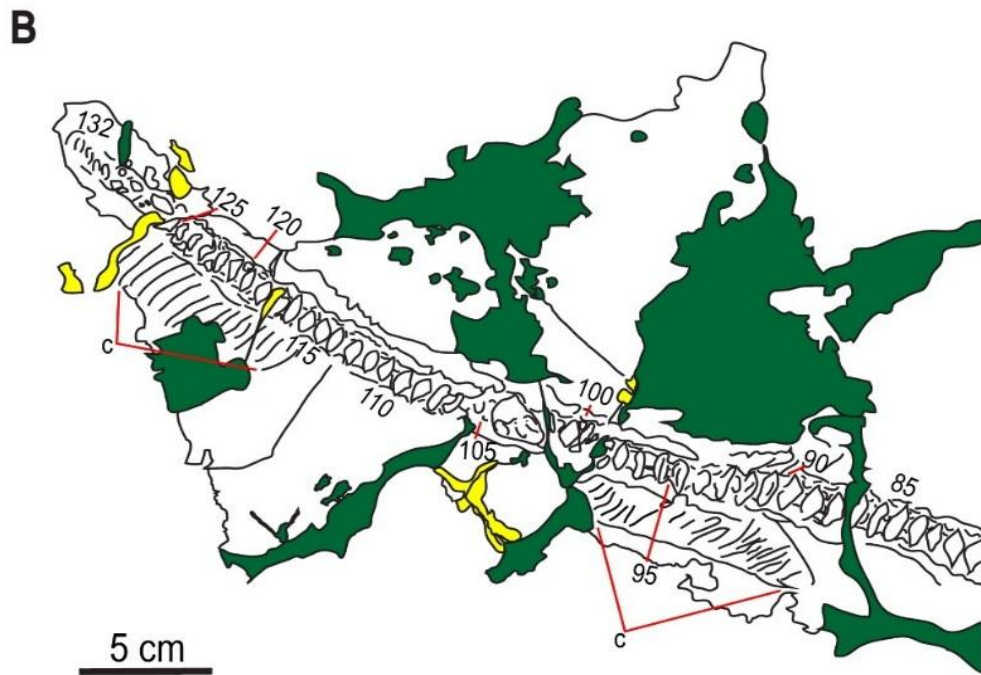


Figure 21: Photograph of the distal region of the trunk under UV light (A) and interpretative drawing (B) of the anatomical components (MSNPV 17716). The clusters of ceratotrichia ventrally extend from 88th to 98th and among the 115th - 125th. Yellow and green patches represent the different typologies of mortar glue. *Abbreviations:* c) ceratotrichia.

Patches of dermal denticles occur discontinuously along the entire length of the shark (**Fig. 22: A and D**). Skin samples collected from the head region and the distal part of the trunk (the latter collected on the counter – slab 17717) were analyzed using SEM imaging (**Fig. 21: B, C, E**), revealing two different morphotypes:

- 1) *Morphotype A* (distal trunk area; **Fig. 22: A, B, C**). Arrow – shaped scales and higher than wide. The number of peaks vary from 5 to 7; the edges of peaks are rounded. The crown measures approximately 420 μm in average. The overall thickness is about 100 μm . Hexagonal, micro – cells cover the bottom outline of the scale. In several individual – scales, the surface is medio – distally thickened by ridges, developing an upward – pointing spine. Ridges diverged apically are well separated and arranged subparallel. The interspace of ridges ranges between 100 and 120 μm .
- 2) *Morphotype B* (Head region; **Fig. 22D, E**). Teardrop – shaped scales, higher than wide, about 75 μm thick. The crown size is about 450 μm . 6 subparallel ridges develop on surface, in which the medial ones converge apically. Ridges decrease progressively in thickness apically until they merge with the surface. The ridge interspace average is approximately 74 μm . The apical edge is smooth. The surface is distally covered by hexagonal micro – structures. Medial spines are absent.

A small cluster of bivalves with 5 valves (**Fig. 23**) is preserved posteriorly to the head on both slabs. The valves are wider than high, smooth and ornamented by evident circular growth structures. No taxonomic identification is possible.

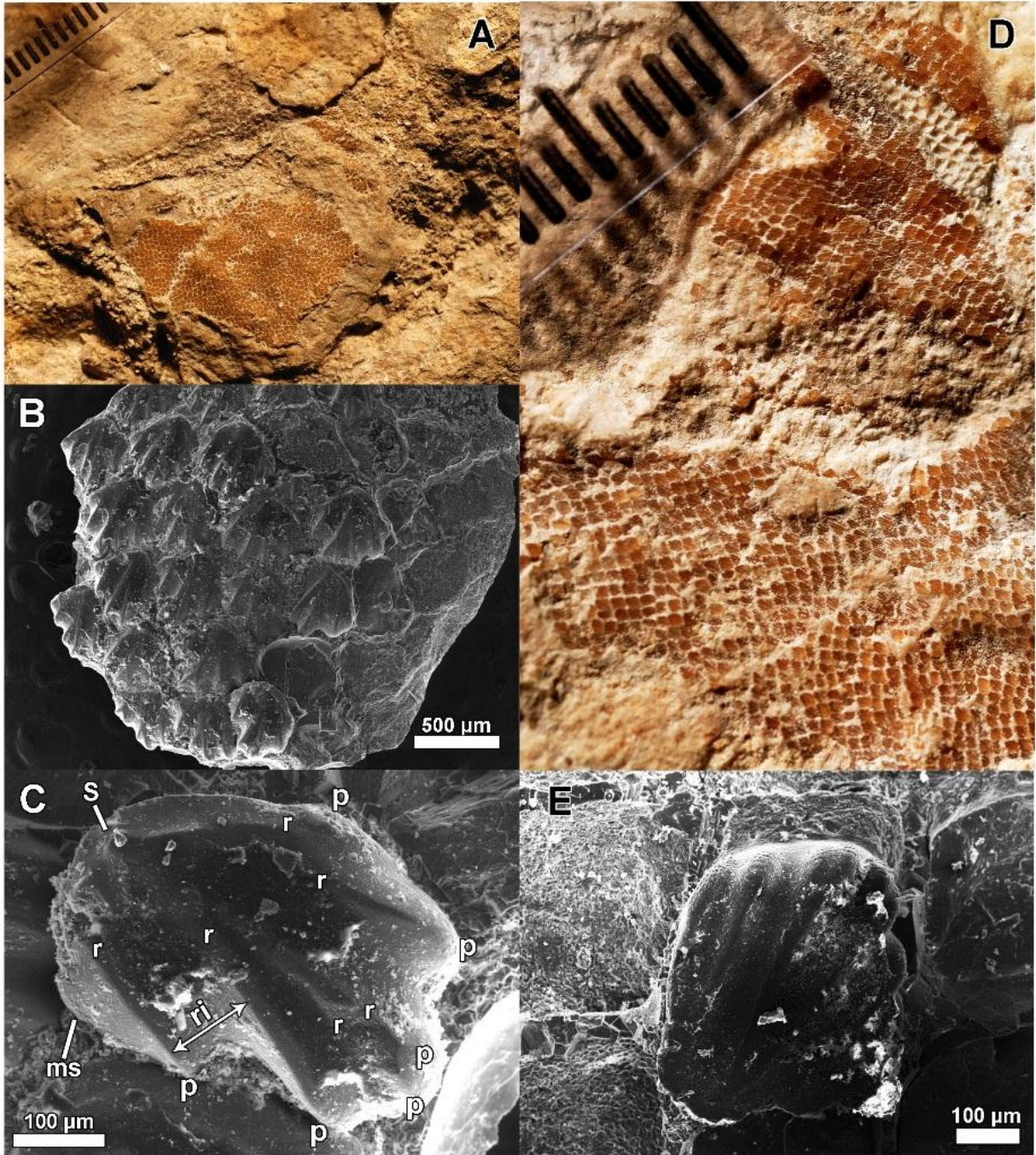


Figure 22: Dermal denticles at different scales: A) Patches of dermal denticles of 17717, arranged ventrally from vertebral column along the distal part of the trunk. Samples scanned in this area (B and C) are thick and well ridged. A pointing spine in medial – distal position occurs in several denticles, forming by the distal convergence of ridges. D) dermal denticles of the head region preserved on 17716. In this area, dermal denticles are teardrop – shaped (E). The ridges interrupt apically, without forming peaks. Medial – distal upward spines are absent. *Abbreviations:* ms) micro – structures; p) peak; r) ridge; ri) ridge interspace; s) spine

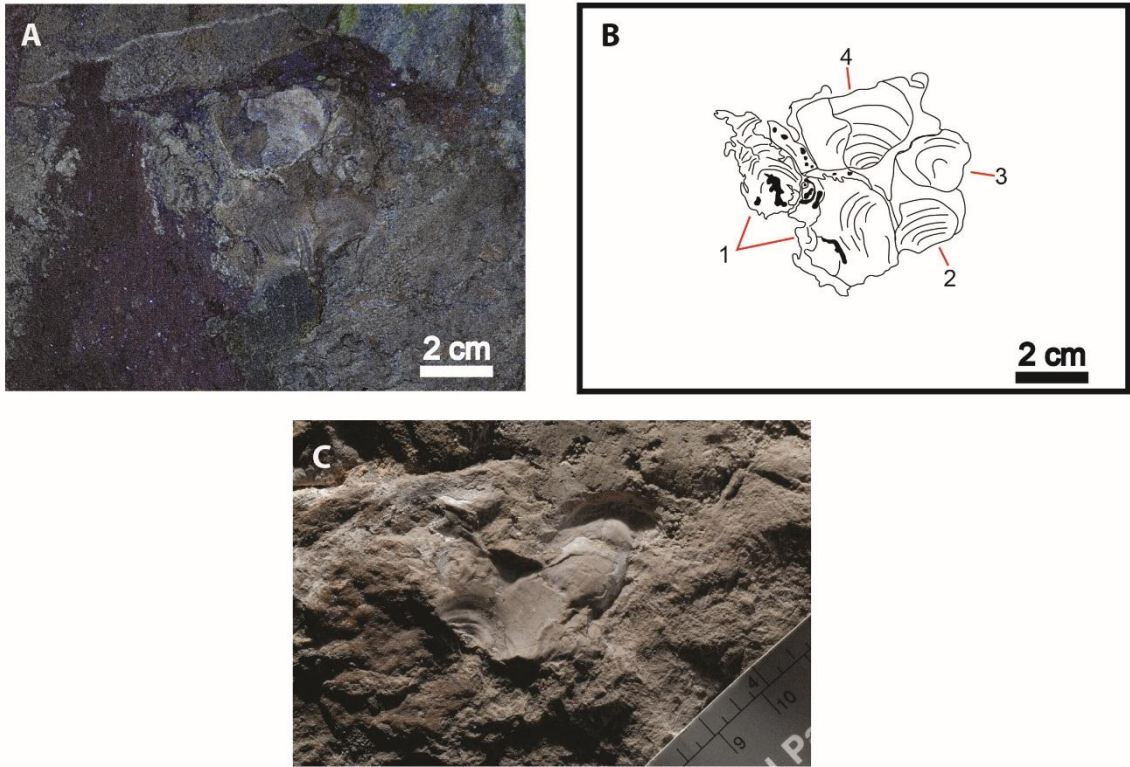


Figure 23: Bivalves clustered posteriorly to head on 17716 (A, B) and 17717 (C). Section A is a photograph under UV light. Section B is an interpretative drawing of the individuals. Section C is a natural colors photograph.

Chapter 5: Historical outline of Bolca shark specimens

The Count Giovan Battista Gazola purchased part of the fossiliferous deposit in Bolca in 1789 and started many excavating activities. After Napoleon armies confiscated several specimens from his private collection in 1797, Gazola also acquired a number of small private collections in order to reconstitute the collections exposed in his museum (Sorbini, 1972; Frigo & Sorbini, 1997; Roghi et al., 2014). Around the same time, Serafino Volta (1796 – 1808), in his masterwork *“Ittiologia Veronese”*, analyzed the fossils of various private collections including those in Gazola’s care. Among the bony fish specimens drawn by the author, he illustrated the first detailed descriptions of two fossilized sharks from Bolca, classified as *“Squalus carcharias”* and *“Squalus fasciatus”*. The latter is currently exposed in the Museo Civico di Storia Naturale di Verona (MCSNV VII.B.97; **Fig. 24**).

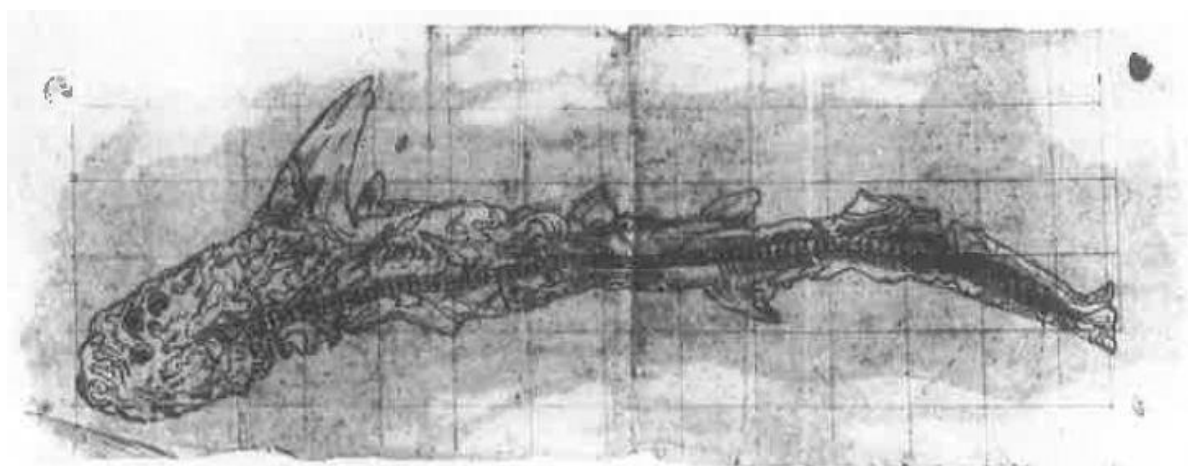


Figure 24: Original illustration of Gazola's *“Squalus fasciatus”* (MCSNV VII.B.97; after Sorbini, 1972)

The Gazola collection in Paris was studied by de Blainville (1818) and afterwards by Agassiz (1833 – 1844). The latter, on his *“Recherches sur les poissons fossiles”*, analyzed and illustrated the specimen previously classified *“Squalus carcharias”* by Volta. Agassiz classified shark individuals as *“Galeus cuvieri”*, which is housed in the Muséum National d'Histoire Naturelle of Paris (MNHN.F.Bol.516). Meanwhile, the professor of mineralogy Tommaso Antonio Catullo (1818 – 1822; 1827; Sorbini, 1972) studied the large collection of Bolca specimens in the museum of Castelfomberto, founded by Luigi Castellini near the end of the XVIII century. Catullo (1827) classified the specimens following Volta’s field marks. During the second half of XIX century, Catullo moved the collection of Castellini to the Museo Geologico – Paleontologico dell’Università di Padova (Sorbini, 1972), including sharks, for a total of five slabs: MGP – PD 8869 – 8870; 8871 – 8872; 26878.

The botanist Achille De Zigno (1850) was the first author who dated the succession to the Eocene. His private collection was helpfully offered to the Museo Geologico di Bologna, founded by Giovanni Capellini, celebrating the “Congresso Geologico Internazionale di

Bologna” on 1881. Among the samples there is an individual of shark consisting of slab and counter - slab; the fossils are currently preserved in Museo Geologico Giovanni Capellini (MGGC 1976 or 7444 and 7431).

Table 1 outlines the total number of shark specimens collected from Bolca area and include a description of their original provenance according to stratigraphic and paleoenvironment settings. Despite exhaustive anatomical description of all specimens, at the time of writing fossils lack any information on their original quarry (i.e. Pesciara or Monte Postale).

Systematic of Bolca’s sharks has been object of different revisions in the last centuries following latest to the improvement of methodological analysis. After Agassiz, Molin (1860) revisited the specimens preserved in Padua and changed the genus in *Protogaleus*. Lioy (1865) converted the species in *Alopiopsis plejodon* based on the description of a specimen 1,51 m long preserved in Vicenza; he counted 176 preserved vertebral centra, considering about 50 more, and specifying that teeth counted 105 right after the excavation. Unfortunately, this specimen was destroyed during the Second World War (Cappetta, 1975). The specimens preserved in MGGC were classified by De Zigno as *Alopiopsis cuvieri* (1874). Following, Jackel (1894) reexamined the sharks from Monte Bolca and instituted the genus *Pseudogaleus*. De Beaumont (1960) analyzed the specimen preserved in MNHN (Paris) and included the sample within the genus *Notidianus*.

Cappetta (1975) studied all specimens preserved in the museum of Paris, Bologna, Padova and Verona in order to provide a comprehensive systematic of Bolca’s sharks. His research resulted in the definition of two distinct taxa:

- 1) *Galeorhinus cuvieri* (Agassiz, 1835). Referred specimens: MNHN 11005 P, currently referred to the I.D. F.Bol.516, holotype; B 70, now referred to BM 70 and preserved in Museo dei Fossili di Bolca; MCSNV VII.B.97; MGP – PD 8871 – 8872; MGGC 1976 – 7431. Head with well – developed supraorbital process. Pectoral fin large and falcate. Second dorsal slender and tilted to caudal region. Caudal fin well developed, with a falcate basal lobe. Vertebral centra count 200 to 220. Teeth with a triangular crown and labial face slightly convex. The mesial edge is smooth or slightly convex with a marked inflection point. The main cusp shows varied inclinations to the commissure according to their position in the dental series. Root flat in labial view. The distal edge bears cusplets. Sub – rhomboidal – shaped dermal denticles.
- 2) *Eogaleus bolcensis* (Cappetta, 1975). Referred specimens: MCSNV T.311 (holotype); MCSNV VII.B.94; MGP – PD 8869 – 8870. Broad head. Second dorsal fin moderately large, about 2/3 of first dorsal. Presence of dorsal caudal depression (i.e. precaudal pit). Total vertebra counts around 150. Lower central teeth with narrow main cusp, thick and lacking inflection points on their edge. Lower lateral teeth with mesial inflection points and maximum 4 cusplets on distal edge. 2 main morphotype of dermal denticles, sub – rhomboidal or rhomboidal - shaped, with deep or shallow furrows, according to different arrangement on the body surface.

Recently, Adnet & Cappetta (2008) reviewed all Bolca specimens assigned to *Galeorhinus* and suggested close similarities with tooth morphologies of *Physogaleus*, despite the latter genus has too a controversial systematic position (Cappetta, 2012). Fanti et al. (2016) focused on the excellent preservation of anatomical components of the specimens MGGC 1976 and its ecological implications, remarking that the paper has no systematic reassessments to

consider *G. cuvieri* as a valid species among the family Triakidae. Marammà et al., (2017) recently depicted an overview about shark communities of Pesciara – Monte Postale succession.

Table 1: List of total shark individuals from Bolca fossiliferous area and their relatives I.D., taxonomic assessments, museums where are preserved and provenance. The individuals assigned to the inventory ID MGP – PD 26878, MCSNV T,311 and VII.B.94 consist to one slab each. The cross before taxonomic assessments indicates extinct taxa. The systematic is according to Cappetta (1975).

| I.D. | Species | Institutional abbreviations | Provenance |
|----------------------------------|--|---|-------------------|
| MGGC 1976 - 7431 | † <i>Galeorhinus cuvieri</i> | MGGC, Bologna (BO), Italy | Pesciara |
| MGP – PD 8871 – 8872 | † <i>Galeorhinus cuvieri</i> | MGP - PD, Padova (PD), Italy | Pesciara |
| MGP – PD 8869 - 8870 | † <i>Eogaleus bolcensis</i> | MGP - PD, Padova (PD), Italy | Pesciara |
| MGP – PD 26878 | Unclassified | MGP - PD, Padova (PD), Italy | Pesciara |
| MCSNV VII.B.96 – VII.B.97 | † <i>Galeorhinus cuvieri</i> | MCSNV, Verona (VR), Italy | Pesciara |
| MCSNV T.1124/ BM 70 | † <i>Galeorhinus cuvieri</i> | MCSNV, Verona (VR), Italy/ Museo dei Fossili di Bolca, Vestenanova, Bolca (VR), Italy | Pesciara |
| MCSNV T.311 | † <i>Eogaleus bolcensis</i> (holotype) | MCSNV, Verona (VR), Italy | Pesciara |
| MCSNV VII.B.94 | † <i>Eogaleus bolcensis</i> | MCSNV, Verona (VR), Italy. Preserved in Arsenale Franz Josef, Verona (VR), Italy | ? |
| MSNPV 17716 - 17717 | Unclassified | MSNPV, Pavia (PV), Italy | Monte Postale |
| MNHN F.Bol.516 | † <i>Galeorhinus cuvieri</i> (holotype) | MNHN, Paris, France | Pesciara |

Fanti et al. (2016) also remarked the low biodiversity of the assemblage of Bolca Elasmobranchii and the excellent status of preservations of the related carcharhinids, without going to cladistics analysis.

Chapter 6: Discussion

Among Paleogene deposits, the Bolca locality is one of the few Eocene fossiliferous sites in which sharks are preserved. The completeness of non – dental features of fossil specimens is pivotal to properly document the evolutionary patterns during the Cenozoic. Extant shark species are classified almost exclusively on the basis of remarkable specimens. On the contrary, single characters used for taxonomic purposes have low resolutions to establish evolutive divergences among taxa. In this study, the comparison among both fossils and living taxa is addressed to properly define relationships within the Bolca shark assemblage. In so doing, this work provides a comprehensive review, based on qualitative and morphometric characters of: 1) overall body morphology and ratios against total length; 2) dermal denticles; 3) teeth. All anatomical components are analyzed in consequent order from family to genus levels.

6.1: *Galeorhinus* Vs *Eogaleus* and size estimates of MSNPV 17716 – 17717

Overall morphologies documented in Bolca carcharhinids clearly support a differentiation between preserved taxa (Cappetta, 1975; Fanti et al., 2016; Marammà et al., 2017). The completeness of individuals varies from medium to excellent preserved – specimens. However, detailed analysis of fossils is usually biased due to multiple restorations (i.e. vegetal or artificial resins, sustain blocks and pigmented mortar glues). The best example is MCSNV T.311 (*Eogaleus bolcensis*, holotype; Cappetta, 1975). The specimen measures 125 cm, with a ventrally curved, “S” - shaped vertebral column. The body is deceptively stocky, and fins show different patterns of preservation: Pelvic and anal fins are not preserved, whereas the second dorsal fin is triangular and higher than antero – posteriorly wide; The first dorsal fin and the pectorals fins are poorly preserved. The early description of Cappetta (1975) considers the individual as a complete specimen. Fin outlines and skin patches clearly delineate the external outline of the individual, suggesting an incomplete shark lacking part of the tail and the entire caudal fin (**Fig. 25**). The head is exposed in dorso – ventral view, whereas the trunk is preserved in lateral view. The outline of the braincase and a tripodal rostrum are preserved. 139 vertebral centra are preserved, and each centrum display wedge - shaped intermedial calcification.

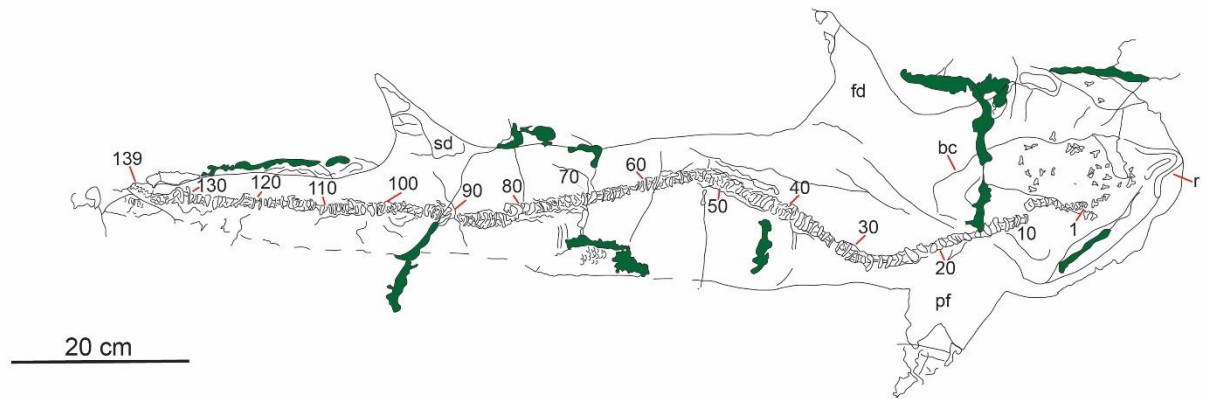


Figure 25: Interpretative drawing of the specimen MCSNV T.311. Fin attachments and skin patches delineate the real outline, displaying an uncomplete soecimen. The individual lies in lateral view with the head turned clockwise. The vertebral column shows a “S” – shaped bent anteriorly. The green patches indicate pigmented mortar glue. *Abbreviation:* bc, braincase; fd, first dorsal fin; pf, pectoral fin; r, rostrum; sd, second dorsal fin.

The dentition is strongly heterodont, with 64 teeth preserved (**Fig. 26A**; morphometrical measurement in **Appendix B**). Five morphotypes of holaulachorhizid teeth (i.e. vascularization type. The root has a deep transverse notch in lingual view and several foramina running on both root faces; Hermann et al., 1991) are observed:

- 1) *Morphotype A* (Teeth No. 1, 3, 4, 5, 6, 7, 8, 9, 10, 11, 12, 13, 14, 15, 16, 17, 18, 21, 41, 42, 43, 43, 44, 45, 46, 47, 57, 58; **Fig. 26B**). Subtriangular teeth, wider than high and asymmetric. The d/c ratio ranges from 0,42 to 0,89. The main cusp is inclined distally. Mesial edge is straight or slightly convex (f/e ratio approximately 0,50), usually smooth and poorly serrated distally. The mesial edge and the main cusp are well separated by a marked inflection point, generally sharp. The distal angle is acute or approximately right. The distal edge is flat, about the 40% of root length (“c”), bearing from 2 to 4 cusplets that decreasing in size distally. The neck is prominent. In labial view, the root is slightly convex with a medial narrow nutritive groove. The root is divided in 2 lobes by a deep transverse notch lingually.
- 2) *Morphotype B*. Tooth No. 33 is subtriangular and symmetric, preserved in labial view. The d/c ratio is 1,2. The crown is smooth, lacking transverse ridges. The neck is massive. The main cusp is slightly inclined distally. The height of main cusp is about 3/4 of the total height. The mesial edge is straight, lacking serrations or cusplets. The distal angle is obtuse. The distal edge lacks cusplets. The root height is 1/6 of the total height.
- 3) *Morphotype D*. Tooth No. 60 (**Fig. 26B**) is subtriangular and asymmetric, higher than wide, with a slender main cusp. The crown lacks basal ornamentations. The d/c ratio is 1,6. The main cusp (approximately 2/3 of total height) is slightly inclined distally. The mesial edge is concave, lacking serrations (f/e ratio = 0,45). The distal angle is obtuse. The distal edge bears one small cusplet. The root is 1/6 of the total height.
- 4) *Morphotype E* (teeth No. 25, 26, 29, 32, 35, 36, 37, 38, 39, 51, 52, 56; **Fig. 26B**). Teeth are subtriangular and asymmetric, higher than wide, with a slender main cusp. The main cusp is approximately 2/3 of the total height. The d/c ratio ranges from 1,11 to 2. The edges lack cusplets and serrations. The distal angle is obtuse. In rare cases on distal edge

occurs 1 cusplet (tooth No.39). The root is thick and slightly convex in labial view, with an arched nutritive groove. Transverse notch is well developed, covering the circular, central foramina.

- 5) *Morphotype F* (teeth No. 27, 28, 48, 59, 61, 62; **Fig. 26B**). Triangular and symmetric teeth preserved in mesial or labial views. The crown is smooth. The labial face is convex in mesial view, despite the lingual face is straight. The main cusp is approximately the half of the total height (i/c ratio is 0,6 in average). The edges lack serrations and cusplets. The distal angle is obtuse.

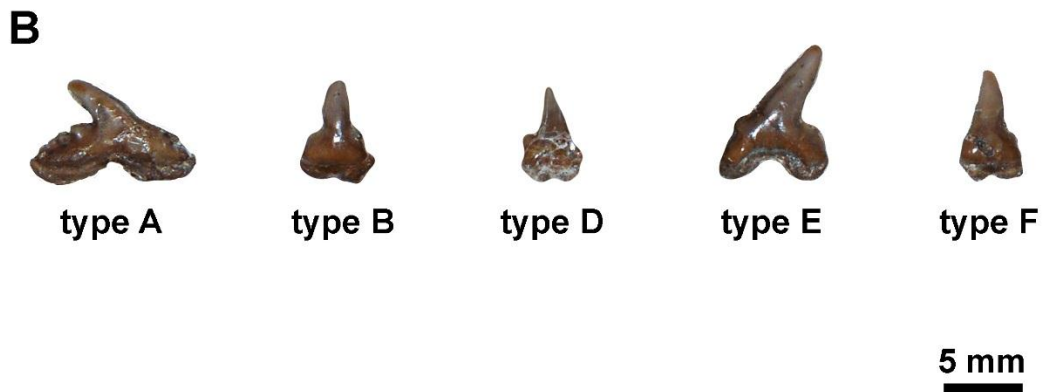
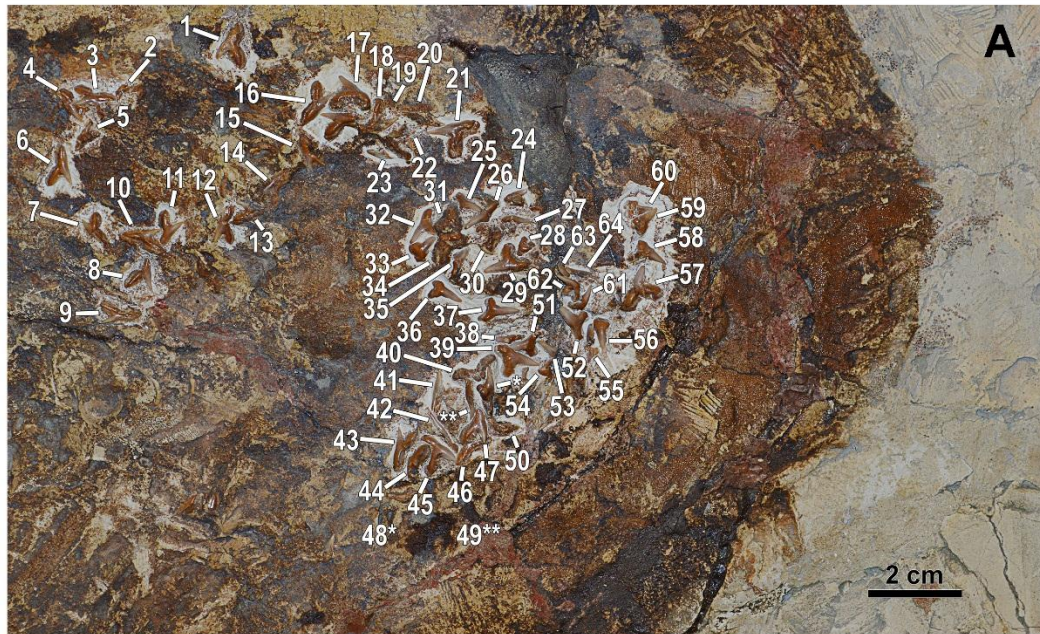


Figure 26: Focus on the head region of MCSNV T.311. A) teeth count; B) Characteristic teeth morphotypes of the specimens. All teeth illustrated for each type are in labial view.

Specimen MGP – PD 8869 – 8870, classified as *E. bolcensis* (Cappetta, 1975), measures 135 cm. The head is stocky showing teeth lined on the preserved jaw. Unfortunately, most of the preserved teeth are partially exposed, thus limiting accurate description. However, the overall morphologies of teeth resemble MCSNV T.311 (morphometrical measurements and teeth

counts on **Appendix B, C**). The trunk and the caudal fin are preserved in lateral view. The first dorsal fin is triangular, slightly tilted distally. The base is about the 10% TL and partially overlap the pectoral fin from its posterior juncture. The second dorsal fin is triangular, higher than wide, and its size is about more than the half of first dorsal. Both pectoral fins are preserved. They are triangular and slender, but not falcate. The anterior edge is about the 14% TL. The pelvic and the anal fins are not preserved. Several ceratotrichia are preserved ventrally to the second dorsal fin and most likely referable to the anal fin. The basal lobe of the caudal fin is partially preserved. The vertebral column shows multiple distortions between the first and second dorsal fins. Centra count is 202, considerably higher than T.311 and the range proposed by Cappetta (1975). It supports the non – completeness of the holotype. Indeed, count of centra and trends of T.311 remark similar taphonomic features of MSNPV 17716 – 17717: the trends show a slight decrease toward caudal region due to the lack of caudal vertebrae. Trends and averages are illustrated in **Fig 27**. Measurements, vertebral centra counts, correspondences body regions/number of centra and fin arrangement/number of centra are listed in **Table 2, 3, 4**.

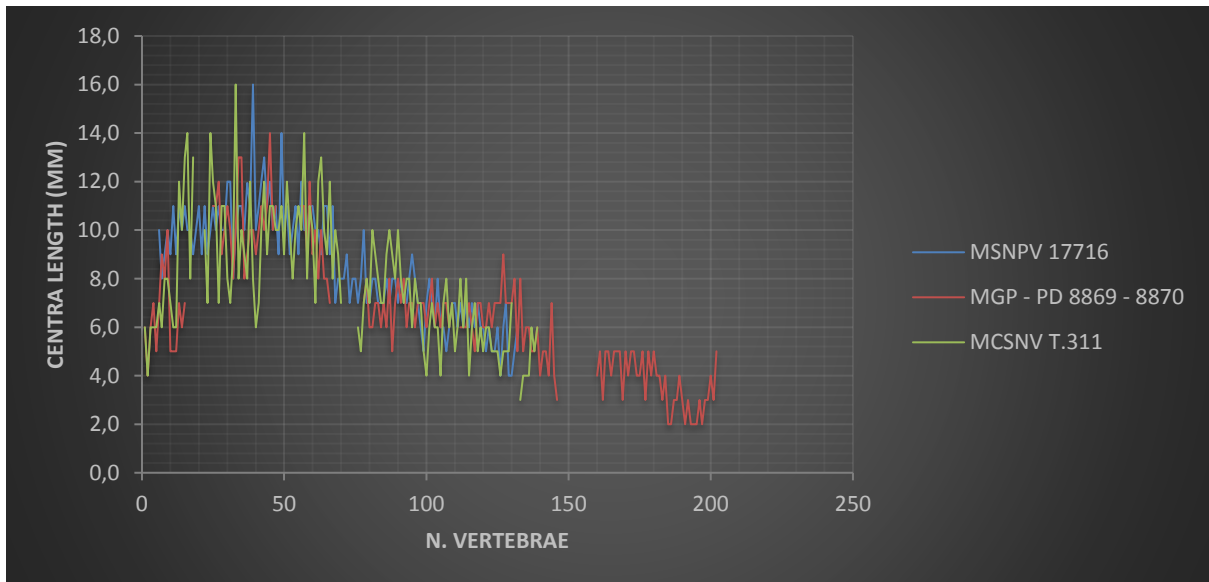


Figure 27: Trends of vertebrae length against the number of centra of specimens MSNPV 17716, MGP – PD 8869 – 8870 and MCSNV T.311. Each curve shows a relative rapid increasing until the 40th centrum, then the size of centra decreases in several steps posteriorly. The decreasing of centra size of specimens MSNPV 17716 and MCSNV T.311 is slightly emphasized than MGP – PD 8869 – 8870 due to the lack of the most of caudal vertebrae, therefore the specimens MCSNV T.311 is an uncomplete individual as well as 17716. Centra are numbered from anterior (0) to posterior.

MNHN F.Bol.516 is the holotype of *Galeorhinus cuvieri* (Agassiz, 1975), and is represented by a single slab. The specimen measures 67 cm with the head turned clockwise. The caudal fin is not preserved. Preservation of teeth, soft tissues and skeletal component is poor. Cappetta (1975) based his diagnosis mainly on the best preserved Bolca shark MGGC 1976. Fanti et al. (2016) recently highlighted that both hard and soft tissues (i.e. cerebrum, cerebellum, medulla oblongata, myomeres, endolymphatic sac, lobes of the liver, stomach, intestine) are easier to discriminate under UV light. All specimens measure less than 1 m in total length. Specimens 1976, MCSNV VII.B.96 – 97, MGP – PD 8871 – 8872 and the holotype are preserved with the head turned clockwise. The cranium is triangular – shaped in dorsal view with a slender rostrum. The first dorsal fin is better preserved on T.1124, 8869 – 70 and MGGC

7431. It is triangular, usually wider than high (**Fig. 28A**) and slightly inclined toward the caudal fin. The base of first dorsal fin partially overlap posteriorly the pectoral fin. The pectoral fin is slender, ventrally elongated and falcate (**Fig. 28B**). The second dorsal fin overlaps with the anal fin; it is about the 2/3 in size when compared to the first dorsal. The anal fin is slightly smaller than the second dorsal. The second dorsal and anal fins are inclined posteriorly (**Fig. 28 C**). The pelvic fin is higher than wide.

Fanti et al. (2016) documented sexual dimorphism among the specimens assigned to *G. cuvieri*, based on presence/absence of claspers. Specimens 1976 and T.1124 were considered, respectively, as male and female individuals (**Fig. 29**).



Figure 28: Focus on fin morphologies of the specimen MCSNV T.1124: A) first dorsal fin; B) pectoral fins; C) second dorsal, anal and caudal fins.

The holotype (F.Bol.516) lacks the pelvic region and therefore is not possible to infer the sex of the individual. Vertebral centra count ranges from 200 to 207 (**Table 4**). Soft tissues show different degree of preservations among the specimens. Usually, intestine and myomeres of fin attachments are preserved in all samples. Centra show wedge – shaped intermedial calcification. The vertebral column is commonly preserved without evidence of disarticulation, except for T.1124 that shows a “V” – shaped distortion between the pectoral and first dorsal fins. The individual VII.B.96 – 97 measures 83 cm, lacking the proximal part of the caudal fin. The total length of the specimen is estimated in 89 cm according to apical lobe – caudal tip/caudal fin ratio of the referred specimens. MGP – PD 26878 is an incomplete individual, with 87 centra. The second dorsal fin is well preserved. The number of centra is normalized according to the correspondence between centra – fins origins of the fossil specimens. Correspondences of body regions/number of centra, fin position/number of centra and measurements of specimens are listed in **Table 2, 3, 4**.

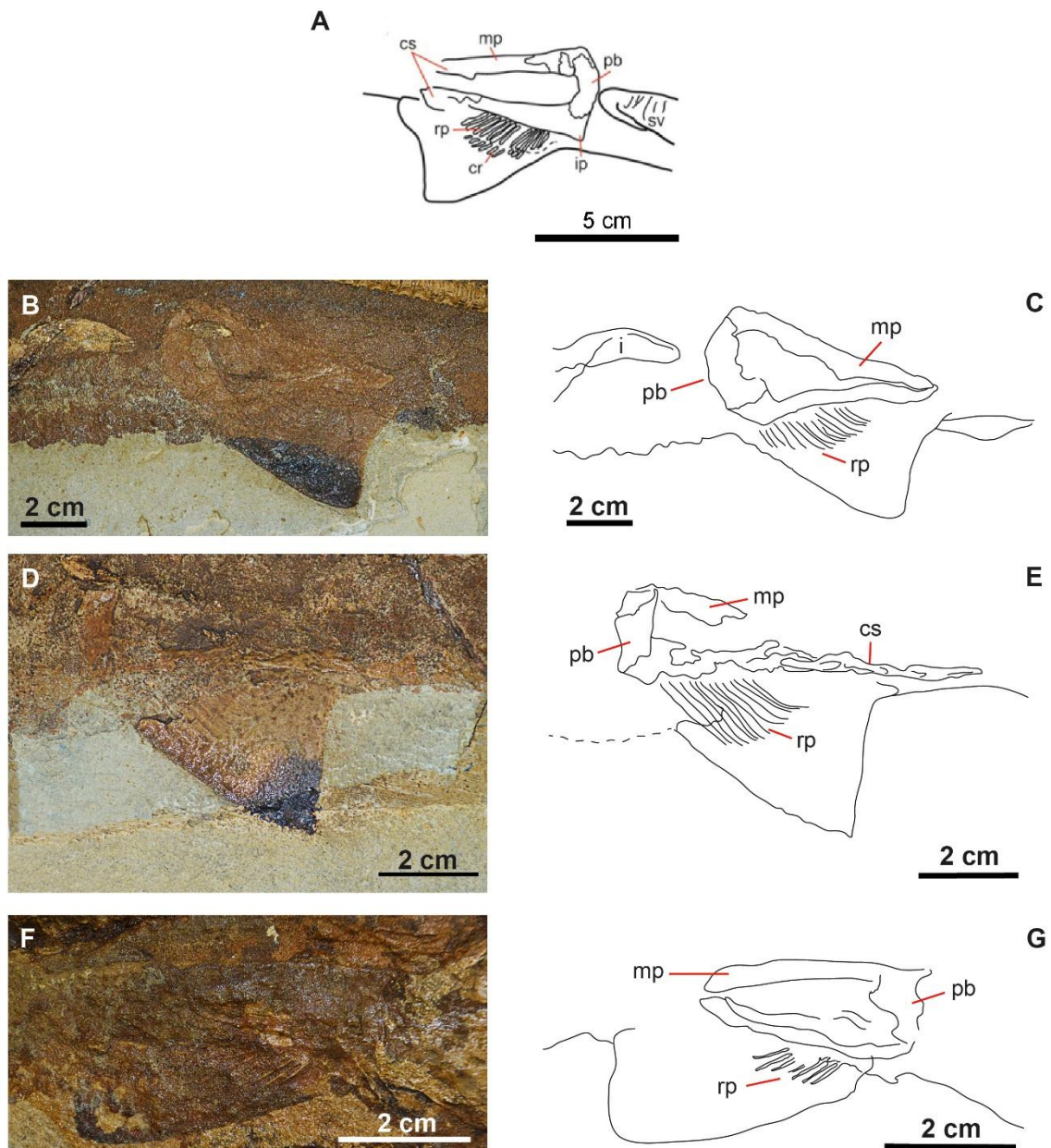


Figure 29: Pelvic region of specimens MGGC 1976 (A; Fanti et al., 2016), MCSNV T.1124 (B, C); VII.B.96 (D, E) and MGP – PD 8871 (F, E). The male individuals (1976 and VII.B.96) show the claspers that extend from the metapterygia. *Abbreviations:* cr, ceratotrichia; cs, claspers; i, intestine; ip, iliac process; mp, metapterygium; pb, puboischiatic bar; rp, radial pterygophores.

Teeth vascularization is holaulacorhizid type. *G. cuvieri* is characterized by a weakly heterodonty. The numerical system adopted for teeth counts doesn't reflect the anatomical position. The teeth counts are illustrated in **Appendix C**. Four morphotypes are preserved:

- 1) *Morphotype A* (**Fig. 30**). Teeth are subtriangular and asymmetrical, with smooth crowns. The d/c ratio is 0,7 in average. The neck is thick and clearly split the root from crown. The main cusp is never longer than the mesial edge (f/e ratio is 0,55 in average). The mesial edge varies from smooth to convex, bearing maximum 3 serration. No

cuspelets adorn the mesial edge. Mesial – inflection point well defined, usually sharp. The distal angle varied from acute to approximately right. The distal edge always bears cuspelets, from 2 to 4. The root is broad, with one narrow medial groove. The transverse notch well divides the root in two lobes in lingual view.

- 2) *Morphotype B* (**Fig. 30**). This type is represented by only one tooth preserved on VII.B.96 (n.13; **Appendix C2**). The tooth is preserved in labial view. It is subtriangular and symmetric, higher than wide. The crown is smooth, lacking basal ornamentation. The edges are smooth, lacking cuspelets and serrations. The Distal angle is obtuse. The main cusp is narrow and erected (g/b ratio = 0,50). The root is absent.
- 3) *Morphotype D* (**Fig. 30; Appendix C1**). This type is represented only in MGGC 1976. Teeth are subtriangular and asymmetrical, usually preserved in labial view. Teeth are higher than wide (d/c ratio about 1,1 in average). The crown is smooth, lacking basal ornamentation. The width of the main cusp is about $2/3$ of the root length. The mesial edge is straight and lacks serrations. The distal angle is obtuse. The distal edge bears 1 or 2 small cusplets.
- 4) *Morphotype E* (**Fig. 30**). This morphotype is preserved only in MCSNV T.1124 (No.10; **Fig. 30; Appendix C4**). The tooth is sub – triangular and asymmetric, preserved in lingual view. The main cusp is slender and erected main cusp (g/d ratio = 0.4; g/b ratio = 0,67). Edges are smooth, with a well defined mesial inflection point. The crown is smooth, lacking basal ornamentations. The distal angle is obtuse. The tooth is preserved in lingual view. The lingual face is broad. The transverse notch separates the root in two lobes.

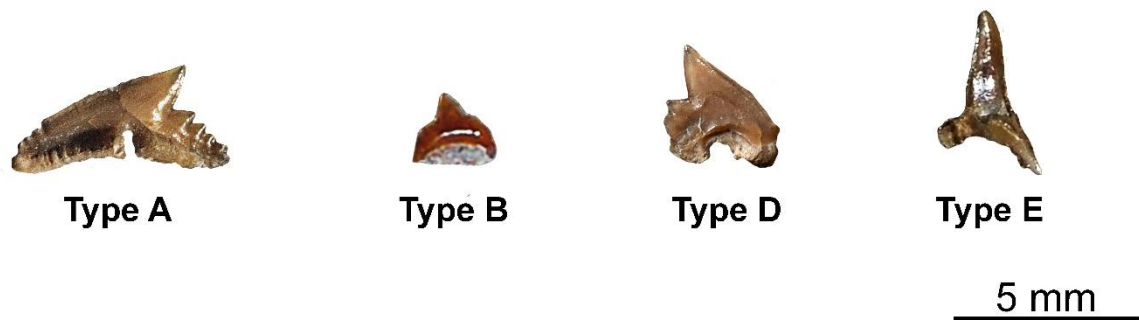


Figure 30: Characteristic morphotypes of *Galeorhinus cuvieri*. The tooth that represents “Type E” is in lingual view.

Fanti et al. (2016) classified the stomach content of MGGC 1976 as an articulated caudal vertebrae and dismembered fin rays of the acanthomorph *Sphyræna bolcensis*. Curiously, vertebral remains are found in ventral region of specimens MGP – PD 8871 – 8872 and 26878. The stomach content of MGP – PD 8871 – 8872 counts approximately 30 articulated centra (centra length approximately 5 mm each) and spines. The scattered fin rays around the centra marks the outline of the stomach of the individual (**Fig. 31**). Specimen MGP – PD 26878 contains approximately 12 articulated centra (length of centra from 5 to 10 mm; **Appendix D**)

and scattered spines as well as the stomach content of the specimens MGP – PD 8871 – 8872. Overall morphology and vertebral size suggest perciform fishes as potential victims.

According to qualitative and morphometrical analysis, considered taxa share several symplesiomorphies: 1) the general body ratios and correspondence to vertebral centra of head, trunk and caudal regions against total length are similar (**Table 2 and 4**); 2) vertebrae count around 200 (**Table 4**), following a similar trend from anterior to posterior (**Fig. 32**). The morphology of centra coincides among the specimens (i.e. strongly wedge – shaped intermedial calcification); 3) the fins show several variations of correspondences to vertebral column, shape and size among and within specimens, as suggested by ratios and percentage errors (**Table 2 and 3**). However, fins attachments and inter – spaces between them follow the same general arrangement.

According to overall descriptions of *G. cuvieri* and *E. bolcensis*, the external morphology of specimens MSNPV 17716 has been discriminated with the following criteria:

- 1) the head region extends to the 15th centrum for a total length of 12,4 cm, including 2,2 cm estimated from 2nd to 5th centra;
- 2) the basal cartilage preserved between the 16th and the 22th is referred to the pectoral fin. The 16th centrum marks the trunk region. Ceratotrichia clustered among the 88th – 98th centra are considered as components of the anal fin. The 114th centrum marks the end of the trunk area (total centra of the trunk = 99). According to vertebral centra length, the trunk is 89,3 cm long. The ventral ceratotrichia between the 115th – 125th are considered components of the caudal fin. The 115th centrum is the first the caudal region, which measures 10,1.

In order to estimate the body length of MSNPV 17716, the ratios of first the trunk and then the centra of the head region were plotted against every other body segments for 5 Bolca carcharhinids (MCSNV T.1124, VII.B.97; MGGC 1976; MGP – PD 8869 – 8870, 8871 – 8872). This dataset was then performed following two approaches (see **Tables 5 and 6**):

- 1) The averages of each ratio types, calculated for each specimen, (see **Table 5** for ratios description) were used as standards to calculate the different body segments of the exanimated specimen.
- 2) The estimates of every segment of the Pavia specimen has been computed considering one specimen per time. For each external region, two different types of values were estimated, one based on the ratios referred to the trunk region, the other based on the ratios referred to the centra of the head region. The average of this values, gave in the end 5 estimates, one for each specimen. The averages of this averages are shown in **Table 6** (yellow cells) and represents the estimated size of MSNPV 17716 – 17717.

A comparison between the two approaches in terms of errors (**Tables 5 and 6**) indicate that the accuracy of the standard ratios method is higher ($\epsilon\%$ of TL = 0,12). The length of MSNPV 17716 is here estimated in 175 cm (**Table 5**). This approach has been consequently extended to MCSNV T.311 and MNHN F.Nol.516, with estimated length of 168 cm and 81,2 cm respectively.

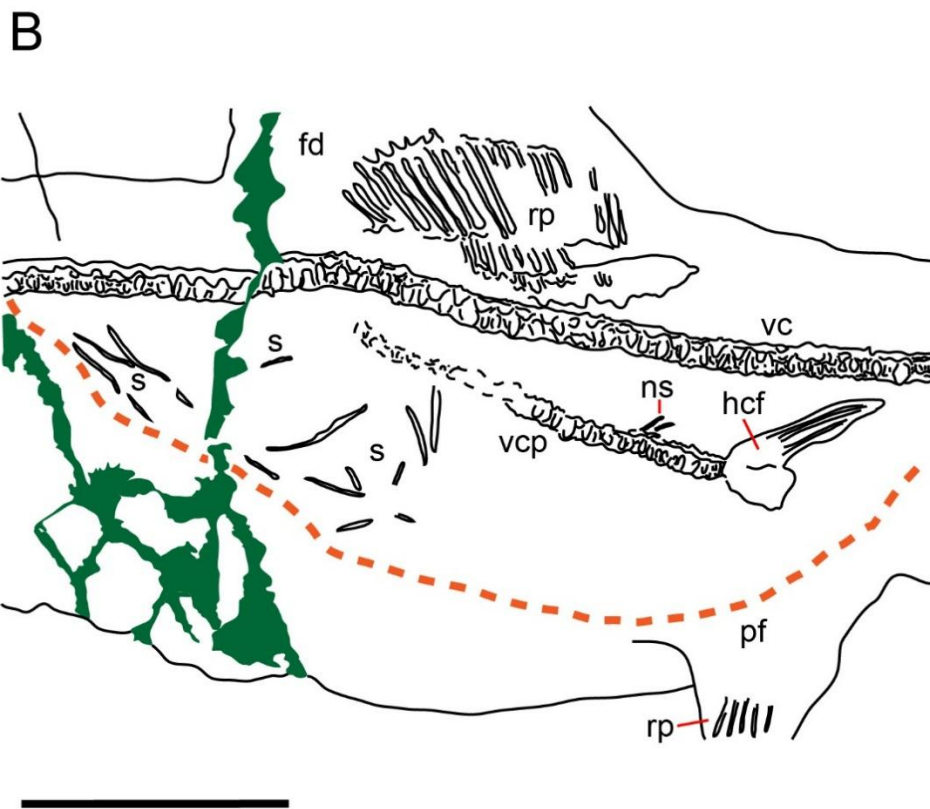


Figure 31: (A) Focus on abdominal region of MGP - PD 8871; B) interpretative drawing of anatomical components and stomach content. The orange trace indicates the hypothetical outline of the stomach. The green patches represent the mortar glue. Scale bar = 5 cm. *Abbreviations:* fd, first dorsal fin; hcf, homocercal caudal fin; ns, neural spines; pf, pectoral fin; rp, radial pterygophores; s, spines; vc, vertebral column of the shark specimen; vcp, vertebral column of the perciform prey.

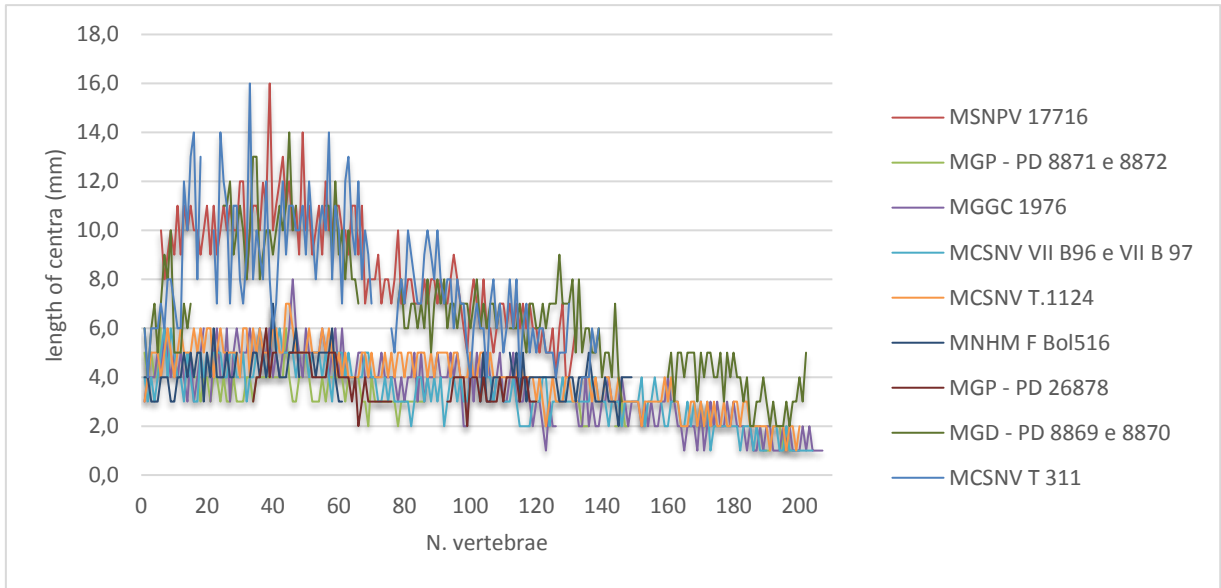


Figure 32: Trends of centra length of Bolca specimens. Centra are numbered from anterior to posterior. All specimens show a slowly increase in size on the anterior area of the trunk. Peaks of rapid increasing is around the 40th centrum, close to the first dorsal. The length of centra decreases in several steps trough the caudal fin. Centra are numbered from anterior (0) to posterior.

Table 2: Correspondence between body regions and number of vertebral centra. For each area are reported the absolute and the percentage errors.

| | ID | Precaudal | | Caudal | Total |
|----------------------------|----------------------------|-------------|-------|------------|--------------|
| | | head region | trunk | caudal fin | total length |
| <i>Galeorhinus cuvieri</i> | MGP - PD 8871/8872 | 15 | 99 | 92 | 206 |
| | MCSNV T.1124 | 14 | 98 | 88 | 200 |
| | MCSNV VII.B.96 - 97 | 14 | 100 | 90 | 204 |
| | MGGC 1976 | 15 | 100 | 92 | 207 |
| | MNHN F.Bol.516 | 15 | 97 | ? | ? |
| <i>Eogaleus bolcensis</i> | MCSNV T.331 | 14 | 98 | ? | ? |
| | MGP - PD 8869/8870 | 15 | 98 | 89 | 202 |
| | Average | 14,6 | 98,6 | 90,2 | 203,8 |
| | Δa | 0,5 | 1 | 2 | 3,5 |
| | ε% | 3,4 | 1,0 | 2,2 | 1,7 |

Table 3: Correspondence between fin positions and number of centra. The total number of centra covered by fins is shown between parentheses.

| | i.D. | Pectoral fin | 1 st dorsal | Pelvic fin | 2 nd dorsal | anal fin | caudal fin |
|----------------------------|----------------------|------------------|------------------------|------------------|------------------------|-------------------|---------------|
| <i>Galeorhinus cuvieri</i> | MGP - PD 8871 - 8872 | 16th - 26th (11) | 24th - 42th (19) | 61th - 71st (11) | 87th - ? | 88th - ? | 115th - 206th |
| | MCSNV T.1124 | 15th - 29th (15) | 26th - 49th (24) | 64th - 78th (15) | 90th - 103th (14) | 88th - 99th (12) | 113th - 200th |
| | MCSNV VII.B.96/97 | 15th - 29th (15) | ? | 64th - 76th (13) | ? | 88th - 101th (14) | 115th - 204th |
| | MGGC 1976 | 16th - 32st (17) | 21th - 41th (21) | 61th - 76th (16) | 86th - 102th (17) | 89th - 98th (10) | 116th - 207th |
| | MNHN F. Bol.516 | 16th - 32th (17) | ? | ? | ? | ? | 113th - ? |
| <i>Eogaleus bolcensis</i> | MCSNV T.331 | 15th - 24th (10) | 22th - ? | ? | 86th - 102th (17) | ? | 113th - ? |
| | MGP - PD 8869 - 8870 | 16th - 27th (12) | 27th - 45th (19) | ? | 87th - 99th (13) | ? | 114th - 202th |
| | Average | 13,9 | 20,8 | 13,8 | 15,6 | 12 | |
| | Δa | 3,5 | 2,5 | 2,5 | 2 | 2 | |
| | $\epsilon\%$ | 25,3 | 12,0 | 18,2 | 12,8 | 17,0 | |

Table 4: Measurements of well – preserved specimens assigned to *G. cuvieri* and *E. bolcensis*, expressed in cm and %TL. The estimated vertebral centra of the characters 24, 25 and 26 are highlighted in orange.

| Fig.19 | <i>Galeorhinus cuvieri</i> | | | | | | | | <i>Eogaleus bolcensis</i> | |
|--------|----------------------------|-------|--------------|-------|-----------------|-------|-----------|-------|---------------------------|-------|
| | MGP - PD 8871 - 8872 | | MCSNV T.1124 | | MCSNV VII.B. 97 | | MGGC 1976 | | MGP - PD 8869 e 8870 | |
| | cm | %TL | cm | %TL | cm | %TL | cm | %TL | cm | %TL |
| 1 | 69,4 | 1 | 92,0 | 1 | 89,0 | 1 | 92,0 | 1 | 135,0 | 1 |
| 2 | 13,9 | 20,03 | 16,0 | 17,39 | 18,0 | 20,22 | 14,6 | 15,89 | 23,0 | 17,04 |
| 3 | 35,5 | 51,15 | 46,0 | 50,00 | 42,0 | 47,19 | 48,3 | 52,48 | 73,0 | 54,07 |
| 4 | 20,0 | 28,82 | 30,0 | 32,61 | 29,0 | 32,58 | 28,9 | 31,41 | 39,0 | 28,89 |
| 5 | 16,0 | 23,05 | 22,0 | 23,91 | ? | ? | 24,5 | 26,61 | 41,0 | 30,37 |
| 6 | 37,0 | 53,31 | 52,0 | 56,52 | 46,0 | 51,69 | 50,0 | 54,33 | 84,5 | 62,59 |
| 7 | 29,5 | 42,51 | 41,0 | 44,57 | ? | ? | 40,1 | 43,61 | ? | ? |
| 8 | 37,5 | 54,03 | 51,0 | 55,43 | 47,0 | 52,81 | 51,0 | 55,43 | ? | ? |
| 9 | 49,4 | 71,18 | 62,0 | 67,39 | 60,0 | 67,42 | 62,9 | 68,37 | 105,0 | 77,78 |
| 10 | 10,2 | 14,70 | 13,0 | 14,13 | ? | ? | 11,9 | 12,93 | ? | ? |
| 11 | 3,5 | 5,04 | 4,0 | 4,35 | 3,2 | 3,60 | 3,4 | 3,70 | 6,0 | 4,44 |

| | | | | | | | | | | |
|--------------------------------|------|-------|------|-------|------|-------|------|-------|------|-------|
| 12a | 6,0 | 8,65 | 10,0 | 10,87 | ? | ? | 10,0 | 10,87 | 14,0 | 10,37 |
| 12b | 8,2 | 11,82 | 14,0 | 15,22 | ? | ? | 13,0 | 14,13 | 19,0 | 14,07 |
| 12c | 8,0 | 11,53 | 5,0 | 5,43 | ? | ? | 7,8 | 8,48 | 8,5 | 6,30 |
| 13a | 4,0 | 5,76 | 5,0 | 5,43 | ? | ? | 6,4 | 6,96 | 6,0 | 4,44 |
| 13b | 7,8 | 11,24 | 6,0 | 6,52 | ? | ? | 8,6 | 9,35 | 11,0 | 8,15 |
| 13c | 5,8 | 8,36 | 4,0 | 4,35 | ? | ? | 4,2 | 4,57 | 8,0 | 5,93 |
| 14a | 4,0 | 5,76 | 5,0 | 5,43 | 6,5 | 7,30 | 8,2 | 8,87 | 10,0 | 7,41 |
| 14b | 8,6 | 12,39 | 10,0 | 10,87 | 15,0 | 16,85 | 14,3 | 15,52 | 19,0 | 14,07 |
| 14c | 6,6 | 9,51 | 10,0 | 10,87 | 11,5 | 12,92 | 11,9 | 12,93 | 15,5 | 11,48 |
| 15a | 4,2 | 6,05 | 5,8 | 6,30 | ? | ? | 4,2 | 6,52 | ? | ? |
| 15b | 4,5 | 6,48 | 4,7 | 5,11 | ? | ? | 5,1 | 5,54 | ? | ? |
| 15c | 1,2 | 1,73 | 3,5 | 3,80 | ? | ? | 2,0 | 3,80 | ? | ? |
| 16a | 4,6 | 6,63 | 5,0 | 5,43 | 5,0 | 5,62 | 4,1 | 4,43 | ? | ? |
| 16b | 5,2 | 7,49 | 7,0 | 7,61 | 7,0 | 7,87 | 4,4 | 4,80 | ? | ? |
| 16c | 1,8 | 2,59 | 2,5 | 2,72 | 3,5 | 3,93 | 1,7 | 1,85 | ? | ? |
| 17 | 15,0 | 21,61 | 18,0 | 19,57 | ? | ? | 17,3 | 18,80 | 31,6 | 23,41 |
| 18 | 4,5 | 6,48 | 5,5 | 5,98 | 6,7 | 7,53 | 5,3 | 5,76 | 9,0 | 6,67 |
| 19 | 13,5 | 19,45 | 19,0 | 20,65 | ? | ? | 16,2 | 17,61 | ? | ? |
| 20 | 3,5 | 5,04 | 4,2 | 4,57 | ? | ? | 5,1 | 5,54 | ? | ? |
| 21 | 4,3 | 6,20 | 5,0 | 5,43 | 4,0 | 4,49 | 7,1 | 7,72 | ? | ? |
| 22 | 6,5 | 9,37 | 9,0 | 9,78 | 7,0 | 7,87 | 7,0 | 7,61 | 6,5 | 4,81 |
| 23 | 11,3 | 16,28 | 16,0 | 17,39 | 11,8 | 13,26 | 15,9 | 17,28 | 24,0 | 17,78 |
| Vertebral centra counts | | | | | | | | | | |
| 24 | 206 | 106 | 200 | 0 | 204 | 1 | 207 | 6 | 202 | 42 |
| 25 | 114 | 37 | 112 | 0 | 114 | 0 | 115 | 1 | 113 | 29 |
| 26 | 92 | 69 | 88 | 0 | 90 | 1 | 92 | 5 | 89 | 13 |

Table 5: Measurements, ratios and estimates according to standard ratios of trunk and head region centra. Yellow highlighted values are the estimates performed according to trunk length. Turquoise highlighted values are the estimates according to centra of the head region. The orange cells indicate the averages of the estimated measurements for MSNPV 17716 (orange cells).

| Sample measurements | | | | | | |
|---|----------------|----------------------------|--|-----------------|------------------------------|--------------|
| | MSNPV 17716 | MGP - PD 8871 - 8872 | MGP - PD 8869 - 8870 | MCSNV T.1124 | MCSNV VII B 96 e VII B 97 | MGGC 1976 |
| Trunk (cm) | 89,3 | 35,5 | 73,0 | 46,0 | 42,0 | 48,3 |
| H. r. centra (cm) | 12,4 | 5,0 | 9,7 | 6,7 | 6,0 | 6,5 |
| Ratios according to trunk region and centra of the head region | | | | | | |
| | ratio (trunk) | | | | ratio (h. r. centra) | |
| Trunk (3) / Total length (1) | 0,51 | | Head region centra/Total length (1) | | 0,07 | |
| Trunk (3) / Head region (2) | 2,85 | | Head region centra/Head region (2) | | 0,36 | |

| | | | | |
|------------------------------|--------------------------|-----------------------------------|--------------------------|-------------------------------|
| Trunk (3) / Trunk (3) | 1 | Head region centra/Trunk (3) | 0,14 | |
| Trunk (3) / Caudal fin (4) | 1,66 | Head region centra/Caudal fin (4) | 0,25 | |
| Estimates | | | | |
| | Total length (cm) | Head region length (cm) | Trunk length (cm) | Caudal fin length (cm) |
| MSNPV 17716 (cm) | 175,2 | 31,4 | 89,3 | 53,8 |
| MSNPV 17716 (cm) | 174,8 | 31,3 | 89,0 | 53,7 |
| MSNPV 17716 (Average) | 175 | 31,4 | 89,1 | 53,8 |
| Δa | 0,21 | 0,01 | 0,16 | 0,03 |
| ε% | 0,12 | 0,03 | 0,18 | 0,1 |

Table 6: estimates of MSNPV 17716 according to the second approach. The yellow underlined values represent the estimated body measurements of 17716.

| | Total length (cm) | head region (cm) | Trunk length (cm) | caudal fin length (cm) |
|--|--------------------------|-------------------------|--------------------------|-------------------------------|
| MGP - PD 8871 e 8872 (Average, cm) | 173,3 | 34,7 | 88,7 | 50,0 |
| MCSNV T.1124 (Average, cm) | 174,4 | 30,3 | 71,7 | 56,9 |
| MCSNV VII B 96 e VII B 97 (Average, cm) | 186,6 | 37,7 | 88,1 | 60,8 |
| MGGC 1976 (Average, cm) | 172,8 | 27,5 | 90,7 | 54,3 |
| MGP - PD 8869 e 8870 (Average, cm) | 179,7 | 32,6 | 89,4 | 57,5 |
| MSNPV 17716 (Average, cm) | 177,4 | 32,6 | 85,7 | 55,9 |
| Δa | 6,9 | 5,1 | 9,5 | 5,4 |
| ε% | 3,9 | 15,8 | 11,1 | 9,7 |

6.2: Comparison of body ratios between extant and living specimens

The dataset of longitudinal measurements, counts of vertebral centra, and body ratios vs TL of both fossils specimens and thirty-four taxa belonging to the families Carcharhinidae, Hemigaleidae, Triakidae, Scyliorhinidae and Sphyrnidae was consequently performed in order to test the taxonomic resolutions for selected anatomical characters at family level. Data collected in this study were compared with those available in the literature (Compagno & Gilbert, 1983; Compagno & Stevens, 1993; Compagno et al., 1996; Compagno, et al., 2008;

Choy et al., 1998; Sato et al., 1999; Nakaya & Séret, 2000; White & Last, 2006; Séret & Last, 2007; Schaaf – Da Silva & Ebert, 2008; White & Ebert, 2008; Iglésias et al., 2012; McCosker et al., 2012; Weigmann, 2012; White & Harris, 2013; White & Weigmann, 2014; Famhi & White, 2015) The taxonomic identification of fossils follows Cappetta (1975). The matrix includes 68 characters (**Appendix E**).

The PCA produces 39 PC axes (**Fig. 33**). The PC1 and PC2 explain the 87,3% of the variance (PC1 = 70,2%; PC2 = 17,1%). The total length and total vertebral centra counts are the main characters, related to PC1, to contribute for the distribution of groups. Negative scores are correlated to small sized individuals, around < 73 cm total length. The fossil specimens of *G. cuvieri* are closely related and well separated from the unique individual of *E. bolcensis* plotted (MGP – PD 8869 – 8870; “fill square” symbols on **Fig. 33**). Indeed, *G. cuvieri* specimens are distant from the superimposition area, marking the bottom outline of the Triakidae morpho – space. The morpho – space of Hemigaleidae overlaps all projected areas of the considered families, excepted Sphyrnidae area. The Carcharhinidae area superimposes partially the groups of Scyliorhinidae and Triakidae. The one – way PERMANOVA test (Anderson, 2001a) apparently indicates that all clusters are well separated ($p = 0,0006$). A pairwise comparison indicates that the morphometrical characters among the Triakidae, Carcharhinidae and Sphyrnidae show no statistical significance ($p > 0,05$). The family Scyliorhinidae is well separated from Triakidae and Carcharhinidae clusters ($p < 0,05$), whereas uncorrected significances reveal no variance among Scyliorhinidae, Hemitriakidae and Sphyrnidae (**Table 7**).

Table 7: Pairwise p – values computed on the clusters considered. The orange cells indicate uncorrected significance between groups ($p > 0,05$).

| | Pairwise p - values | | | | |
|----------------|-----------------------|----------------|--------------|------------|----------------|
| | Triakidae | Carcharhinidae | Hemigaleidae | Sphyrnidae | Scyliorhinidae |
| Triakidae | | 0,4493 | 0,0616 | 0,2806 | 0,0001 |
| Carcharhinidae | 0,4493 | | 0,3974 | 0,4675 | 0,0017 |
| Hemigaleidae | 0,0616 | 0,3974 | | 0,1934 | 0,0533 |
| Sphyrnidae | 0,2806 | 0,4675 | 0,1934 | | 0,9359 |
| Scyliorhinidae | 0,0001 | 0,0017 | 0,0533 | 0,9359 | |

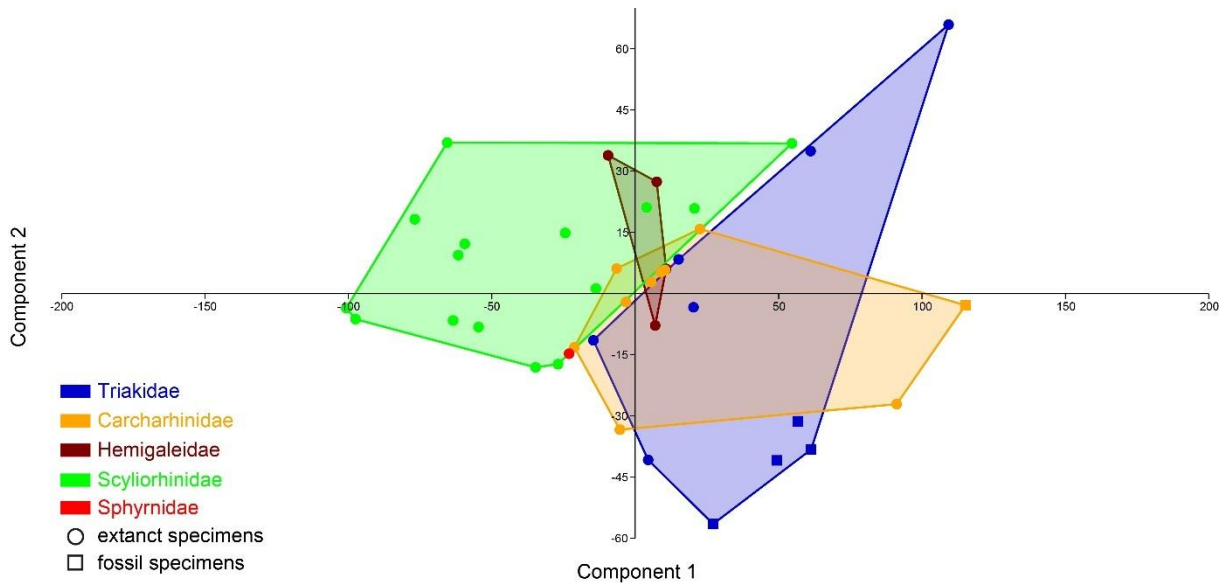


Figure 33: PCA diagram performed on longitudinal measurements, vertebral centra counts and body ratios dataset of Bolca Carcharhinids assemblage and extant taxa.

To provide the hierarchical groups computed by PCA, the analysis is supported by a neighbor joining – Cluster analysis. The cluster analysis performed with the same dataset supports PCA results (**Fig. 34**). Among the taxa considered, none of the specimens form phylogenetic outgroup. The shortest trees found arrange in two main monophyletic lineages: one including several species of Triakidae (*Galeorhinus galeus* and *Mustelus widodoi*), Carcharhinidae (*Glyphis glyphis*, *Carcharhinus humani*, *Eogaleus bolcensis*) and Scyliorhinidae (*Cephaloscyllium umbratile*, *Apristurus exsanguis*); the other lineage including taxa of all families considered. The fossil specimens of *G. cuvieri* closely cluster within a monophyletic group including taxa of Carcharhinidae, Hemigaleidae and Triakidae families. Excepted *C. umbratile* and *A. exsanguineus*, the family Scyliorhinidae is a paraphyletic group; the results are according to Iglésias et al. (2005), who provides the systematic affinities of the order Carcharhiniformes based on nuclear and mitochondrial – ribosomal genes.

Detailed analyses on body proportions within Carcharhinidae do not allow to infer the manner and timing of evolutive divergences. Ontogenetic variations, partly highlighted by morphometric analyses discussed here, appear a crucial aspect of the analyses as living sharks display remarkable inter- and intra-specific variations (Compagno & Gilbert, 1983; Compagno, 1984; Compagno & Stevens, 1993; Compagno et al., 1996; Compagno, et al., 2008; Choy et al., 1998; Sato et al., 1999; Nakaya & Séret, 2000; White & Last, 2006; Séret & Last, 2007; Schaaf – Da Silva & Ebert, 2008; White & Ebert, 2008; Iglésias et al., 2012; McCosker et al., 2012; Weigmann, 2012; White & Harris, 2013; White & Weigmann, 2014; Famhi & White, 2015). According to Compagno (1984), the arrangement of fins within Carcharhinidae, Hemigaleidae and Triakidae are related. The position of the first dorsal fin of scyliorhinid taxa is strongly posterior to head and pectoral fin (i.e. *Apristurus*, *Atelomycterus*, *Bythaelurus*, *Cephaloscyllium*, *Parmaturus*, *Pentanchus*, *Scyliorhinus*. Compagno, 1984; Sato et al., 1999; Nakaya & Séret, 2000; Séret & Last, 2007; Schaaf – Da Silva & Ebert, 2008; White & Ebert, 2008; Iglésias et al., 2012; McCosker et al., 2012). Moreover, the first dorsal fin is usually much smaller than the caudal fin (excepted in *Atelomycterus*) and the second dorsal could be absent (*Pentanchus*). The 1st dorsal fin arrangement remark higher ratios of the morphometrical character “head – 1st dorsal distance” (around 50%TL).

Body measurements representative of the Bolca shark assemblage display consistent affinities with living taxa, confirming little morphological variation the Carcharhiniformes. Wedge – shaped intermedial calcification of vertebral centra is a common anatomical component shared among Carcharhinidae, Hemigaleidae, Sphyrnidae and Triakidae. The number of vertebral centra is the sole character that significantly varies at species level. A total number of vertebrae close to or higher than 200 is rare. Among carcharhinids, several species of the genera *Carcharhinus*, *Galeocerdo*, *Glyphis*, *Hemitriakis*, *Prionace*, *Sphyrna*, *Triaenodon* show this diagnostic feature (Compagno & Stevens, 1993; Compagno et al., 2008; Ebert & Stehmann, 2013). Francis & Mulligan (1998) reported vertebral – precaudal centra length measurements for different ontogenetical classis of *Galeorhinus galeus*. Documented trends of living individual show several affinities with those of Bolca specimens (**Fig. 35**):

- 1) Vertebrae display a consistent increase in size from the 40th centrum; this trend is even more evident in adult individuals. The same trend has been observed in *G. galeus*.
- 2) decreasing after the maximum size peak. The grade of decreasing is higher in *G. galeus*, whereas the decreasing in fossils specimens is graded. Occasionally, peaks of maximum length occur around the 70th centrum.

G. galeus has 123 to 146 total centra, substantially less than vertebrae counts of *G. cuvieri* (200 – 207) and *E. bolcensis* (202 in the sole complete specimen MGP – PD 8869 – 8870). The 40th centrum in *G. galeus* correspond to the attachment of the pelvic fin (Francis & Mulligan, 1999), although in Bolca carcharhinids it is located anteriorly to the first dorsal fin. The size of individual centra is higher in *G. galeus* according to ontogenetical classis (**Fig. 35**).

Porter et al. (2016) recently studied the biomechanism of vertebral bending during swimming. Vertebral column acts as a non – linear viscoelastic spring due to the combined hyper – mineralized and unmineralized nature of centra. The frequency and amplitude of oscillations is strictly related to propulsion – brake balance of the individuals; high frequencies and low curvatures mark elastic behaviors, allowing to store and release the energy for swimming, whereas low frequencies and higher amplitude confer viscous behave that dissipate energy, essential for the brake. Probably, higher number of centra increase the plasticity of the vertebral column, although the energy carried by caudal fin is portioned proportionally to the number of centra, increasing viscous behave during swimming. On the contrary, low numbers of large centra allows more efficient swimming performances due to the higher stiffness of the vertebral column. According to size and number of centra in living and fossils taxa (Cappetta, 1987, 2012; Ebert & Stehmann, 2013), high vertebrae counts could be considered as an ancestor character. Therefore, Bolca specimens provide crucial data for our understanding of the origin of these anatomical features and their ecologically implications.

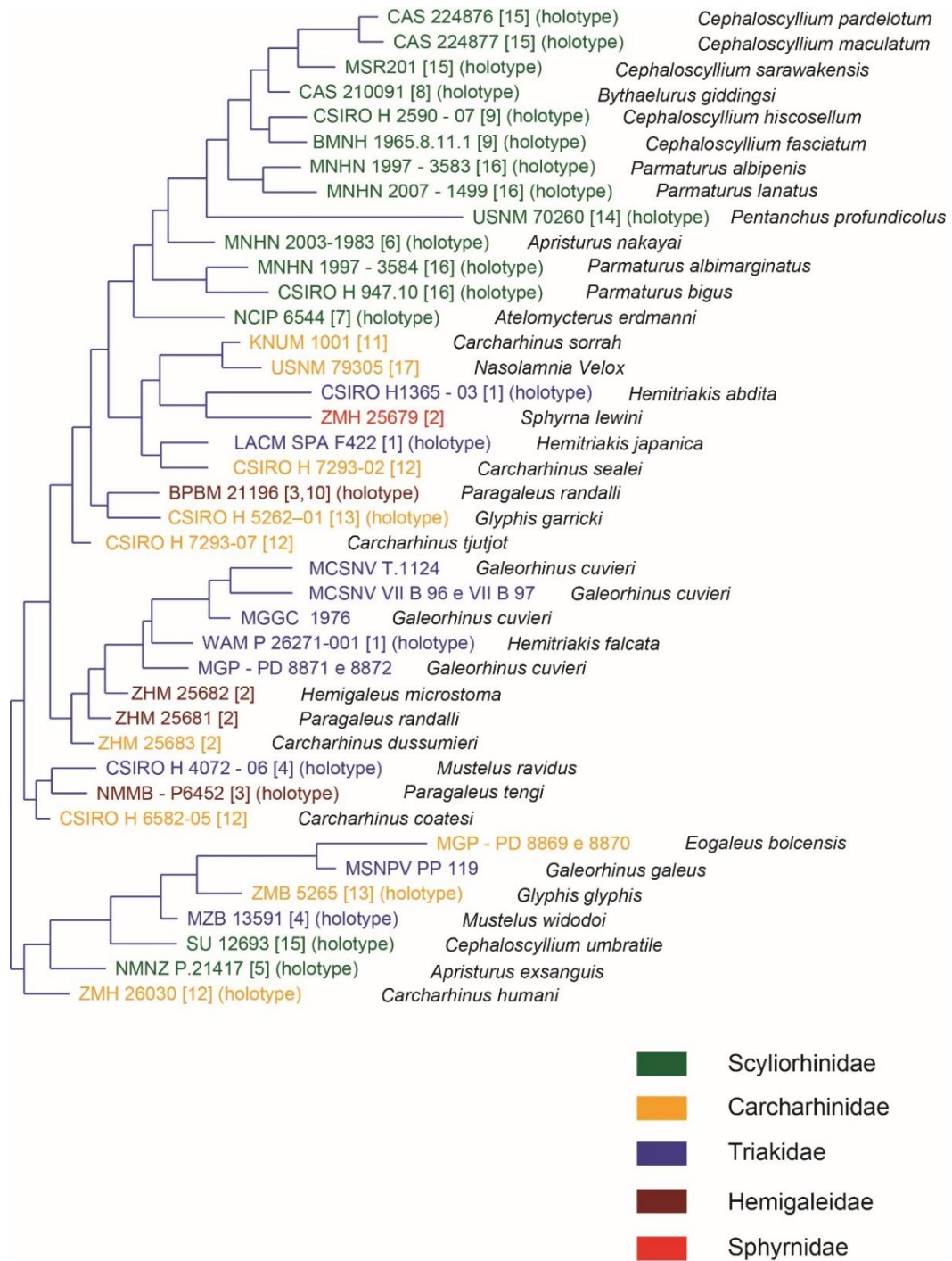


Figure 34: Strict topology of the shortest tree found by cluster analysis based on morphometrical dataset. The phylogenetic reconstruction computes two main groups. Specimens of *G. cuvieri* are well separated from *E. bolcensis*. The colors of I.D. indicate the family assessment of specimens. Numbers between squared parenthesis [#] indicate the referred paper found in references.

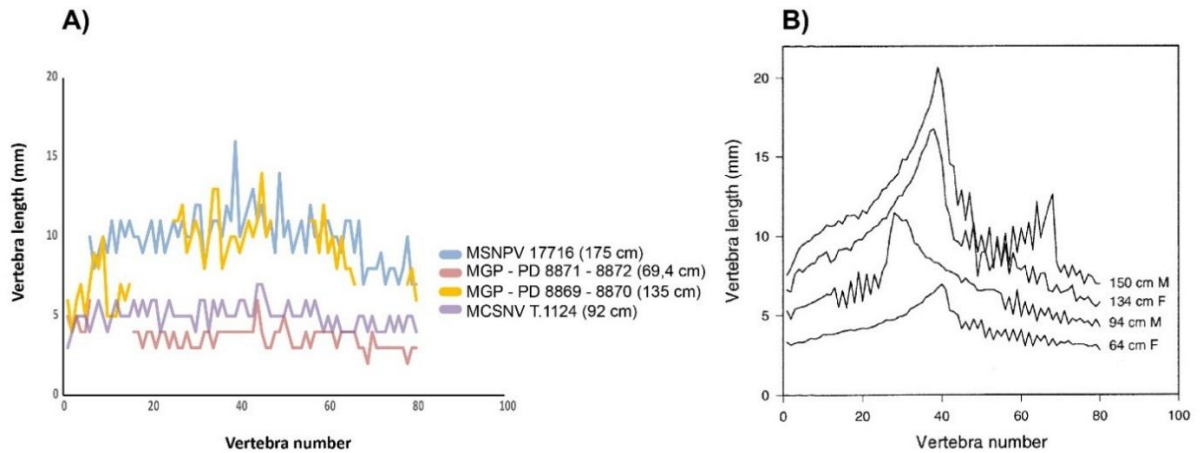


Figure 35: Comparison of trends of vertebra length between Bolca carcharhinids (A) and different ontogenetical classes of *G. galeus* (B; after Francis & Mulligan, 1999). Both graphs show similar trends from apical to distal part of the trunk. Vertebrae are numbered from anterior (0) to posterior (80).

6.3: Comparison of scale morphotypes between extant and living specimens

Dermal tissues of selachians is covered by dermal denticles, also known as placoid scales. The denticles consist of orthodontine and are anchored to skin with a pedestal. The top is a cusp laterally expanded (Helfman et al., 2009; Cappetta, 2012). The morphology of dermal denticles varies among species and within the same individual in different part of the body according to their specialized functions (Cappetta, 1975, 1987, 2012; Dillon et al., 2016; Ferrón & Botella, 2017). Fanti et al. (2016) provided additional information on skin patches of *Galeorhinus cuvieri* from Bolca. Samples of scales were collected from head, pectoral fin and trunk region of MGGC 1976. Three mainly morphotypes arrange on body areas (**Fig. 36; Table 8**):

- 1) *Morphotype C* (**Fig. 36A**): lanceolate scales with hexagonal micro – structures on the basal surface. The crown size measures approximately 160 μm . The crown thickness ratio is around 37 μm . Three distinct V – shaped peaks on the apical edge. Four subparallel ridges cross the denticle and join apically; the ridge spacing measures 40 μm in average. The upward pointing – spine is absent. The morphotype been reported from the cephalic area (Fanti et al., 2016);
- 2) *Morphotype D* (**Fig. 36B**): squared – shaped scales displaying hexagonal patterns on the basal surface. The crown size measures approximately 220 μm . The thickness ratio measures about 40 μm . No peaks are observed; denticle show a rounded apex. Four incomplete and parallel ridges extend up to the medial region, merging with the surface apically. Ridges are equidistantly arranged (ridge space approximately 40 μm). The upward pointing spine is absent. The scales morphotype has been recovered from the dorsal area of pectoral fins.

- 3) *Morphotype E* (**Fig. 36C**): elliptical to rounded, aligned scales with a smooth crown. Pecks, ridge, median spine and micro – ornamentations are absent. The crown size measures approximately 15 μm . The crown thickness is $< 5 \mu\text{m}$ in average. Fanti et al. (2016) reported this type from the abdominal region.

Cappetta (1975) described scales morphologies of *E. bolcensis*, focusing his diagnosis on preserved denticles patches of specimen MCSNV VII.B.94 (**Fig. 37A, B**). According to different areas of the body, he distinguished two mainly morphologies placoid scales:

- 1) irregular and relative large scales. The ridges vary in number. The furrows between ridges are shallow. This type of scale is reported from the head, pelvic and caudal regions of the specimens (**Fig. 37B**);
- 2) thick and sub – lozenge shaped scales, with longitudinal and deep furrows (**Fig. 37 A**). The number of furrows varies from 3 to 5. The anterior edge is irregular, and the posterior edge is rounded. The morphotype usually cover the second dorsal fin and ventral regions.

Data presented in this study document clear morphologic and morphometric differences between placoid scales of *G. cuvieri* and *E. bolcensis*. Overall, size and thickness values documented in morphotypes A and B are higher than in *G. cuvieri* (**Table 8**).

A comparison between preserved scales in *G. cuvieri*, *E. bolcensis* and MSNPV 17716 /17 support Cappetta (1975) assignments of specimen VII.B.94 to *E. bolcensis* (**Fig. 37C, D**). Consequently, MSNPV 17716 /17 is here referred to *Eogaleus bolcensis* (Cappetta, 1975).

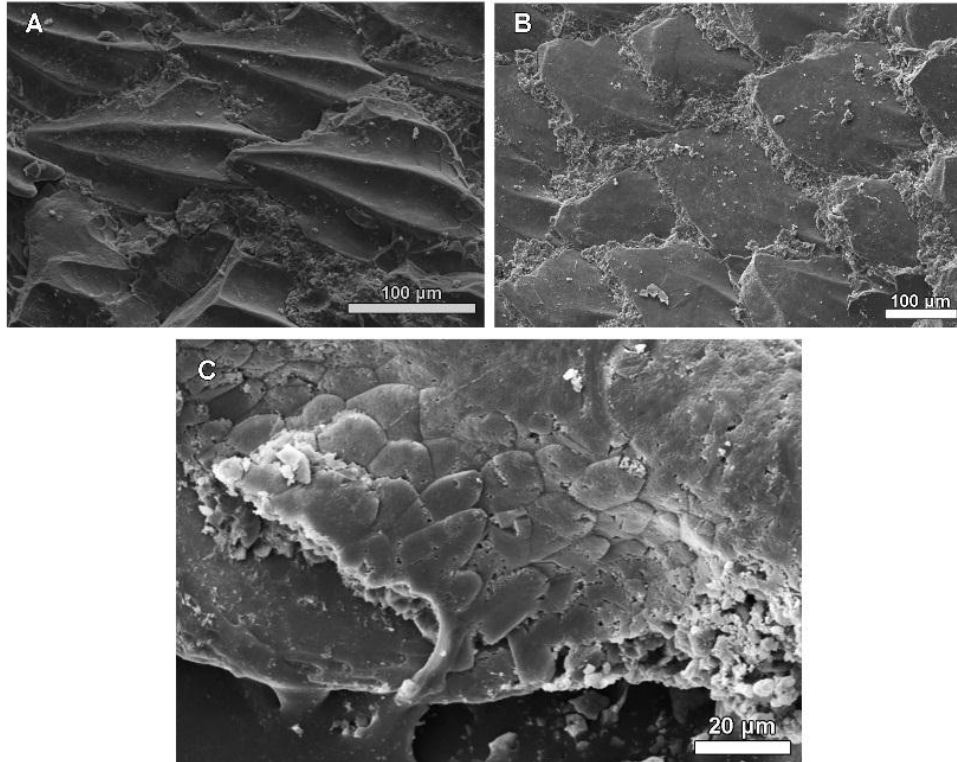


Figure 36: SEM micrographs of scale morphotypes from head (A), pectoral (B) and trunk regions of *G. galeus* (MGGC 1976). Scales varies in shape and dimension according to different body areas. Sections A and C after Fanti et al. (2016).

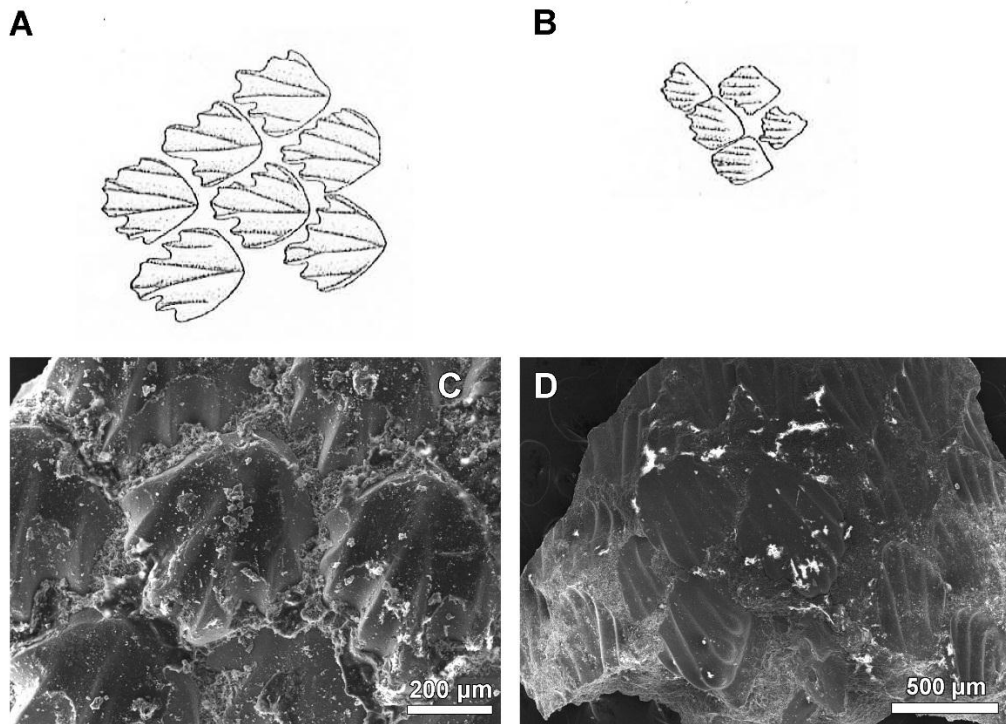


Figure 37: Comparison between the interpretative drawing of scales of MCSNV VII.B.94 (A, B; Cappetta, 1975) and scanned skin patches of MSNPV 17716 – 17717 (C, D). According to Cappetta (1975), “thick scales” (A) and “irregular – shaped denticles” (B) cover respectively the trunk and the pelvic fin of the individual. The description indicates affinities with *Morphotypes A* and *B* (images C, D) of MSNPV 17716 – 17717. Images A and B after Cappetta (1975), scale: 25x

Table 8: Approximately measurements of scale morphotypes. All values are expressed in μm . Morphotypes A, B refer to MSNPV 17716 – 17717 (yellow cells). Green cells indicate scale morphotypes of *G. cuvieri* (MGGC 1976). Measurements follow Dillon et al. (2016). *Abbreviations:* CL = crown length; CT = crown thickness; CW = crown width.

| | crown size ($\sqrt{\text{CL} \times \text{CW}}$) | thickness ratio ($\sqrt{\text{CL} \times \text{CW}}/\text{CT}$) | ridge spacing |
|---------------------|--|---|---------------|
| Morphotype A | 420 | 52 | > 100 |
| Morphotype B | 450 | 49 | < 100 |
| Morphotype C | 163 | 37 | < 100 |
| Morphotype D | 220 | 39 | < 100 |
| Morphotype E | 13 | 3 | - |

In a recent study, Dillon et al. (2016) documented scale morphological characters representative of different body areas for several species of sharks. In so doing, they defined six morphotypes based on overall shape and size providing for each a bio-mechanic interpretation. In particular, Dillon et al. (2016) recognize scales adaptations to: 1) *drag reduction*; 2) *abrasion strength*; 3) *defense type*; 4) *generalized functions*; 5) *ridged abrasion strength*; 6) *luminescence type*. The suggested categorization has also taxonomic resolution to a family level, based on shared morphological characters and variation across individuals/populations of the same species.

However, a few exceptions have been reported. The genus *Galeocerdo* is covered solely by defense – type placoid scales. This type of scale is virtually indistinguishable from *Morphotype A* of *E. bolcensis* (17716 – 17717). According to Applegate (1967) and Reif (1985a), the spines could prevent the settlement of epibionts and ectoparasites.

Morphotype B scales follow under the description of *general function* type scale. The shape is tear – dropped with rounded edges. Ridges are well separated, despite they apically decrease in size. Abrasion grooves or spines are absent. *Morphotypes C, D, E* collected from *G. cuvieri* follow under the description of *generalized function* – type scales. Although all types differ in shape and dimension, no anatomical characters suggest any specialized functions (i.e. lack of well separated ridges crossing the entire surface, superficial and random grooves, spines).

According to Dillon et al. (2016), a unique combination of defense and general functions morphotypes characterize the family Carcharhinidae. Defense type scales of *Eogaleus bolcensis* show closely morphological affinities to denticles of the genus *Galeocerdo* (**Fig. 38**). The analysis also supported the interpretation proposed by Applegate (1978), who suggested an *Eogaleus* – *Galeocerdo* lineage. Within Carcharhiniformes, the species characterized by the sole generalized function – type scales correspond to the family Triakidae (Dillon et al., 2016). In addition, *Galeorhinus galeus* reveals ontogenetic variations in scales morphologies; juvenile individuals are mainly covered by defense – type scales and generalized function denticles (Ferrón & Botella, 2017).

Defense – type scales are replaced by drag – reduction scales in adults. Moreover, Fanti et al. (2016) remarked the morphological denticle affinities between *Galeorhinus cuvieri* and an adult female individual of *G. galeus*.

Two main functional morphotypes cover the skin of *G. galeus* (**Fig. 39**).

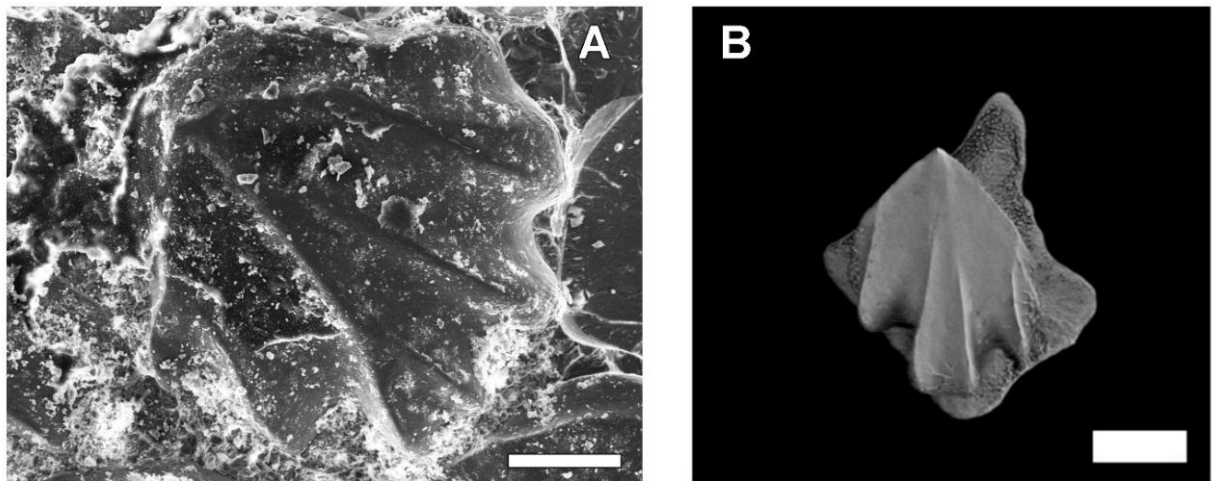


Figure 38: Comparison between MSNPV 17717 (A) and *Galeocerdo cuvieri* (B) based on SEM imaging. Both scales are defense – type. Skin samples were collected from the trunk region (17717; A) and the dorsal edge of caudal fin (*Galeocerdo*; B). Scales are arched, with thick ridges arranged subparallel. The upward pointing – spine emerges posteriorly on surface, due to the convergence of ridges. Peaks are rounded. The scales differ in number of ridges and sizes. Image B after Dillon et al. (2016). Scale bar = 100 μ m

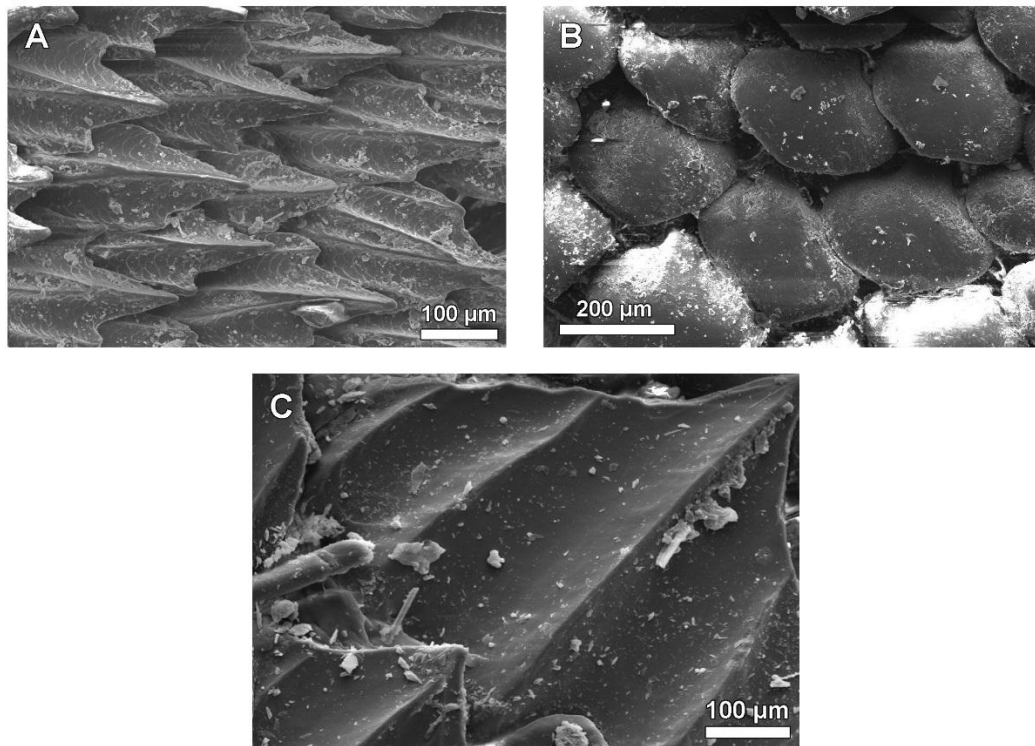


Figure 39: SEM micrographs of *Galeorhinus galeus* denticles from pectoral fin (A), trunk (B) and head (C) regions. Placoid scales of sections A and B are *generalized function* types, showing close morphological affinities to those of *G. cuvieri*. Section C is a detailed imaging of *drag reduction* type scale; ridges are thick, arranged parallel and well separated.

6.4: Comparison of tooth morphotypes between extant and living specimens

The dentition of Chondrichthyes are polyphyodont (i.e. teeth are replaced many times during the life of individuals. Moss, 1967; Kemp, 1999) and lyodont (i.e. teeth are not strongly anchored on jaws. Moss, 1967; Kemp, 1999). Teeth are formed by biogenic phosphate and consist of an enameloid – covered part, the crown, and a basal part, the root (Cappetta, 2012). The morphologies and their disposition on jaws (i.e. number of teeth per rows and number of files) are differentiated among taxa, at genus and species levels (Cappetta, 1987; 2012). Numerical data are nowadays commonly elaborated to further define affinities and divergences among taxa or to identify tooth position on jaws according to their functional morphologies (Adnet, 2006; Nyberg et al., 2006; Whitenack & Gottfried, 2010; Takács, 2012; Marammà & Krivet, 2017; Maramma et al., 2017). In this study, two complete jaws of *Galeorhinus galeus*

(uncatalogued, kindly lent from private collection) and *Galeocerdo cuvieri* (MACB 2428) were used as standards of the respective families, Triakidae and Carcharhinidae, in order to test statistic methodologies. Teeth of each samples were plotted separately to the referred standards. All matrices include 29 characters, including quantitative and qualitative features, as well as significative ratios (**Appendix F**). The significance of the variances between groups clustered by PCA were tested with the non – parametric, one – way PERMANOVA (Anderson, 2001a). To solve the Gaussian distributions, the measurements were log – transformed, “flattening” values on their fitted trends. This step overcomes the problem of a non – normal distribution of dataset according to Marammà & Kriwet (2017). The authors elaborated data even with standardization to remove any size – effects of isolated teeth. However, this approach is not applied in this thesis as the total height of teeth is one of the main character that reflect tooth positions on jaws.

The jaws of *Galeorhinus galeus* (Linnaeus, 1758) counts 34 teeth on Meckel’s cartilage, arranged in 5 files, and 36 teeth on palatoquadrate, arranged in 4 files. Teeth of each file are arranged alternate on jaws (**Fig. 40**). The dentition is slightly heterodont and cutting – type (Compagno, 1987; 2012). The vascularization of root is holaulacorhizid type (Hermann et al., 1991). The statistical analysis does not consider the posteriormost, lateral lower tooth (i.e. 34th according to the established counts); the size of this tooth is under the nearest resolution adopted for measurements. The PCA analysis produces 29 PC axes, in which PC1 and PC2 explain the 74,9% of the variance ($p < 0,05$; **Fig. 41**). The number of cusplets and serrations on mesial edge are the main characters, related to PC1 and PC2, which contribute for the distribution of teeth. Morphospaces of lateral and anterior teeth of both jaws show clear superimposition. Anterior teeth are more differentiated on the upper jaw. Nevertheless, the central teeth are clearly distinct, reflecting different functional roles in predation. d/c ratio ranges vary for lower and upper teeth (**Table 10**).

Teeth of *Galeocerdo cuvier* (MACB 2428; Müller & Henle, 1837; **Fig. 42**) count 23 per file on lower jaw (total file number = 5) and 20 per file (total file number = 4) on upper jaw. The dentition is homodont and cutting – type (Cappetta, 1987, 2012; Hermann et al., 1991), with teeth aligned and well separated to each on jaws. The vascularization of the root is anaulacorhizid due to lack of median groove (i.e. the most archaic root vascularization type; Casier. 1947 A, B, C; Cappetta, 2012); it is atypical character for a carcharhinid. The PCA analysis produces 28 PC axis. The PC1 and PC2 explain the 78,9% of the variance ($p < 0,05$; **Fig. 43**). The mesial edge measures and the morphology of labial face are the main characters, related to PC1 and PC2, which contribute for the distribution of teeth. The morphospaces of lateral teeth of both jaws show a strongly overlap. Anterior and central teeth are well separated to each them. A pairwise comparison of p – values marks strongly affinities between anterior and central and anterior upper teeth. Teeth are sub – triangular and asymmetric. The d/c ratio values are listed in **Table 10**.

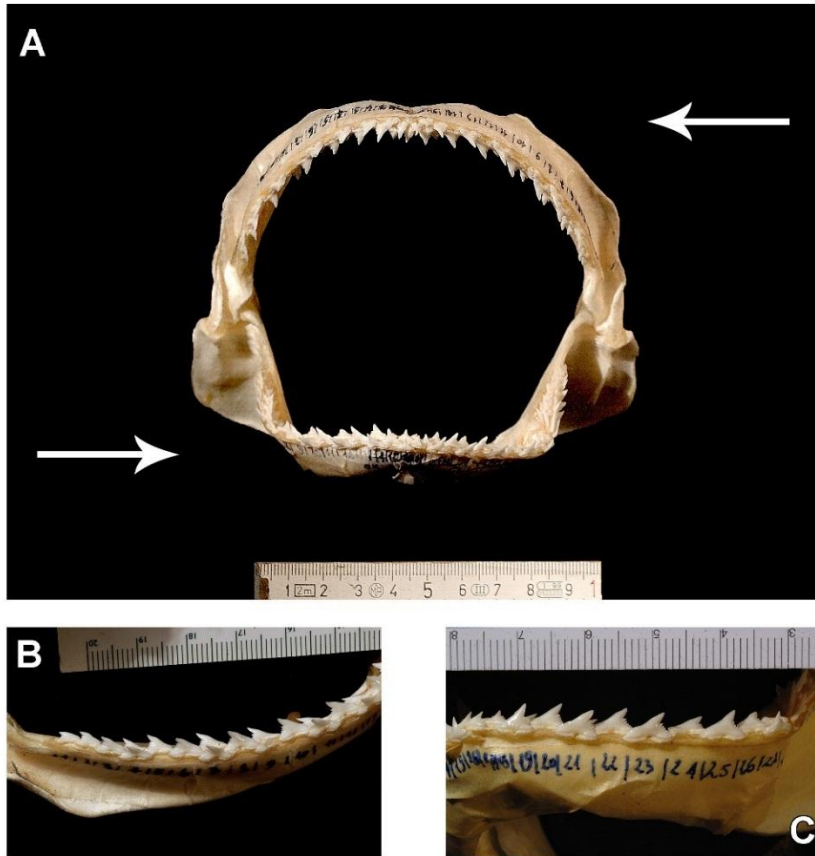


Figure 40: A) Upper and lower jaws of *Galeorhinus galeus*. The arrows indicate the direction of the numerical system adopted for teeth counts: from lateral left to lateral right teeth for upper jaw and from lateral right to lateral left teeth for lower jaw. B) Focus of the upper left lateral teeth; C) focus of the lower left hemimandible.

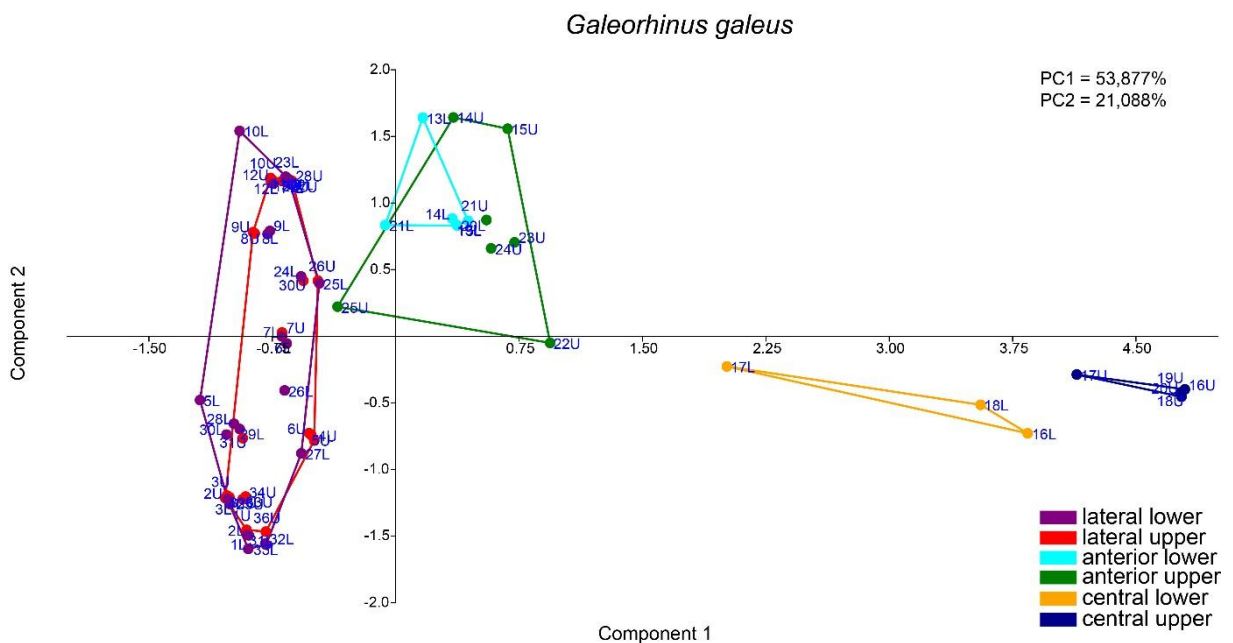


Figure 41: PCA computed on teeth dataset of *G. galeus*. The colored morphospaces indicate the tooth categories for each jaw.

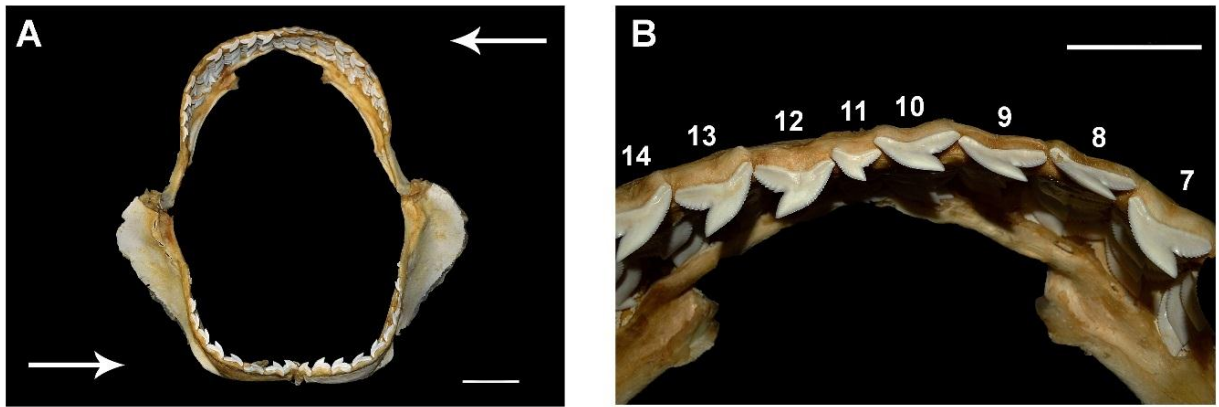


Figure 42: A) Upper and lower jaws of *Galeocerdo cuvier* (MACB 2428). The arrows indicate the direction of the numerical system adopted for teeth counts: from lateral left to lateral right teeth for upper jaw and from lateral right to lateral left teeth for lower jaw. B) Focus of the upper teeth from the 7th to 14th (7th, 8th, 9th, 13th, 14th upper lateral; 10th, 12th, upper anterior; 11th, upper central). Scale bar = 5 cm

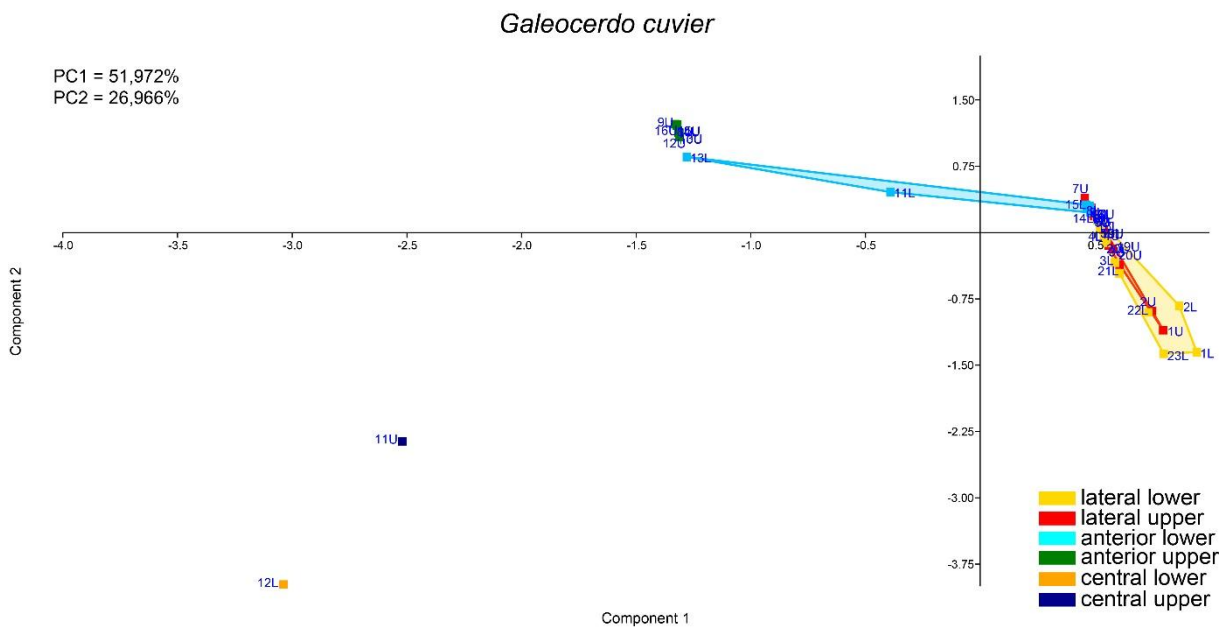


Figure 43: PCA performed on teeth dataset of *G. cuvier*. Colored morphospaces indicate the tooth position on upper and lower jaws.

Table 9: pairwise comparison of p – values between teeth of *G. cuvieri*. The orange cells indicate uncorrected significance among groups ($p > 0,05$).

| | lateral upper | anterior upper | central upper | lateral lower | anterior lower | central lower |
|----------------|---------------|----------------|---------------|---------------|----------------|---------------|
| lateral upper | | 0.0001 | 0.085 | 0.1261 | 0.0001 | 0.0795 |
| anterior upper | 0.0001 | | 0.1109 | 0.0001 | 0.0001 | 0.11 |
| central upper | 0.085 | 0.1109 | | 0.0786 | 0.0913 | 1 |
| lateral lower | 0.1261 | 0.0001 | 0.0786 | | 0.0014 | 0.0753 |
| anterior lower | 0.0001 | 0.0001 | 0.0913 | 0.0014 | | 0.0892 |
| central lower | 0.0795 | 0.11 | 1 | 0.0753 | 0.0892 | |

Table 10: d/c ratio values of *G. galeus* and *G. cuvieri*.

| | lateral lower | anterior lower | central lower | lateral upper | anterior upper | central upper |
|---------------------------------------|---------------|----------------|---------------|---------------|----------------|---------------|
| <i>Galeorhinus galeus</i> | 0,38 - 0,67 | 0,71 - 0,83 | 0,88 - 0,89 | 0,5 - 0,77 | 0,89 - 1,13 | 1,25 - 1,67 |
| <i>Galeocerdo cuvieri</i> (MACB 2428) | 0,54 - 0,68 | 0,77 - 0,86 | 1,14 | 0,42 - 0,74 | 0,8 - 0,87 | 0,92 |

Teeth of the genus *Galeorhinus* are problematic to discriminate on statistic approach due to the strong similarities shared by lateral and anterior teeth of both jaws (Compagno, 1984; Cappetta, 1987, 2012; Hermann et al., 1991; this study). With the exception of the central teeth, a qualitative analysis simply discriminate lateral from anterior teeth. In so doing, outputs remark that the inclination of the main cusp, the serrations on mesial edge, the distal angle, number of cusplets are the main key features to define general classes. The d/c ratio values reflect the same assessment. Teeth of *G. cuvieri* reveals several affinities to *G. galeus* dentition:

- 1) The morphotypes “A” and “D” are considered as lateral and anterior teeth. The total height is never higher than 5 mm. Both morphotypes are subtriangular with the distal edge bearing cusplets as anterior and lateral teeth of *G. cuvieri*. Lateral teeth are wider than high. On the contrary, anterior teeth are more developed in height. The mesial edge of *G. galeus* is strongly sigmoidal – shaped; these character lacks in *G. cuvieri* dentition. The cusplets on distal edge count from 3 to 5 on *G. galeus* and maximum 4 in *G. cuvieri*. The distal edge of *G. galeus* is more inclined apically than *G. cuvieri*. According to d/c ratios of *G. galeus* (Table 10), teeth No. 25, 27, 31 and 50 of MGGC 1776 are probably anterior upper teeth; the d/c ratio ranges from 1 to 1,17.
- 2) The morphotype “B”, exclusively preserved in the specimen MCSNV VII.B.96, is a lower central tooth. The tooth is subtriangular and symmetrical as those of *G. galeus*, despite lacks cusplets on edges. Indeed, the main cusp in slender, with its height approximately the half of crown height.
- 3) The morphotype “C” is absent in *G. galeus*. The tooth is preserved solely on the upper jaw of the specimen MCSNV T.1124 and it represents most likely an upper tooth; the morphology has several affinities with anterior upper teeth of *G. galeus*, despite the edges lack serrations and cusplets.

The tooth positions along the dental series of *E. bolcensis* can be interpreted as follows: morphotype “A” and “D” are lateral and anterior teeth. Cappetta (1975) classified the cutting – type of the specimens as lower lateral or upper lateral teeth. The interpretation is not valid; according to Carcharhiniformes field marks (Compagno, 1984; Ebert & Stehmann, 2013), the individuals characterized by a strongly dignathic heterodonty have cutting – type teeth on upper jaw and blade – like teeth arranged on lower jaw. Therefore, the bladelike – morphotypes “B” and “E” are lower central and lateral/anterior teeth. Among teeth clustered in morphotype “B”, the overall morphology and ratios are similar, hence the correct anatomical position of teeth is uncertain. The morphotype “C” is exclusively preserved on the specimens MSNPV 17716 and MGP – PD 8870 (tooth No. 17; **Appendix C8**). The morphologies of tooth show several affinities with the triangular – asymmetric upper central teeth of *G. galeus*. Teeth belonging to morphotype “F” are upper central, probably the most closer to the symphysis of the palatoquadrate. The PCA analysis indicates optimal distributions of teeth classes for singular individuals or for populations of the same species (Marammà & Kriwet 2017), marking the functional variety of dental types. To provide the anatomical categorization of fossil teeth based on statistical approach, Bolca specimens are compared one by one with teeth dataset of the adopted standard. The analysis reveals conflicting results: for example, the comparison between MCSNV VII.B.96 – 97 and *G. galeus* show a partial overlap among morphotype “A” and lateral upper – lower teeth of *G. galeus* and an isolated cluster for the morphotype “B” (**Fig. 44**). According to pairwise comparison of *p* – values (PERMANOVA test), the morphotype “A” clearly discriminated from all categorized teeth of *G. galeus* ($p < 0,05$), despite the morphotype “B” shows no significant variance with *G. galeus* teeth (**Table 11**). Comparing the same fossil specimen to *Galeocerdo cuvier*, all morphotypes are diversified from teeth of the chosen standard (**Fig. 45**). The pairwise comparison (PERMANOVA test) among considered clusters indicates that the morphotype “A” is similar to lower central teeth of *G. cuvier* ($p > 0,05$), whereas the morphotype “B” has no significant variance with both central upper and lower teeth of *G. cuvier* (**Table 12**). The comparison between the other fossil specimens indicate the same results (pairwise *p* – values in **Appendix G**). Hence, the qualitative characters of each tooth and significant ratios have higher resolution than the statistical approach to categorize the tooth position.

Table 11: Pairwise comparison between teeth categories of *G. galeus* and morphotypes “A” (A) and “B” (B) of MCSNV VII.B.96 – 97. The orange cells indicate uncorrected significance among groups ($p > 0,05$).

| MCSNV VII.B.96 – 97/ <i>Galeorhinus galeus</i> pairwise comparison | | | | | | | | |
|--|---------------|----------------|---------------|---------------|----------------|---------------|--------|--------|
| | lateral upper | anterior upper | central upper | lateral lower | anterior lower | central lower | A | B |
| lateral upper | | 0.0003 | 0.0001 | 0.0154 | 0.0001 | 0.0003 | 0.0001 | 0.157 |
| anterior upper | 0.0003 | | 0.0039 | 0.0884 | 0.0007 | 0.0102 | 0.0001 | 0.1258 |
| central upper | 0.0001 | 0.0039 | | 0.0002 | 0.226 | 0.1941 | 0.0005 | 0.4986 |
| lateral lower | 0.0154 | 0.0884 | 0.0002 | | 0.0001 | 0.001 | 0.0001 | 0.1543 |
| anterior lower | 0.0001 | 0.0007 | 0.226 | 0.0001 | | 0.5312 | 0.0001 | 0.4263 |
| central lower | 0.0003 | 0.0102 | 0.1941 | 0.001 | 0.5312 | | 0.0009 | 0.2531 |
| A | 0.0001 | 0.0001 | 0.0005 | 0.0001 | 0.0001 | 0.0009 | | 0.3587 |
| B | 0.157 | 0.1258 | 0.4986 | 0.1543 | 0.4263 | 0.2531 | 0.3587 | |

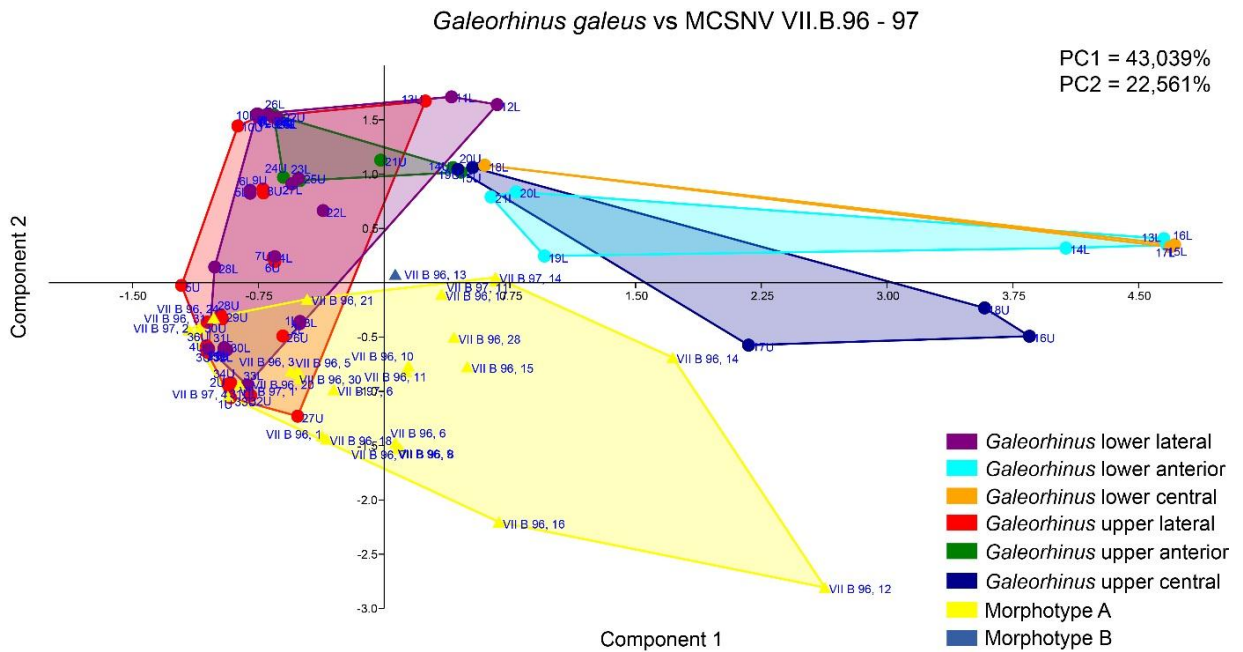


Figure 44: PCA computed between *G. galeus* and MCSNV VII.B.96 – 97 teeth dataset. The morphotype “A” (yellow morphospace area) show a partial superimposition with both lateral upper and lower teeth (red and violet areas). The morphotype “B” (light blue filled triangle) clusters as a diversified morphospace.

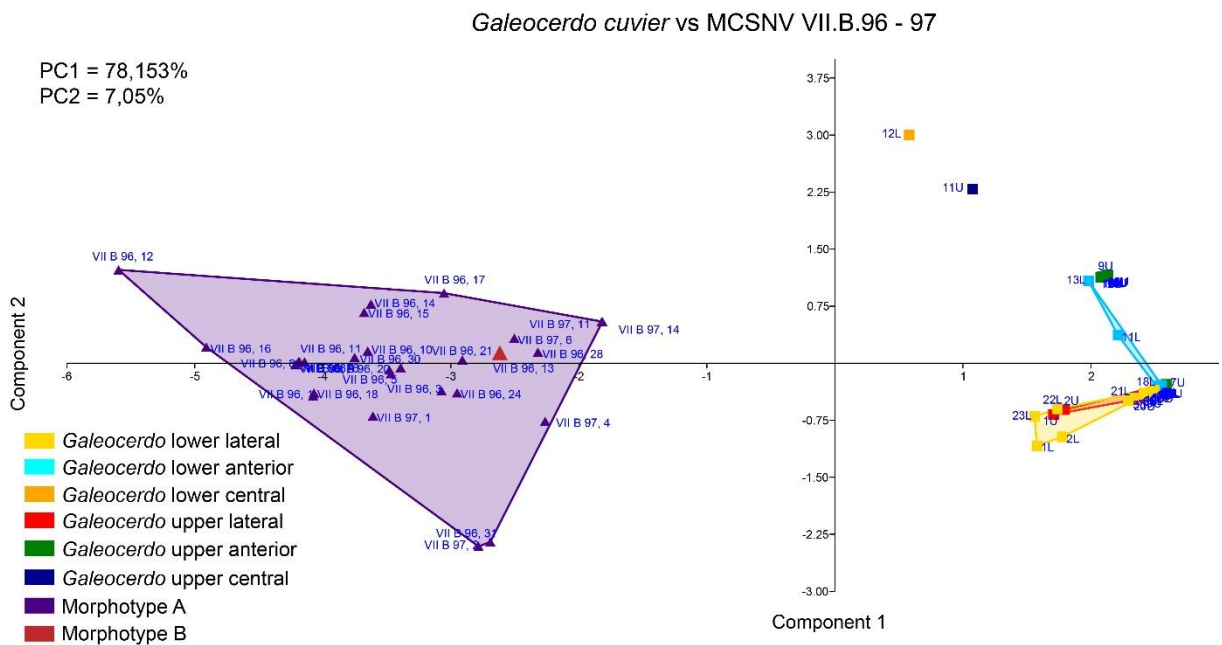


Figure 45: PCA computed between *G. cuvier* and MCSNV VII.B.96 – 97 teeth dataset. The morphotypes “A” (violet morphospace area) and “B” (red coral filled triangle) cluster as a diversified morphospaces.

Table 12: Pairwise comparison between teeth of *G. cuvier* and morphotypes “A” (A) and “B” (B) of MCSNV VII.B.96 – 97. The orange cells indicate uncorrected significance among groups ($p > 0,05$).

| MCSNV VII.B.96 – 97/ <i>Galeocerdo cuvier</i> pairwise comparison | | | | | | | | |
|---|---------------|----------------|---------------|---------------|----------------|---------------|--------|--------|
| | lateral upper | anterior upper | central upper | lateral lower | anterior lower | central lower | A | B |
| lateral upper | | 0.0001 | 0.083 | 0.127 | 0.0002 | 0.0843 | 0.0001 | 0.0859 |
| anterior upper | 0.0001 | | 0.1152 | 0.0001 | 0.0001 | 0.1061 | 0.0001 | 0.1123 |
| central upper | 0.083 | 0.1152 | | 0.075 | 0.0891 | 1 | 0.0368 | 1 |
| lateral lower | 0.127 | 0.0001 | 0.075 | | 0.001 | 0.0728 | 0.0001 | 0.0798 |
| anterior lower | 0.0002 | 0.0001 | 0.0891 | 0.001 | | 0.0941 | 0.0001 | 0.0911 |
| central lower | 0.0843 | 0.1061 | 1 | 0.0728 | 0.0941 | | 0.0385 | 1 |
| A | 0.0001 | 0.0001 | 0.0368 | 0.0001 | 0.0001 | 0.0385 | | 0.3638 |
| B | 0.0859 | 0.1123 | 1 | 0.0798 | 0.0911 | 1 | 0.3638 | |

All teeth included in the database are compared with dental morphologies of both extant and living specimens found in literature to provide affinities at genus level. The dataset includes 220 teeth, arranged in 20 species (*Chaenogaleus macrostoma*, *Eogaleus bolcensis*, *Galeocerdo cuvier*, *Galeorhinus cuvieri*, *G. duchaussoisi*, *G. galeus*, *G. louisi*, *G. minor*, *G. ypresiensis*, *Galeorhinus sp.*, *Galeorhinus sp.1*, *Galeorhinus sp.2*, *Hemigaleus microstoma*, *Hemitriakis falcata*, *Pachygaleus lefevrei*, *Paragaleus pectoralis*, *Physogaleus latecuspidatus*, *P. secundus*, *P. tertius*, *Physogaleus sp.*; Cappetta, 1975, 1980; Hermann et al., 1991; Compagno & Stevens, 1993; Müller, 1999; Rana et al., 2004, 2006; Adnet & Cappetta, 2008) 9 genera (*Chaenogaleus*, *Eogaleus*, *Galeocerdo*, *Galeorhinus*, *Hemigaleus*, *Hemitriakis*, *Pachygaleus*, *Paragaleus*, *Physogaleus*) and 3 families (Carcharhinidae, Hemigaleidae, Triakidae). The PC components 1 and 2 explicate the 55,9% of the variance (**Fig. 46**). The p – values permuted 9999 times is $< 0,05$. The distribution shows a general superimposition among taxa, with the exception of the genus *Galeocerdo*. The pairwise comparison of the significance between groups (**Table 13**) indicates:

- 1) The genus *Eogaleus* shows no variance between *Pachygaleus* and *Chaenogaleus*. *Pachygaleus* (Cappetta, 1992b; Adnet & Cappetta, 2008) is an extinct taxon belonging to the family Triakidae. Teeth are cutting – type and exceed 1 cm of total width. The size of teeth shows several affinities with the lateral upper teeth of *E. bolcensis*. Nevertheless, the mesial edge is concave, and the distal edge bears higher number of cusplets than *Eogaleus* teeth. Indeed, the dentition of *Pachygaleus* is homodont – type. The dentition of *Chaenogaleus* (Family Hemigaleidae) is dignathic heterodonty (Hermann et al., 1991). The mesial edge of cutting – type teeth in *Chaenogaleus* is sigmoid and the distal edge might bear up to 5 cusplets. Unlike *E. bolcensis*, the edges of bladelike – lower teeth are well rounded and upward inclined in *Chaenogaleus*. Moreover, the size of teeth is different between the two considered taxa. Both the species *E. bolcensis* and *G. cuvier* show several affinities to the extinct triakid *Pachygaleus*.

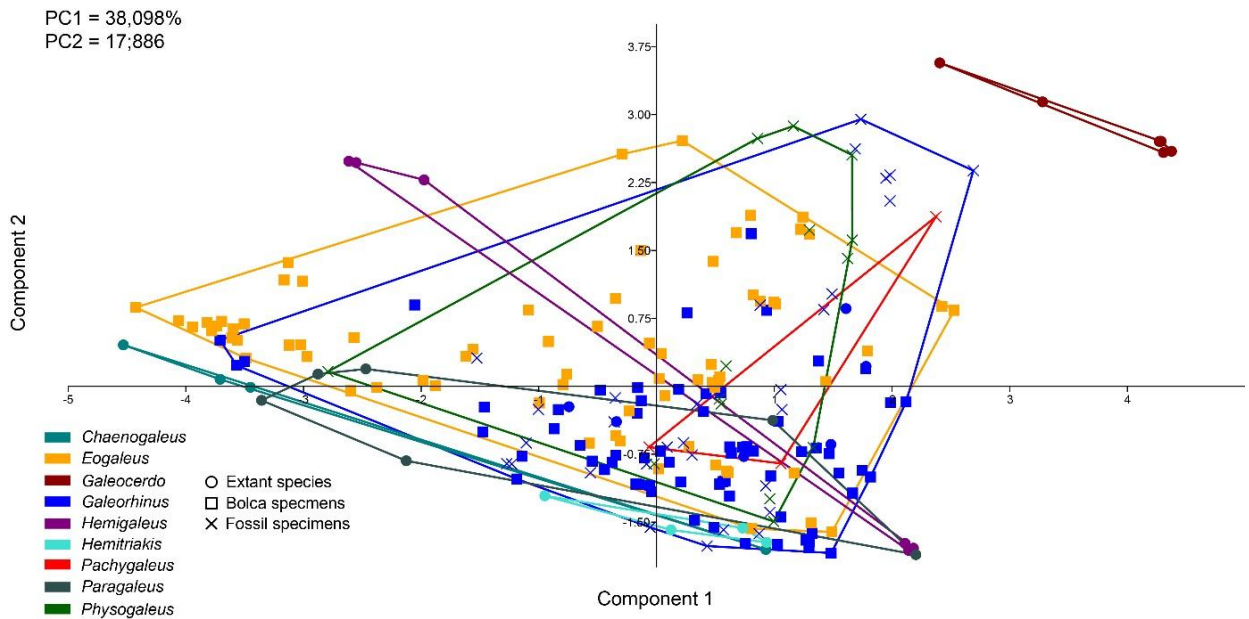


Figure 46: PCA performed on teeth dataset of extant and fossil specimens. The genus *Galeocerdo* is well differentiated

Table 13: pairwise comparison of p - values computed with one - way PERMANOVA. The orange cells indicate the uncorrected significance ($p > 0,05$)

| | <i>Eogaleus</i> | <i>Galeorhinus</i> | <i>Pachygaleus</i> | <i>Physogaleus</i> | <i>Hemigaleus</i> | <i>Chaenogaleus</i> | <i>Paragaleus</i> | <i>Hemitriakis</i> | <i>Galeocerdo</i> |
|---------------------|-----------------|--------------------|--------------------|--------------------|-------------------|---------------------|-------------------|--------------------|-------------------|
| <i>Eogaleus</i> | | 0.0001 | 0.0246 | 0.0011 | 0.004 | 0.0122 | 0.0043 | 0.0007 | 0.0001 |
| <i>Galeorhinus</i> | 0.0001 | | 0.049 | 0.002 | 0.0036 | 0.0008 | 0.0009 | 0.0093 | 0.0001 |
| <i>Pachygaleus</i> | 0.0246 | 0.049 | | 0.1031 | 0.3536 | 0.0352 | 0.0813 | 0.0187 | 0.0114 |
| <i>Physogaleus</i> | 0.0011 | 0.002 | 0.1031 | | 0.0466 | 0.0022 | 0.0024 | 0.0052 | 0.0001 |
| <i>Hemigaleus</i> | 0.004 | 0.0036 | 0.3536 | 0.0466 | | 0.2761 | 0.3174 | 0.1787 | 0.0025 |
| <i>Chaenogaleus</i> | 0.0122 | 0.0008 | 0.0352 | 0.0022 | 0.2761 | | 0.5537 | 0.074 | 0.0028 |
| <i>Paragaleus</i> | 0.0043 | 0.0009 | 0.0813 | 0.0024 | 0.3174 | 0.5537 | | 0.0781 | 0.002 |
| <i>Hemitriakis</i> | 0.0007 | 0.0093 | 0.0187 | 0.0052 | 0.1787 | 0.074 | 0.0781 | | 0.002 |
| <i>Galeocerdo</i> | 0.0001 | 0.0001 | 0.0114 | 0.0001 | 0.0025 | 0.0028 | 0.002 | 0.002 | |

2) The genus *Galeorhinus* differs from all the genera considered, but not with the genus *Pachygaleus*. The size, mesial edge shape and number of cuspltes arranged on distal edge are clearly characters that differs from the two genera. The hypothesis suggested by Adnet & Cappetta (2008), concerning the similarities between Bolca triakids and the genus *Physogaleus*, is not valid ($p = 0,002$; **Table 13**). Unlike *G.*

cuvieri, the dentition of the genus *Physogaleus* is characterized by a strong dental dimorphism marked in anterior teeth (Cappetta, 2012).

6.5: Age and size estimates

Despite efforts to discriminate genus/species variability based on vertebral centra (number, size, etc.), analyses must include ontogenetic calibrations (**Fig. 47, 48**). Values referred to trunk length, sum of centra of the head region and centra length averages of the respectively body regions are listed in **Table 14 and 15**. Trend lines of both diagrams indicate a consistent linearity between specimens (see R^2 values; **Fig. 47, 48**), due to affinities of morphological, number and morphometrical proportions of centra. All specimens of *G. cuvieri* cluster in discrete groups. The centra length averages of the trunk region range from a minimum of 3,5 mm (MGP – PD 8871 – 8872) to a maximum value of 4,6 mm (MCSNV T.1124) proportionally to the trunk length of each specimen (**Table 14**). Analogously, the correlation between the averages computed on centra of the caudal region and head region length reflects the same correlation. These trends indicate small ontogenetic variations among triakid individuals. On the contrary, the specimens of *E. bolcensis* cluster on both diagrams although displaying relative high variations among individuals. This trend is clearly shown in **Fig. 48** and probably reflects the paucity of number of vertebrae in the head regions of specimens. The centra length averages of *E. bolcensis* specimens proportionally vary according to the size of body segments, in the same way as fossil triakids (see **Fig. 47, 48** and **Table 14, 15**). Nevertheless, diagrams (**Fig. 47, 48**) indicate three main ontogenetic classes according to proportional increasing of size among the individuals.

To provide ontogenetic classes among Bolca carcharhinids, the Von Bertalanffy growth equation (Bertalanffy, von, 1938) is applied to estimate the ages among the individuals, according to age – growth curves of extant sharks living in different estuarine – marine environments (*Carcharhinus brevipinna*, *C. leucas*, *C. longimanus*, *Galeocerdo cuvier*, *Galeorhinus galeus*, *Galeus sauteri*, *Isogomphodon oxyrhynchus*, *Mustelus antarcticus*, *M. californicus*, *M. lenticulatus*, *M. antarcticus*, *Negaprion brevirostris*, *Prionace glauca*, *Rhizoprionodon porosus*, *R. lalandii*, *Sphyrna lewini*, *S. tiburo*, *S. zygaena*, *Triakis semifasciata*; Olsen, 1984; Kusher, 1987; Brown & Gruber, 1988; Yudin & Caillet, 1990, 1990; Francis & Francis, 1992; Kusher et al., 1992; Moulton et al., 1992; Parsons, 1993; Goosen & Smale, 1997; Francis & Mulligan, 1998; Lessa et al., 1999, 2000, 2009; Wintner & Dudley, 2000; Skomal & Natanson, 2002; Martinez, 2004; Joung et al., 2005; Piercy et al., 2007; Coelho et al., 2011; Liu et al., 2011):

$$t1 = \left(\frac{1}{k}\right) * \ln \frac{L_{\infty}}{L_{\infty} - Lt} + t0$$

where $t1$ is the age of the individual, k is a growth coefficient based on the rate of growth of length increment for the individual per year, L_{∞} is the mean maximum total length for the population, Lt is the length of the individual at the age $t1$, $t0$ is the hypothetical age computed from the growth curve when the total length equals zero. All curves are performed according to the total length or head – caudal fin length of Bolca specimens as Lt , whereas the remaining parameters of the equations refer to extant populations. For example, the dataset for combined sex growth curve of *Mustelus mustelus* from South Africa (Goosen & Smale, 1997), has the following parameters: $L_{\infty} = 198,94$ cm; $k = 0,06$; $t0 = - 3,82$. As $Lt = 175$ cm for MSNPV 17716, the estimated age for the specimens is:

$$t1 = \left(\frac{1}{0,06} \right) * \ln \frac{198,94}{198,94 - 175} - 3,82 = 31,47 \approx 31 \text{ years}$$

The growth curves rates have regional variations among the populations of the same species. All estimated ages for the Bolca fossil sharks aim to provide a comprehensive overlook over the preserved community. Estimated values are listed in **Table 16**. The estimates of the specimens of *E. bolcensis* ranges from adult to sexual immature individual following the fits from different shark species. Indeed, the total length of the carcharhinids fossil specimens is higher than the L_{∞} of several shark populations (**Table 16**). All the estimated ages refer to the maximum ages predicted of the living specimens. The fits of age – length of specimens follows shark populations with higher predicted total length than the fossil assemblage.

The performed curves suggest 3 hypotheses:

- 1) the growth curves of *Carcharhinus leucas*, *Galeorhinus galeus* (Bass Strait populations, curve for combined sex), *Mustelus antarcticus*, *M. mustelus*, *Negaprion brevirostris*, *Prionace glauca*, *Sphyrna lewini*, (Brown & Gruber, 1988; Moulton, 1992; Goosen & Smale, 1997; Francis & Mulligan, 1998; Skomal & Natanson, 2002; Cruz – Martinez, 2004; Piercy et al., 2007) are not valid. The correlation age – total length is strongly polynomial ($R^2 = 1$; **Fig. 49, 50; Appendix H3 – H9**). According to triakids specimens, the growth curves reveal two distinct ontogenetic three ontogenetic classes; the sexual and somatically immature individuals of *G. cuvieri*, the young specimens MGP – 8869 – 8870 and the adult individuals MCSNV T.311 and MSNPV 17716. Observing the fits according to non – triakid carcharhiniforms, all specimens are sexual immatures comparing the estimated values with the age of maturity for the referred populations (**Table 16**).

Table 14: Values of trunk length and centra length averages of Bolca shark specimens

| id | Trunk length (mm) | centra length average (mm) |
|-----------------------------|----------------------|-------------------------------|
| MSNPV 17716 | 893,0 | 9,0 |
| MGP - PD 8871 - 8872 | 355,0 | 3,5 |
| MGP - PD 8869 - 8870 | 730,0 | 8,5 |
| MCSNV T.1124 | 460,0 | 4,6 |
| MCSNV VII.B.96 - 97 | 420,0 | 4,1 |
| MCSNV T 311 | 857,0 | 8,9 |
| MGGC 1976 | 483,0 | 4,5 |
| MNHN F.Bol.516 | 414,0 | 4,4 |

Table 15: Values of sum of centra in the head region and centra length averages of Bolca shark specimens

| id | Head region (mm) | centra length average (mm) |
|----------------------|------------------|----------------------------|
| MSNPV 17716 | 124,0 | 9,3 |
| MGP - PD 8871 - 8872 | 64,0 | 4,7 |
| MGP - PD 8869 - 8870 | 97,0 | 6,5 |
| MCSNV T.1124 | 62,0 | 4,8 |
| MCSNV VII.B.96 - 97 | 60,0 | 4,3 |
| MCSNV T 311 | 98,0 | 7,0 |
| MGGC 1976 | 65,0 | 4,3 |
| MNHN F.Bol.516 | 53,0 | 3,8 |

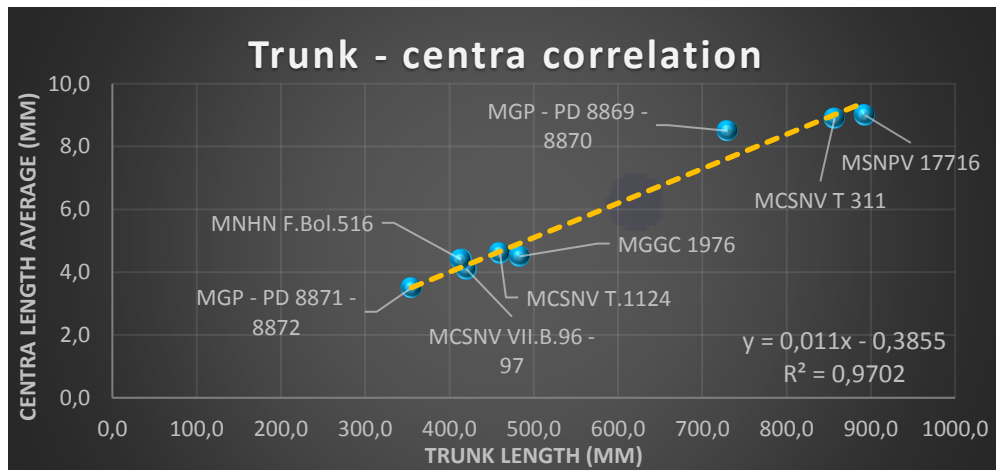


Figure 47: Correlation between trunk length and averages of centra length of Bolca specimens. All the individuals show a robust linear distribution ($R^2 = 0,97$).

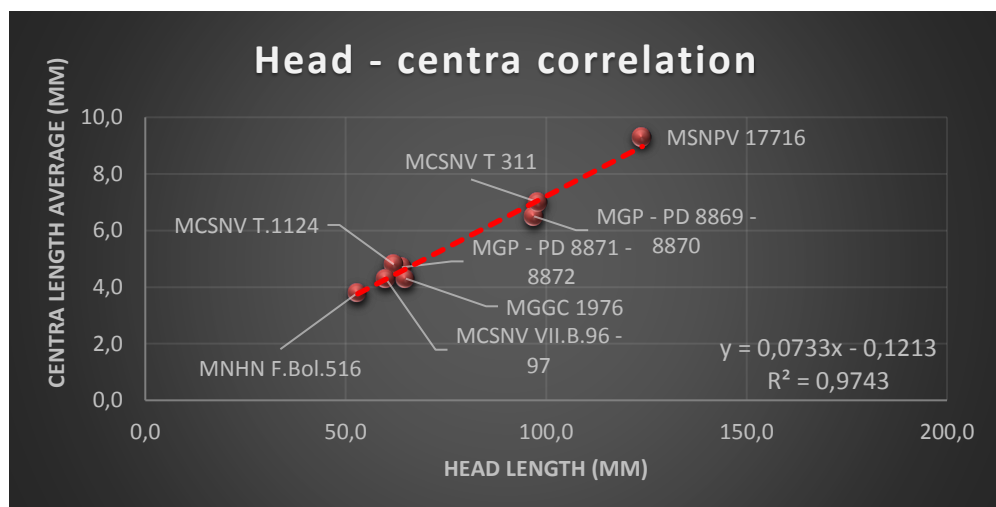


Figure 48: Correlation between sum of centra of the head region and averages of centra length of Bolca specimens. All the individuals show a robust linear distribution ($R^2 = 0,97$).

Table 16: age estimates of Bolca specimens according to growth parameters of different extant populations of sharks. The parameters of *G. galeus* (Moulton et al., 1992 [18]) refer to combined sex growth curves for the Bass Strait (BS), South Australia (SA) and combined populations (total) during the caught periods. The symbol “ $\hat{\alpha}$ ” indicates the estimated ages according to head – caudal fin length. The highlighted cells indicate the geographic provenience of different shark populations: yellow = New Zealand; orange = Australia; green = West USA; light blue = South Africa; coral red = North Atlantic Sea; grey = Gulf of Mexico; blue = Western Central Pacific Sea; violet = South Atlantic Sea, North Brazil; light orange = Philippine Sea. The references are indicated with the numbers between squared parenthesis. *Abbreviations:* C, combined sex; F, female; M, male.

| Taxon | S | k | L_{∞} | t_0 | Age at maturity | MGP - PD 8871 - 8872 | MGP - PD 8869 - 8870 | MCSNV T.1124 | MCSNV VII.B.96 - 97 | MGGC 1976 | MCSNV T.311 | MNHN F.Bol.516 | MSNPV 17716 | Source |
|-------------------------------------|---|--------|--------------|---------|-----------------------|-------------------------------|-------------------------------|-----------------|------------------------------|--------------|----------------|-------------------|----------------|--------|
| <i>Galeorhinus galeus</i> | | | | | | | | | | | | | | |
| <i>Galeorhinus galeus</i> | F | 0,086 | 179,2 | -2,68 | 13 - 15 | 3,02 | 13,6 | 5,7 | 5,3 | 5,7 | 29,6 | 4,34 | 40,96 | [17] |
| <i>Galeorhinus galeus</i> | C | 0,086 | 180,4 | -2,48 | (12) - (17) | 3,17 | 13,56 | 5,81 | 5,43 | 5,81 | 28,69 | 4,47 | 38,32 | [17] |
| <i>Galeorhinus galeus</i> (BS) | C | 0,084 | 215,8 | -0,9 | ? | 3,72 | 10,79 | 5,72 | 5,43 | 5,72 | 17,05 | 4,72 | 18,93 | [18] |
| <i>Galeorhinus galeus</i> (SA) | C | 215,8 | 173,7 | 182,9 | ? | 2,62 | 9,51 | 4,32 | 4,07 | 4,32 | 22,86 | 3,45 | 23+ | [18] |
| <i>Galeorhinus galeus</i> (Total) | C | 0,124 | 182,9 | -1,29 | ? | 2,56 | 9,52 | 4,35 | 4,09 | 4,35 | 18,95 | 3,44 | 24,05 | [18] |
| <i>Galeorhinus galeus</i> | M | 0,1675 | 158,33 | -1,2545 | 8+ | 2,19 | 10,18 | 3,94 | 3,68 | 3,94 | 30+ | 3,04 | 30+ | [19] |
| <i>Galeorhinus galeus</i> | F | 0,1600 | 161,83 | -1,2818 | 10+ | 2,22 | 9,95 | 3,97 | 3,71 | 3,97 | 30+ | 3,07 | 30+ | [19] |
| <i>Galeorhinus galeus</i> | C | 0,1639 | 160,04 | -1,2669 | 8+ - 10+ | 2,2 | 10,05 | 3,95 | 3,69 | 3,95 | 30+ | 3,05 | 30+ | [19] |
| Triakidae | | | | | | | | | | | | | | |
| <i>Mustelus californicus</i> | M | 0,35 | 101,8 | -1,002 | (1) - (2) | 2,27 | 9+ | 5,69 | 4,92 | 5,69 | 9+ | 3,56 | 9+ | [20] |
| <i>Mustelus californicus</i> | F | 0,218 | 142,4 | -1,032 | (2) - (3) | 2,03 | 12,53 | 3,73 | 3,47 | 3,73 | 13+ | 2,84 | 13+ | [20] |
| <i>Mustelus californicus</i> | C | 0,168 | 154,4 | -1,271 | (1) - (3) | 2,28 | 11,08 | 4,12 | 3,84 | 4,12 | 12+ | 3,17 | 12+ | [20] |
| <i>Mustelus lenticulatus</i> | M | 0,11 | 161,1 | -1,91 | 5 | 3,21 | 14,64 | 5,79 | 5,4 | 5,79 | 15+ | 4,46 | 15+ | [21] |
| <i>Mustelus lenticulatus</i> | C | 0,1 | 176,9 | -2,12 | (3) - (5) | 2,86 | 12,28 | 5,22 | 4,87 | 5,22 | 27,82 | 4,02 | 43,22 | [21] |
| <i>Mustelus antarticus</i> | M | 0,16 | 155,9 | -1,94 | ? | 1,74 | 10,62 | 3,63 | 3,35 | 3,63 | 16+ | 2,66 | 16+ | [18] |
| <i>Mustelus antarticus</i> | F | 0,094 | 223,6 | -2,05 | ? | 1,9 | 7,8 | 3,59 | 3,35 | 3,59 | 12,76 | 2,75 | 14,19 | [18] |
| <i>Mustelus mustelus</i> | M | 0,12 | 145,1 | -2,14 | (6) - (9) | 3,28 | 20,07 | 6,24 | 5,78 | 6,24 | 21+ | 4,69 | 21+ | [22] |
| <i>Mustelus mustelus</i> | F | 0,06 | 204,96 | -3,55 | (12) - (15) | 3,34 | 14,36 | 6,38 | 5,94 | 6,38 | 25,02 | 4,85 | 28,50 | [22] |
| <i>Mustelus mustelus</i> | C | 0,06 | 198,94 | -3,82 | (6) - (15) | 3,33 | 15,1 | 6,53 | 6,06 | 6,53 | 27,22 | 4,92 | 31,47 | [22] |
| <i>Triakis semifasciata</i> | M | 0,089 | 149,9 | -2,03 | 7+ | 4,96 | 23,91 | 8,66 | 8,09 | 8,66 | 24+ | 6,73 | 24+ | [23] |
| <i>Triakis semifasciata</i> | F | 0,073 | 153,6 | -2,74 | 10+ | 5,5 | 26,18 | 9,78 | 9,12 | 9,78 | 24+ | 7,56 | 24+ | [23] |
| <i>Triakis semifasciata</i> | C | 0,082 | 160,2 | -2,31 | 7 - 10+ | 4,61 | 20,25 | 8,1 | 7,58 | 8,1 | 24+ | 6,31 | 24+ | [23] |
| <i>Triakis semifasciata</i> | M | 0,089 | 157,7 | -1,06 | 7+ | 5,46 | 20,72 | 8,78 | 8,28 | 8,78 | 24+ | 7,06 | 24+ | [24] |
| <i>Triakis semifasciata</i> | F | 0,134 | 144,9 | 0,325 | 10+ | 5,19 | 20,35 | 7,84 | 7,43 | 7,84 | 24+ | 6,46 | 24+ | [24] |
| <i>Triakis semifasciata</i> | C | 0,0717 | 172,4 | -2,302 | 8 - 10+ | 4,88 | 19,01 | 8,34 | 7,83 | 8,34 | 48,98 | 6,58 | 49+ | [24] |
| Non-triakid carcharhiniforms | | | | | | | | | | | | | | |
| <i>Prionace glauca</i> | F | 0,13 | 371,2 | 1,77 | 2+ | 3,36 | 5,25 | 3,96 | 3,88 | 3,96 | 6,41 | 3,67 | 6,67 | [25] |
| <i>Carcharhinus leucas</i> | C | 0,1397 | 256,4 | -1,935 | (9) - (10) | 0,32 | 3,42 | 1,25 | 1,12 | 1,25 | 5,69 | 0,79 | 6,28 | [26] |
| <i>Carcharhinus longimanus</i> | C | 0,099 | 284,9 | -3,4 | 7 | -0,58 | 3,09 | 0,54 | 0,38 | 0,54 | 5,6 | -0,01 | 6,22 | [27] |
| <i>Isogomphodon oxyrinchus</i> | C | 0,121 | 171,4 | -2,612 | M: 5 - 6; F: 6 - 7 | 1,68 | 10,19 | 3,75 | 3,44 | 3,75 | 29,88 | 2,69 | 30+ | [31] |
| <i>Carcharhinus brevipinna</i> | M | 0,2 | 319 | -0,44 | 7,9 | -0,16 | 1,95 | 0,47 | 0,38 | 0,47 | 3,5 | 0,16 | 3,90 | [32] |
| <i>Carcharhinus brevipinna</i> | F | 0,203 | 257,4 | -1,709 | 7,8 | -0,16 | 2,20 | 0,56 | 0,46 | 0,56 | 3,81 | 0,20 | 4,20 | [32] |
| <i>Negaprion brevirostris</i> | C | 0,151 | 288,2 | -1,988 | M:11,6; F:12,7 | 0,66 | 4,74 | 1,51 | 1,37 | 1,57 | 5,87 | 1,18 | 6,29 | [33] |
| <i>Rhizoprionodon porosus</i> | C | 0,17 | 112,9 | -1,75 | 3,3 | 3,86 | 9+ | 8,17 | 7,38 | 8,17 | 9+ | 5,72 | 9+ | [34] |

| | | | | | | | | | | | | | | |
|--|---|-------|--------|--------|--------------|-------|------|-------|-------|-------|------|-------|------|------|
| <i>Sphyrna lewini</i> | M | 0,13 | 278,9 | -1,63 | < 15 | 0,57 | 3,46 | 1,45 | 1,33 | 1,45 | 5,47 | 1,02 | 5,97 | [35] |
| | F | 0,09 | 302,6 | -2,22 | < 15 | 0,67 | 4,34 | 1,81 | 1,65 | 1,81 | 6,78 | 1,25 | 7,37 | [35] |
| <i>Sphyrna tiburo</i> | F | 0,34 | 115 | -1,1 | 2,2 | 1,62 | 6+ | 3,63 | 3,27 | 3,63 | 6+ | 2,50 | 6+ | [36] |
| | F | 0,37 | 103,3 | -0,6 | 2,3 | 2,41 | 6+ | 5,38 | 4,74 | 5,38 | 6+ | 3,56 | 6+ | [36] |
| Non-triakid carcharhiniforms unrealistic age estimates | | | | | | | | | | | | | | |
| <i>Sphyrna zygaena</i> | C | 0,06 | 315,45 | -8,3 | ? | -4,16 | 1,01 | -2,55 | -2,78 | -2,55 | 4,38 | -3,34 | 5,19 | [28] |
| <i>Galeus sauteri</i> | M | 0,036 | 118,8 | -0,307 | 9+ | 56,56 | - | - | - | - | - | - | - | [29] |
| | F | 0,046 | 101,6 | -0,527 | 7+ | 57,47 | - | - | - | - | - | - | - | [29] |
| <i>Galeocerdo cuvier</i> ° | C | 0,202 | 301 | -1,11 | M:8, F:11 | -0,22 | 1,01 | 0,03 | -0,01 | 0,05 | 1,36 | -0,07 | 1,49 | [30] |
| <i>Rhizoprionodon lalandii</i> | C | 0,057 | 317,65 | -2,302 | 2,6 | 5,86 | - | - | - | - | - | - | - | [34] |
| <i>Sphyrna tiburo</i> | M | 0,58 | 88,8 | -0,77 | 2 | 1,85 | - | - | - | - | - | 3,46 | - | [36] |
| <i>Sphyrna tiburo</i> | M | 0,5 | 81,5 | -0,64 | 2 | 3,17 | - | - | - | - | - | 10,42 | - | [36] |

- 2) Among the growth curves of the triakids, the New Zealand and Australian populations represent a reliable term of comparison for the Bolca assemblage of *G. galeus* (growth parameters for female individuals and combined sex; Moulton et al, 1992; Francis & Mulligan, 1998) and *M. lenticulatus* (growth parameter for combined sex; Francis & Francis, 1992). The best trend is logarithmic (R^2 values 0,99; **Fig. 51, 52; Appendix H1, H2**). The fits separate sexual and somatic individuals (*G. cuvieri* specimens), from young – adult individuals (*E. bolcensis* specimens). The estimated ages of *G. cuvieri* ranges from 2,56 (MGP – PD 8871 – 8872, the youngest of the assemblage) to 5,81 years (MGGC 1976). Fanti et al. (2016) recently provided the ecological affinities between the fossil specimens and Australian populations of *G. galeus*. Data presented here are also consistent with the x – ray imaging of centra collected from specimen MCSNV T.1124. The counts of vertebral bands (i.e. hypermineralized circular structures of centra) indicates 4 years – old individual.
- 3) The estimated ages of the carcharhinids show a larger variability. All specimens are mature young – adult individuals. The youngest of the series is the specimen MGP – PD 8869 – 8870 (age between 9,52 – 13,52 years). The estimated values for MCSNV T.311, and in particular for MSNPV 17716, display a significant variability (**Table 17**) probably reflecting the decreasing of growth rate during the life of the individuals within population. The total length of 17716 is close to the plateau level of fits (i.e. the total length is similar to the L_{∞} computed for the surrogated populations). The **Table 17** lists the valid estimated ages.

Tabella 17: Valid estimated ages according to the Australian (orange cells) and New Zealand populations (yellow cells) of the triakids *Galeorhinus galeus* and *Mustelus lenticulatus*. The estimates fall in a range variable to each specimen.

| Taxon | S | k | L _∞ | t ₀ | Age at maturity | MGP - PD 8871 - 8872 | MGP - PD 8869 - 8870 | MCSNV T.1124 | MCSNV VII.B.96 - 97 | MGGC 1976 | MCSNV T.311 | MNHN F.Bol.516 | MSNPV 17716 | Source |
|-----------------------------------|---|-------|----------------|----------------|-----------------|----------------------|----------------------|--------------|---------------------|-----------|-------------|----------------|-------------|--------|
| <i>Galeorhinus galeus</i> | | | | | | | | | | | | | | |
| <i>Galeorhinus galeus</i> | F | 0,086 | 179,2 | -2,68 | 13 - 15 | 3,02 | 13,6 | 5,7 | 5,3 | 5,7 | 29,6 | 4,34 | 40,96 | [17] |
| <i>Galeorhinus galeus</i> | C | 0,086 | 180,4 | -2,48 | (12) - (17) | 3,17 | 13,56 | 5,81 | 5,43 | 5,81 | 28,69 | 4,47 | 38,32 | [17] |
| <i>Galeorhinus galeus</i> (Total) | C | 0,124 | 182,9 | -1,29 | ? | 2,56 | 9,52 | 4,35 | 4,09 | 4,35 | 18,95 | 3,44 | 24,05 | [18] |
| <i>Mustelus lenticulatus</i> | C | 0,1 | 176,9 | -2,12 | (3) - (5) | 2,86 | 12,28 | 5,22 | 4,87 | 5,22 | 27,82 | 4,02 | 43,22 | [21] |

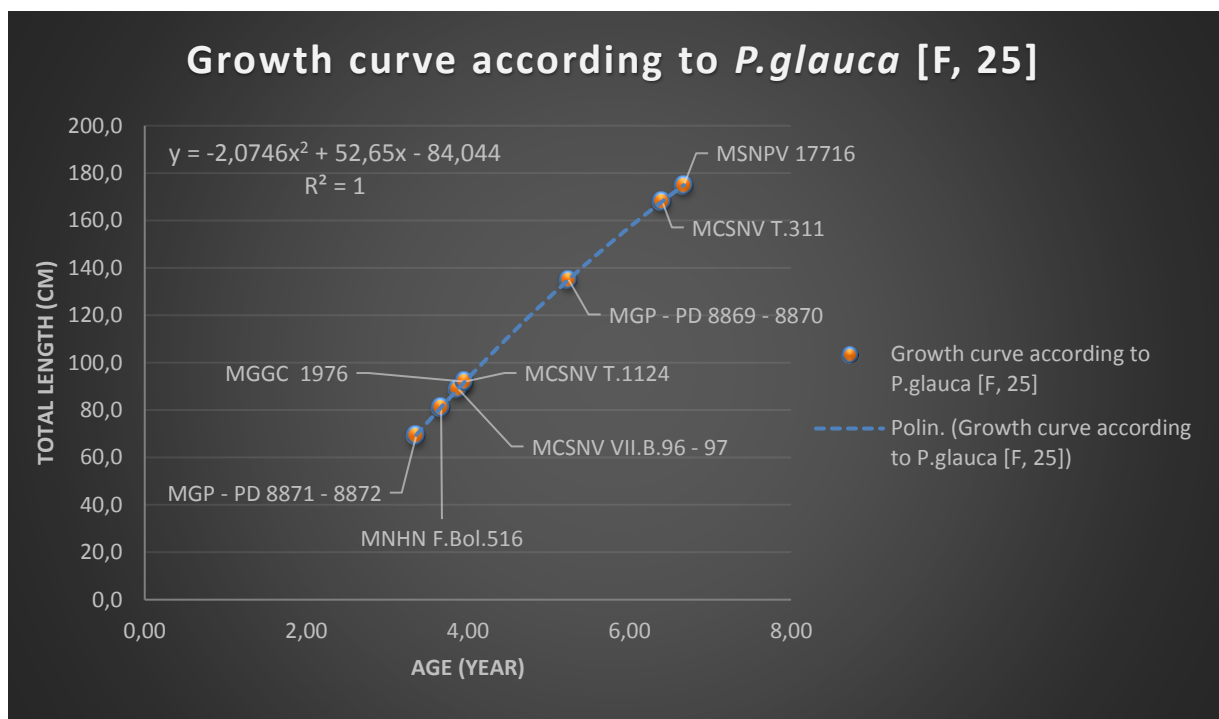


Figure 49: Estimated ages – total length correlation computed follows the growth curve for combined sex of the North Atlantic Sea populations of *Prionace glauca* (Skomal & Natanson, 2002 [25]). Abbreviations: C, combined sex.

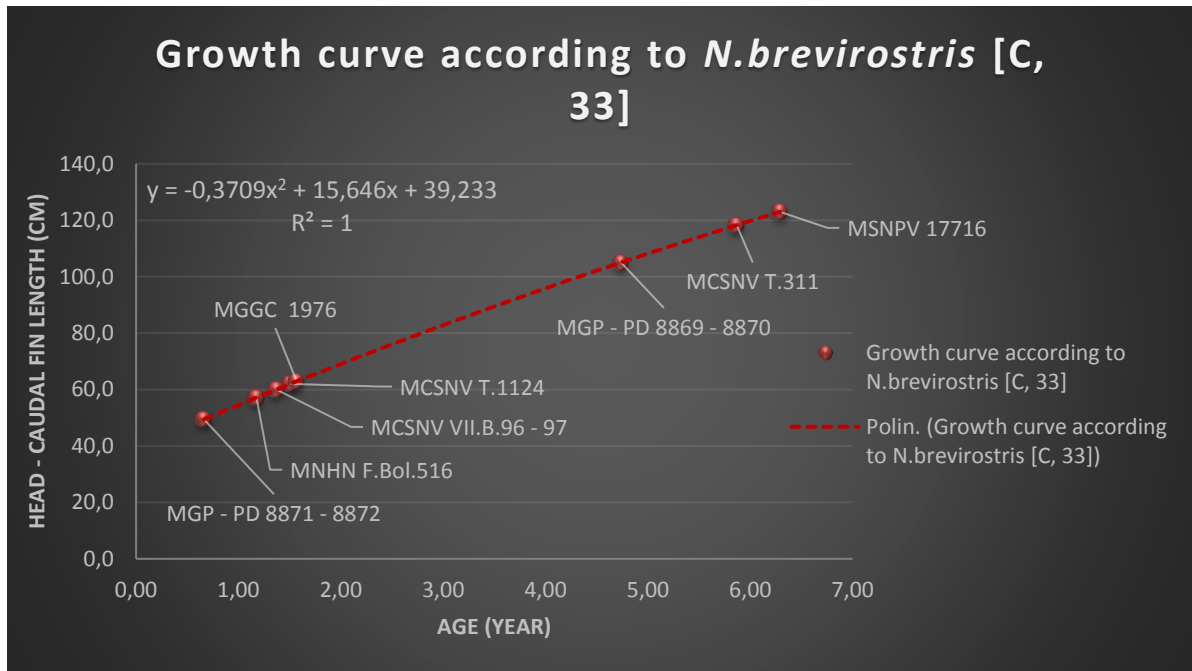


Figure 50: Estimated ages – head caudal fin length correlation computed follows the growth curve for combined sex of the Gulf of Mexico populations of *Negaprion brevirostris* (Brown & Gruber, 1988 [33]). *Abbreviations:* C, combined sex.

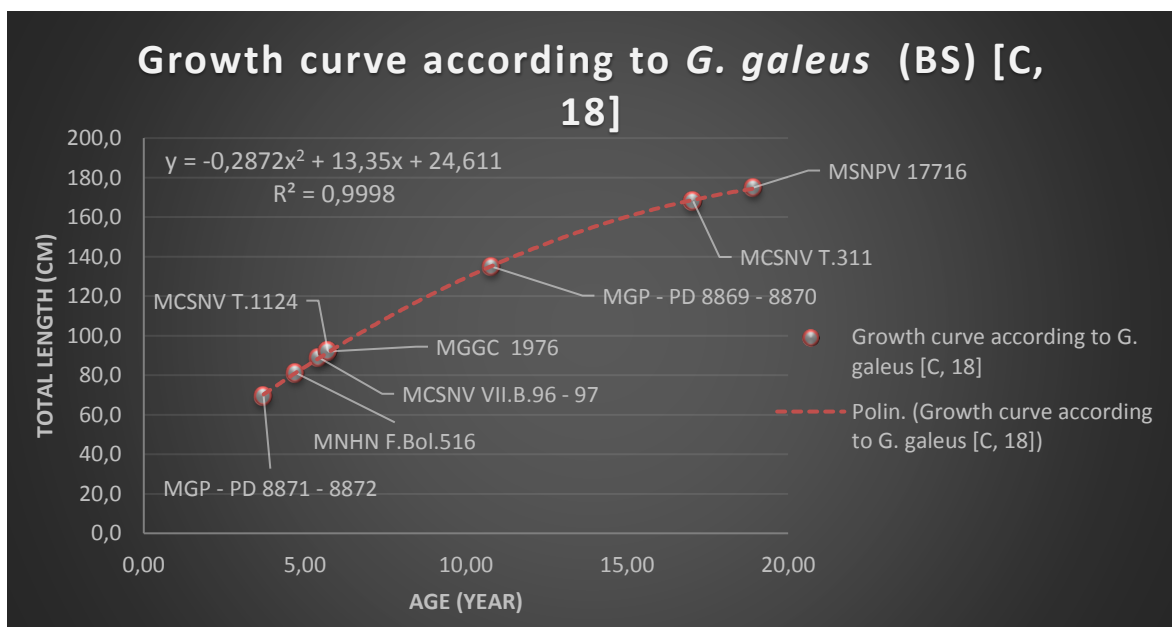


Figure 51: Estimated ages – total length correlation computed follows the growth curve for combined sex of the Australian populations (Bass strait, BS) of *Galeorhinus galeus* (Moulton et al., 1992 [18]). *Abbreviations:* C, combined sex.

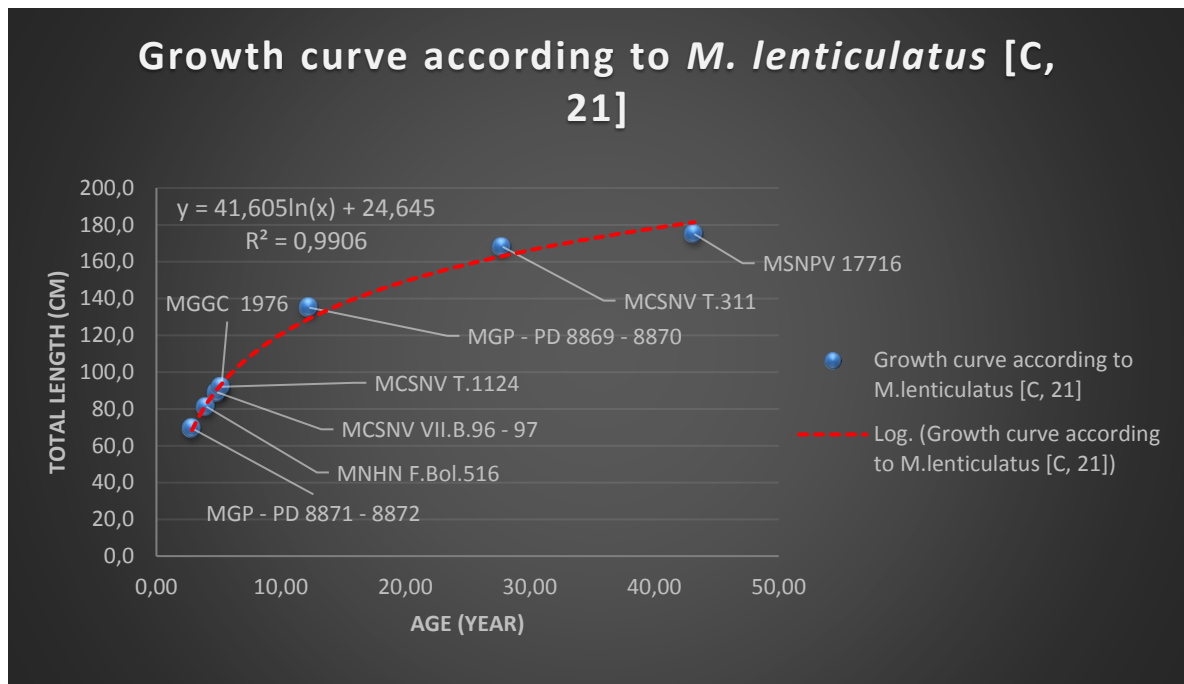


Figure 52: Estimated ages – total length correlation computed follows the growth curve for combined sex of the New Zealand populations of *Mustelus lenticulatus* (Francis & Francis, 1992 [21]). *Abbreviations:* C, combined sex.

6.6: Paleoecologically and Paleogeographic significances

The 1999 – 2011 excavation performed at both Pesciara and Monte Postale localities documented high abundance of bony fishes among the two fossiliferous sites with several different compositions. Clupeids and secondary perciforms are the most abundant family among the Pesciara site, whereas the perciforms are the dominant taxa in laminated limestones of Monte Postale (Marammà et al., 2016). However, the Pesciara – Monte Postale system is considered as one of the earliest coral reef fish assemblages (c.f. Homocitratae, Ephippidae, Acanthuridae, Apogonidae, Serranidae, Gobiidae, Labridae, Pomacentridae; Bellwood, 1995). On the contrary, the chondrichthyan assemblage of Bolca is less diverse (Marammà et al., 2017). Both extant triakids and carcharhinids are top – predators inhabiting different marine – brackish environments (Compagno, 1984; Cailliet et al. 2005; Ebert & Stehmann, 2013). According to Dillon et al. (2016) and Ferrón & Botella (2017), the functional morphologies of dermal denticles reflect ecological groups of shark communities in coral reef and marine environments. The combination of defense – generalized types scale of *E. bolcensis* indicates coastal – pelagic behaviors as the living tiger shark species *Galeocerdo cuvier* (Dillon et al., 2016; Ferrón & Botella, 2017). *G. cuvier* inhabits tropical and warm – temperate latitudes, from continental or insular shelves to coral atolls and lagoon environments, within a maximum depth possibly to 140 m. Usually, the species prefers area with abundant runoff of freshwater. The

tiger shark is a top predator – scavenger, feeding from bony – cartilaginous fishes to reptiles and mammals (Ebert & Stehmann, 2013).

None of the triakids taxa are coral – reef specialists, but several species as *Galerhinus galeus* inhabits muddy – sandy habitats such as enclosed bay and lagoonal setting (Compagno, 1984; Ebert & Stehmann, 2013; Morash et al., 2016). *G. galeus* is a mesopredator inhabiting warm and tropical waters of continental shelf (Compagno, 1984). Ferrón & Botella (2017) provided ontogenetic variations in scales morphologies, reflecting different life styles among the somatic classes; the juveniles have school behaviors, usually inhabiting protected bay or lagoon – estuarine habitats, whereas the adults tend to cluster in pelagic environments. (Compagno, 1984; Ebert & Stehmann, 2013; Ferrón & Botella, 2017). The drag – reduction type scales cover the overall body of adult individuals, increasing considerably the hydrodynamic performance (Oeffner & Lauder, 2011).

According to Von Bertalanffy estimated ages, all the specimens of *G. cuvieri* are sexual and somatic immature individuals. Fanti et al. (2016) hypothesized the Bolca setting as a possible nursery area for *G. cuvieri* specimens based on the anatomical and ecological affinities with the extant species *G. galeus*. Nevertheless, the authors specified that none of the criteria adopted to define a geographical area as a nursery for a population of a species are identified in the assemblage; the hypothesis is also questioned by Marammà et al. (2017). According to Heupel et al. (2007), the criteria to recognize an area as a nursery for extant populations of shark are based on the occurrence and the frequency to remain or return in a particular geographical area for extend periods. These conditions are *a priori* not valid for a fossil assemblage due to the impossibility to survey the yearly dynamic of a population in fossils. Moreover, the fossils criteria to establish a nursery are:

- 1) Occurrence of egg cases (Fischer et al., 2011; Sallan & Coeates, 2014). The egg cases are an exclusively behavior of ovipare shark specimens as scyliorhinids. Comparing *G. cuvieri* to the extant species of *G. galeus*, the development is viviparous without a yolk – sac placenta (i.e. organ formed from the embryonic yolk – sac of the maternal uterus, through which maternal nutrient is passed to the embryo; Ebert & Stehmann, 2013). The number of young varies from 6 to 52 per litter, increasing according to the size of the mother (Ebert & Stehmann, 2013). Olsen (1984) provided that the female pregnant individuals of the Australian populations of *G. galeus* reach the protected bay – estuarine environments when the temperature of water is approximately 14 °C. Therefore, the absence of egg cases among the laminated limestones of Pesciara – Monte Postale build up is due to different reproductive behaviors of the populations.
- 2) Occurrence of abundant isolated teeth samples of the same species, varying in size, collected in a specific locality (Pimiento et al., 2010). This approach is valid for species characterized by homodonty dentition, which the teeth have approximately equal size along the jaws of the same specimen (i.e. *Carcharodon carcharias*, *Carcharhinus brachyurus*; Pimiento et al., 2010; Landini et al., 2016) or when the life history and morphometric parameters of ontogenetic classes for a species are well known. Considering the teeth of all the specimens of fossil assemblage as isolated, the classes of different size is strongly influenced by the heterodonty of the specimens and none adult individuals are found in the fossil assemblage according to estimated ages for *G. cuvieri*. Moreover, the stratigraphic position of the specimens is unclear.

The combination of biologic and abiotic proxies is consistent to nursery area. The Bolca succession was a shallow lagoon – buildup setting, bordered by active fluvial and coral reef systems and associated to the Early Eocene Climatic Optimum (Papazzoni and Trevisani, 2006;

Trevisani, 2015; Vescogni et al, 2016); these environmental features agree to modern nursery area. The Ypresian protected lagoon offered an optimal shelter against top predators, such as the mesopelagic specimens of *E. bolcensis*, and high availability of invertebrates and fishes preys. The diet of juvenile individuals of *G. galeus* is mainly based on molluscs, crustaceans and frequently bony fishes (Olsen, 1984); all the mentioned taxa are found in the Bolca assemblage (Papazzoni et al., 2014). The stomach content of MGP – PD 8871 – 8872, 26878 and the remains of caudal region of *Sphyræna bolcensis* within MGGC 1976, suggests feeding relationships near top of the trophic network (Fanti et al., 2016). The *Galeorhinus* – Perciformes interactions was probably a shift at higher trophic level correlated to the post – Cretaceous increasing of morphological disparities among herbivorous Bolca fish, suggesting a niche – filling scenario into the coral reef habitats (Friedman M., 2010; Bellwood et al., 2014; Lobato et al., 2014; Price et al., 2014; Fanti et al., 2016). However, it is necessary to establish additional criteria to provide nursery areas for heterodonty – viviparous specimens within fossil assemblages.

The fossil records of the genus *Galeorhinus* range from the Upper Cretaceous (Cenomanian) to recent, represented by at list nine species occurred from Europe, North and Central America, Nord Africa, Russia, India and Australia deposits (Rana et al., 2004, 2006; Adnet & Cappetta, 2008; Cappetta, 2012, Marammà et al., 2017; **Fig. 53**). Rana et al. (2004, 2006) provided the presence of the genus *Galeorhinus* in the Lower Eocene deposits of India (i.e. Cambay Basin and Kapurdi Formation) based on the general description of several isolated teeth classified at genus level. The chronostratigraphic ranges of *G. bolcensis* (Agassiz, 1835), *G. duchaussoisi* (Adnet & Cappetta, 2008), *G. louisi* (Adnet & Cappetta, 2008), *G. minutissimus* (Arambourg, 1935F), *G. ypresiensis* (Casier, 1946), suggests higher diversification of the genus during the Eocene among European and Moroccan assemblages than today, with *G. galeus* as the only extant representative (Adnet & Cappetta, 2008; Marammà et al., 2017; **Fig. 53**). The reorganization of *Galeorhinus* distribution is probably a recent phenomenon, according to geographical distributions of triakid specimens among the Cenozoic (Adnet & Cappetta, 2008; **Fig. 54**). The genus *Eogaleus* is uniquely represented by the Ypresian individuals from Bolca deposits. However, the systematics is still unclear (Cappetta, 2012) and none paleogeographic distribution could provide the evolutionary history for the taxon.

Chapter 7: Conclusions

Detailed analyses on MSNPV 17716 – 17717 allowed to increase our knowledge on Bolca carcharhinids assemblage within a famous ancient lagoon – buildup system.

Furthermore:

- 1) the overall external morphology between *G. cuvieri* and *E. bolcensis* shows no significative differences. The standardized morphometrical ratios against the total length of the body for each specimen allowed to accurately estimate the size of the partly disarticulated individual MSNPV 17716 – 17717 in 175 cm;
- 2) morphometrical measurements of body proportions is a conservative character shared between fossil and living carcharhinids. The morphology and higher number of centra among the Carcharhiniformes also follows the same criterion although it is not possible to infer taxonomic informations;
- 3) SEM images of dermal denticles reveals that specimen MSNPV 17716 – 17717 is an individual of *Eogaleus bolcensis*. The morphology of dermal denticles has usually taxonomic resolution at family level. The comparison with extant family reveal high affinities to the carcharhinid *Galeocerdo cuvier*. All specimens referred to *Galeorhinus cuvieri* from Bolca show affinities to the family Triakidae, in particular to the genus *G. galeus*;
- 4) The statistic prediction of anatomical position of teeth, compared to jaws arrangements of living taxa, reveals conflicting associations. The Bolca triakids shows affinities to the genus *Galeorhinus*. The genus *Eugaleus* is well diversified from the extant species *Galeocerdo cuvier*, despite both genera are related to the triakid *Pachygaleus*;
- 5) the correlation between length of centra and body region of the fossil specimens supports three ontogenetic classes. A comparison with growth curves of living taxa document affinities with Australian and New Zealand populations of the triakids *Galeorhinus galeus* and *Mustelus lenticulatus*. Furthermore, all the specimens of *G. cuvieri* from Bolca are juvenile individuals, whereas the specimens of *E. bolcensis* are young – adult individuals.
- 6) Given the age and paleoenvironmental setting, the Bolca ecosystem was a possible nursery area for *G. cuvieri*. The stomach content of four specimens of *G. cuvier* clearly document trophic networks among higher – consumers as the modern food – network observed in modern coral reef.

References:

- Adnet S., 2006. Biometric analysis of the teeth of fossil and Recent hexanchid sharks and its taxonomic implications. *Acta Palaeontol Pol.* 51(3): 477 – 488.
- Adnet S., Cappetta H., 2008. New fossil triakid sharks from the early Eocene of Prémontré, France, and comments on fossil record of the family. *Acta Palaeontol. Pol.* 53 (3): 433–448. <http://app.pan.pl/acta53/app53-433.pdf>
- Agassiz L., 1833-1844. *Recherches sur les poissons fossiles*. Petitpierre, Neuchâtel: Tome IV: 296 pp.; Tome V, pt 1: 122 p.
- Agnini C., Fornaciari E., Raffi I., Catanzariti R., Pälke H., Backman J., Rio D., 2014. Biozonation and biochronology of Paleogene calcareous nannofossils from low and middle latitudes. *Newsl Stratigr* 47(2):131–181.
- Applegate S., 1967. A survey of shark hard parts. In: Gilbert P, Mathewson R, Rall D (eds) *Sharks, skates, and rays*. Johns Hopkins Press, Baltimore, MD. 37 – 67.
- Applegate, S.P. 1978. Phyletic studies. Part. I. Tiger sharks. *Universidad Nacional Autonoma de Mexico, Instituto de Geologia Revista.* 2(1): 55–64.
- Anderson M.J., 2001a. A new method for non-parametric multivariate analysis of variance. *Austral Ecology.* 26: 32 – 46.
- Arambourg, 1935F. Note preliminaire sur les vertebres fossiles des phosphates du Maroc. - *Bull. Soc. geol. France.*, 1940. 5 (5): p. 413 – 439. Le groupe des Ganopristines. - *Bull. Soc. geol. France.* 10(5): 127 – 147.
- Balbino A C., 1995. *Selaceos (Pisces) do Miocenico terminal da bacia de Alvalade (Portugal)*. - These Doctorat, Evora. 200 p.
- Barbieri, G., 1972. Sul significato geologico della Faglia di Castelvero (Lessini veronesi). *Atti e Memorie dell'Accademia Patavina di Scienze. Lettere ed Arti.* 84: 297–302.
- Barbieri G., Medizza F., 1969. Contributo alla conoscenza geologica della regione di Bolca. *Mem. Ist. Geol. Miner. Univ. Padova.* 27: 1 – 36.
- Barbieri, G., De Zanche, V., Medizza, F., Sedea, R., 1982. Considerazioni sul vulcanismo terziario del Veneto occidentale e del Trentino meridionale. *Rendiconti della Società Geologica Italiana.* 4: 267 – 270.
- Barbieri, G., De Zanche, V., Sedea, R., 1991. Vulcanismo paleogenico ed evoluzione del semigraben Alpone-Agno (Monti Lessini). *Rendiconti della Società Geologica Italiana.* 14: 5–12.
- Barbieri G, Zampieri D, 1992. Deformazioni sinsedimentarie eoceniche con stile a domino nel semigraben Alpone-Agno e relativo campo di paleostress (Monti Lessini orientali-Prealpi Venete). *Atti Ticinensi di Scienze della Terra.* 35: 25–31.

- Beccaro, L., Fornaciari, E., Mietto, P., Preto, N., 2001. Analisi di facies e ricostruzione paleoambientale dei “Calcari nummulitici” (Eocene, Monti Lessini orientali-Vicenza): dati preliminari. Studi Trentini di Scienze Naturali. Acta Geologica. 76 (1999): 3 –16.
- Bellwood D.R., 1995. The Eocene fishes of Monte Bolca: the earliest coral reef assemblage. Coral Reefs. 15: 11 – 19.
- Bellwood D.R., 2003. Origins and escalation of herbivory in fishes: a functional perspective. Paleobiology. 29 :71 – 83.
- Bellwood D.R., Goatley C.H.R., Brandl S.J., Bellwood O., 2014. Fifty million years of herbivory on coral reefs: fossils, fish and functional innovations. Proc R Soc Lond B Biol Sci. 281: 8 p.
- Bellwood D.R., Hoey A.S., Bellwood O., Goatley C.H.R., 2014. Evolution of long-toothed fishes and the changing nature of fish–benthos interactions on coral reefs. Nat Commun. 5: 3144 p..
- Bertalanffy, L. von. (1938). A quantitative theory of organic growth. Human Biology. 10: 181 – 213.
- Blainville H. M. D. de, 1818. Des ichthyolites du Monte Bolca, ou Vestena Nuova dans le Veronais. Nouveau dictionnaire d’histoire naturelle. 27: 334 – 361.
- Bosellini A.,1989. Dynamics of Tethyan carbonate platforms. In Crevello P.D., Wilson J.L., Sarg J.F. & Read J.F. (eds), Controls on Carbonate Platform and Basin Platform. S.E.P.M. Special Publication. 44: 3 – 13.
- Bosellini A., Carraro F., Corsi M., De Vecchi G.P., Gatto G.O., Malaroda R., Sturani C., Ungaro S., Zanettin B., 1967. Note illustrative della carta geologica d’Italia alla scala 1:100.000. Foglio 49 Verona. Ministero dell’Industria, del Commercio e dell’Artinato. Servizio Geologico d’Italia. Nuova Tecnica grafica, Roma. 61 p.
- Bosellini A., Masetti D., Sarti M., 1981. A Jurassic, “Tongue of Ocean” infilled with oolitic sands: the Belluno Trough, Venetian Alps, Italy. Mar Geol. 44: 59 – 95.
- Bosellini F.R., Papazzoni C.A., 2003. Paleoecological significance of coral – encrusting foraminifera associations. A case – study from the Upper Eocene of Northern Italy. Acta Palaeontologica Polonica. 48(2): 279 – 292.
- Brown C.A., Gruber S., 1988 [33]. Age Assessment of the Lemon Shark, *Negaprion brevirostris*, Using Tetracycline Validated Vertebral Centra. Copeia. 3: 747 – 753.
- Cailliet G. M., Musick J.A., Simpfendorfer C.A., Stevens J.D., 2005. Ecology and Life History Characteristics of Chondrichthyan Fish. Chapter 3. In: Fowler L., Cavanagh R.D., Camhi M., Burgess G.H., Cailliet G.M., Fordham S.V., Simpfendorfer C.A., Musick J.A. (eds.). Sharks, Rays and Chimaeras: The Status of the Chondrichthyan Fishes. IUCN/SSC Shark Specialist Group. IUCN, Gland, Switzerland and Cambridge, UK. 461 p.

- Cappetta H., 1975. “Les Selaciens Eocenes du Monte Bolca. I. Les Carcharhinidae” in *Miscellanea paleontologica di Sorbini L. et al.*, Verona. Museo Civico di Storia Naturale. 279 – 305.
- Cappetta H., 1987. Chondrichthyes II, Mesozoic and Cenozoic Elasmobranchii. In: SCHULTZE, H.-P. (ed.), *Handbook of Paleichthyology*, 3B, 193 p.; Stuttgart (Gustav Fischer Verlag).
- Cappetta H., 1992b. Carcharhiniformes nouveaux (Chondrichthyes, Neoselachii) de l'Ypresien du Bassin de Paris. – *Geobios*. 25(5): 639 – 646.
- Cappetta H., 2012. Chondrichthyes. Mesozoic and Cenozoic Elasmobranchii: Teeth. Volume 3E. Verlag Dr. Friedrich Pfeil- München. 512 p.
- Carrillo – Bricegño J.D., González – Barba G., Landaeta M.F., Nielsen S.N., 2013. Condriactios fósiles del Plioceno Superior de la Formación Horcón, Región de Valparaíso, Chile central. *Revista Chilena de Historia Natural* 86: 191 – 206.
- Casier E., 1946. La faune ichthyologique de l'Ypresien de la Belgique. *Mem. Mus. roy. Hist. natur. Belg.* 104: 1 – 267.
- Casier E., 1947A. Constitution et evolution de la racine dentaire des Euselachii. I - Note preliminaire. *Bull. Inst. roy. Hist. natur. Belgique, BioI.* 23(13): 1 – 15.
- Casier E., 1947B. Constitution et evolution de la racine dentaire des Euselachii. II - Note preliminaire. *Bull. Inst. ray. Sci. natur. Belg.* 23(14), 1 – 32.
- Casier E., 1947C. Constitution et evolution de la racine dentaire des Euselachii. III - Note preliminaire. *Bull. Inst. ray. Sci. natur. Belg.* 23(15):1 – 45.
- Castro, J.I. 1993. The shark nursery of Bulls Bay, South Carolina, with a review of the shark nurseries of the southeastern coast of the United States. *Environmental Biology of Fishes*. 38: 37–48.
- Catullo T.A., 1818 – 1822. Memorie sopra li corpi organizzati fossili del Bolca e degli altri monti terziari della provincia veronese. *Giornale di Pavia*.
- Catullo T.A. 1827. Saggio si Zoologia fossile, ovvero osservazioni sopra li petrefatti delle province Austro – Venete. *Tip. Seminario, Padova*. 30 p.
- Cerato M., 2011. Cerato. I pescatori del tempo. Grafica Alpone Srl. San Giovanni Ilarione (VR). 178 p.
- Coelho R., Fernandez-Carvalho J., Amorim S., Santos M.N., 2011 [28]. Age and growth of the smooth hammerhead shark, *Sphyrna zygaena*, in the Eastern Equatorial Atlantic Ocean, using vertebral sections. *Aquat. Living Resour.* 24: 351 – 357.
- Choi Y., Kim I., Nakaya K., 1998 [11]. A taxonomic revision of the Genus *Carcharhinus* (Pisces: Elasmobranchii) with description of two new records in Korea. *The Korean Journal of Systematic Zoology*. 14(1): 43 – 49.

- Cohen K.M., Harper D.A.T., Gibbard P.L., 2017. ICS International Chronostratigraphic Chart 2017/02. International Commission on Stratigraphy, IUGS.
- Compagno, L.J.V., 1984. Vol. 4. Sharks of the world. An annotated and illustrated catalogue of sharks species known to date. Part 2, Carcharhiniformes. FAO species catalogue. 251 – 655.
- Compagno, 1988. Sharks of the order Carcharhiniformes. - XXII + 486 p.; Princeton, New Jersey (Princeton Univ. Press)
- Compagno, L.J.V., Garrick J.R.F., 1983 [17]. *Nasolamia*, new genus, for the shark *Carcharhinus velox* Gilbert, 1898(Elasmobranchii: Carcharhinidae). Zool.Publ.Vict.Univ.Wellington, (76): 16 p.
- Compagno L.J.V., Stevens, 1993 [1]. *Hemitriakis falcata* n.sp. and *H. abdita* n.sp., Two New Houndsharks (Carcharhiniformes: Triakidae) from Australia. Records of the Australian Museum. 45: 195 – 220. ISSN 0067-1975
- Compagno L.J.V., Krupp F., Kent C.E., 1996 [10]. New Weasel Shark of the Genus *Paragaleus* from the Northwestern Indian Ocean and the Arabian Gulf (Carcharhiniformes: Hemigaleidae). FAUNA OF SAUDI ARABIA. 15: 391 – 401.
- Compagno L.J.V., White W.T., Last P.R., 2008 [13]. *Glyphis garricki* sp. nov., a new species of river shark (Carcharhiniformes: Carcharhinidae) from northern Australia and Papua New Guinea, with a redescription of *Glyphis glyphis* (Müller & Henle, 1839). CSIRO Marine and Atmospheric Research Paper. 22: 203 – 225.
- Cruz – Martínez A., Chiappa – Carrara X., Arenus – Fuentes V., 2004 [26]. Age and Growth of the Bull Shark, *Carcharhinus leucas*, from Southern Gulf of Mexico. J. Northw. Atl. Fish. Sci. 35: 367 – 374. doi:10.2960/J.v35.m481
- De Beaumont G., 1960. Un *Notidianus* de l'Eocène du Mont Bolca. Schweiz. Paleont. Gesellesch. 53(1): 308 – 314.
- De Zigno, 1850. Coup d'oeil sur les Terrains stratifiés des Alpes Venitiennes, Braumuller, Wien
- De Zigno, 1874. Catalogo ragionato dei pesci fossili del calcare eoceno di M. Bolca e M. Postale, Grimaedo, Venezia.
- Dillon E.M., O’dea A., Norris R.D., 2017. Dermal denticles as a tool to reconstruct shark communities. Marine Ecology Progress Series. 566: 117–134. doi: 10.3354/meps12018
- Ebert D.A., Stehmann M.F.W., 2013. Sharks, batoids, and chimaeras of the North Atlantic FAO Species Catalogue for Fishery Purposes. No. 7. Rome, FAO. 523 p.
- Fhami, White W.T., 2015 [7]. *Atelomycterus erdmanni*, a new species of catshark (Scyliorhinidae: Carcharhiniformes) from Indonesia. Journal of the Ocean Science Foundation. 14: 14 – 27.

- Fanti, F., Minelli D., Larocca Conte G., and Miyashita T., 2016. An exceptionally preserved Eocene shark and the rise of modern predatory-prey interaction in the coral reef food web. *Zoological Letters* 2(9): 18p. doi:[10.1186/s40851-016-0045-4](https://doi.org/10.1186/s40851-016-0045-4).
- Ferrón H.G., Botella H., 2017. Squamation and ecology of thelodonts. *PLoS ONE* 12(2): 40 p. e0172781. doi:[10.1371/journal.pone.0172781](https://doi.org/10.1371/journal.pone.0172781)
- Fischer J., Voigt S., Schneider J.W., Buchwitz M., Voigt S., 2011. A selachian freshwater fauna from the Triassic of Kyrgyzstan and its implication for Mesozoic shark nurseries. *Journal of Vertebrate Paleontology*. 31 (5): 937–953.
- Francis M.P., Francis R.I.C.C., 1992 [21]. Growth Rate Estimates for New Zealand Rig (*Mustelus lenticulatus*). *Aust. J. Mar. Freshwater Res.* 43: 1157 – 76.
- Francis M.P., Mulligan K.P., 1998 [17]. Age and growth of the New Zealand school shark, *Galeorhinus galeus*. *New Zealand Journal of Marine and Freshwater Research*. 32: 427 – 440.
- Friedman M., 2010. Explosive morphological diversification of spiny-finned teleost fishes in the aftermath of the end-Cretaceous extinction. *Proc R Soc Lond B Biol Sci.* 277: 1675 – 1683.
- Friego M., Sorbini L., 1997. 600 fossili per Napoleone, catalogo della mostra. Verona. 31 p.
- Goosen A.J.J., Smale M.J., 1997 [22]. A preliminary study of age and growth of the smooth-hound shark *Mustelus mustelus* (Triakidae). *South African Journal of Marine Science*. 18(1): 85 – 91.
- Hammer, Ø., Harper, D.A.T., P. D. Ryan, 2001. PAST: Paleontological Statistics Software Package for Education and Data Analysis. *Palaeontologia Electronica*. 4(1): 9p.
- Helfman G.S., Collette B.B., Facey D.E., Bowen B.W., 2009. The diversity of fishes. Biology, evolution and ecology. Second edition. Rev. and ed. of Helfman G.S., Collette B.B., Facey D.E., Bowen B.W., 1997. The diversity of fishes. Wiley – Blackwell. 720 p.
- Heupel M.R, Carlson J.K., Simpfendorfer C.A., 2007 Shark nursery areas: concepts, definition, characterization and assumptions. *Mar Ecol: Prog Ser.* 337: 287 – 97.
- Höntzsch S., Brock J.P., Scheibner C., Kuss J., 2013. Circum-Tethyan carbonate platform evolution during the Palaeogene: the Prebetic platform as test case for climatically-controlled facies shifts. *Turk J Earth Sci.* 22: 891 – 918.
- Hottinger, L., 1960. Recherches sur les Alvéolines du Paléocène et de l'Eocène. *Schweizerische Paläontologische Abhandlungen.* 75–76: 1 – 243.
- Iglésias S. P., 2012 [6]. *Apristurus nakayai* sp. nov., a new species of deepwater catshark (Chondrichthyes: Pentanchidae) from New Caledonia. *Cybium*, 36(4): 511 – 519.
- Iglésias S. P., Lecointre G. and Sellos D.Y., 2005. Extensive paraphyly within sharks of the order Carcharhiniformes inferred from nuclear and mitochondrial genes. *Mol. Phylog. Evol.* 34: 569 – 583.

- Joung S.J., Liao Y.Y., Liu K.M., Chen C.T., Leu L.C., 2005 [32]. Age, Growth, and Reproduction of the Spinner Shark, *Carcharhinus brevipinna*, in the Northeastern Waters of Taiwan. *Zoological Studies*. 44(1): 102 – 110.
- Jucci C., 1939. L'Istituto di Zoologia "Lazzaro Spallanzani" della R. Università di Pavia. Cenno sulla storia dell'Istituto – sulla sua organizzazione e sulla attività svolta durante il quinquennio 1934-1938. Tipografia già Cooperativa di Bortolo Bianchi, Pavia. 152 p.
- Kapellos C.C., Schaub H., 1973. Zur Korrelation von Biozonierungen mit Grossforaminiferen und Nannoplankton im Paläogen der Pyrenäen. *Eclogae geologicae Helvetiae*. 66 (3): 687 – 737.
- Kemp N.R., 1999. Integumentary system and teeth. - In: Hamlett W. C., (ed.), *Biology of elasmobranch fishes: sharks, skates and rays*, Baltimore, MD (The Jolms Hopkins University.; Press). 43 – 68.
- Kusher D.I., 1987 [24]. Age and growth of the Leopard shark, *Triakis semifasciata*, from Central California. MLML/S.F. State Thesis. 36 p.
- Kusher D.I., Smith S.E., Caillet G.M., 1992 [23]. Validated age and growth of the leopard shark, *Triakis semifasciata*, with comments on reproduction. *Environmental Biology of Fishes*. 35: 187 – 203.
- Landini W., Collareta A., Pesci F., Di Celma C., Urbina M., Bianucci G., 2017. A secondary nursery area for the copper shark *Carcharhinus brachyurus* from the late Miocene of Peru. *Journal of South American Earth Sciences*. 78: 164 – 174.
- Lessa R., Santana M. F., P. Renato, 1999 [27]. Age, growth and stock structure of the oceanic whitetip shark, *Carcharhinus longimanus*, from the southwestern equatorial Atlantic. *Fisheries Research*. 42: 21 – 30. doi:[10.1016/S0165-7836\(99\)00045-4](https://doi.org/10.1016/S0165-7836(99)00045-4)
- Lessa R., Santana F.M., Batista V., Almeida Z., 2000 [31]. Age and growth of the daggenose shark, *Isogomphodon oxyrinchus*, from northern Brazil. *Mar. Freshwater Res.* 51: 339 – 347.
- Lessa R., Santana F.M., Almeida Z., 2009 [34]. Age and growth of the Brazilian sharpnose shark, *Rhizoprionodon lalandii* and Caribbean sharpnose shark, *R. porosus* (Elasmobranchii, Carcharhinidae) on the northern coast of Brazil (Maranhão). *Pan-American Journal of Aquatic Sciences*. 4(4): 532 – 544.
- Linnaeus C., 1758. *Systema naturae*. Vol.1. Regnum animale. Holmiae. 824 p.
- Lioy, P. 1865. Sopra alcuni avanzi di plagiostomi fossili del Vicentino e specialmente sull' *Alopiopsis plejodon* Lioy (*Galeus cuvieri* Ag.). *Atti della Società Italiana di Scienze Naturali e del Museo Civico di Storia Naturale di Milano*. 8: 398–405.
- Liu K.M., Lin C.P., Joung S.J., Wang S.B., 2011 [29]. Age and Growth Estimates of the Blacktip Sawtail Catshark *Galeus sauteri* in Northeastern Waters of Taiwan. *Zoological Studies*. 50(3): 284 – 295.

- Lobato F.L., Barneche D.R., Siqueira A.C., Liedke A.M.R., Lindner A., Pie M.R., Bellwood D.R., Floeter S.R., 2014. Diet and diversification in the evolution of coral reef fishes. *PLoS One*. 9(7): 11 p.
- Luciani V., Dickens G.R., Backman J., Fornaciari E., Giusberti L., Agnini C., D'Onofrio R., 2016. Major perturbations in the global carbon cycle and photosymbiont-bearing planktic foraminifera during the early Eocene. *Clim Past* 12: 981 – 1007.
- Marcinowski R., Radwanski A., 1983. The Mid-Cretaceous transgression on to the central Polish Uplands (marginal part of the central European Basin). – *Zitteliana*. 10: 65 – 95.
- Marramà, G., Bannikov A.F., Tyler J.C., Zorzin R., Carnevale G., 2016. Controlled excavations in the Pesciara and Monte Postale sites provide new insights about the palaeoecology and taphonomy of the fish assemblages of the Eocene Konservat - Lagerstätte, Italy. *Palaeogeogr. Palaeoclimatol. Palaeoecol.* 454: 228 – 245. <http://dx.doi.org/10.1016/j.palaeo.2016.04.021>
- Marramà G., Carnevale G., Andrea Engelbrecht A., Claeson K.M., Zorzin R., Fornasiero M., Kriwet J., 2017. A synoptic review of the Eocene (Ypresian) cartilaginous fishes (Chondrichthyes: Holocephali, Elasmobranchii) of the Bolca Konservat-Lagerstätte, Italy. *PalZ*. 31p. <https://doi.org/10.1007/s12542-017-0387-z>
- Marramà G., Engelbrecht A., Carnevale G., Kriwet J., 2017. Eocene sand tiger sharks (Lamniformes, Odontaspidae) from the Bolca Konservat - Lagerstätte, Italy: palaeobiology, palaeobiogeography and evolutionary significance. *Historical Biology*. 15 p.
- Marramà G., Kriwet J., 2017. Principal component and discriminant analyses as powerful tools to support taxonomic identification and their use for functional and phylogenetic signal detection of isolated fossil shark teeth. *Plos One*. 12(11): 1 – 22 pp. <https://doi.org/10.1371/journal.pone.0188806>
- Martini E., 1971. Standard Tertiary and Quaternary calcareous nannoplankton zonation. In: Farinacci A (ed) *Proceedings of the 2nd planktonic conference, Roma*. 2: 739 – 785.
- Massari, F., Sorbini, L., 1975. Aspects sédimentologiques des couches à poissons de l'Éocène de Bolca (Vérone–Nord Italie). *IXe Congrès International de Sédimentologie*. 55–61.
- McCosker J.E., Long D.J., Baldwin C.C., 2012 [8]. Description of a new species of deepwater catshark, *Bythaelurus giddingsi* sp. nov., from the Galápagos Islands (Chondrichthyes: Carcharhiniformes: Scyliorhinidae). *Zootaxa*. 3221: 48 – 59.
- Medizza, F., 1975. Il nannoplancton calcareo della Pesciara di Bolca (Monti Lessini). *Studi e Ricerche sui Giacimenti Terziari di Bolca*. 2: 433 – 444.
- Morash A.J., Mackellar S.R.C., Tunnah L., Barnett D. A., Stehfest K.M., Semmens J.M., Currie S., 2016. Pass the salt: physiological consequences of ecologically relevant hyposmotic exposure in juvenile gummy sharks (*Mustelus antarcticus*) and school sharks (*Galeorhinus galeus*). *Conservation Physiology*. 4: 13 p.

- Moss S. A., 1967. Tooth replacement in the lemon shark, *Negaprion brevirostris*. - In: Gilbert P. W., Mathewson R. F., Rall D. P. (eds.), *Sharks, skates and rays*, Baltimore (John Hopkins Press). 319 – 329.
- Moulton P.L., Walker T.I., Saddler S. R., 1992 [18]. Age and Growth Studies of Gummy Shark, *Mustelus antarcticus* Giinther, and School Shark, *Galeorhinus galeus* (Linnaeus), from Southern Australian Waters. *Aust. J. Mar. Freshwater Res.* 43: 1241 – 67.
- Müller A., 1999. Ichthyofaunen aus dem atlantischen Tertiär der USA. *Leipziger Geowissenschaften*, 9(10): 360 p.
- Müller J., Henle J., 1837. Gattungen der Haifische und Rochen nach einer von ihm mit Hr. Henle unternommenen gemeinschaftlichen Arbeit über die Naturgeschichte der Knorpelfische. - *Ber. Akad. Wiss. Berlin*. 2: 111 – 118.
- Nakaya K., Stehmann M., 1998. A new species of deep-water catshark, *Apristurus aphyodes* n. sp., from the Eastern North Atlantic (Chondrichthyes: Carcharhiniformes: Scyliorhinidae). *Archives of Fishery and Marine Research*. 46: 77 – 90.
- Nakaya K., Séret B., 2000 [14]. Re – description and taxonomy of *Pentanchus profundicolus* (Smith & Radcliff), based on a second specimen from the Philippines (Chondrichthyes, Carcharhiniformes, Scyliorhinidae). *Ichthyol. Res.* 47(4): 373 – 378.
- Nakaya K., Sato K., Iglésias P., White W.T., 2008b. Methodology for the taxonomic description of members of the genus *Apristurus* (Chondrichthyes: Carcharhiniformes: Scyliorhinidae). In: *CSIRO Marine & Atmospheric Research Paper* (eds). *Descriptions of New Australian Chondrichthyans*. 358 p.
- Noubhani A., Cappetta H., 1997. Les Orectolobiformes, Carcharhiniformes et Myliobatiformes (Elasmobranchii, Neoselachii des bassins à phosphate du Maroc (Maastrichtien-Lutétien basal). *Systematique, biostratigraphie, evolution et dynamique des faunes. – Palaeo Ichthyologica*. 8: 327 p.
- Nyberg JG, Ciampaglio CN, Wray GA. Tracing the ancestry of the great white shark, *Carcharodon carcharias*, using morphometric analyses of fossil teeth. *J Vert Paleontol.* 2006; 26(4): 806±814.
- Olsen, A. M., 1984 [19]. Synopsis of biological data on the school shark *Galeorhinus australis* (Macleay 1881). *FAO Fisheries Synopsis*. 139: 49 p.
- Oeffner J., Lauder G.V., 2011. The hydrodynamic function of shark skin and two biomimetic applications. *The Journal of Experimental Biology*. 215: 785 – 795.
- Papazzoni C.A., Trevisani E., 2006. Facies analysis, palaeoenvironmental reconstruction, and biostratigraphy of the “Pesciara di Bolca” (Verona, northern Italy): An early Eocene Fossil-Lagerstätte. *Palaeogeography, Palaeoclimatology, Palaeoecology*. 242: 21 – 35.
- Papazzoni C.A., Giusberti L., Carnevale G., Roghi G., Bassi D. and Zorzini R., 2014. The Bolca Fossil-Lagerstätten: A window into the Eocene World. *Excursion guidebook CBEP 2014-EPPC 2014-EAVP 2014-Taphos 2014 Conferences. Rendiconti della Società Paleontologica Italiana*. 4: 19 – 28.

- Papazzoni C. A., Bassi D., Fornaciari E., Giusberti L., Luciani V., Mietto P., Roghi G., Trevisani E., 2014. 3. Geological and stratigraphical setting of the Bolca area. In: Papazzoni C.A, Giusberti L., Carnevale G., Roghi G., Bassi D. and Zorzin R., 2014. The Bolca Fossil-Lagerstätten: A window into the Eocene World. Excursion guidebook CBEP 2014-EPPC 2014-EAVP 2014-Taphos 2014 Conferences. Rendiconti della Società Paleontologica Italiana. 4: 19 – 28.
- Papazzoni C.A., Trevisani E. (2002) - Risultati preliminari dello studio delle alveoline della Pesciara di Bolca (VR). Giornate di Paleontologia Società Paleontologica Italiana, Bolca 6-8 giugno 2002, p. 40.
- Papazzoni C.A., Fornaciari E., Giusberti L., Vescogni A., Fornaciari B., 2017. Integratic shallow benthic and calcareous nannofossil zones: the Lower Eocene of the Monte Postale section (Northern Italy). PALAIOS. 32: 6 – 17.
- Parsons G.R., 1993 [36]. Geographic variation in reproduction between two populations of the bonnethead shark, *Sphyrna tiburo*. Environmental Biology of Fishes. 38: 25 – 35.
- Piercy A.N., Carlson J.K., Sulikowski J.A., Burgess G.H., 2007 [35]. Age and growth of the scalloped hammerhead shark, *Sphyrna lewini*, in the north-west Atlantic Ocean and Gulf of Mexico. Marine and Freshwater Research. 58: 34 – 40.
- Pimiento P., Ehret D.J., MacFadden B.J., Hubbell G., 2010. Ancient nursery area for the extinct giant shark Megalodon from the Miocene of Panama. PLoS One: 5 (5): e10552. doi: [10.1371/journal.pone.0010552](https://doi.org/10.1371/journal.pone.0010552).
- Porter M.E., Ewoldt R.H., Long J.H., Jr, 2016. Automatic control: the vertebral column of dogfish sharks behaves as a continuously variable transmission with smoothly shifting functions. Journal of Experimental Biology. 219: 2908 – 2919. doi:10.1242/jeb.135251
- Price S.A., Schmitz L., Oufiero C.E., Eytan R.I., Dornburg A., Smith W.L., Friedman M., Near T.J., Wainwright P.C., 2014. Two waves of colonization straddling the K–Pg boundary formed the modern reef fish fauna. Proc R Soc Lond B Biol Sci. 281: 7 p.
- Rana R.S., Kumar K., Singh H., 2004. Vertebrate fauna from the subsurface Cambay Shale (Lower Eocene), Vastan Lignite Mine, Gujarat, India. CURRENT SCIENCE. 87(12): 1726 – 1733.
- Rana R.S., Kumar K., Loyal R.S., Sahni A. Rose K.D., Nussel J., Singh H. Kulshreshtha S.K., 2006. Selachians from the Early Eocene Kapurdi Formation (Fuller’s Earth), Barmer District, Rajasthan. Journal Geological Society of India. 67: 509 – 522.
- Reif W.E., 1985a. Squamation and ecology of sharks. Cour Forschungsinstitut Senckenb Band 78, Schweizerbart Science Publishers, Stuttgart. 101 p.
- Rovati C., 1999. Storia del Museo dall’ottocento a oggi. In: Il Museo di Lazzaro Spallanzani 1771 – 1799 una camera delle meraviglie tra l’Arcadia e Linneo. Greppi Editore, Cava Manara (Pavia). 106 – 116.

- Roghi G., Dominici S., Giusberti L., Cerato M., Zorzin R., 2008. 2. Historical outline. In Papazzoni C.A, Giusberti L., Carnevale G., Roghi G., Bassi D. and Zorzin R., 2014. The Bolca Fossil-Lagerstätten: A window into the Eocene World. Excursion guidebook CBEP 2014-EPPC 2014-EAVP 2014-Taphos 2014 Conferences. Rendiconti della Società Paleontologica Italiana, 2014. 4: 19 – 28.
- Roghi G., Giusberti L., Papazzoni C.A., Fornaciari E., Zorzin R., Deiana R. 2015. Relazione preliminare sul carotaggio effettuato in prossimità della Pesciara di Bolca – giugno 2015. Studi e ricerche sui giacimenti terziari di Bolca, XVI - Miscellanea Paleontologica, 2015. 13: 27 – 32.
- Sato K., Nakaya K., Stewart A.L., 1999 [5]. A new species of the deep-water catshark genus *Apristurus* from New Zealand waters (Chondrichthyes: Scyliorhinidae). Journal of the Royal Society of New Zealand. 29: 325 – 335.
- Schaub, H., 1981. Nummulites et Assilines de la Téthys Paléogène. Taxonomie, phylogénèse et biostratigraphie. Schweizerische Paläontologische Abhandlungen. 104: 1 – 236.
- Schwark L., Ferretti A., Papazzoni C.A., Trevisani E., 2008. Organic geochemistry and paleoenvironment of the Early Eocene “Pesciara di Bolca” Konservat-Lagerstätte, Italy. Palaeogeography, Palaeoclimatology, Palaeoecology. 273: 272 – 285.
- Schaaf – Da Silva J.A., Ebert D.A., 2008 [15]. A revision of the western North Pacific swellsharks, genus *Cephaloscyllium* Gill 1862 (Chondrichthyes: Carcharhiniformes: Scyliorhinidae), including descriptions of two new species. Zootaxa 1872: 1–28 pp
- Scheibner C., Speijer R.P., 2008. Decline of coral reefs during late Paleocene to early Eocene global warming. eEarth. 3: 19 – 26.
- Séret B., Last P.R., 2007 [16]. Four new species of deep-water catsharks of the genus *Parmaturus* (Carcharhiniformes: Scyliorhinidae) from New Caledonia, Indonesia and Australia. Zootaxa. 1657: 23–39.
- Serra-Kiel, J., Hottinger, L., Caus, E., Drobne, K., Ferràndez, C., Jauhri, A.K., Less, G., Pavlovec, R., Pignatti, J., Samsó, J.M., Schaub, H., Sirel, E., Strougo, A., Tambareau, Y., Tosquella, J., Zakrevskaya, E., 1998. Larger foraminiferal biostratigraphy of the Tethyan Paleocene and Eocene. Bulletin de la Société Géologique de France: 169 (2): 281 – 299.
- Skomal G.B., Natanson L.J., 2002 [25]. Age and growth of the blue shark, *Prionace Glauca*, in the North Atlantic Ocean. Col.Vol.Sci.Pap. ICCAT. 54(4): 1212 – 123.
- Sorbini L., 1967. Contributo alla sedimentologia della “Pesciara” di Bolca. Memorie del Museo Civico di Storia Naturale di Verona. 15: 213 – 221.
- Sorbini L., 1972. I fossili di Bolca. 1ª edizione. Corev., Verona. 133 p.
- Sallan L., Coates M., 2014. The long-rostrumed elasmobranch *Bandringa* Zangerl, 1969 and taphonomy within a Carboniferous shark nursery. Journal of Vertebrate Paleontology. 34: 22–33.

- Takács P., 2012. Morphometric differentiation of gudgeon species inhabiting the Carpathian Basin. *Int J Limnol.* 48: 53 – 61.
- Trevisani E., 2015. Upper Cretaceous-Lower Eocene succession of the Monte Postale and its relationship with the “Pesciara di Bolca” (Lessini Mountains, northern Italy): deposition of a fossil-fish lagerstätte. *Facies.* 61: 7 p.
- Trevisani E., Papazzoni C.A., 2003. Le più antiche piattaforme del Lessini Shelf: biostratigrafia e paleoambiente dello “Spilecciano” di Spilecco (M. Lessini, Provincia di Verona). In: *Geitalia 2003, 4° Forum Italiano di Scienze della Terra (Bellaria) 16–18 settembre 2003. Riassunti: 309 – 311.*
- Trevisani E., Papazzoni C.A., Ragazzi E., Roghi G., 2005. Early Eocene amber from the “Pesciara di Bolca” (Lessini Mountains, Northern Italy). *Palaeogeography, Palaeoclimatology, Palaeoecology.* 223: 260 – 274.
- Vescogni A., Bosellini F.R., Papazzoni A. C., Giusberti L., Roghi G., Fornaciari E., Dominici S., Roberto Z., 2016. Coralgall buildups associated with the Bolca Fossil-Lagerstätten: new evidence from the Ypresian of Monte Postale (NE Italy). *Facies.* 62: 21 p.
- Volta S., (1796 – 1808). *Ittiolitologia Veronese del Museo Bozziano ora annesso a quello del Conte Giovambattista Gazola e di altri gabinetti di fossili veronesi.* Tip. Giuliari, Verona, 323 pp
- Walker, T.I., Cavanagh, R.D., Stevens, J.D., Carlisle, A.B., Chiaramonte, G.E., Domingo, A., Ebert, D.A., Mancusi, C.M., Massa, A., McCord, M., Morey, G., Paul, L.J., Serena, F. and Vooren, C.M. 2006. *Galeorhinus galeus*. The IUCN Red List of Threatened Species 2006: e.T39352A10212764. <http://dx.doi.org/10.2305/IUCN.UK.2006.RLTS.T39352A10212764.e>
- Weigmann S., 2012 [2]. Contribution to the Taxonomy and Distribution of Six Shark Species (Chondrichthyes, Elasmobranchii) from the Gulf of Thailand. *ISRN Zoology Volume 2012, Article ID 860768, 24 pp.*
- White W.T., Last P.R., 2006 [4]. Description of two new species of smooth-hounds, *Mustelus widodoi* and *M. ravidus* (Carcharhiniformes: Triakidae) from the western central Pacific. *Cybium.* 30(3): 235 - 246.
- White W. T., Ebert D. A., 2008 [9]. *Cephaloscyllium hiscosellum* sp. nov., a new swellshark (Carcharhiniformes: Scyliorhinidae) from northwestern Australia. pp. 171- 178. In *Descriptions of New Australian Chondrichthyans.* Eds P. R. Last, W. T. White & J. J. Pogonoski, CSIRO Marine and Atmospheric Research Paper No. 022, Australia. 358 p.
- White W.T., Harris M., 2013 [3]. Redescription of *Paragaleus tengi* (Chen, 1963) (Carcharhiniformes: Hemigaleidae) and first record of I Compagno, Krupp & Carpenter, 1996 from the western North Pacific. *Zootaxa.* 3752(1): 172 – 184.
- White W.T., Weigmann S., 2014 [12]. *Carcharhinus humani* sp. nov., a new whaler shark (Carcharhiniformes: Carcharhinidae) from the western Indian Ocean. *Zootaxa.* 3821(1): 71– 87.

- Winterer E.L., Bosellini A., 1981. Subsidence and sedimentation on Jurassic passive continental margin, Southern Alps, Italy. AAPG Bull. 65: 394 – 421.
- Wintner S.P., Dudley S.F.J., 2000 [30]. Age and growth estimates for the tiger shark, *Galeocerdo cuvier*, from the east coast of South Africa. Marine and Freshwater Research. 51(1): 43 – 53.
- Yano K., Ahmad A., Gambang A.C., Hamid I.A., Razak S.A., Zainal A., 2005. Sharks and Rays of Malaysia and Brunei Darussalam. Kuala Terengganu, SEAFDEC-MFRDMD. 530 p.
- Yudin K.G., Caillet G.M., 1990 [20]. Age and Growth of the Gray Smoothhound, *Mustelus californicus*, and the Brown Smoothhound, *M. henlei*, Sharks from Central California. Copeia. 1: 191 – 204.
- Zampieri D., 1992. Extensional mesostructures in the Cretaceous limestones of Paleogene Alpone – Agno half-graben (Eastern Lessini Mountains, northern Italy). Studi Trentini di Scienze Naturali Acta Geologica. 67: 75 – 85.
- Zampieri D., 1995. Tertiary extension in the southern Trento Platform, Southern Alps, Italy. Tectonics. 14: 645–657.

Supplementary materials

Appendix A: conversion between the criteria adopted and those found in literature for external measurements.

| Compagno 1988 | Cappetta 1975 | Nakaya & Stehmann (1998) | Nakaya et al. (2008b) |
|---|--|----------------------------------|--|
| TL = Total length | Total length (1) | Total length | 1 Total length (TL) |
| PP1 = prepectoral length | head region (2) | Snout tip to pectoral origin | 6 PreP1 |
| PCL - PP1 = precaudal length - prepectoral length | Trunk length (3) | ? | ? |
| TL - PRC = Total length - precaudal length | caudal fin length (4) | Lower caudal origin to tip | 68 Caudal length Distance from ventral caudal-fin origin to the tip |
| PD1 = pre 1 st dorsal length | Head – 1 st dorsal length (5) | Snout tip to 1° dorsal origin | 5 PreD1 |
| PD2 = pre 2 nd dorsal length | Head – 2 nd dorsal length (6) | Snout tip to 2° dorsal origin | 3 PreD2 |
| PP2 = prepelvic length | Head - pelvic fin length (7) | Snout tip to pelvic origin | 7 PreP2 |
| PAL = preanal length | Head - anal fin length (8) | Snout tip to anal origin | 9 Preanal length Distance |
| PCL = precaudal length | Head - caudal fin width (9) | Snout tip to lower caudal origin | 10 Precaudal length Distance |
| ? | Basal lobe width (10) | ? | 69 Caudal height Greatest height |
| ? | apical lobe width (11) | ? | 72 Caudal terminal lobe height |
| D1B = 1 st dorsal base | 1 st Dorsal fin (12a) | ? | 44 D1 base length Distance |
| D1A = 1 st dorsal anterior margin | 1 st Dorsal fin (12b) | ? | 43 D1 length Distance from first dorsal-fin origin to posterior end of the free lobe |
| D1H = 1 st dorsal height | 1 st Dorsal fin (12c) | ? | 45 D1 height Greatest |
| D2B = 2 nd dorsal base | 2 nd Dorsal fin (13a) | ? | 47 D2 length Distance from second dorsal-fin origin to posterior end of the free lobe |
| D2A = 2 nd dorsal anterior margin | 2 nd Dorsal fin (13b) | ? | 48 D2 base length Distance from second dorsal-fin origin to the insertion |
| D2H = 2 nd dorsal height | 2 nd Dorsal fin (13c) | ? | 49 D2 height Greatest height of second dorsal-fin free lobe |
| P1B = pectoral base | Pectoral fin (14a) | ? | 51 P1 base length Distance from pectoral-fin origin to the insertion |
| P1A = pectoral anterior margin | Pectoral fin (14b) | ? | 52 P1 anterior margin Distance from pectoral-fin origin to the outer corner |
| P1H = pectoral height | Pectoral fin (14c) | ? | 53 P1 posterior margin Distance between pectoral-fin outer and inner corners |
| P2B = pelvic base | Pelvic fin (15a) | ? | 58 P2 base length Distance from pelvic-fin origin to the insertion |
| P2A = pelvic anterior margin | Pelvic fin (15b) | ? | 56 P2 anterior margin Distance from pelvic-fin origin to the outer corner |
| P2H = pelvic height | Pelvic fin (15c) | ? | 60 P2 inner margin Distance from pelvic-fin insertion to the inner corner |
| ANB = anal base | Anal fin (16a) | ? | 62 Anal base length (muscle) Distance from origin of anal-fin muscle to the insertion |
| ANA = anal anterior margin | Anal fin (16b) | Anal fin Base length | 63 Anal anterior margin Distance from origin of anal-fin ceratotrichia to the outer corner |

| | | | |
|---|--|----------------------------------|---|
| ANH = anal height | Anal fin (16c) | Anal fin vertical height | 66 Anal inner margin Distance |
| IDS interdorsal space | 1 st dorsal - 2 nd dorsal fins length (17) | Interspace 1° and 2° dorsal fins | 34 D1-D2 space Direct distance |
| DCS = 2 nd dorsal - caudal space | 2 nd dorsal - caudal fins length (18) | ? | ? |
| PPS = pectoral - pelvic space | Pectoral - pelvic fins length (19) | ? | 37 P1-P2 space Distance between two lines connecting right and left insertions of pectoral fin |
| PAS = pelvic - anal space | Pelvic - anal fins length (20) | ? | 41 P2-anal space Direct distance from pelvic-fin insertion to anal-fin origin (ceratotrichia) |
| ACS = anal - caudal space | Anal - caudal fins length (21) | ? | ? |
| CTR = terminal caudal margin | Apical lobe - caudal tip (22) | ? | 73 Caudal terminal lobe length Distance from subterminal notch to the tip |
| CPU = upper postventral margin | Basal - apical lobes length (23) | ? | 71 Caudal postventral margin Distance from apex of caudal-fin ventral lobe to subterminal notch |
| Vertebrae | Vertebrae | ? | ? |
| Total | Total (24) | ? | ? |
| MP + DP (precaudal) | precaudal (25) | ? | ? |
| DC | caudal (26) | ? | ? |

Appendix B: morphometrical measurements (a, b, c, d, e, f, g, h, i) and ratios (d/c, f/e, g/f) of tooth characters for each Bolca specimens. The measures are expressed in mm

| Specimen | N. tooth | a (mm) | b (mm) | c (mm) | d (mm) | e (mm) | f (mm) | g (mm) | h (mm) | i (mm) | d/c | f/e | g/f | |
|-------------------|----------|--------|--------|--------|--------|--------|--------|--------|--------|--------|------|------|------|------|
| MSNPV 17716 | 1 | 1,0 | 3,0 | 9,0 | 4,0 | 8,0 | 5,0 | 3,0 | 3,0 | 2,0 | 0,44 | 0,63 | 0,60 | |
| | 3 | 1,0 | 2,0 | 8,0 | 3,0 | 6,0 | 4,0 | 2,0 | 2,0 | 2,0 | 0,38 | 0,67 | 0,50 | |
| | 11 | 1,0 | 5,0 | 8,0 | 6,0 | 7,5 | 5,0 | 2,5 | 3,0 | 2,0 | 0,75 | 0,67 | 0,50 | |
| | 12 | 1,0 | 3,0 | 4,0 | 4,0 | 3,0 | 1,0 | 2,0 | 1,0 | 1,0 | 1,00 | 0,33 | 2,00 | |
| | 13 | ? | 3,0 | 4,0 | ? | 3,0 | 2,0 | 1,0 | 1,5 | 1,5 | ? | 0,67 | 0,50 | |
| | 16 | 1,0 | 3,0 | 5,0 | 4,0 | 5,0 | 3,0 | 2,0 | 2,0 | 2,0 | 2,0 | 0,80 | 0,60 | 0,67 |
| | 17 | 1,0 | 2,0 | 4,0 | 3,0 | 4,0 | 2,0 | 2,0 | 1,0 | 2,0 | 2,0 | 0,75 | 0,50 | 1,00 |
| | 18 | 1,0 | 3,0 | 5,0 | 4,0 | 5,0 | 4,0 | 1,0 | 2,0 | 2,0 | 2,0 | 0,80 | 0,80 | 0,25 |
| | 19 | 1,0 | 5,0 | 4,0 | 6,0 | 6,5 | 3,5 | 3,0 | 0,5 | 1,0 | 1,0 | 1,50 | 0,54 | 0,86 |
| | 21 | 1,0 | 6,0 | 7,0 | 7,0 | 6,0 | 4,0 | 2,0 | ? | 2,0 | 2,0 | 1,00 | 0,67 | 0,50 |
| MCSNV VII.B.96 | | | | | | | | | | | | | | |
| | 1 | 1,0 | 2,0 | 5,0 | 3,0 | 4,0 | 3,0 | 1,0 | 2,0 | 1,0 | 0,60 | 0,75 | 0,33 | |
| | 2 | ? | ? | ? | ? | ? | ? | ? | ? | ? | ? | ? | ? | |
| | 3 | ? | 2,0 | 5,0 | ? | 5,0 | 4,0 | 1,0 | 1,0 | 1,0 | ? | 0,80 | 0,25 | |
| | 4 | ? | ? | ? | ? | ? | ? | ? | ? | ? | ? | ? | ? | |
| | 5 | 1,0 | 2,0 | 5,0 | 3,0 | 5,0 | 3,0 | 2,0 | 2,0 | 2,0 | 1,0 | 0,60 | 0,60 | 0,67 |
| | 6 | 1,0 | 2,0 | 5,0 | 3,0 | 5,0 | 3,0 | 2,0 | 2,0 | 2,0 | 1,0 | 0,60 | 0,60 | 0,67 |
| | 7 | 1,0 | 2,0 | 4,0 | 3,0 | 4,0 | 2,0 | 2,0 | 2,0 | 2,0 | 1,0 | 0,75 | 0,50 | 1,00 |
| | 8 | 1,0 | 2,0 | 5,0 | 3,0 | 3,0 | 2,0 | 1,0 | 2,0 | 2,0 | 1,0 | 0,60 | 0,67 | 0,50 |
| 9 | 1,0 | 2,0 | 5,0 | 3,0 | 4,0 | 2,0 | 2,0 | 2,0 | 2,0 | 1,0 | 0,60 | 0,50 | 1,00 | |

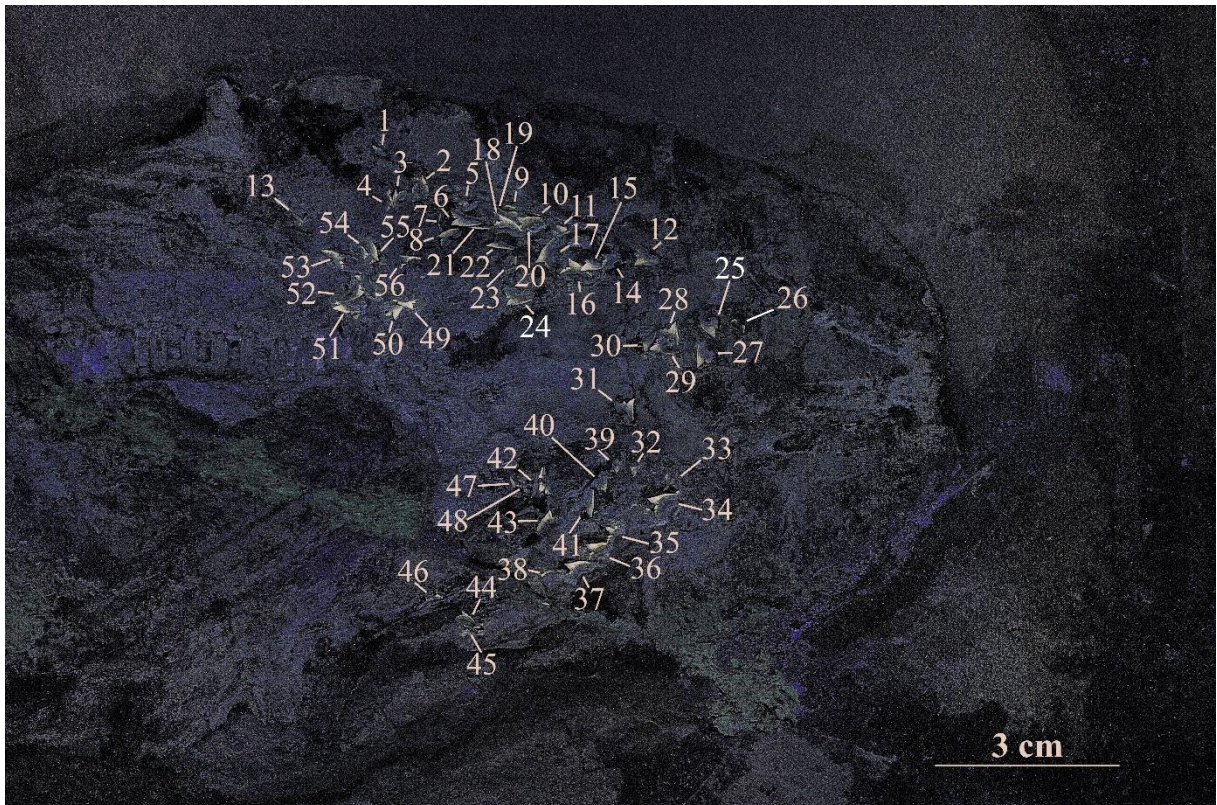
| | | | | | | | | | | | | | |
|---------------------------|----|-----|-----|------|-----|-----|------|-----|-----|-----|------|------|------|
| | 10 | 1,0 | 3,0 | 5,0 | 4,0 | 5,0 | 3,0 | 2,0 | 2,0 | 1,0 | 0,80 | 0,60 | 0,67 |
| | 11 | 1,0 | 2,0 | 5,0 | 3,0 | 4,0 | 3,0 | 1,0 | 1,0 | 1,0 | 0,60 | 0,75 | 0,33 |
| | 12 | 1,0 | 2,0 | ? | 3,0 | ? | ? | 2,0 | 2,0 | 1,0 | ? | ? | ? |
| | 13 | ? | 2,0 | 2,0 | ? | 2,0 | 1,0 | 1,0 | 1,0 | 1,0 | ? | 0,50 | 1,00 |
| | 14 | 1,0 | 2,0 | 5,0 | 4,0 | 5,0 | 3,0 | 2,0 | 2,0 | 2,0 | 0,80 | 0,60 | 0,67 |
| | 15 | ? | 3,0 | 3,0 | ? | 3,0 | 1,0 | 2,0 | 2,0 | 1,5 | ? | 0,33 | 2,00 |
| | 16 | 1,0 | 2,0 | 4,0 | 3,0 | 4,0 | 2,0 | 2,0 | 2,0 | 1,0 | 0,75 | 0,50 | 1,00 |
| | 17 | 0,5 | 1,5 | 3,0 | 2,0 | 2,0 | 1,0 | 1,0 | 1,0 | 1,0 | 0,67 | 0,50 | 1,00 |
| | 18 | 0,5 | 3,0 | 4,0 | 3,5 | 5,0 | 3,0 | 2,0 | 2,0 | 1,0 | 0,88 | 0,60 | 0,67 |
| | 19 | ? | ? | 4,0 | ? | ? | ? | ? | ? | ? | ? | ? | ? |
| | 20 | 1,0 | 2,0 | 5,0 | 3,0 | 4,0 | 2,0 | 2,0 | 2,0 | 1,0 | 0,60 | 0,50 | 1,00 |
| | 21 | ? | 2,0 | 4,0 | ? | 4,0 | 2,0 | 2,0 | 1,0 | 1,0 | ? | 0,50 | 1,00 |
| | 24 | ? | 2,0 | ? | ? | 5,0 | 3,0 | 2,0 | 2,0 | 1,0 | ? | 0,60 | 0,67 |
| | 28 | 0,5 | 2,5 | 6,0 | 3,0 | 5,0 | 3,0 | 2,0 | 2,0 | 1,5 | 0,50 | 0,60 | 0,67 |
| | 30 | ? | 2,0 | ? | ? | 3,5 | 2,0 | 1,5 | ? | ? | ? | 0,57 | 0,75 |
| | 31 | ? | 3,0 | ? | ? | 4,0 | 2,5 | 1,5 | 1,5 | 1,0 | ? | 0,63 | 0,60 |
| MCSNV VII.B.97 | | | | | | | | | | | | | |
| | 1 | ? | 2,0 | ? | 4,0 | 2,0 | 2,0 | 2,0 | 2,0 | 1,0 | ? | 1,0 | 1,0 |
| | 2 | 0,5 | 2,0 | 5,0 | 2,5 | 4,0 | 2,0 | 2,0 | 2,0 | 1,0 | 0,50 | 0,50 | 1,00 |
| | 4 | 0,5 | 2,0 | 4,5 | 2,5 | 4,0 | 2,0 | 2,0 | 2,0 | 1,0 | 0,56 | 0,50 | 1,00 |
| | 5 | ? | ? | ? | ? | ? | ? | ? | ? | ? | ? | ? | ? |
| | 6 | 0,5 | 2,0 | 4,0 | 2,5 | 4,0 | 2,0 | 2,0 | 2,0 | 1,5 | 0,63 | 0,50 | 1,00 |
| | 11 | 1,0 | 2,0 | 5,0 | 3,0 | 4,0 | 2,0 | 2,0 | 1,5 | 1,5 | 0,60 | 0,50 | 1,00 |
| | 12 | 1,0 | 2,0 | ? | 3,0 | 4,5 | 2,00 | 2,5 | ? | 1,5 | ? | 0,44 | 1,25 |
| | 13 | ? | ? | ? | ? | 3,5 | 2,00 | 1,5 | ? | ? | ? | 0,57 | 0,75 |
| | 14 | 1,0 | 2,0 | ? | 3,0 | ? | ? | 2,0 | 2,0 | 1,5 | ? | ? | ? |
| | 15 | ? | ? | ? | ? | ? | ? | ? | ? | ? | ? | ? | ? |
| MCSNV T.1124 | | | | | | | | | | | | | |
| | 2 | 1,0 | 2,0 | 5,0 | 3,0 | 5,0 | 3,0 | 2,0 | 2,0 | 1,5 | 0,60 | 0,60 | 0,67 |
| | 3 | 0,5 | 1,5 | 4,0 | 2,0 | 5,0 | 3,0 | 2,0 | 1,0 | 1,5 | 0,50 | 0,60 | 0,67 |
| | 4 | ? | ? | ? | ? | 5,5 | 3,0 | 2,5 | ? | ? | ? | 0,55 | 0,83 |
| | 5 | 1,0 | 2,0 | 5,0 | 3,0 | 3,0 | 1,0 | 2,0 | 2,0 | 1,5 | 0,60 | 0,33 | 2,00 |
| | 6 | 0,5 | 2,5 | ? | 3,0 | ? | 1,0 | 2,0 | 2,0 | ? | ? | ? | 2,00 |
| | 7 | 1,0 | 2,0 | 6,0 | 3,0 | 5,0 | 3,0 | 2,0 | 2,0 | 1,5 | 0,50 | 0,60 | 0,67 |
| | 10 | 2,0 | 3,0 | 4,0 | 5,0 | 3,0 | 1,0 | 2,0 | 1,0 | 1,0 | 1,25 | 0,33 | 2,00 |
| MCSNV T.311 | | | | | | | | | | | | | |
| | 1 | 1,5 | 4,5 | 10,0 | 6,0 | 9,0 | 5,0 | 4,0 | 4,2 | 2,5 | 0,60 | 0,56 | 0,80 |
| | 3 | 1,0 | 3,5 | 9,0 | 4,5 | 8,5 | 5,0 | 3,5 | 3,0 | 2,5 | 0,50 | 0,59 | 0,70 |
| | 4 | 1,0 | 3,5 | 8,0 | 4,5 | 8,0 | 3,0 | 5,0 | 2,0 | 3,0 | 0,56 | 0,38 | 1,67 |
| | 5 | 1,0 | 3,0 | 6,5 | 4,0 | 6,5 | 3,5 | 3,0 | 2,0 | 2,0 | 0,62 | 0,54 | 0,86 |
| | 6 | 1,0 | 4,0 | 9,5 | 4,0 | 8,5 | 4,5 | 4,0 | 3,5 | 2,5 | 0,42 | 0,53 | 0,89 |
| | 7 | 1,0 | 3,5 | 8,5 | 4,5 | 8,0 | 4,5 | 3,0 | 2,5 | 2,5 | 0,53 | 0,56 | 0,67 |
| | 8 | 1,0 | 5,0 | 8,0 | 6,0 | 7,0 | 4,0 | 3,0 | 4,0 | 2,0 | 0,75 | 0,57 | 0,75 |
| | 9 | 1,0 | 4,0 | 8,5 | 4,5 | 9,0 | 5,5 | 3,5 | 3,0 | 2,0 | 0,53 | 0,61 | 0,64 |

| | | | | | | | | | | | | | |
|----------------------|----|-----|-----|------|-----|------|-----|-----|-----|-----|------|------|------|
| | 10 | 1,5 | 5,0 | 10,5 | 6,5 | 8,5 | 4,0 | 4,5 | 3,5 | 3,0 | 0,62 | 0,47 | 1,13 |
| | 11 | 1,0 | 4,0 | 7,5 | 5,0 | 6,0 | 3,0 | 3,0 | 3,5 | 2,0 | 0,67 | 0,50 | 1,00 |
| | 12 | 1,0 | 3,0 | 8,5 | 4,0 | 8,0 | 4,0 | 4,0 | 2,5 | 2,5 | 0,47 | 0,50 | 1,00 |
| | 15 | 1,0 | 4,0 | ? | 5,0 | 8,0 | 4,0 | 4,0 | 2,5 | 2,5 | ? | 0,50 | 1,00 |
| | 16 | 1,0 | 4,0 | 10,0 | 5,0 | 9,5 | 6,0 | 3,0 | 3,0 | 2,0 | 0,50 | 0,63 | 0,50 |
| | 17 | 1,5 | 6,0 | 8,5 | 7,5 | 8,5 | 6,5 | 3,0 | 4,0 | 2,5 | 0,88 | 0,76 | 0,46 |
| | 18 | 1,5 | 5,0 | 9,0 | 6,5 | 8,5 | 4,5 | 4,0 | 4,0 | 2,5 | 0,72 | 0,53 | 0,89 |
| | 21 | 1,0 | 7,5 | 9,5 | 8,5 | 10,5 | 6,0 | 4,5 | 4,0 | 3,0 | 0,89 | 0,57 | 0,75 |
| | 25 | 0,5 | 4,5 | 4,0 | 5,0 | 7,0 | 3,0 | 4,0 | 1,0 | 1,5 | 1,25 | 0,43 | 1,33 |
| | 26 | ? | 5,5 | ? | ? | 8,5 | 3,5 | 5,0 | ? | 2,5 | ? | 0,41 | 1,43 |
| | 27 | 0,5 | 6,5 | 3,5 | 7,0 | 7,0 | 3,0 | 4,0 | 3,0 | 2,5 | 2,00 | 0,43 | 1,33 |
| | 28 | 1,5 | 3,0 | 3,0 | 4,5 | 3,5 | 2,0 | 1,5 | 2,0 | 1,5 | 1,50 | 0,57 | 0,75 |
| | 29 | 2,0 | 6,5 | 7,0 | 8,5 | 8,5 | 3,0 | 5,5 | 3,0 | 3,0 | 1,21 | 0,35 | 1,83 |
| | 32 | 1,0 | 6,0 | 6,0 | 7,0 | 8,5 | 4,0 | 4,5 | 2,5 | 2,0 | 1,17 | 0,47 | 1,13 |
| | 33 | 1,0 | 5,0 | 5,0 | 6,0 | 5,0 | 1,5 | 3,5 | 2,5 | 1,5 | 1,20 | 0,30 | 2,33 |
| | 36 | 1,0 | 6,5 | 4,0 | 7,5 | 7,0 | 2,5 | 4,5 | 1,0 | 2,0 | 1,88 | 0,36 | 1,80 |
| | 37 | 1,0 | 7,0 | 5,5 | 8,0 | 8,5 | 3,0 | 5,5 | 2,5 | 2,5 | 1,45 | 0,35 | 1,83 |
| | 39 | 1,0 | 8,0 | 7,0 | 9,0 | 10,5 | 4,5 | 6,0 | 3,5 | 2,5 | 1,29 | 0,43 | 1,33 |
| | 41 | ? | 7,5 | ? | ? | 9,0 | 4,0 | 5,0 | 3,5 | 3,0 | ? | 0,44 | 1,25 |
| | 43 | 1,5 | 3,5 | 9,5 | 5,0 | 9,0 | 4,0 | 5,0 | 3,0 | 3,0 | 0,53 | 0,44 | 1,25 |
| | 45 | 1,0 | 6,0 | 9,0 | 7,0 | 7,0 | 5,5 | 3,5 | 4,0 | 2,5 | 0,78 | 0,79 | 0,64 |
| | 47 | 1,0 | 4,5 | 8,5 | 5,5 | 7,5 | 4,5 | 3,0 | 3,5 | 2,0 | 0,65 | 0,60 | 0,67 |
| | 48 | 2,0 | 4,0 | 4,0 | 6,0 | 6,0 | 1,0 | 5,0 | 1,0 | 2,5 | 1,50 | 0,17 | 5,00 |
| | 51 | 1,0 | ? | 6,0 | ? | ? | 3,5 | ? | 2,0 | 2,5 | ? | ? | ? |
| | 52 | 0,5 | 6,5 | 4,5 | 7,0 | 8,5 | 3,5 | 5,0 | 2,0 | 3,0 | 1,56 | 0,41 | 1,43 |
| | 56 | 0,5 | 6,0 | 3,5 | 7,0 | 6,5 | 2,0 | 4,5 | 1,5 | 2,0 | 2,00 | 0,31 | 2,25 |
| | 57 | 2,5 | 5,0 | 10,0 | 7,5 | 9,5 | 5,5 | 4,0 | 3,5 | 2,5 | 0,75 | 0,58 | 0,73 |
| | 58 | ? | 7,5 | ? | ? | 7,5 | 4,0 | 3,5 | 3,5 | 2,5 | ? | 0,53 | 0,88 |
| | 59 | 1,0 | 6,0 | 4,0 | 7,0 | 6,0 | 2,0 | 4,0 | 2,0 | 2,5 | 1,75 | 0,33 | 2,00 |
| | 60 | 1,0 | 5,0 | 4,0 | 6,0 | 5,5 | 2,5 | 3,0 | 2,0 | 2,0 | 1,50 | 0,45 | 1,20 |
| | 61 | 1,0 | 5,5 | 3,5 | 6,5 | 5,5 | 2,0 | 3,5 | ? | 1,5 | 1,86 | 0,36 | 1,75 |
| | 62 | 1,0 | 5,5 | 3,5 | 6,5 | 6,0 | 1,5 | 4,5 | 1,5 | 1,5 | 1,86 | 0,25 | 3,00 |
| MGP - PD 8871 | | | | | | | | | | | | | |
| | 1 | 0,5 | 2,5 | 3,5 | 3,0 | 4,0 | 2,0 | 2,0 | 1,0 | 2,0 | 0,86 | 0,50 | 1,00 |
| | 3 | 0,5 | 2,5 | 3,5 | 3 | 3,5 | 2 | 1,5 | ? | 1 | 0,86 | 0,57 | 0,75 |
| MGP - PD 8872 | | | | | | | | | | | | | |
| | 1 | 1,0 | 2,0 | 4,0 | 3,0 | 4,0 | 3,0 | 1,0 | 1,0 | 1,0 | 0,75 | 0,75 | 0,33 |
| | 2 | 1,0 | 3,0 | ? | 4,0 | 4,0 | 2,0 | 2,0 | ? | ? | ? | 0,50 | 1,00 |
| | 4 | 1,0 | 3,0 | 4,0 | 3,0 | 3,0 | 2,0 | 1,0 | 2,0 | 1,0 | 0,75 | 0,67 | 0,50 |
| | 5 | 1,0 | 2,0 | 5,0 | 2,0 | 4,0 | 3,0 | 1,0 | 1,0 | 1,0 | 0,40 | 0,75 | 0,33 |
| | 7 | ? | 3,0 | ? | 3,0 | 3,0 | 1,0 | 2,0 | 1,0 | 1,0 | ? | 0,33 | 2,00 |
| MGP - PD 8869 | | | | | | | | | | | | | |
| | 1 | 1,0 | 3,0 | ? | 4,0 | ? | ? | 4,0 | 1,0 | 2,0 | ? | ? | ? |
| | 2 | ? | 4,0 | ? | ? | 4,0 | 2,0 | 2,0 | 2,0 | 2,0 | ? | 0,50 | 1,00 |
| | 3 | 1,0 | 4,0 | 8,0 | 5,0 | 6,0 | 4,0 | 2,0 | 3,0 | 2,5 | 0,63 | 0,67 | 0,50 |

| | | | | | | | | | | | | | |
|----------------------|----|-----|-----|------|-----|-----|-----|-----|-----|-----|------|------|------|
| | 7 | ? | ? | ? | ? | 8,0 | 4,0 | 4,0 | 4,0 | 1,5 | ? | 0,50 | 1,00 |
| | 8 | 1,0 | 2,0 | 5,0 | 3,0 | 5,0 | 3,0 | 2,0 | 1,0 | 1,0 | 0,60 | 0,60 | 0,67 |
| | 14 | 1,5 | 2,5 | 6,0 | 4,0 | 5,0 | 2,5 | 2,5 | 1,5 | 3,0 | 0,67 | 0,50 | 1,00 |
| | 17 | 1,0 | 5,0 | 5,0 | 6,0 | 6,0 | 2,0 | 4,0 | 2,0 | 2,5 | 1,20 | 0,33 | 2,00 |
| | 19 | 1,5 | 2,5 | 3,0 | 4,0 | 5,5 | 2,5 | 3,0 | 1,5 | 2,0 | 1,33 | 0,45 | 1,20 |
| | 22 | 2,0 | 4,0 | 4,5 | 6,0 | 7,0 | 3,0 | 4,0 | 1,0 | 2,0 | 1,33 | 0,43 | 1,33 |
| | 23 | 1,5 | 4,5 | 8,0 | 6,5 | 7,0 | 3,0 | 4,0 | 4,0 | 2,0 | 0,81 | 0,43 | 1,33 |
| | 24 | ? | 4,0 | 3,0 | ? | 4,0 | 2,0 | 2,0 | 2,0 | 2,0 | ? | 0,50 | 1,00 |
| | 25 | 1,5 | 5,5 | 9,0 | 7,0 | 8,0 | 3,5 | 4,5 | 3,0 | 2,5 | 0,78 | 0,44 | 1,29 |
| | 28 | ? | 9,0 | ? | ? | 7,0 | 3,0 | 4,0 | 2,0 | 2,0 | ? | 0,43 | 1,33 |
| | 31 | ? | 4,0 | ? | ? | 5,5 | 3,0 | 2,5 | 3,0 | 2,5 | ? | 0,55 | 0,83 |
| | 35 | 1,0 | 3,5 | 4,5 | 4,5 | 5,0 | 5,0 | 2,0 | 2,0 | 2,0 | 1,00 | 1,00 | 0,40 |
| | 36 | 1,5 | 3,5 | 7,0 | 5,0 | 5,0 | 2,0 | 3,0 | 2,0 | 3,0 | 0,71 | 0,40 | 1,50 |
| | 37 | ? | 4,5 | ? | ? | 7,0 | 4,0 | 3,0 | ? | 2,5 | ? | 0,57 | 0,75 |
| | 49 | 1,0 | 3,0 | 6,0 | 4,0 | 6,0 | 3,0 | 3,0 | 2,5 | 2,5 | 0,67 | 0,50 | 1,00 |
| MGP - PD 8870 | | | | | | | | | | | | | |
| | 5 | ? | 4,0 | ? | ? | 7,5 | 4,5 | 3,0 | ? | ? | ? | 0,60 | 0,67 |
| | 6 | ? | 4,5 | ? | ? | 6,5 | 4,5 | 2,0 | 3,0 | 2,5 | ? | 0,69 | 0,44 |
| | 7 | 1,0 | 3,0 | 6,0 | 4,0 | 6,0 | 3,0 | 3,0 | 2,5 | 2,5 | 0,67 | 0,50 | 1,00 |
| | 10 | ? | 5,0 | ? | ? | 7,5 | 4,5 | 3,0 | 2,0 | 3,0 | ? | 0,60 | 0,67 |
| | 17 | 1,0 | 4,0 | 4,0 | 5,0 | 4,5 | 2,0 | 2,5 | 1,5 | 1,0 | 1,25 | 0,44 | 1,25 |
| | 21 | 1,0 | 3,0 | 6,0 | 4,0 | 5,0 | 3,0 | 2,0 | 3,0 | 2,0 | 0,67 | 0,60 | 0,67 |
| | 23 | ? | 3,0 | 5,0 | ? | 4,0 | 3,0 | 1,0 | 2,5 | 1,0 | ? | 0,75 | 0,33 |
| | 26 | 1,0 | 4,0 | 10,0 | 5,0 | ? | ? | ? | 3,0 | ? | 0,50 | ? | ? |
| | 35 | ? | 4,0 | 7,0 | ? | 7,0 | 4,0 | 3,0 | 2,0 | 1,0 | ? | 0,57 | 0,75 |
| | 41 | 1,0 | 3,0 | 8,5 | 4,0 | 7,0 | 4,0 | 3,0 | 2,5 | 1,5 | 0,47 | 0,57 | 0,75 |
| MGGC 1976 | | | | | | | | | | | | | |
| | 2 | 0,5 | 1,5 | 4,0 | 2,0 | 4,0 | 3,0 | 1,0 | 2,0 | 1,0 | 0,50 | 0,75 | 0,33 |
| | 3 | 0,5 | 1,5 | 3,0 | 2,0 | 3,0 | 2,0 | 1,0 | 1,0 | 1,0 | 0,67 | 0,67 | 0,50 |
| | 4 | ? | 3,0 | 3,0 | ? | 2,0 | 1,0 | 1,0 | 1,0 | 1,0 | ? | 0,50 | 1,00 |
| | 6 | 1,0 | 2,0 | 6,0 | 3,0 | 5,0 | 3,0 | 2,0 | 2,0 | 1,0 | 0,50 | 0,60 | 0,67 |
| | 8 | 1,0 | 2,0 | 4,0 | 3,0 | 4,0 | 3,0 | 1,0 | 1,0 | 1,0 | 0,75 | 0,75 | 0,33 |
| | 12 | 0,5 | 3,0 | 4,5 | 3,5 | 4,0 | 2,0 | 2,0 | 2,0 | 1,0 | 0,78 | 0,50 | 1,00 |
| | 13 | 0,5 | 1,0 | 3,0 | 1,5 | 3,0 | 2,0 | 1,0 | 1,0 | 0,5 | 0,50 | 0,67 | 0,50 |
| | 14 | 1,0 | 2,0 | 5,0 | 3,0 | 5,0 | 3,0 | 2,0 | 2,0 | 2,0 | 0,60 | 0,60 | 0,67 |
| | 16 | 1,0 | 3,0 | 6,0 | 4,0 | 5,0 | 3,0 | 2,0 | 2,0 | 2,0 | 0,67 | 0,60 | 0,67 |
| | 17 | 1,0 | 3,0 | 6,0 | 4,0 | 5,0 | 3,0 | 2,0 | 2,0 | 2,0 | 0,67 | 0,60 | 0,67 |
| | 18 | 1,0 | 2,0 | ? | 3,0 | 6,0 | 3,0 | 3,0 | ? | 2,0 | ? | 0,50 | 1,00 |
| | 22 | 0,5 | 2,5 | ? | 3,0 | 5,0 | 3,0 | 2,0 | ? | ? | ? | 0,60 | 0,67 |
| | 23 | 0,5 | 1,5 | 3,0 | 2,0 | 3,0 | 2,0 | 1,0 | 1,0 | 1,0 | 0,67 | 0,67 | 0,50 |
| | 24 | 1,0 | 2,0 | 5,0 | 3,0 | 5,0 | 3,0 | 2,0 | 2,0 | 2,0 | 0,60 | 0,60 | 0,67 |
| | 25 | 0,5 | 3,0 | 3,0 | 3,5 | 3,0 | 1,0 | 2,0 | 1,0 | 2,0 | 1,17 | 0,33 | 2,00 |
| | 27 | 1,0 | 3,0 | 4,0 | 4,0 | 4,0 | 3,0 | 1,0 | 1,0 | 2,0 | 1,00 | 0,75 | 0,33 |
| | 28 | ? | 3,0 | ? | ? | 4,0 | 1,0 | 3,0 | 1,0 | 2,0 | ? | 0,25 | 3,00 |
| | 29 | 1,0 | 3,0 | 5,0 | 4,0 | 5,0 | 2,0 | 3,0 | ? | 2,0 | 0,80 | 0,40 | 1,50 |

| | | | | | | | | | | | | | |
|--|----|-----|-----|-----|-----|-----|-----|-----|-----|-----|------|------|------|
| | 31 | 1,0 | 3,0 | 5,0 | 4,0 | 4,0 | 2,0 | 2,0 | 2,0 | 1,0 | 0,80 | 0,50 | 1,00 |
| | 34 | 1,0 | 3,0 | 6,0 | 4,0 | 5,0 | 2,0 | 3,0 | 2,0 | 2,0 | 0,67 | 0,40 | 1,50 |
| | 37 | 0,5 | 3,0 | 5,0 | 3,5 | 4,0 | 2,0 | 2,0 | 1,0 | 2,0 | 0,70 | 0,50 | 1,00 |
| | 41 | 1,0 | 2,0 | 5,0 | 3,0 | 5,0 | 3,0 | 2,0 | ? | 1,0 | 0,60 | 0,60 | 0,67 |
| | 42 | 1,0 | 3,0 | 5,0 | 4,0 | 5,0 | 3,0 | 2,0 | 2,0 | ? | 0,80 | 0,60 | 0,67 |
| | 43 | ? | 2,0 | ? | ? | 4,0 | 2,0 | 2,0 | ? | 2,0 | ? | 0,50 | 1,00 |
| | 44 | 0,5 | 1,5 | 3,0 | 2,0 | 3,0 | 1,0 | 2,0 | 1,0 | 2,0 | 0,67 | 0,33 | 2,00 |
| | 49 | ? | 2,0 | ? | ? | 4,0 | 3,0 | 1,0 | 1,0 | 1,0 | ? | 0,75 | 0,33 |
| | 50 | 1,0 | 2,0 | 3,0 | 3,0 | 3,0 | 1,0 | 2,0 | 1,0 | 1,0 | 1,00 | 0,33 | 2,00 |
| | 52 | 1,0 | 2,0 | 5,0 | 3,0 | 4,0 | 3,0 | 1,0 | 2,0 | 1,0 | 0,60 | 0,75 | 0,33 |
| | 53 | 0,5 | 1,5 | 5,0 | 2,0 | 4,0 | 3,0 | 1,0 | 2,0 | 1,0 | 0,40 | 0,75 | 0,33 |
| | 54 | ? | 1,0 | 2,0 | ? | 2,0 | 1,0 | 1,0 | 1,0 | 1,0 | ? | 0,50 | 1,00 |
| | 55 | 1,0 | 1,0 | 4,0 | 2,0 | 4,0 | 2,0 | 2,0 | 1,0 | 1,0 | 0,50 | 0,50 | 1,00 |
| | 56 | ? | 2,0 | 4,0 | ? | 4,0 | 2,0 | 2,0 | ? | ? | ? | 0,50 | 1,00 |

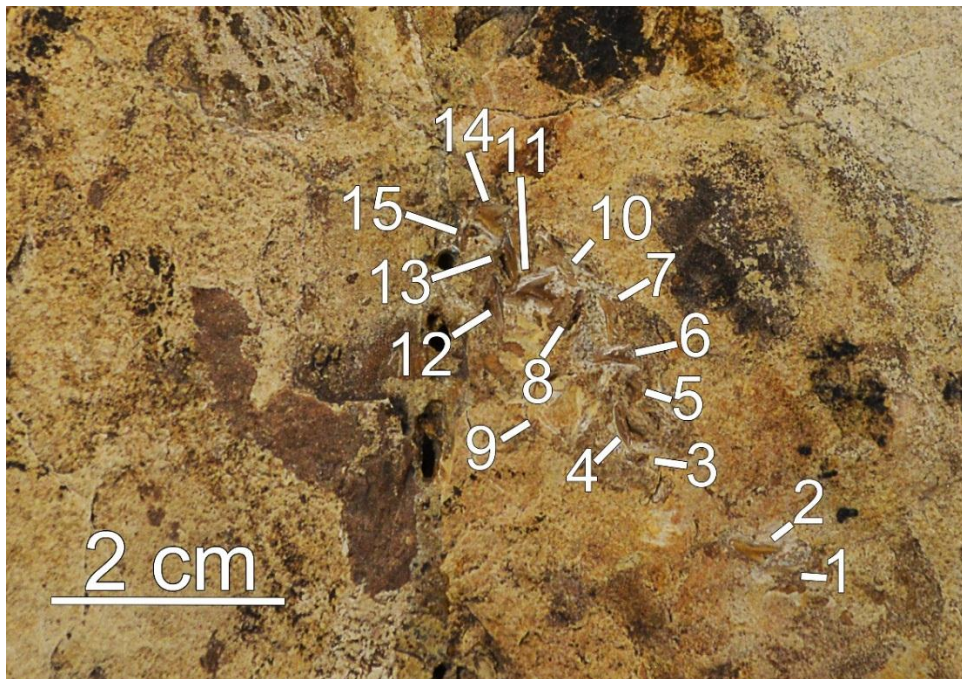
Appendix C: Teeth counts.



C1: Head region of the specimen MGGC 1976. Photograph under UV rays.



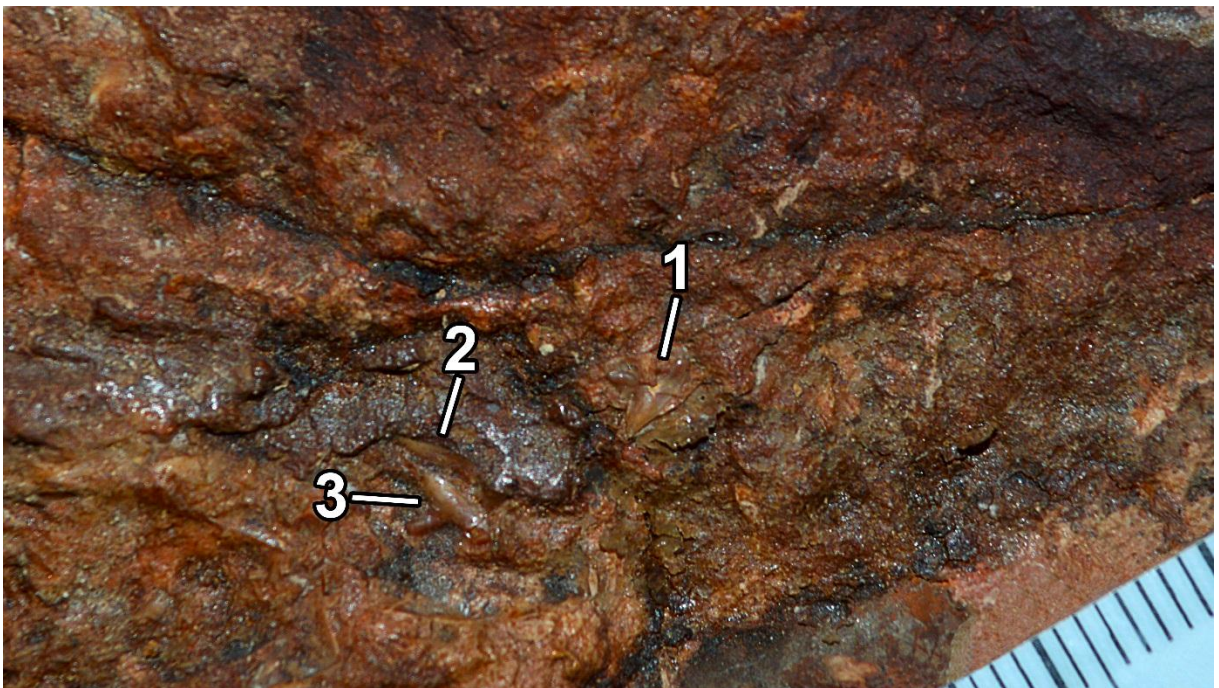
C2: Head region of MCSNV VII.B.96



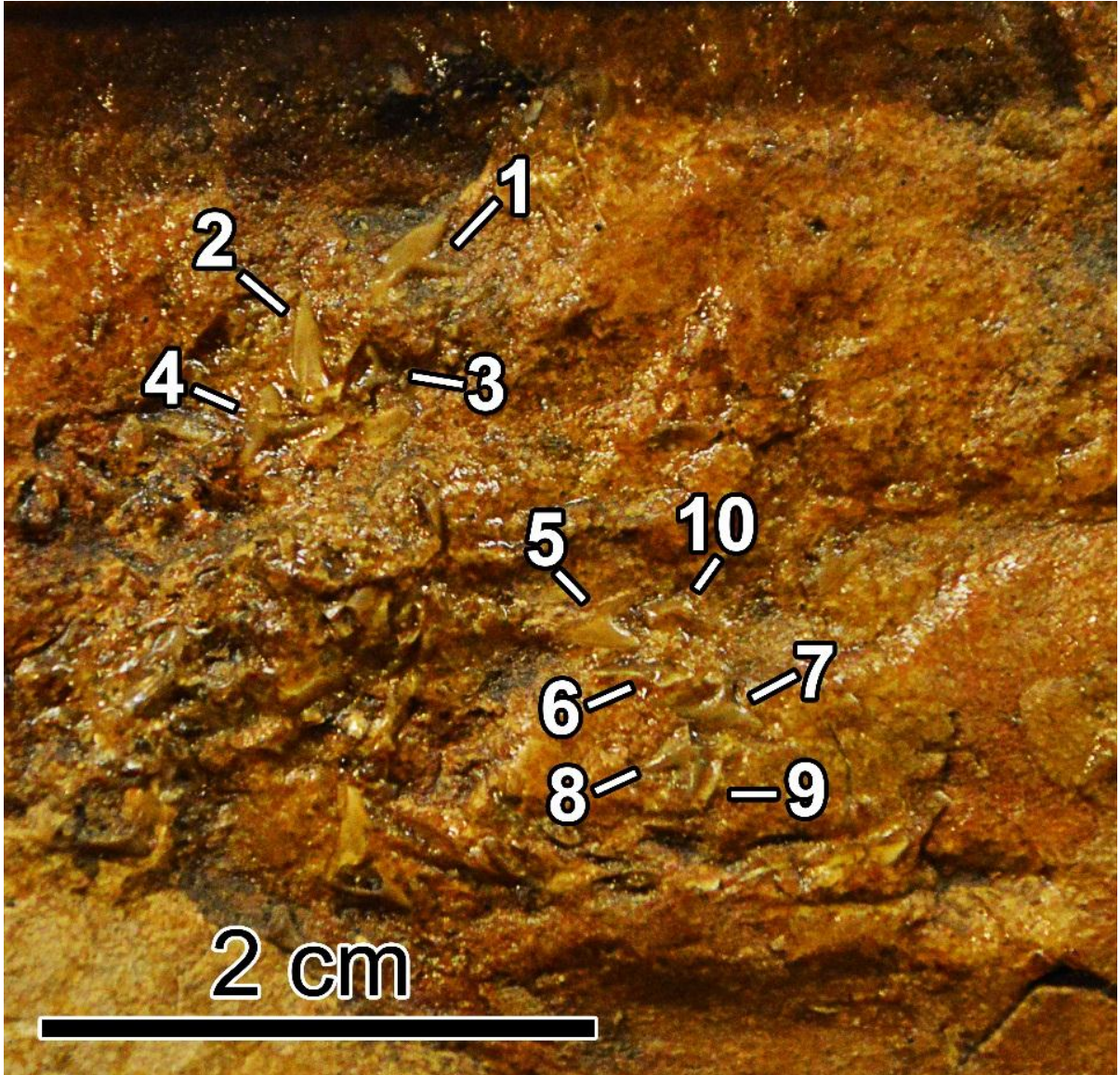
C3: Head region of MCSNV VII.B.97



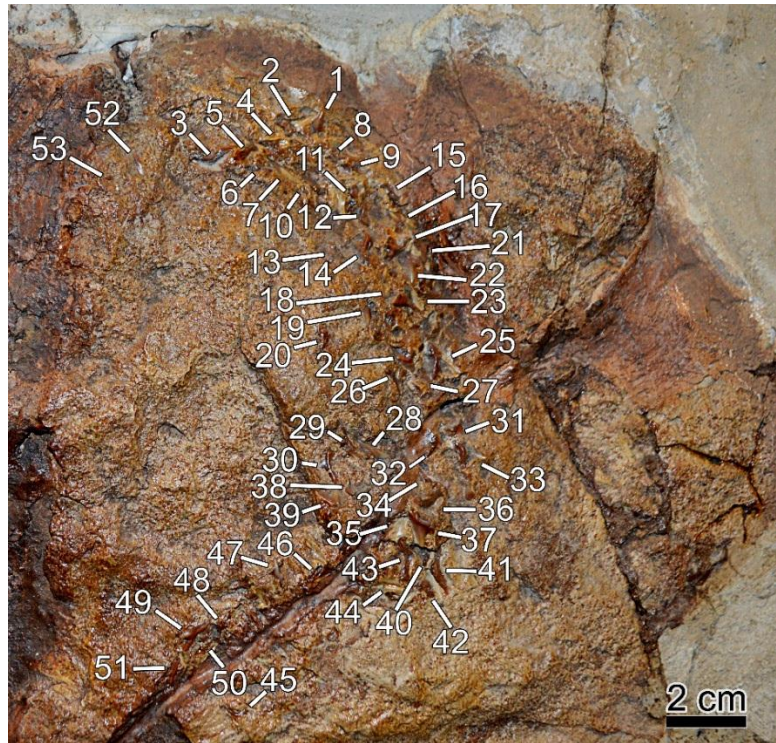
C4: Head region of MCSNV T.1124



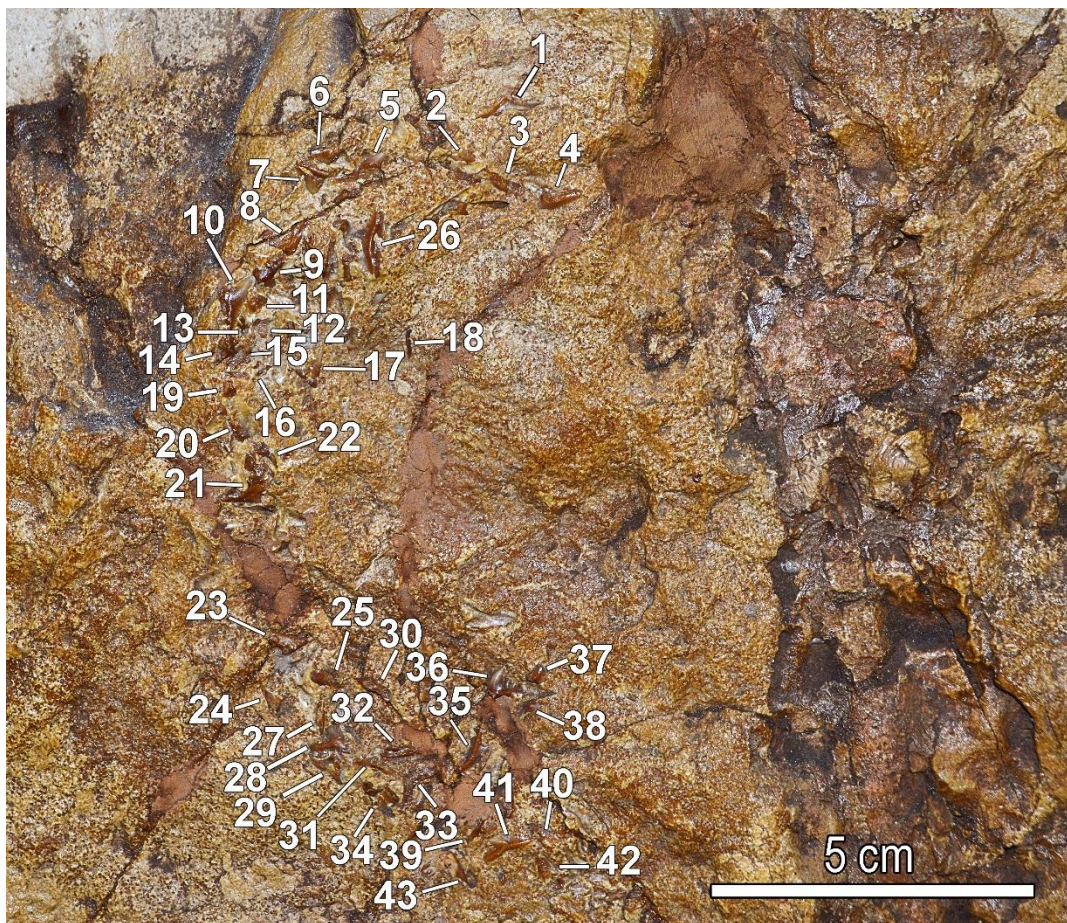
C5: Head region of MGP - PD 8871



C6: Head region of MGP – PD 8872

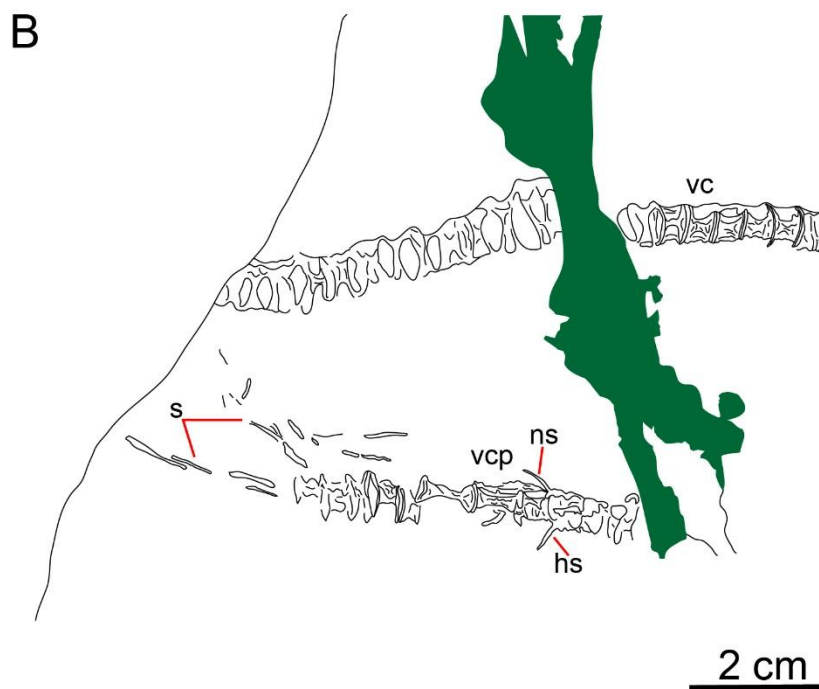


C7: Head region of MGP – PD 8869



C8: Head region of MGP – PD 8870

Appendix D: Focus of the abdominal region of the specimen MGP – PD 26878: A) photograph under natural color; B) interpretative drawing. The perciform individual counts 12 centra and several scattered spines. The green patches indicate pigmented mortar glue. *Abbreviations:* hs, haemal spine; ns, neural spine; s, spines; vc, vertebral column of the shark specimen; vcp, vertebral column of the perciform specimen.



Appendix E: List of the 68 characters considered to statistical analysis.

| | |
|---|--|
| Total length (1) | precaudal vertebrae (25) |
| Head region (2) | caudal vertebrae (26) |
| Trunk length (3) | Trunk (3) / total length (1) |
| caudal fin length (4) | Head (2) / total length (1) |
| Head - 1st dorsal length (5) | Caudal region (4) / total length (1) |
| Head - 2nd dorsal length (6) | Head - 1st dorsal (5) / total length (1) |
| Head - pelvic fin length (7) | Head - 2nd dorsal (6) / total length (1) |
| Head - anal fin length (8) | Head - pelvic fin (7) / total length (1) |
| Head - caudal fin width (9) | Head - anal fin (8) / total length (1) |
| Basal lobe width (10) | Head - caudal fin (9) / total length (1) |
| Apical lobe width (11) | Basal lobe (10) / total length (1) |
| 1st dorsal (12a) | Apical lobe (11) / total length (1) |
| 1st dorsal (12b) | 1st dorsal (12a) / total length (1) |
| 1st dorsal (12c) | 1st dorsal (12b) / total length (1) |
| 2nd dorsal (13a) | 1st dorsal (12c) / total length (1) |
| 2nd dorsal (13b) | 2nd dorsal (13a) / total length (1) |
| 2nd dorsal (13c) | 2nd dorsal (13b) / total length (1) |
| Pectoral fin (14a) | 2nd dorsal (13c) / total length (1) |
| Pectoral fin (14b) | Pectoral fin (14a) / total length (1) |
| Pectoral fin (14c) | Pectoral fin (14b) / total length (1) |
| Pelvic fin (15a) | Pectoral fin (14c) / total length (1) |
| Pelvic fin (15b) | Pelvic fin (15a) / total length (1) |
| Pelvic fin (15c) | Pelvic fin (15b) / total length (1) |
| Anal fin (16a) | Pelvic fin (15c) / total length (1) |
| Anal fin (16b) | Anal fin (16a) / total length (1) |
| Anal fin (16c) | Anal fin (16b) / total length (1) |
| 1st dorsal - 2nd dorsal fins length (17) | Anal fin (16c) / total length (1) |
| 2nd dorsal - caudal fins length (18) | 1st dorsal - 2nd dorsal (17) / total length (1) |
| Pettoral - pelvic fins length (19) | 2nd dorsale - caudal fin (18) / total length (1) |
| Pelvic - anal fins length (20) | Pectoral - pelvic fins (19) / total length (1) |
| Anal - caudal fins length (21) | Pelvic - anal fins (20) / total length (1) |
| Apical lobe - caudal tip (22) | Anal - caudal fins (21) / total length (1) |
| Basal - apical lobes length (23) | Apical lobe - caudal tip (22) / total length (1) |
| Total vertebrae (24) | Basal - apical lobes (23) / total length (1) |

Appendix F: Tooth characters list

- 1) **Overall tooth morphology (labial view):** 0) triangular; 1) sub – triangular
- 2) **Tooth morphology, mesio – distal view:** 0) pressed labio – lingually; 1) thick
- 3) **Tooth symmetry:** 0) asymmetric; 1) symmetric
- 4) **Crown, labial view:** 0) smooth; 1) basal transverse ridge
- 5) **Neck, labial view:** 0) present; 1) absent
- 6) **Crown, labial face in mesio – distal view:** 0) flat or slightly convex; 1) convex;
- 7) **Crown, lingual face in mesio – distal view:** 0) flat or slightly convex; 1) convex
- 8) **Main cusp, morphology:** 0) restricted; 1) wide; 2) slender
- 9) **Main cusp, inclination:** 0) strongly tilted distally; 1) tilted distally; 2) slightly tilted distally; 3) erected
- 10) **Main cusp, serration:** 0) absent; 1) present
- 11) **Mesial edge:** 0) Straight or slightly convex; 1) concave; 2) convex
- 12) **Mesial edge, serrations:** 0) absent; 1) 1 – 2 distal serrations; 2) 3 distal serrations; 3) ≥ 4 distal serrations; 4) totally serrated
- 13) **Mesial edge, cusplets:** 0) absent; 1) 1 cusplet; 2) 2 cusplets; 3) 3 – 4 cusplet; 4) 5 cusplets; 5) 6 + cusplets
- 14) **Distal angle:** 0) acute; 1) approximately right; 2) right; 3) obtuse
- 15) **Distal edge:** 0) smooth; 1) with cusplets; 2) serrated; 3) with cusplets and serrated
- 16) **Number of cusplets:** 0) absent; 1) 1 cusplet; 2) 2 cusplets; 3) 3 - 4 cusplets; 4) 5 cusplets; 5) ≥ 6 cusplets
- 17) **Root, labial view:** 0) 1 nutritive groove; 1) 2 nutritive grooves; 2) absent
- 18) **Root height (a)**
- 19) **Crown height (b)**
- 20) **Root length (c)**
- 21) **Tooth height (d)**
- 22) **Mesial edge + main cusp length (e)**
- 23) **Mesial edge length (f)**
- 24) **Main cusp length (g)**
- 25) **Distal edge length (h)**
- 26) **Main cusp width (i)**
- 27) **Total height/root length (d/c)**
- 28) **Main cusp length/mesial edge (f/e)**
- 29) **Distal edge length/Main cusp length (g/f)**

Appendix G: *p* - values of a the pairwise comparison between teeth of the extant species *Galeorhinus galeus*, *Galeocerdo cuvier* and Bolca fossil specimens.

Table G1: Pairwise comparison between teeth categories of *Galeorhinus galeus* and morphotypes of fossil specimens. The blue, yellow and orange cells indicate the tooth categories of *G. galeus*, the morphotypes of the fossils and uncorrected variances among groups ($p > 0,05$), respectively.

| <i>Galeorhinus galeus</i> - MGGC 1976 | | | | | | | | | | |
|---|---------------|----------------|---------------|---------------|----------------|---------------|--------|--------|--|--|
| | lateral upper | anterior upper | central upper | lateral lower | anterior lower | central lower | A | D | | |
| lateral upper | | 0.0007 | 0.0002 | 0.0153 | 0.0001 | 0.0003 | 0.0113 | 0.0002 | | |
| anterior upper | 0.0007 | | 0.0035 | 0.0951 | 0.0003 | 0.0087 | 0.0088 | 0.004 | | |
| central upper | 0.0002 | 0.0035 | | 0.0001 | 0.2346 | 0.1971 | 0.0011 | 0.0081 | | |
| lateral lower | 0.0153 | 0.0951 | 0.0001 | | 0.0001 | 0.001 | 0.0009 | 0.0001 | | |
| anterior lower | 0.0001 | 0.0003 | 0.2346 | 0.0001 | | 0.5376 | 0.0001 | 0.0197 | | |
| central lower | 0.0003 | 0.0087 | 0.1971 | 0.001 | 0.5376 | | 0.0019 | 0.0287 | | |
| A | 0.0113 | 0.0088 | 0.0011 | 0.0009 | 0.0001 | 0.0019 | | 0.0114 | | |
| D | 0.0002 | 0.004 | 0.0081 | 0.0001 | 0.0197 | 0.0287 | 0.0114 | | | |
| <i>Gleorhinus galeus</i> - MGP - PD 8871 - 8872 | | | | | | | | | | |
| | lateral upper | anterior upper | central upper | lateral lower | anterior lower | central lower | A | | | |
| lateral upper | | 0.0003 | 0.0001 | 0.0161 | 0.0001 | 0.0004 | 0.0001 | | | |
| anterior upper | 0.0003 | | 0.0031 | 0.0914 | 0.0007 | 0.0085 | 0.0005 | | | |
| central upper | 0.0001 | 0.0031 | | 0.0001 | 0.2328 | 0.1909 | 0.0123 | | | |
| lateral lower | 0.0161 | 0.0914 | 0.0001 | | 0.0001 | 0.0006 | 0.0001 | | | |
| anterior lower | 0.0001 | 0.0007 | 0.2328 | 0.0001 | | 0.5298 | 0.0033 | | | |
| central lower | 0.0004 | 0.0085 | 0.1909 | 0.0006 | 0.5298 | | 0.0251 | | | |
| A | 0.0001 | 0.0005 | 0.0123 | 0.0001 | 0.0033 | 0.0251 | | | | |
| <i>Galeorhinus galeus</i> - MCSNV T.1124 | | | | | | | | | | |
| | lateral upper | anterior upper | central upper | lateral lower | anterior lower | central lower | A | C | | |
| lateral upper | | 0.0009 | 0.0002 | 0.0159 | 0.0001 | 0.0004 | 0.0054 | 0.0415 | | |
| anterior upper | 0.0009 | | 0.0035 | 0.0901 | 0.0006 | 0.0085 | 0.0017 | 0.1285 | | |
| central upper | 0.0002 | 0.0035 | | 0.0001 | 0.2243 | 0.192 | 0.0393 | 0.1661 | | |
| lateral lower | 0.0159 | 0.0901 | 0.0001 | | 0.0002 | 0.0005 | 0.0006 | 0.0397 | | |
| anterior lower | 0.0001 | 0.0006 | 0.2243 | 0.0002 | | 0.5356 | 0.0268 | 0.1461 | | |
| central lower | 0.0004 | 0.0085 | 0.192 | 0.0005 | 0.5356 | | 0.0334 | 0.2478 | | |

| | | | | | | | | | | | |
|--|----------------------|-----------------------|----------------------|----------------------|-----------------------|----------------------|----------|----------|----------|----------|----------|
| A | 0.0054 | 0.0017 | 0.0393 | 0.0006 | 0.0268 | 0.0334 | | 0.1639 | | | |
| C | 0.0415 | 0.1285 | 0.1661 | 0.0397 | 0.1461 | 0.2478 | 0.1639 | | | | |
| Galeorhinus galeus - MSNPV 17716 | | | | | | | | | | | |
| | lateral upper | anterior upper | central upper | lateral lower | anterior lower | central lower | A | B | D | C | |
| lateral upper | | 0.0009 | 0.0001 | 0.0179 | 0.0001 | 0.0007 | 0.0002 | 0.0389 | 0.0436 | 0.0429 | |
| anterior upper | 0.0009 | | 0.0039 | 0.0947 | 0.0008 | 0.0073 | 0.0038 | 0.1263 | 0.122 | 0.1253 | |
| central upper | 0.0001 | 0.0039 | | 0.0001 | 0.2309 | 0.1943 | 0.027 | 0.1651 | 0.17 | 0.1685 | |
| lateral lower | 0.0179 | 0.0947 | 0.0001 | | 0.0001 | 0.0012 | 0.0002 | 0.0416 | 0.0357 | 0.043 | |
| anterior lower | 0.0001 | 0.0008 | 0.2309 | 0.0001 | | 0.5315 | 0.0013 | 0.1458 | 0.1471 | 0.1528 | |
| central lower | 0.0007 | 0.0073 | 0.1943 | 0.0012 | 0.5315 | | 0.0272 | 0.242 | 0.2526 | 0.2532 | |
| A | 0.0002 | 0.0038 | 0.027 | 0.0002 | 0.0013 | 0.0272 | | 0.1281 | 0.7491 | 0.2445 | |
| B | 0.0389 | 0.1263 | 0.1651 | 0.0416 | 0.1458 | 0.242 | 0.1281 | | 1 | 1 | |
| D | 0.0436 | 0.122 | 0.17 | 0.0357 | 0.1471 | 0.2526 | 0.7491 | 1 | | 1 | |
| C | 0.0429 | 0.1253 | 0.1685 | 0.043 | 0.1528 | 0.2532 | 0.2445 | 1 | 1 | | |
| Galeorhinus galeus - MGP - PD 8869 - 8870 | | | | | | | | | | | |
| | lateral upper | anterior upper | central upper | lateral lower | anterior lower | central lower | A | F | E | D | C |
| lateral upper | | 0.0001 | 0.0827 | 0.1316 | 0.0006 | 0.0807 | 0.0001 | 0.0133 | 0.0126 | 0.0008 | 0.0833 |
| anterior upper | 0.0001 | | 0.1162 | 0.0001 | 0.0001 | 0.1161 | 0.0001 | 0.0216 | 0.0213 | 0.0022 | 0.1089 |
| central upper | 0.0827 | 0.1162 | | 0.075 | 0.0943 | 1 | 0.0707 | 0.3291 | 0.333 | 0.1961 | 1 |
| lateral lower | 0.1316 | 0.0001 | 0.075 | | 0.0007 | 0.0728 | 0.0001 | 0.0108 | 0.012 | 0.0011 | 0.0792 |
| anterior lower | 0.0006 | 0.0001 | 0.0943 | 0.0007 | | 0.0899 | 0.0001 | 0.0163 | 0.017 | 0.001 | 0.0946 |
| central lower | 0.0807 | 0.1161 | 1 | 0.0728 | 0.0899 | | 0.077 | 0.3371 | 0.3341 | 0.1971 | 1 |
| A | 0.0001 | 0.0001 | 0.0707 | 0.0001 | 0.0001 | 0.077 | | 0.0092 | 0.0088 | 0.0276 | 0.0727 |
| F | 0.0133 | 0.0216 | 0.3291 | 0.0108 | 0.0163 | 0.3371 | 0.0092 | | 0.6596 | 0.0653 | 0.6655 |
| E | 0.0126 | 0.0213 | 0.333 | 0.012 | 0.017 | 0.3341 | 0.0088 | 0.6596 | | 0.3368 | 0.6685 |
| D | 0.0008 | 0.0022 | 0.1961 | 0.0011 | 0.001 | 0.1971 | 0.0276 | 0.0653 | 0.3368 | | 0.2016 |
| C | 0.0833 | 0.1089 | 1 | 0.0792 | 0.0946 | 1 | 0.0727 | 0.6655 | 0.6685 | 0.2016 | |
| Galeorhinus galeus - MCSNV T.311 | | | | | | | | | | | |
| | lateral upper | anterior upper | central upper | lateral lower | anterior lower | central lower | A | E | F | B | D |
| lateral upper | | 0.0015 | 0.0017 | 0.001 | 0.0001 | 0.0004 | 0.0001 | 0.0001 | 0.0001 | 0.0032 | 0.0401 |
| anterior upper | 0.0015 | | 0.0035 | 0.1632 | 0.0011 | 0.0085 | 0.0001 | 0.0001 | 0.0019 | 0.0298 | 0.1244 |
| central upper | 0.0017 | 0.0035 | | 0.0005 | 0.2964 | 0.2813 | 0.0002 | 0.0004 | 0.0059 | 0.0482 | 0.1636 |
| lateral lower | 0.001 | 0.1632 | 0.0005 | | 0.0002 | 0.0014 | 0.0001 | 0.0001 | 0.0001 | 0.0032 | 0.0437 |

| | | | | | | | | | | | |
|----------------|--------|--------|--------|--------|--------|--------|--------|--------|--------|--------|--------|
| anterior lower | 0.0001 | 0.0011 | 0.2964 | 0.0002 | | 0.4676 | 0.0001 | 0.0003 | 0.0016 | 0.0384 | 0.1434 |
| central lower | 0.0004 | 0.0085 | 0.2813 | 0.0014 | 0.4676 | | 0.0006 | 0.0038 | 0.0142 | 0.1017 | 0.2469 |
| A | 0.0001 | 0.0001 | 0.0002 | 0.0001 | 0.0001 | 0.0006 | | 0.0001 | 0.0001 | 0.0041 | 0.0459 |
| E | 0.0001 | 0.0001 | 0.0004 | 0.0001 | 0.0003 | 0.0038 | 0.0001 | | 0.0095 | 0.0168 | 0.2781 |
| F | 0.0001 | 0.0019 | 0.0059 | 0.0001 | 0.0016 | 0.0142 | 0.0001 | 0.0095 | | 0.3954 | 0.8596 |
| B | 0.0032 | 0.0298 | 0.0482 | 0.0032 | 0.0384 | 0.1017 | 0.0041 | 0.0168 | 0.3954 | | 0.6606 |
| D | 0.0401 | 0.1244 | 0.1636 | 0.0437 | 0.1434 | 0.2469 | 0.0459 | 0.2781 | 0.8596 | 0.6606 | |

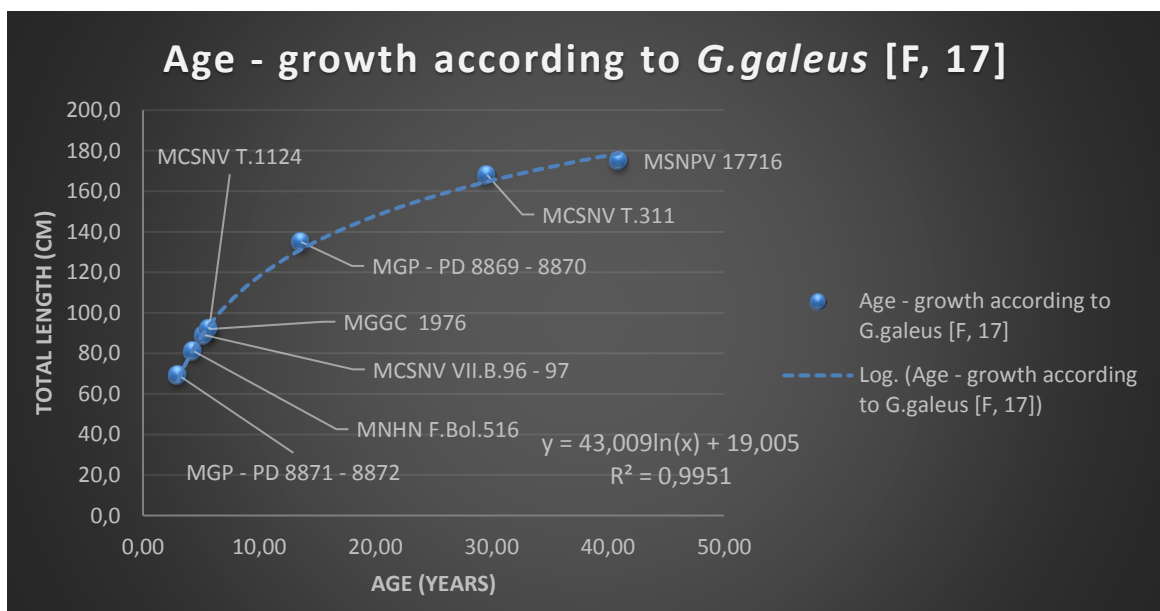
Table G2: Pairwise comparison between teeth categories of *Galeocerdo cuvier* and morphotypes of fossil specimens. The blue, yellow and orange cells indicate the tooth categories of *G. cuvier*, the morphotypes of the fossils and uncorrected variances among groups ($p > 0,05$), respectively.

| <i>Galeocerdo cuvier</i> - MGGC 1976 | | | | | | | | | | | |
|---|---------------|----------------|---------------|---------------|----------------|---------------|--------|--------|--|--|--|
| | lateral upper | anterior upper | central upper | lateral lower | anterior lower | central lower | A | D | | | |
| lateral upper | | 0.0001 | 0.0832 | 0.1374 | 0.0003 | 0.0805 | 0.0001 | 0.0005 | | | |
| anterior upper | 0.0001 | | 0.12 | 0.0002 | 0.0002 | 0.1086 | 0.0001 | 0.0014 | | | |
| central upper | 0.0832 | 0.12 | | 0.0811 | 0.0904 | 1 | 0.045 | 0.2014 | | | |
| lateral lower | 0.1374 | 0.0002 | 0.0811 | | 0.0008 | 0.0805 | 0.0001 | 0.001 | | | |
| anterior lower | 0.0003 | 0.0002 | 0.0904 | 0.0008 | | 0.0856 | 0.0001 | 0.001 | | | |
| central lower | 0.0805 | 0.1086 | 1 | 0.0805 | 0.0856 | | 0.0434 | 0.1953 | | | |
| A | 0.0001 | 0.0001 | 0.045 | 0.0001 | 0.0001 | 0.0434 | | 0.0135 | | | |
| D | 0.0005 | 0.0014 | 0.2014 | 0.001 | 0.001 | 0.1953 | 0.0135 | | | | |
| | | | | | | | | | | | |
| <i>Galeocerdo cuvier</i> - MGP - PD 8872 - 8871 | | | | | | | | | | | |
| | lateral upper | anterior upper | central upper | lateral lower | anterior lower | central lower | A | | | | |
| lateral upper | | 0.0002 | 0.0808 | 0.1285 | 0.0005 | 0.0849 | 0.0001 | | | | |
| anterior upper | 0.0002 | | 0.1149 | 0.0001 | 0.0001 | 0.112 | 0.0001 | | | | |
| central upper | 0.0808 | 0.1149 | | 0.0834 | 0.0911 | 1 | 0.1435 | | | | |
| lateral lower | 0.1285 | 0.0001 | 0.0834 | | 0.0007 | 0.0787 | 0.0001 | | | | |
| anterior lower | 0.0005 | 0.0001 | 0.0911 | 0.0007 | | 0.0934 | 0.0001 | | | | |
| central lower | 0.0849 | 0.112 | 1 | 0.0787 | 0.0934 | | 0.1473 | | | | |
| A | 0.0001 | 0.0001 | 0.1435 | 0.0001 | 0.0001 | 0.1473 | | | | | |
| | | | | | | | | | | | |
| <i>Galeocerdo cuvier</i> - MCSNV T.1124 | | | | | | | | | | | |
| | lateral upper | anterior upper | central upper | lateral lower | anterior lower | central lower | A | C | | | |

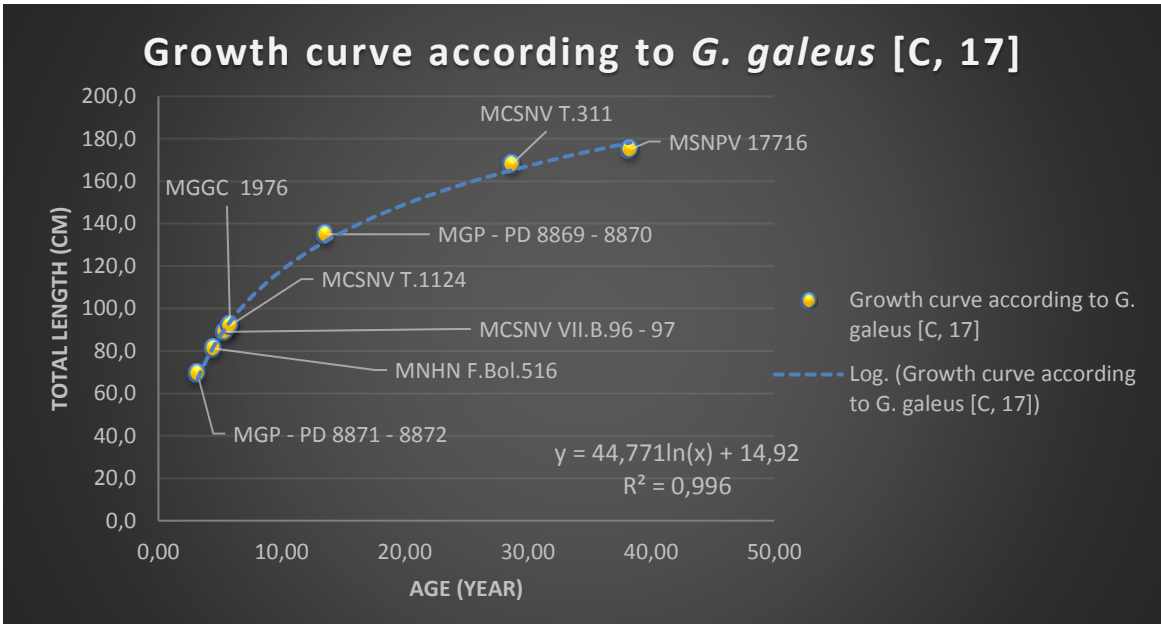
| | | | | | | | | | | | |
|---|---------------|----------------|---------------|---------------|----------------|---------------|--------|--------|--------|--------|--------|
| lateral upper | | 0.0001 | 0.0804 | 0.1306 | 0.0001 | 0.0868 | 0.0003 | 0.0824 | | | |
| anterior upper | 0.0001 | | 0.1092 | 0.0001 | 0.0002 | 0.1148 | 0.0011 | 0.1094 | | | |
| central upper | 0.0804 | 0.1092 | | 0.0789 | 0.0924 | 1 | 0.164 | 1 | | | |
| lateral lower | 0.1306 | 0.0001 | 0.0789 | | 0.0013 | 0.075 | 0.0005 | 0.077 | | | |
| anterior lower | 0.0001 | 0.0002 | 0.0924 | 0.0013 | | 0.0904 | 0.0008 | 0.0879 | | | |
| central lower | 0.0868 | 0.1148 | 1 | 0.075 | 0.0904 | | 0.1711 | 1 | | | |
| A | 0.0003 | 0.0011 | 0.164 | 0.0005 | 0.0008 | 0.1711 | | 0.1521 | | | |
| C | 0.0824 | 0.1094 | 1 | 0.077 | 0.0879 | 1 | 0.1521 | | | | |
| | | | | | | | | | | | |
| Galeocerdo cuvier - MSNPV 17716 | | | | | | | | | | | |
| | lateral upper | anterior upper | central upper | lateral lower | anterior lower | central lower | A | B | D | C | |
| lateral upper | | 0.0001 | 0.0788 | 0.1372 | 0.0001 | 0.08 | 0.0001 | 0.0805 | 0.0872 | 0.085 | |
| anterior upper | 0.0001 | | 0.1134 | 0.0001 | 0.0002 | 0.1119 | 0.0004 | 0.1142 | 0.1118 | 0.1108 | |
| central upper | 0.0788 | 0.1134 | | 0.0824 | 0.0888 | 1 | 0.124 | 1 | 1 | 1 | |
| lateral lower | 0.1372 | 0.0001 | 0.0824 | | 0.0006 | 0.0756 | 0.0001 | 0.0799 | 0.0799 | 0.0815 | |
| anterior lower | 0.0001 | 0.0002 | 0.0888 | 0.0006 | | 0.0882 | 0.0001 | 0.0926 | 0.0929 | 0.0911 | |
| central lower | 0.08 | 0.1119 | 1 | 0.0756 | 0.0882 | | 0.1212 | 1 | 1 | 1 | |
| A | 0.0001 | 0.0004 | 0.124 | 0.0001 | 0.0001 | 0.1212 | | 0.1257 | 0.7432 | 0.2424 | |
| B | 0.0805 | 0.1142 | 1 | 0.0799 | 0.0926 | 1 | 0.1257 | | 1 | 1 | |
| D | 0.0872 | 0.1118 | 1 | 0.0799 | 0.0929 | 1 | 0.7432 | 1 | | 1 | |
| C | 0.085 | 0.1108 | 1 | 0.0815 | 0.0911 | 1 | 0.2424 | 1 | 1 | | |
| | | | | | | | | | | | |
| Galeocerdo cuvier - MGP - PD 8869 - 8870 | | | | | | | | | | | |
| | lateral upper | anterior upper | central upper | lateral lower | anterior lower | central lower | A | F | E | D | C |
| lateral upper | | 0.0001 | 0.0848 | 0.1351 | 0.0003 | 0.0858 | 0.0001 | 0.0143 | 0.0152 | 0.0009 | 0.0794 |
| anterior upper | 0.0001 | | 0.1048 | 0.0001 | 0.0002 | 0.11 | 0.0001 | 0.0206 | 0.0215 | 0.0016 | 0.1168 |
| central upper | 0.0848 | 0.1048 | | 0.0817 | 0.0885 | 1 | 0.0644 | 0.3303 | 0.3394 | 0.1948 | 1 |
| lateral lower | 0.1351 | 0.0001 | 0.0817 | | 0.0009 | 0.077 | 0.0001 | 0.0105 | 0.0108 | 0.0005 | 0.0762 |
| anterior lower | 0.0003 | 0.0002 | 0.0885 | 0.0009 | | 0.0927 | 0.0001 | 0.0131 | 0.012 | 0.0009 | 0.0911 |
| central lower | 0.0858 | 0.11 | 1 | 0.077 | 0.0927 | | 0.0694 | 0.3308 | 0.3356 | 0.195 | 1 |
| A | 0.0001 | 0.0001 | 0.0644 | 0.0001 | 0.0001 | 0.0694 | | 0.0098 | 0.0081 | 0.024 | 0.0704 |
| F | 0.0143 | 0.0206 | 0.3303 | 0.0105 | 0.0131 | 0.3308 | 0.0098 | | 0.6661 | 0.0645 | 0.6648 |
| E | 0.0152 | 0.0215 | 0.3394 | 0.0108 | 0.012 | 0.3356 | 0.0081 | 0.6661 | | 0.3292 | 0.6617 |
| D | 0.0009 | 0.0016 | 0.1948 | 0.0005 | 0.0009 | 0.195 | 0.024 | 0.0645 | 0.3292 | | 0.2106 |
| C | 0.0794 | 0.1168 | 1 | 0.0762 | 0.0911 | 1 | 0.0704 | 0.6648 | 0.6617 | 0.2106 | |
| | | | | | | | | | | | |

| Galeocерdo cuvier - MCSNV T.311 | | | | | | | | | | | |
|---------------------------------|---------------|----------------|---------------|---------------|----------------|---------------|--------|--------|--------|--------|--------|
| | lateral upper | anterior upper | central upper | lateral lower | anterior lower | central lower | A | E | F | B | D |
| lateral upper | | 0.0001 | 0.0842 | 0.1287 | 0.0003 | 0.0781 | 0.0001 | 0.0001 | 0.0001 | 0.0032 | 0.0896 |
| anterior upper | 0.0001 | | 0.1163 | 0.0001 | 0.0002 | 0.1052 | 0.0001 | 0.0001 | 0.0002 | 0.0066 | 0.1075 |
| central upper | 0.0842 | 0.1163 | | 0.078 | 0.0923 | 1 | 0.0408 | 0.0867 | 0.1392 | 0.2546 | 1 |
| lateral lower | 0.1287 | 0.0001 | 0.078 | | 0.0009 | 0.0827 | 0.0001 | 0.0001 | 0.0003 | 0.0029 | 0.079 |
| anterior lower | 0.0003 | 0.0002 | 0.0923 | 0.0009 | | 0.0863 | 0.0001 | 0.0001 | 0.0001 | 0.0044 | 0.0923 |
| central lower | 0.0781 | 0.1052 | 1 | 0.0827 | 0.0863 | | 0.0435 | 0.0885 | 0.1425 | 0.2473 | 1 |
| A | 0.0001 | 0.0001 | 0.0408 | 0.0001 | 0.0001 | 0.0435 | | 0.0001 | 0.002 | 0.0424 | 0.092 |
| E | 0.0001 | 0.0001 | 0.0867 | 0.0001 | 0.0001 | 0.0885 | 0.0001 | | 0.1024 | 0.4005 | 0.8165 |
| F | 0.0001 | 0.0002 | 0.1392 | 0.0003 | 0.0001 | 0.1425 | 0.002 | 0.1024 | | 0.7508 | 0.5721 |
| B | 0.0032 | 0.0066 | 0.2546 | 0.0029 | 0.0044 | 0.2473 | 0.0424 | 0.4005 | 0.7508 | | 0.7463 |
| D | 0.0896 | 0.1075 | 1 | 0.079 | 0.0923 | 1 | 0.092 | 0.8165 | 0.5721 | 0.7463 | |

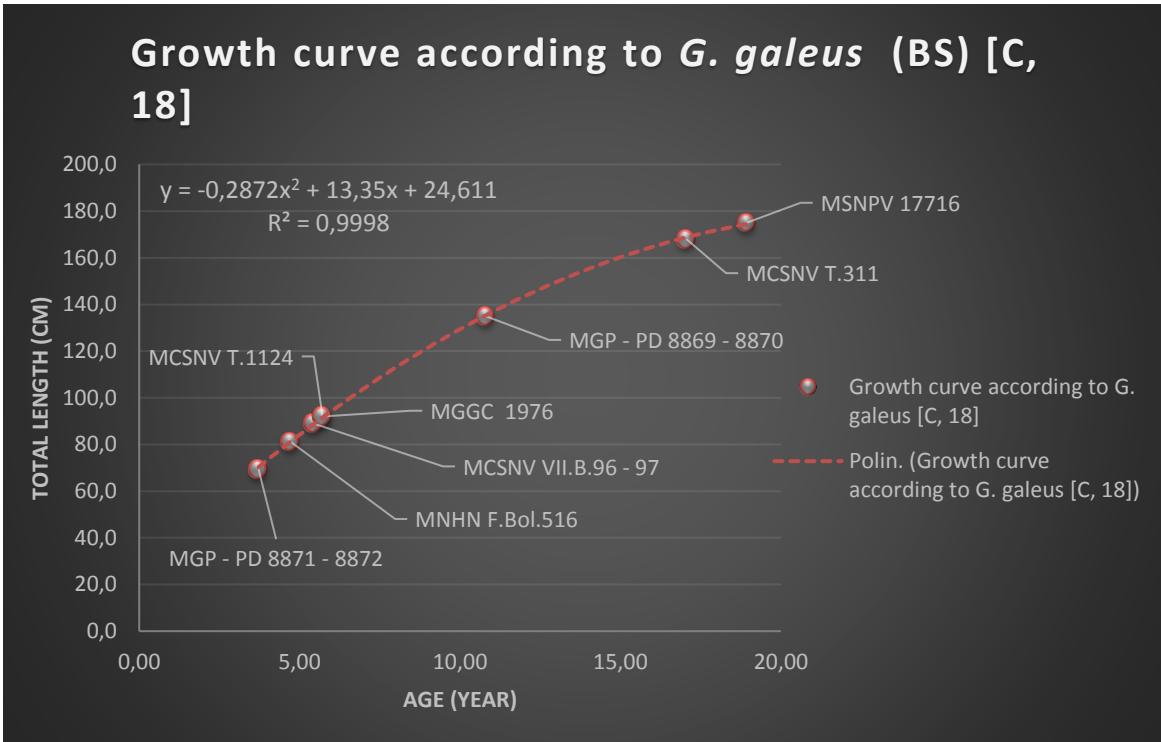
Appendix H: Growth curves of fossil specimens according to growth parameters of living shark populations.



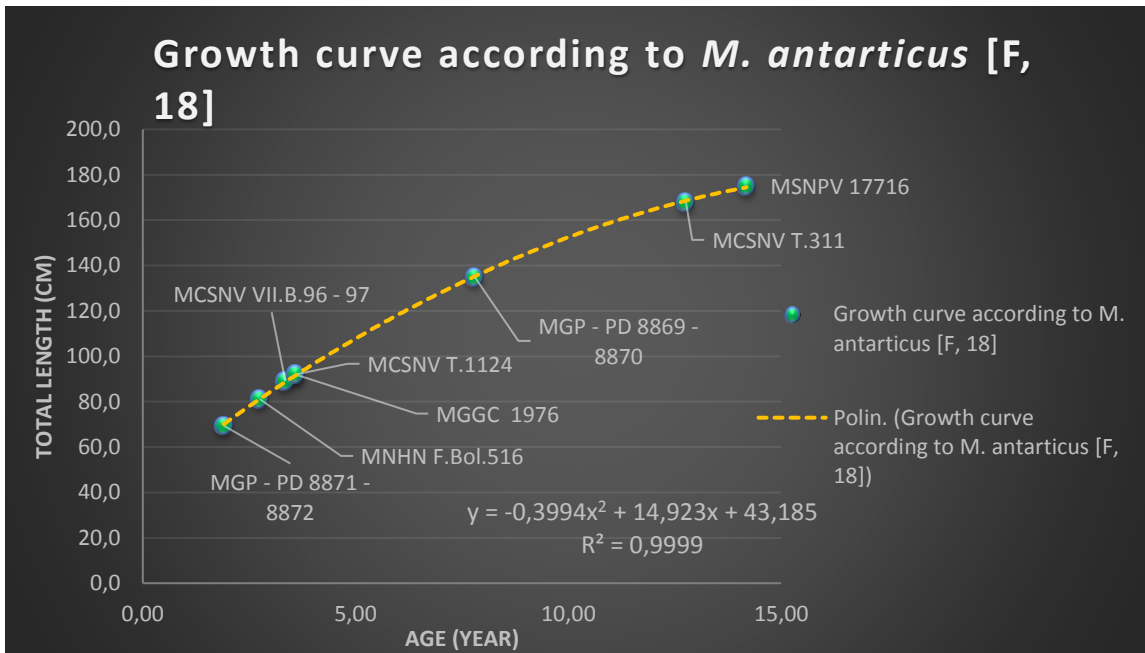
H1: Estimated ages – total length correlation computed follows the growth curve for female individuals of the New Zealand populations of *Galeorhinus galeus* (Francis & Mulligan, 1998 [17]). *Abbreviations:* F, female individuals.



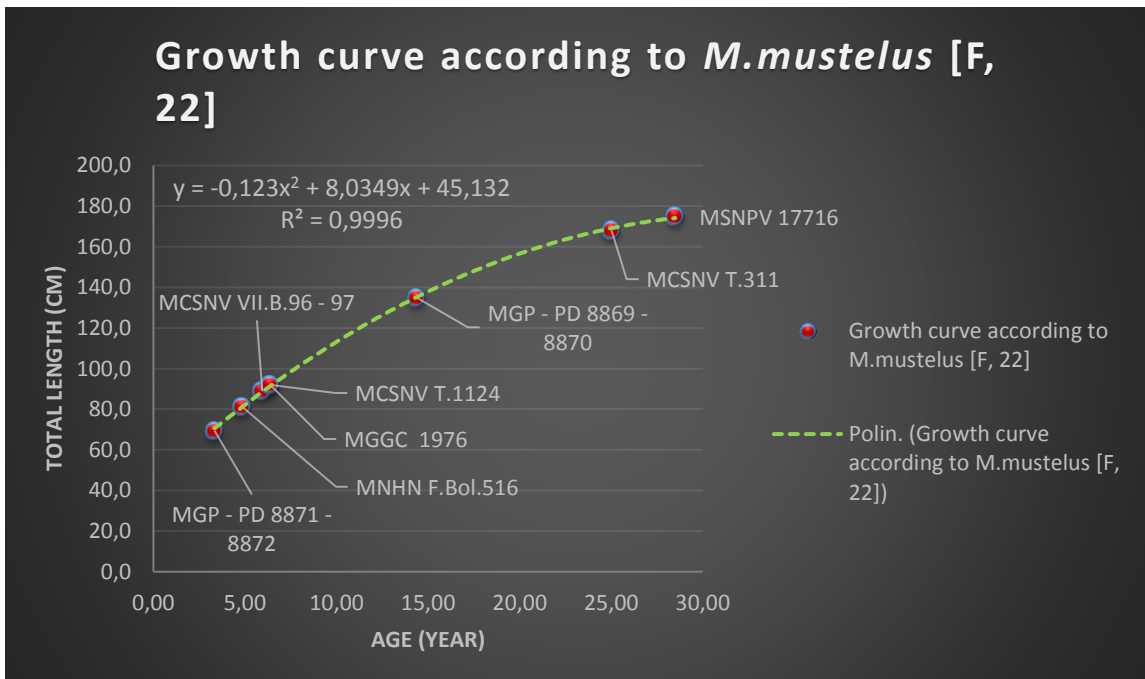
H2: Estimated ages – total length correlation computed follows the growth curve for combined sex of the New Zealand populations of *Galeorhinus galeus* (Francis & Mulligan, 1998 [17]). *Abbreviations:* C, combined sex.



H3: Estimated ages – total length correlation computed follows the growth curve for combined sex of the Bass Strait populations (Australia) of *Galeorhinus galeus* (Moulton et al., 1992 [18]). *Abbreviations:* BS, Bass Strait; C, combined sex.

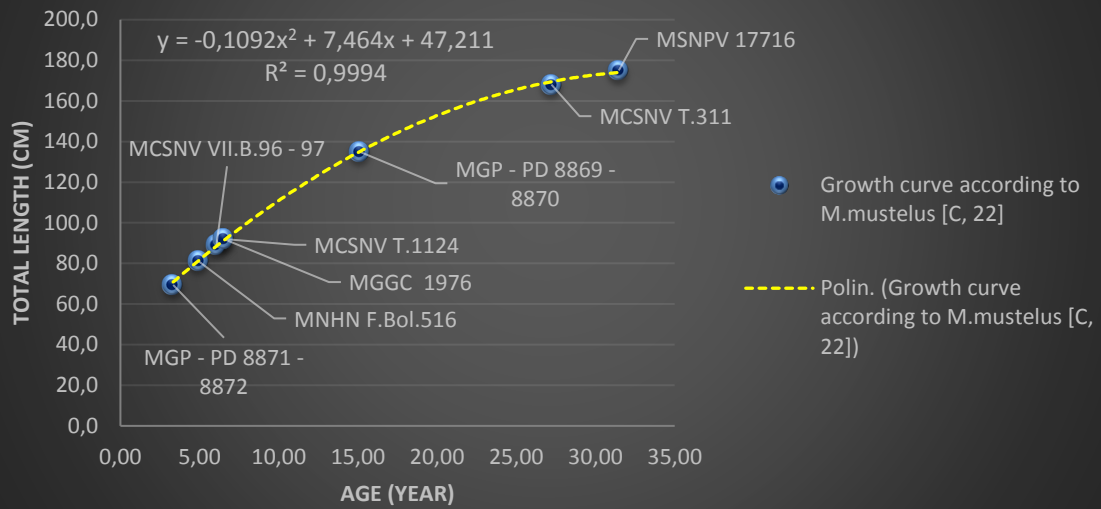


H4: Estimated ages – total length correlation computed follows the growth curve for female individuals of Australian populations of *Mustelus antarcticus* (Moulton et al., 1992 [18]). Abbreviations: F, female individuals.



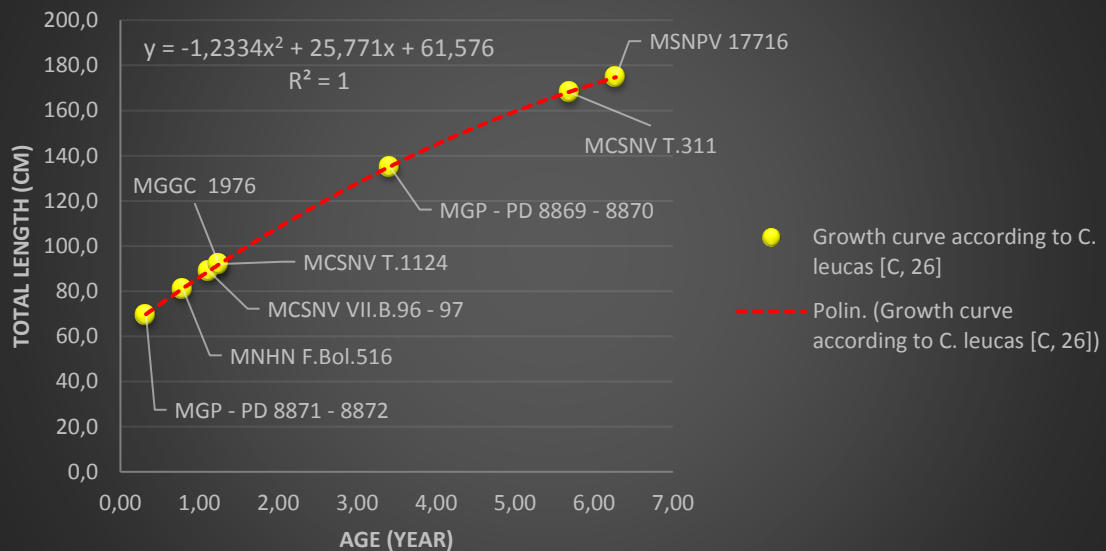
H5: Estimated ages – total length correlation computed follows the growth curve for female individuals of South Africa populations of *Mustelus mustelus* (Goosen & Smale, 1997 [22]). Abbreviations: F, female individuals.

Growth curve according to *M. mustelus* [C, 22]

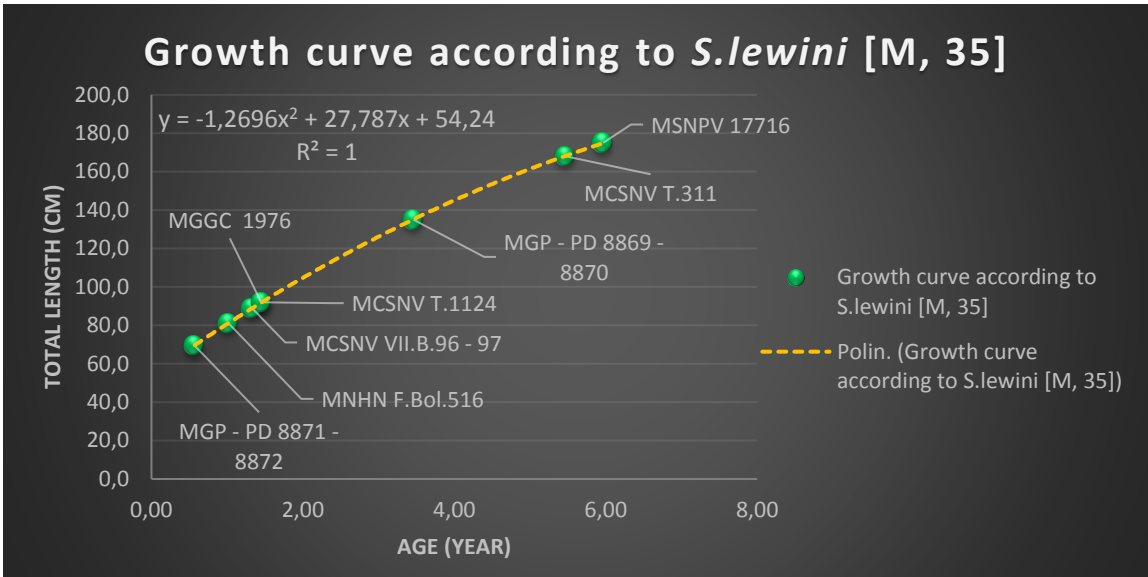


H6: Estimated ages – total length correlation computed follows the growth curve for combined sex of South Africa populations of *Mustelus mustelus* (Goosen & Smale, 1997 [22]). Abbreviations: C, combined sex.

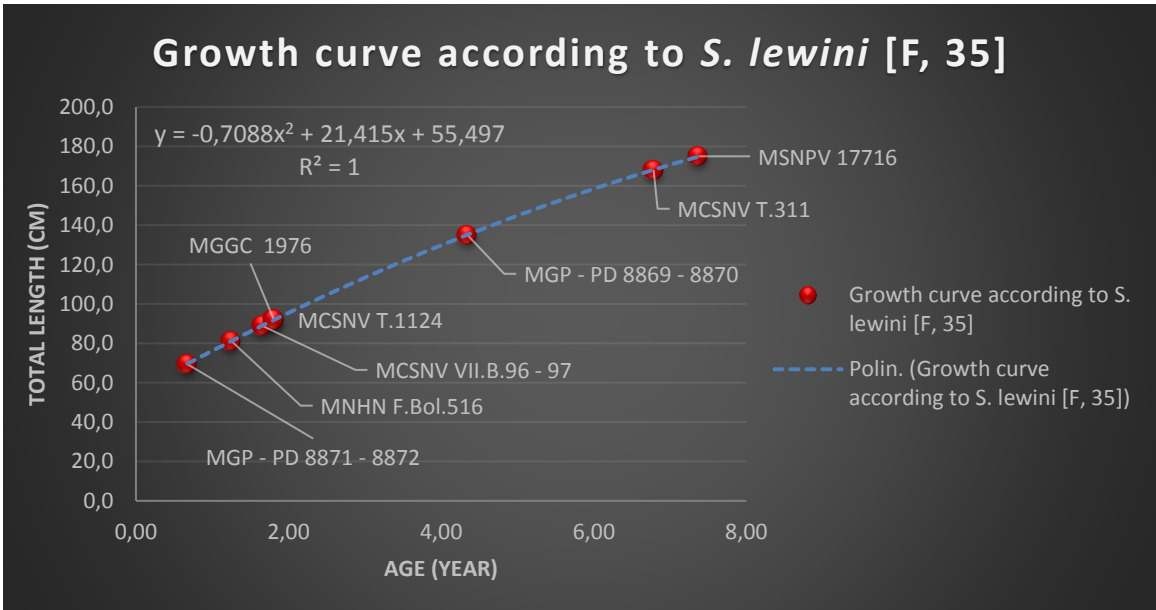
Growth curve according to *C. leucas* [C, 26]



H7: Estimated ages – total length correlation computed follows the growth curve for combined sex of Gulf of Mexico populations of *Carcharhinus leucas* (Cruz – Martines, 2004 [26]). Abbreviations: C, combined sex.



H8: Estimated ages – total length correlation computed follows the growth curve for male individuals of Gulf of Mexico populations of *Sphyrna lewini* (Piercy et al., 2007 [35]). Abbreviations: M, male individuals.



H9: Estimated ages – total length correlation computed follows the growth curve for female individuals of Gulf of Mexico populations of *Sphyrna lewini* (Piercy et al., 2007 [35]). Abbreviations: F, female individuals.

Ringraziamenti

Uno speciale ringraziamento va al Prof. Federico Fanti, Enrico Trevisani e Paolo Guaschi non solo per il contributo della ricerca, ma anche per la massima disponibilità e cordialità mostratami in questi mesi. Ringrazio il direttore del Museo di Scienze Naturali dell'Università di Pavia, il Prof. Giorgio Mellerio, per l'accessibilità dei reperti. Ringrazio il Prof. Pietro Galinetto e la dott.ssa Ilenia Tredici del "Centro interdipartimentale di studi e ricerche per la conservazione del patrimonio culturale dell'Università di Pavia (CISRIC)" per le eccellenti acquisizioni al SEM dei campioni. Ringrazio inoltre la dott.sa Mariagabriella Fornasiero, dott.sa Letizia Del Favero, dott. Roberto Zorzin, Prof. Valeria Franceschini, dott.sa Daniela Minelli per avermi messo a disposizione tutto il materiale di cui avevo bisogno, indispensabile per questo studio. Ringrazio inoltre Paolo "Paolino" Ferrieri per le eccellenti fotografie e per la sua disponibilità.

Ringrazio la mia famiglia e mio fratello, per avermi sostenuto e aiutato in ogni situazione. Ringrazio Carlotta, per sopportarmi di continuo e placare le mie incertezze. Ringrazio: tutti i compagni di corso; Sgamos; Amedeo; St**zes; "Social bolo"; Lo Spezz, Paolo e Alessandra per l'indimenticabile Wacken Open Air 2017 e tutte le belle persone conosciute in tale occasione; In the Vault; vari ed eventuali dispersi in parte in Oceania ed in parte in America; Rush, 883, The Offspring, Nofx, Septicflesh e tutti i gruppi musicali che ho ascoltato durante la stesura di questa tesi.

